Evaluation of cultured cochlear fibrocytes as a cell replacement therapy: comparison with native fibrocytes

Anya Helen Osborn

School of Life Sciences

Keele University

A thesis submitted for the degree of

Doctor of Philosophy

March 2020

Abstract

Fibrocyte degeneration in the cochlear lateral wall is one possible pathology of age-related metabolic hearing loss (presbyacusis). Fibrocytes play a role in potassium recycling and maintenance of the endocochlear potential (EP). It has been proposed that a cell replacement therapy could prevent fibrocyte degeneration in the CD/1 mouse model of hearing loss. One source of replacement cells is cultured spiral ligament fibrocytes (SLFs) as they do not require significant differentiation or development so may integrate into the cochlea better than stem cells. This research employs the techniques of whole-cell voltage clamping and immunolabelling to examine and compare the characteristics of native and cultured fibrocytes. The aim to see whether the cultured SLFs display similar features and characteristics to that of native SLFs, in aid of building the case of these cells being a suitable cell replacement to treat age-related hearing loss.

Fibrocytes cultured as monolayers or on 3-D collagen I gels were compared with fibrocytes in cochlear slices or micro-dissected spiral ligament (SL) from ~P7 cochlea of CD/1 mice. Fibrocytes successfully grown for short periods on a 3-D collagen I matrix exhibited rounded cell bodies with extending processes, compared to a flatter morphology when grown in a monolayer. Immunofluorescence showed expression of aquaporin 1 (AQP1) which, in the cochlea, is confined to type III fibrocytes and to a lesser extent for S-100 found in several fibrocyte types. The cultured cells also expressed the inwardly-rectifying potassium channel Kir5.1, as well as labelling for the gap junction proteins connexin 26 and 31. Finally, whole-cell voltage clamp recordings in both the cultured and putative native fibrocytes revealed outwardly- rectifying potassium currents on depolarisation. There was also a large group of linear response recordings, and a subset showing both inward and outward-rectification. There was no significant difference in the resting membrane potentials between the native and

cultured cells in any of the linear or outwardly-rectifying group recordings. Thus 3-D cultured fibrocytes show morphology that more closely resembles that *in vivo* compared to monolayer cultures and appear to possess functional potassium channels. Thus far, this research indicates that these cells are suitable for transplantation into the lateral wall of the cochlea in a cell therapy to treat age-related metabolic presbyacusis.

Table of Contents

Abbreviations

2-D	Two dimensional
3-D	Three dimensional
3-NP	3-nitropropionic acid
ABR	Auditory brainstem response
ACSF	Artificial cerebrospinal fluid
Ahl	Age-related hearing loss gene
AQP	Aquaporin
Atoh1	Atonal BHLH Transcription Factor 1
BM	Basilar membrane
Brn-4	Brain-4
CAEPs	Cortical auditory evoked potentials
CG-JN	Connective-tissue cell gap-junction network
DAB	Days after birth
DMEM	Dulbecco Modified Eagle Media
DMSO	Dimethyl sulfoxide
DPX	Dibutylphthalate polystyrene xylene
EDTA	Ethylenediaminetetraacetic acid
EG-JS	Epithelial cell gap junction system
EP	Endocochlear potential
FCS	Foetal calf serum
FITC	Fluorecein isothiocyanate

G-force	Gravitational force equivalent
GJ-IC	Gap junction mediated intercellular communication
GLAST	Glutamate aspartate transporter
HEPES	4-(2-hydroxyethyl)-1-piperazineethanesulfonic acid
hESCs	Human embryonic stem cells
HSC	Hematopoietic stem cells
IHC	Inner hair cells
ITS-G	Insulin-Transferrin-Selenium-G Supplement
MEM-α	Minimum Essential Medium α
MET	Mechanoelectrical transducer
MSc	Mesenchymal stem cells
NKCC	Na^+K^+Cl transporter
oC	Organ of Corti
OEPs	Otic epithelial progenitors
OHC	Outer hair cells
ONPs	Otic neural progenitors
OSC	Outer sulcus cells
Otos	Otospiralin
P	Postnatal day
PB	Phosphate-buffered
PBS	Phosphate-buffered saline
PDGF- BB	Platelet-derived growth factor
PFA	Paraformaldehyde
pPD	Para-phenyldiamine

PVA	Polyvinyl alcohol
RM	Reissners membrane
RMP	Resting membrane potential
RPM	Revolutions per minute
RT	Room temperature
SL	Spiral ligament
SLFs	Spiral ligament fibrocytes
SNHL	Sensory neural hearing loss
SV	*Stria Vascularis*
TBOA	DL-threo-β-benzyloxyaspartate
TEA	Tetraethylammonium
TGF-β	Transforming growth factor beta
TM	Tectorial membrane
TRITC	Tetramethylrhodamine
UK	United Kingdom
USA	United States of America

List of Tables

List of Figures

Acknowledgement

First and foremost, I would like to thank my supervisors Professor David Furness, Dr Michael Evans and Dr Douglas Caruana for giving me the opportunity to do this PhD. I thank Professor David Furness for helping with the cell cultures and labelling, and Dr Michael Evans and Dr Douglas Caruana for their help with the electrophysiological side of the project. Their expertise, guidance and support throughout this journey is greatly appreciated and their kind patience made it all possible.

Another special thank you to all of my colleagues at the School of Life Sciences and particularly a kind thanks to those based at the EM unit, Karen Walker and Dr Shanthini Mahendrasingam. In addition, the funding sources that made this PhD possible are gratefully acknowledged; Keele University ACORN fund and the Action on Hearing Loss charity.

I would also like to thank all of my friends and family who have been there over this period. Thanks for supporting and encouraging me whilst pretending to understand what it is I have been doing over the past four years! Extra thanks to the friends made whilst at Keele and throughout the course of the PhD, for being there when I needed it and going through this journey with me.

Chapter 1

General Introduction

1. Chapter 1- General Introduction

Hearing impairments are one of the biggest health-related problems reported worldwide. Indeed, the World Health Organisation estimates that over 5% of the world's population (~466 million people) have debilitating hearing loss with approximately 11 million people in the UK alone diagnosed as being deaf or hard of hearing, making it the second most common disability in the UK (Actiononhearingloss.org.uk). It affects more people than epilepsy, multiple sclerosis, spinal injury, stroke, Huntington's and Parkinson's diseases combined (Hudspeth, 1997).

Presbycusis is a form of hearing loss associated with normal ageing, with 71% of individuals over the age of 70 in the UK reporting some form of age-related hearing loss (Actiononhearingloss.org.uk). Schuknecht (1974) identified the four types of human presbycusis: (1) sensory, affecting hair and sensory cells; (2) neural, loss of spiral ganglion neurons; (3) metabolic, deficits in processes maintaining ionic gradients, caused mainly by degeneration of the *stria vascularis* cells and SLFs; and (4) mechanical, stiffening of the basilar membrane and organ of Corti therefore affecting its movement. Animal models have been used extensively to predict patterns of hearing loss associated with human cochlear pathology. The outbred CD/1 mouse model is commonly used and shows accelerated presbycusis (Shone et al, 1991) with hearing loss occurs at about 4 weeks (Le Calvez et al, 1998).

Indeed, audiograms and other advanced measures of auditory function (including, auditory brainstem responses, otoacoustic emissions) have been used in rodents to provide compelling evidence for metabolic, sensory and a mixed metabolic/sensory phenotype of presbycusis (Schuknecht, 1964). Schuknecht and Gacek (1993) later revised his earlier classification to: (1) sensory cell losses are least important type of loss in the aged ear; (2) neuronal losses are a constant pathology of aging; (3) lateral wall pathology is the main lesion in the aging ear.

Therefore, they established the main cause of age-related hearing loss to be the degeneration of the cochlear lateral wall with sensory cell loss being of secondary importance. In order to understand the structures implicated in different forms of presbycusis, a review of the anatomy and functions of the cochlea is required.

1.1 Functional Anatomy of the Cochlea

The human cochlea is the auditory portion of the inner ear and is a ~35mm long coiled bony tube containing three compartments: *the scala tympani*, the *scala vestibuli*, and the *scala media* (Mills & Weber, 2001; fig. 1.1). The *scalae tympani* and *vestibuli* contain perilymph, whilst the *scala media* contains endolymph. The boundaries of the *scala media* are at the top surface of the Organ of Corti, the reticular lamina, which separates it from the *scala tympani;* Reissner's membrane, separating from the *scala vestibuli*; and the *stria vascularis* (fig. 1.1). Beneath the tectorial membrane are interdental cells connected to each other to form a comb-shaped cellular network in the spiral limbus, also containing fibrocytes (Shodo et al, 2017).

The perilymph contains typical extracellular ion concentrations and the endolymph contains a high potassium concentration of 150 mM and an 80 mV EP (Wangemann & Schacht, 1996; Wangemann, 2006; Hibino & Kurachi, 2006). The EP is at a positive voltage of 80-100mV seen in the cochlear endolymphatic spaces and is the main driving force for sensory transduction (Wangemann & Schacht, 1996). Another driving force for this transduction is provided by the large potential difference across the apical membrane of the hair cell (membrane potential), the sensory receptors for the auditory and vestibular system within the organ of Corti. There are two types of hair cells: inner hair cells (IHC) and outer hair cells (OHC).

The hair cells have a membrane potential of –70 mV thereby producing a total driving force across the hair cell apex of 150 mV; these both increase the driving of K^+ recycling. The influx of potassium into the hair cells is driven strongly by the highly positive EP, and this potential is the result of the unique electrical properties of the cochlear lateral wall.

Figure 1. 1 Schematic cross section of the cochlea and Organ of Corti

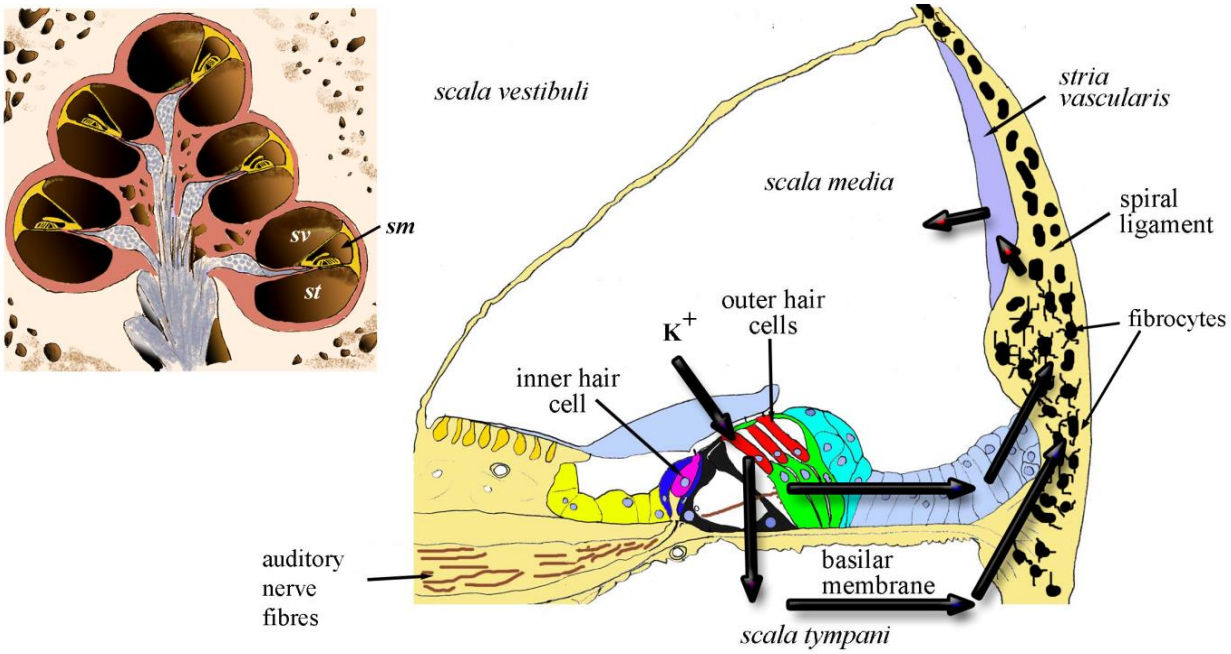

Figure 1.1 Cross-section of the cochlea. Schematic drawing of the cochlear cross-section showing turns of the cochlea. Surrounding structures of the scala media. Potassium is taken up by hair cells and passed through either the epithelial gap junction system or into the perilymph before being taken up by fibrocytes at the bottom of the spiral ligament where it is passed through to the connective tissue gap junction network and back into the endolymph. This potassium recycling maintains the EP crucial to hearing. Arrows indicate potassium transport routes. Image provided by Prof David Furness.

1.2 Structure and Function of the Organ of Corti

The mammalian cochlea contains the transduction organ, the organ of Corti, comprising the two types of sensory hair cells receptors. Acoustic energy that enters the cochlea causes a pressure gradient between the *scala vestibuli* and *scala tympani*, causing movement of the

basilar membrane and a traveling wave which propagates towards the apex of the cochlea. The precise location along the basilar membrane that the traveling wave reaches its maximum vibration depends on the frequency of the stimulus, low frequencies are detected at apex and high frequencies detected at base, the principle of tonopic organisation of the cochlea. Basilar membrane displacement induces deflection of the hair cell stereocilia which sit on this membrane, and this deflection modulates OHC current. The removal of the EP removes the power driving OHC motility (Ruggero & Rich, 1991). The importance of maintaining the EP has been shown in the development of a young gerbil model of metabolic presbycusis through use of furosemide, a loop directic used to treat heart failure and edema, into the round window of the cochlea inducing damage or injury to the lateral wall (Lang et al, 2010). K^+ cycling is essential for hearing as it converts the hair cell sensitivity to mechanical stimulation (reviewed in Hibino & Kurachi, 2006). Essentially, the re-establishment of the K^+ recycling route following damage or injury may result in the normalization of the EP and the recovery of hearing.

IHCs are the sensory cells which convert mechanical stimulation into electrical signals and synaptic activity which is transmitted to the brain. The OHCs are key in the amplification of the basilar membrane motion, which is needed to detect sounds at low sound pressures. Cochlear hair cell bodies are bathed in perilymph and possess stereocilary cell bundles. The bundles of sensory OHCs project up to the tectorial membrane. The vibration of the basilar membrane induced by sound causes hair cell bundle displacement which causes stereocillia deflection, this causes mechanoelectrical transducer channels to open. Tip links seem to couple stereocillia displacement to channel gating (opening) (Corey & Hudspeth, 1983; Pickles et al, 1984; Assad et al, 1991). This then allows Ca^{2+} and predominantly K^+ from the endolymph to enter the hair cells and ultimately leads to the excitation of the auditory nerve

(Hudspeth, 1989). The hair cells then send their signal via neurotransmitter to the primary auditory neurons of the spiral ganglion. One IHC is innervated by 10-15 type I spiral ganglion neurons, and numerous OHCs are innervated by a single type II spiral ganglion neuron. Approximately 90-95% of the spiral ganglion neurons are type I that send peripheral processes to IHCs (Spoendlin, 1985), and are the source of nerve fibres to the brain. The remaining 5-10 % are type II whose functions are still not clear.

1.3 Lateral Wall Structure and Function

The cochlear lateral wall consists of the *stria vascularis* which is located medially and the spiral ligament located laterally (fig. 1.1). The EP is generated by a process of K^+ movement provided by a number of cell types in the lateral wall (Mizuta et al, 1997; Crouch et al, 1997; Takeuchi et al, 2000; Marcus et al, 2002), which may be highly susceptible to aging due to the high metabolic activities of these cells (Gruber et al, 2008). The *stria vascularis* is a secretory epithelium lining the lateral wall of the *scala media* and it is composed of three cell layers: marginal cells, intermediate cells and basal cells (fig. 1.2). The spiral ligament is composed of fibrocytes, of which there are five types.

1.3.1 Spiral Ligament Structure

A function of the spiral ligament is maintaining the ionic balance in the cochlea. Supported by gap junctions and Na^+ K^+ ATPase pumps, the spiral ligament, alongside the *stria vascularis*, is believed to transport K^+ out of the perilymph, and back into the endolymph maintaining its high K^+ concentration (Spicer & Schulte, 1991). The predominant cell types in this structure are SLFs which possess uptake mechanisms for K^+ and contribute towards the generation of

the EP (Mizuta et al, 1997; Crouch et al, 1997). The cell bodies of root cells reside within the outer sulcus and project into the spiral ligament (Galic and Giebel 1989; Spicer and Schulte 1996).The EP in the *scala media* (+80) is due to the actions of complex physiological mechanisms involving Na^+ K^+ ATPase pumps, NKCCs (Na^+K^+Cl transporter) and K^+ channels along the cochlear lateral wall.

Figure 1. 2 Schematic of potassium transport through lateral wall

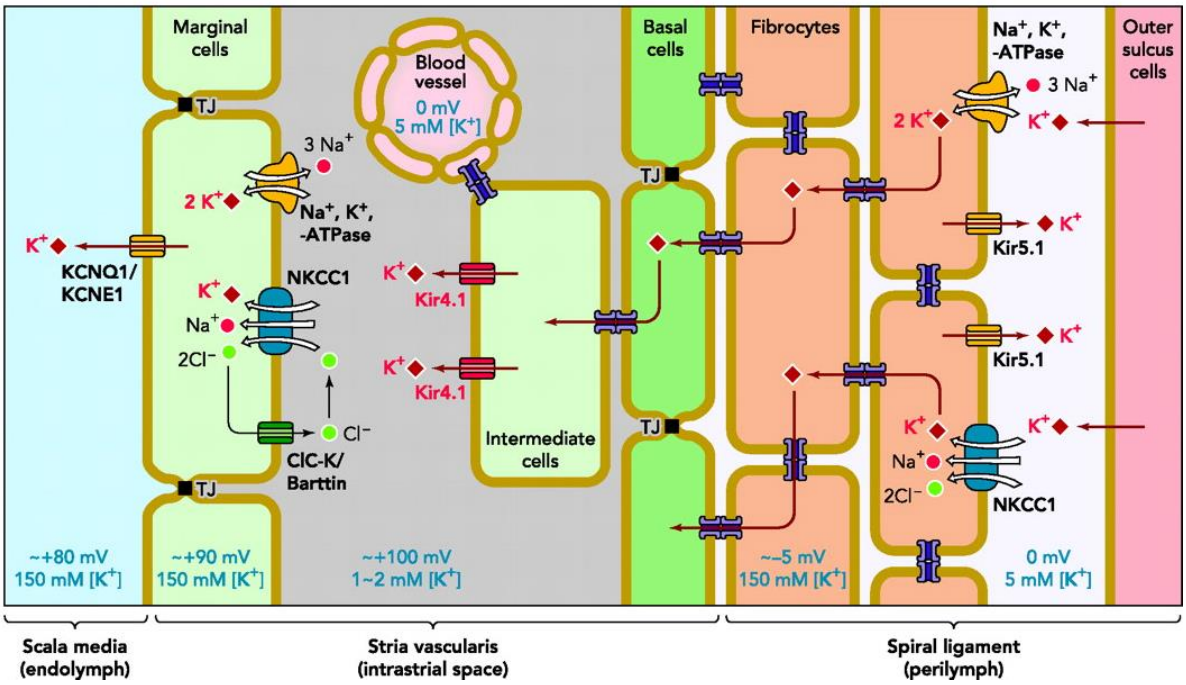

Figure 1.2 Model of cochlear potassium circulation and formation of EP in the lateral wall. Ion-transport expressed in the *stria vascularis* and the spiral ligament involved in potassium circulation. Fibrocytes of the spiral ligament receive potassium from the outer sulcus cells and uptake by the Na^+K^+ATPase transporter and the $Na^+K^+Cl^-$ cotransporter (NKCC). They also contain Kir5.1 inwardly rectifying potassium channels. Gap junctions enable the transport of ions from the fibrocytes to the basal cells, then to the intermediate cells which expel the potassium into the intrastrial space via Kir4.1 potassium channels. It is then actively taken up by marginal cells by transporters cotransporters before being released back into the endolymph ready for use again. NKCC1, $Na^+K^+Cl^-$ cotransporter. TJ, tight junctions. ClC-K/Barttin, Barttin activated chloride channels. KCNQ1/KCNE1, voltage-gated potassium ion channel complex. Taken from Hibino & Kurachi (2006).

Fibrocytes of the cochlear lateral wall are classified into different types based upon their ultrastructure, immunostaining patterns, and anatomical location (Spicer & Schulte, 1996). There are five types of highly specialised fibrocytes which vary in terms of their structural and functional roles (reviewed in Berrocal et al, 2008). Type II and V have been found to have higher levels of Na^+ K^+ ATPase so are believed to be involved in homeostasis (Mahendrasingam et al, 2011); type III are involved in water regulation and tension of the cochlea basilar membrane (Henson et al, 1984; Kuhn & Vater, 1997; Naidu & Mountain, 2007). These type III cells are most numerous in the basal region of the cochlea (Henson & Henson, 1988), and here they possess strong acto-myosin cytoskeletal elements. Type IV are primarily structural but also have some role in K^+ recycling, as do type I. Aiding their K^+ recycling function are the proteins they have been found to express (figure 1.2): the two transporters Na^+K^+ATPase (Schulte & Adams, 1989); $Na^+K^+2Cl^-$ (Crouch et al, 1997); and the Kir5.1 channel (Hibino et al, 2004). There are numerous other proteins and channels found to be expressed by SLFs.

Type I fibrocytes are lateral to the *stria vascularis*, type II below the *stria vascularis*, type III along the external edge of spiral ligament and are most prevalent in the most basal region of the cochlea (high frequency coding), type IV lateral to the basilar membrane and type V are above the *stria vascularis* (figure 1.3) (Spicer & Schulte, 1991; 2002; Weber et al, 2001). Type I, II and V fibrocytes, the intermediate and basal cells of the *stria vascularis*, are interconnected by gap junctions (reviewed in Berrocal et al, 2008). Type I fibrocytes connect via gap junctions to the basal cells of the *stria vascularis* and contain mitochondria in their membrane believed to provide energy required for ion transport. Type II exhibit Na^+-K^+-ATPase in their elongated cell body, where they take up K^+ ions from the roots which they release to type I fibrocytes through these gap junctions.

The use of the three marker proteins (AQP1, S-100 and α1Na-K-ATPase) can distinguish between all fibrocyte types, except II and V (Mahendrasingam et al, 2011a). S-100 is a calcium-binding protein present in a variety of tissues (Haimoto et al, 1987) and believed to be involved in the regulation of diffusion of cations across membranes, modulating membranes, and in regulation of phosphorylation of several proteins (Donato, 1986). It has been indicated that S-100 positive cells may have special functions as type I, II and V SLFs are strongly S-100 positive (Shi et al, 1992; Suko et al, 2000; Mahendrasingam et al, 2011a). AQP1 is a water-transporting channel protein involved in water and ion homeostasis (Carbrey & Agre, 2009), and is associated with the plasma membranes and cytoplasm. Aquaporin is expressed in all cells but six times stronger in type III cells than any other (Mahendrasingam et al, 2011a). The sodium potassium pump, α1Na, K-ATPase (Jorgensen, 1985), is highest in type II and V cells. This pump is membrane associated, however, despite the moderate expression in type III, it was indicated that there was also cytoplasmic labelling which was more evident in type III SLFs (Mahendrasingam et al, 2011a). It could be that the type III cells may be recruited to express this protein and function when other fibrocytes degenerate, as shown in some mouse models (Wu & Marcus, 2003; Mahendrasingam et al, 2011a).

Figure 1. 3 Spiral ligament and areas the five types of SLFs reside

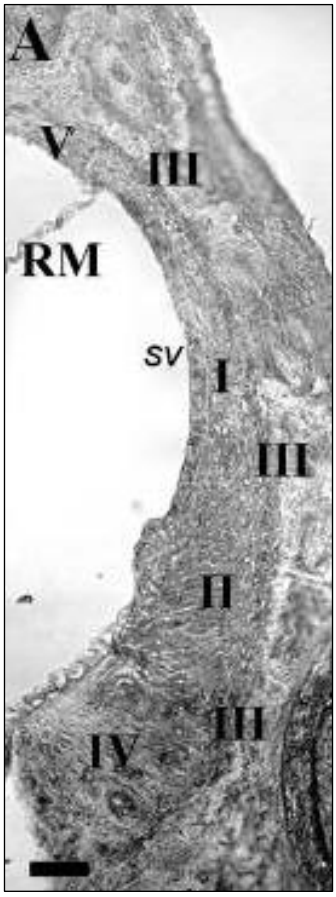

Figure 1.3 Transmitted light microscopy of spiral ligament in a midmodiolar plane. The locations of the different fibrocyte types (I-V), the Reissner membrane (RM), and stria vascularis are shown. Scale bar= 50 μm. Taken from Mahendrasingam *et al*, 2011.

1.3.2 *Stria Vascularis* Structure

The *stria vascularis* is composed of three cell layers, from medial to lateral: marginal cells, intermediate cells and basal cells (fig. 1.2). Basal cells are joined via gap junctions to intermediate cells and fibrocytes; however, unlike most sheets or epithelial cells, strial marginal cells are not coupled to each other or other cells by gap junctions (Kikuchi et al, 2000). As basal cells are connected to fibrocytes via gap junctions, all of these cells are involved in the connective-tissue gap junction network (CG-JN) which transports K^+ from type II and IV fibrocytes to intermediate and basal cells (figure 1.2) (Wangemann, 2002).

1.4 Role of Fibrocytes in maintaining the Endocochlear Potential

The difference in electrical potential between the interior and exterior of the fibrocyte network enables the movement of ions; normally this membrane potential difference is maintained between +5 and +12 mV *in vivo* (Nin et al, 2008; Adachi et al, 2013; Yoshida et al, 2015; 2016). The atypical characteristics of fibrocytes are crucial for maintaining the EP as their highly-positive resting membrane potential underlies a Kir4.1-mediated inwardly-rectifying potassium current that sets the EP to a highly positive value required for hearing. Both the EP and hair cell membrane potentials are driving forces in sensory transduction as the EP is essentially a potassium equilibrium potential generated by the potassium channel, Kir4.1, in the intermediate cells of the *stria vascularis* in conjunction with the low concentration of potassium of the intrastrial fluid and high concentration in the intermediate cells (Takeuchi et al, 2000; Marcus et al, 2002). Spiral ligament fibrocytes, which contain potassium uptake mechanisms, assist with the EP generation by the maintenance of a high concentration of potassium inside the intermediate cells (Schulte & Adams, 1989; Crouch et al, 1997; Mizuta et al, 1997).

1.5 Gap Junction Systems

There are two independent cell systems distinguished by interconnecting gap junctions which function in the recirculation of K^+ (figure 1.4). The first system is the epithelial cell gap junction system (EG-JS), consisting of organ of Corti supporting cells, interdental cells in the spiral limbus and root cells in the SL. The second system is the connective-tissue cell gap-junction network composed of the strial intermediate cells; strial basal cells, SLFs and mesenchymal cells (figure 1.2).

For the EG-JS, membranes of Deiters' cells facing the hair cells express K^+-Cl^- cotransporters. The voltage-gated $K_v7.4$ K^+ channel is a major pathway for K^+ to exit through OHCs which are predominantly present at the basolateral membrane of the hair cells (Kharkovets et al, 2006), and a BK Ca^{2+}-activated K^+ channel (Rüttiger et al, 2004; Navaratnam et al, 1997). The K^+ must be immediately removed from the hair cell surroundings as it would cause continuous depolarisation and affect normal excitability. From the hair cells the K^+ ions are expelled basolaterally and enter cochlear supporting cells, which once inside the supporting cells, move through the EG-JS network.

The CG-JN is expressed by fibrocytes which mediate the K^+ circulation from perilymph to endolymph (reviewed in Kikuchi et al, 2000). There is no cellular connection between outer sulcus cells and type II or IV fibrocytes, therefore K^+ exiting hair cells, is picked up by Deiter's cells and moves down its electrochemical gradient, passing through the CG-JN. It is at this point released to perilymph by the outer sulcus cells (Santos-Sacchi, 2000) and actively up taken by nearby type II and IV fibrocytes which are situated around the root cells within the lower region of the SL. Then this K^+ moves down its electrochemical gradient through type II and type I SLFs, and intermediate cells where it is released through K^+ channels directed into the endolymph (Shen et al, 2004), where they become available to the sensory hair cells again for sensory transduction, thereby maintaining the endolymph K^+ concentration.

Figure 1. 4 K^+ recycling pathways within the cochlea

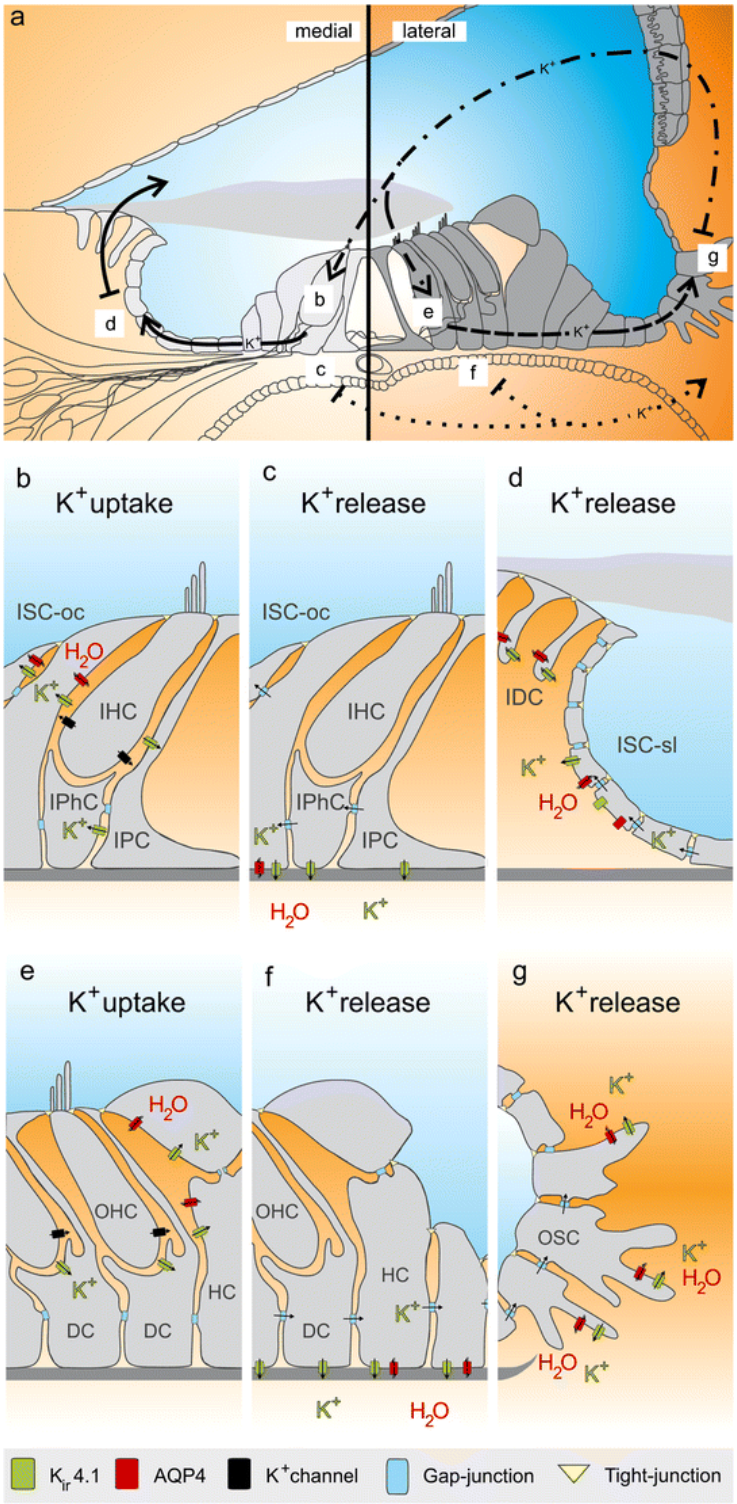

Figure 1.4 Endocochlear K+ recycling routes. **a** proposed K+ recycling routes in the medial (continuous black line: medial route) and lateral parts of the cochlear duct (dashed line: lateral route; dotted line: extraepithelial route). **b** Proposed K+ uptake by epithelial supporting cells **c** Proposed K+ release by the ISC-oc, the IPhC and the IPC. **d** Alternatively, K+ ions in the ISC-oc, IPhC and IPC may be funnelled into the inner sulcus cells of the spiral limbus (ISC-sl) via GJs. **e** The proposed K+ uptake by epithelial supporting cells that are adjacent to the OHC. **f** The proposed volume-equilibrated K+ release. **g** The concept of an intraepithelial lateral K+ recycling route postulates K+ flux into outer sulcus cells (OSC) via gap-junctions. Taken from Eckhard et al (2012).

1.6 Relationship between Types of Hearing Loss and Cochlear Structures

Schuknecht and Gacek (1993) described atrophy of the cochlea lateral wall as the main lesion in human temporal bones. However, Schuknecht and Gacek's (1993) temporal bone studies did not focus specifically in SL, since, more in-depth spiral ligament degenerative changes were investigated which revealed that degeneration of the *stria vascularis,* due to ageing, appears to be slower than that of the spiral ligament (Kusunoki et al, 2004).

1.6.1 Cochlear Conductive Hearing Loss

Conductive hearing loss is usually attributed to external or middle ear abnormalities. Computed tomography scans of the inner ear shows widened internal auditory canal with an incomplete separation of the basal turn of the cochlea from the internal auditory canal, and these inner ear abnormalities are believed to partly cause the conductive hearing loss in X-linked deafness type 3. When the increments of a threshold loss (reduced sensitivity to sound) present a gradually decreasing linear distribution pattern on the audiometric scale and have no pathologic correlate, it is thought the hearing loss is caused by alterations in the physical characteristics of the cochlear duct, and this hearing loss is cochlear conductive presbycusis (Schuknecht and Gacek, 1993).

1.6.2 Sensorineural Hearing Loss

Sensory neural hearing loss (SNHL) is defined by damage to the cochlear hair cells (the sensory hearing organ) or damage to the hearing pathways (nerves). It is not always possible to distinguish which part is damaged with this hearing loss, so is usually stated together as SNHL. Degeneration of the organ of Corti implies sensory presbycusis and loss of word

discrimination indicates neural presbycusis. SNHL results from lesions of the cochlea, VIII cranial nerve, and central auditory pathway.

1.6.2.1 Hair Cell Loss

The loss of sensory cells, supporting cells and neurons in the mammalian cochlea was generally believed to lead to permanent hearing loss as these cells are made only during embryonic development and not regenerated if lost from the mature inner ear so must last an entire lifetime (Ruben, 1967; Michaels, 1987). However, it was found in a guinea pig model that hair cells were replaced after loss induced by amino-glycoside treatment (gentamicin) as by 4 to 7 days most hair cells had been completely replaced by expanded surfaces of supporting cells and only a few degenerating hair cells remained (Forge, 1993). However this was not in the cochlea but the utricle and in very low numbers as after 4 weeks at the end of the treatment, immature hair bundles at different development stages were found in the utricle. These and other similar findings showed that *in vivo* hair cell regeneration in the mature mammalian ear can take place (Lowenheim et al, 1999).

1.6.2.2 Spiral Ganglion Neuron Loss

It has also been found in the CD/1 mouse that acoustic overexposure induces significant degeneration of the cochlear nerve despite the survival of hair cells (Riva et al, 2005; 2007; Kujawa & Liberman, 2009; Makary et al, 2011). Indeed, even where cochlear thresholds have returned to normal there can be up to a 50% loss of spiral ganglion neurons. Large neural degeneration appears to be a primary result of acoustic overexposure and not secondary to hair cell loss. Nevertheless, studies of outbred CD/1 mice displaying accelerated presbycusis have shown different possible causes of this hearing loss (Shone et al, 1991): one suggestion

being that spiral ligament damage precedes hair cell loss, with an endolymphatic K^+ concentration reduction (Wu & Marcus, 2003). It is predicted that fibrocyte degeneration could cause the organ of Corti pathology, later inducing hair cell and spiral ganglion damage (Mahendrasingam et al, 2011b). This damage due to spiral ligament degeneration and consequently *stria vascularis* degeneration could be the cause of K^+ recycling breakdown from the perilymph which surrounds the base of the hair cells, leading to hair cell death (Nouvian et al, 2003). This outcome is only avoided by the process of K^+ being continuously being pumped out of the perilymph, which is dependent upon fibrocytes and cells of the *stria vascularis*.

1.6.2.3 Hidden hearing loss

There are cases of hearing disabilities which display a normal audiogram, and animal experiments which show that noise exposure can cause cochlear neuropathy without affecting sensitivity to weak sounds. This selective neural loss is termed hidden hearing loss (Schaette & McAlpine, 2011). It is likely that individuals with an audiometric hearing loss due to noise exposure or aging have a hidden cochlear pathology. It was long thought that once hearing thresholds return to normal that the ear also would, however this is not the case. Causes of temporary threshold rises can induce irreversible damage to the auditory nerve fibres, which transmit sound information to the brain. This damage might not affect tone detection but the ability to process more complex signals, therefore may allow someone to detect sound but not make out what the person is saying (Liberman, 2015).

1.6.3 Strial/Metabolic Hearing Loss pathology

Strial/metabolic hearing loss is characterised by a decline of EP (Pauler et al, 1988; Gates et al, 2002). Kusunoki et al (2004) conducted a temporal bone study exploring the age-related histopathologic changes in the human cochlea, where compared to Schuknecht & Gacek (1993), they explored these changes in the lateral wall in more detail. Using 39 temporal bones from 24 subjects they found significant degenerative changes of the spiral ligament in the 9-18 year group compared to the 0-2 year group, but decreased areas of the *stria vascularis* only significant in 64-86 year group compared to the 0-2 year group.

In support of Schuknecht and Gacek (1993), work on hearing difficulties in the aging have shown that fibrocytes are progressively lost from the SL, a major pathology in presbycusis, suggesting their importance for auditory capacity (Wu & Marcus, 2003; Adams, 2009). The loss of function of these cells in the cochlear lateral wall can result in disruption of the ion and fluid homeostasis, causing a decline in the EP (Schmiedt, 1996). In this EP maintenance system, a collapse of the endolymphatic compartments occurs if the EP threshold point is not met and a failure of its generation follows (Schulte and Schmiedt, 1992; Friedmann et al, 1966; Wang et al, 2002).

Findings from quiet-aged and furosemide-exposed gerbils (reduced Na^+-K^+-Cl^- co-transport) demonstrated specific contributions of EP loss (Schmiedt et al. 2002) and was key in classifying audiograms and characterizing evidence for metabolic presbycusis (Schulte & Schmiedt, 1992; Gratton et al, 1997; Schmiedt et al, 2002; Schmiedt 1996; 2010). Audiogram patterns from OHC losses due to exposure to noise and drugs are different from those due to chronic EP decline in metabolic presbycusis.

A model of cochlear lateral wall degeneration was performed by applying furosemide as described previously (Lang et al, 2010). This caused a loss of strial intermediate cells and cochlea lateral wall oedema, hence a chronic reduction in EP (Schmiedt et al, 2000). However, this model did not show the characteristic pathological alterations in hair cells and neurons that occur with age as their morphology appeared normal. It was found spontaneous activity of auditory neurons was significantly lower in the furosemide-treated gerbil models, similar to aged gerbils raised in a quiet environment which show a decline in EP and elevated auditory nerve compound action potential (Lang et al, 2010). This suggests that the chronic reduction in the EP induced by cochlear lateral wall dysfunction has a direct effect on the activity of primary auditory neurons similar to that seen in aged gerbils and therefore responsible for much of the hearing loss in metabolic presbycusis.

Nevertheless, some mice strains, such as SAMP1 and C57BL/6 (B6) mice are found to undergo age-related strial and spiral ligament degeneration that is not linked to EP reduction (Ichimiya et al, 2000; Di Girolamo et al, 2001; Hequembourg & Liberman, 2001; Lang et al, 2002). These studies find little changes in EP in aged animals in contrast to other studies, as well as significant degeneration of SLFs prior to that of cochlea hair cells and neurons and this evidence will be explored later in this chapter. It is possible these fibrocytes in the spiral ligament have more to do with trophic factors or K^+ recycling associated with the generation of the silent current than they do with the production of the EP.

Metabolic hearing loss in animals is not necessarily a sensory loss, but results in raised pure-tone thresholds as the gain of the cochlear amplifier is reduced, particularly at higher frequencies. Differences have been found in the lower frequency thresholds for metabolic and sensory phenotypes which averaged 16.5 dB better for sensory than metabolic phenotypes

(Dubno et al, 2013). A hypothesis for the differences is in sensory losses OHC loss cause the reduction of transduction currents (Salt & Konishi, 1979), which reduces the load on the EP generator causing a higher cochlear EP. Additionally, it has been found that the cochlear base is where the EP is most efficiently generated (Wu & Hoshino, 1999) consistent with OHC lesions location in the sensory phenotype. This suggests sensory loss could disguise metabolic loss until significant strial degeneration.

1.7 Evidence of Fibrocyte Involvement in Presbycusis

Wright and Schuknecht (1972) studied spiral ligament morphology in 151 human temporal bones and found age related changes in all samples, which were most significant in the middle and apical turns. Furthermore, a decreased hearing threshold was found in 15 ears with spiral ligament atrophy (shrinking), and in these individuals, the hearing loss was more severe than expected when compared to the limited amount of hair cell and ganglion cell loss. Later, Schuknecht et al (1974) affirmed that four pathologic types of presbycusis are valid, finding out of 101 individuals with presbycusis: 12 had sensory hearing loss, 31 neural, 35 strial (metabolic), and 23 mechanical, therefore proving a significant number of cases of human hearing loss are metabolic. Based on findings, is it reported that many individual cases do not separate into a specific type but possess a mixture of these pathologic types and are termed mixed presbycusis, hence why some believe SNHL is considered most common (Schuknecht & Gacek, 1993). It was then proposed that noise-damaged ears do not ‘age’ at the same rate as ears without evidence of noise damage, therefore, the effect of age is overestimated to do with sensory (Gates et al, 2000).

It has been found that in a C57BL/6 inbred mouse model of presbycusis, that fibrocyte loss precedes significant hair cell loss (Hequembourg & Liberman, 2001). In two cochlear spiral ligament locations, (part of the upper basal turn and the middle of the second turn) there was severe type IV cell loss by just 3 months of age. The SLFs loss extended further apically than the OHC loss, and even up to 7 months of age there was a scarce amount of hair cell loss. The auditory brain stem response (ABR) is an auditory evoked potential in the brain recorded by electrodes and used to determine the ability of one's hearing. It has been shown that fibrocyte loss with age reflects the ABR threshold loss with age, therefore the ABR threshold shift up to 7 month cannot be the result of a loss of hair cells as this loss was minimal (fig. 1.5). The timeline of the decreasing ABR threshold closely resembles that of the degeneration of type IV fibrocytes (fig. 1.5); this could mean the threshold shift could be due to the reduction in EP caused by the loss of these fibrocytes (Hequembourg & Liberman, 2001).

Figure 1. 5 Graph showing the age-related changes in cochlea structures

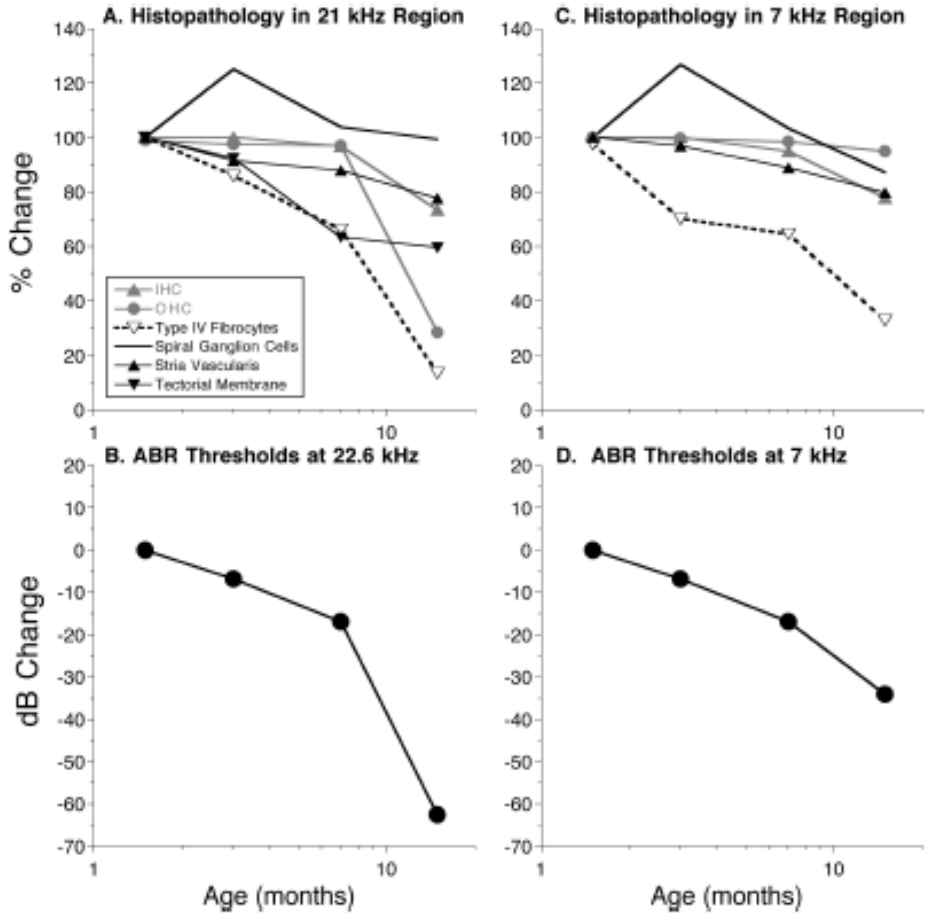

Figure 1.5 Age-related changes in structures of the cochlea C57BL/6 inbred mouse strain. Changes seen in the upper basal turn to about 21kHz(A) or middle of the second turn to about 7kHz(C) compared with the age-related threshold shift at the test frequencies for each region (B and D). Type IV fibrocyte loss after 3 month and no hair cell loss until after 7 month (A and C). Type IV fibrocytes decrease by ~90%, OHC by ~70% and IHC by ~30% in region A. In region B type IV fibrocytes decrease by ~70%, OHC is minimal (~2%) and IHC by ~20%. Changes in ABR thresholds most closely mimic the degeneration patterns of type IV fibrocytes. Taken from Hequembourg & Liberman (2001).

Significantly, this research suggests that as the early-onset degeneration of the type IV fibrocytes occurs, cochlear ion homeostasis is disrupted (*stria vascularis* K^+ recycling), causing an EP reduction. The reduction in EP reduces both the sensitivity and frequency selectivity of hair cells and auditory nerve fibre tuning curves (Evans & Klinke, 1982; Brown et al, 1983; Nouvian et al, 2003). These findings were later supported where the relative time course of degeneration of different cochlear structures in the CD/1 mouse model of

accelerated ageing were investigated (Mahendrasingam et al, 2011b). The outbred CD/1 mouse strain exhibits hearing loss at about 4 weeks, prior to hair cell loss, and display an age-dependent high frequency sloping loss that progresses to a total hearing loss at all frequencies by 24 weeks of age (Shone et al, 1991, Le Calvez et al, 1998, Riva et al, 2005). It was shown that SLFs consistently begin to degenerate and show mitochondrial changes before 3 weeks postnatal, with type II and IV fibrocytes being the most likely to degenerate (Mahendrasingam et al, 2011b). They suggest mitochondrial degeneration could cause functional loss before actual loss of fibrocytes; therefore, the fate of the hair cells is dependent on the fibrocytes that regulate the removal of K^+ from the perilymph highlighting the importance of fibrocytes in auditory transduction (Mahendrasingam et al, 2011b). Together these findings show fibrocyte loss precedes hair cells and/or neuron loss and may be accountable for the loss of sensory cell degeneration and consequently reduced hearing levels.

An important and interesting property of cochlear fibrocytes is that they are present in the mesenchymal nonsensory regions of the cochlea therefore have the capacity for self-renewal whilst maintaining their multipotency. After damage caused by either noise or drug exposure in the inner ear, SLFs are able to repopulate themselves unlike sensory cells (Hirose & Liberman, 2003), although the continuous production of these cells is not sufficient to prevent presbycusis in CD1 mice where the hearing loss is caused by a decrease in EP (Lang et al, 2002). However, loss of fibrocytes from the spiral ligament of humans starts at a young age and progressively increases with age. The replacement or regeneration of mesenchymal cells and fibrocytes of the inner ear is an ideal target for a new therapeutic strategy, an area which has been neglected.

There is some research that links the natural repopulation of fibrocytes and hearing recovery. One example is from a fairly recent study that found, when comparing 15 P6 mice to 6 noise-exposed P28 mice, that noise-damaged mice the number of type III SLFs did not alter, in comparison to the loss of the other fibrocyte subtypes, and these type III fibrocytes increased from day 1 to 14 after noise exposure, (Li et al, 2017). Also the cells repopulating in the type I area, where the cells diminished profoundly after the noise damage, were positive for type III markers and a marker for proliferation. This study suggests type III SLFs possess the regeneration capacity as opposed to other fibrocyte types and may contribute to endogenous regeneration of the lateral wall SL. Therefore, type III cells may potentially be the key to regenerative therapies.

Other research has investigated changes in the EP using a mouse model of acute cochlear energy failure, comprising severe cochlea lateral wall damage by 3-NP (Kitao et al, 2016). They detected recovery of the EP and hearing function at lower frequencies after damage of cochlea lateral wall fibrocytes as they observed the re-expression of Na^+K^+ATPase-β1 in regenerated fibrocytes. The results indicate a mechanism for late-phase hearing recovery after severe deafness, often observed in the clinical setting. This is consistent with previous work that found histological analysis indicated that after 3-NP-treated ear damage, the lateral wall fibrocytes spontaneously recover and the re-expression of Na^+K^+ATPase-β1 occurs in these cells in the cochlea 2 month after 3-NP treatment (Mizutari et al, 2011).

Mechanisms underlying the decline of SLFs remain poorly understood. There may be a potential correspondence between mitochondrial damage and susceptibility of SLFs. Their degeneration is believed to be caused by features of energy depletion, shared by mitochondrial dysfunction, oxidative stress and ischemia (Fujinami et al, 2010). There are animal models in which fibrocyte degeneration is due to a molecular defect involving primarily fibrocytes showing severe ultrastructural alterations, with relatively few structural

alterations in the neurosensory epithelium (Minowa et al, 1999, Xia et al, 2002, Mahendrasingam et al, 2011b). The lack of mitochondrial damage seen in hair cells, and weak levels detected in spiral ganglion neurons suggests there is a tissue-specific difference as well as a genetic susceptibility. It could be that in the spiral ligament, the higher energy demands result in greater damage to susceptible mitochondria through generation of large amounts of free radicals (Seo et al, 2010).

1.8 Treatments for Hearing Loss

The options currently available for the treatment of presbyacusis are limited and consist mainly of prosthetic devices such as hearing aids and cochlear implants (Jongkamonwiwat et al, 2010). For hearing impairments, especially presbycusis, hearing aids can offer significant improvements; however there is no universal benefit. For those with severe hearing loss a better therapeutic option may be cochlear implantation (reviewed in Hildebrand et al, 2008).

1.8.1 Cochlear Implant

Cochlear implants are devices that bypass the organ of Corti and supply electrical stimulation directly to the auditory nerve to mimic the functional properties of the cochlea (Kral & Sharma, 2012). There has been great success with the use of cochlear implantation as 200,000 hearing impaired individuals use them worldwide with most being able to differentiate speech and interpret rudimentary auditory input (Kral & O'Donoghue, 2010). However, despite the success of cochlear implantation, they have some limitations. Outcome differences across subjects in terms of accuracy of auditory cues transmitted by these implants (Brown et al, 1990; Zeng, 2004), as well as electrode placement impact upon the success of cochlear implant outcomes (Finely & Skinner, 2009). The role of electrode placement as a contributor to the differences in the outcomes in cochlear implant was examined and found the location

positioning and depth of the electrode were contributory to the success as lower outcome scores in word recognition task were associated with greater insertion depth and number of contacts being located in the *scala vestibuli* (Finely & Skinner, 2009).

Critical periods in the development of the auditory system also play a role in the success of the implants. Cochlear implantation during the first 3-4 years of life is the most optimal for treating hearing impairments as this is when central auditory pathways show maximal plasticity in response to auditory stimulation. If cochlear implantation is conducted at the end of this critical period, around 6.5-7 years, it results in the reorganisation of cortical areas and pathways (Kral & Sharma, 2012). It was also found that implantation after this critical period caused abnormalities in cortical auditory evoked potentials (CAEPs) thought to result from the functional re-organisation of the cortex (Gilley et al, 2008). One drawback of this is that introducing a new sensory stimulus also introduces new competition for cortical resources, another is the suggestion that the activity in cortical areas observed in children with late implants may have lasting implications for multisensory processing; although this functional relationship is still not clear (Gilley et al, 2008). It was suggested that sensory deprivation compromises learning, which adds to the concept of a sensitive period for recovery in the auditory system within the first 4 years of life (Kral & Eggermont, 2007). Essentially this means that cochlear implantation would be less effective for treating presbycusis as this occurs mainly in older individuals.

An additional problem with this approach is that during cochlear implantation surgery, an electrode is inserted into the *scala tympani* which can often cause mechanical trauma due to disruption of delicate cochlear structures. The mechanisms behind this trauma and residual hearing loss are uncertain, but are thought likely to involve changes in EP that could be the result of spiral ligament and *stria vascularis* injury or due to perilymph and endolymph mixing (Takeuchi et al, 2000; Hequembourg & Liberman, 2001; Wangemann et al, 2004). A

characteristic pattern of cochlear lateral wall and basilar membrane damage in the upper basal turn of the cochlea in individuals who received implants has thought to be related to electrode trauma (Nadol, 1997). Furthermore, it is suggested that mechanical injury to the spiral ligament may cause degeneration of fibrocytes (Bas et al, 2012), and that the loss of these cells may alter the EP and lead to auditory hair cell death (Hequembourg & Liberman, 2001).

1.8.2 Gene Replacement Therapy

Gene therapy has been advocated as a possible way to treat hearing loss. This is where a gene is introduced and used to replace a faulty gene or activate a gene that is switched-off. It was found that inhibiting caspase proteins that play a central role in the apoptosis of cells promotes hair cell survival after treatment with streptomycin, a cochleotoxic and vestibulotoxic aminoglycoside, a molecule that inhibits protein synthesis (Matsui et al, 2003). This followed on from earlier work which found that in the gerbil cochlea the suppression of the expression of the bcl-2 protein may cause apoptosis-induced presbycusis by caspase-3 activation (Alam et al, 2001). These findings suggest inhibiting apoptosis may protect cells affected in presbycusis.

The first gene found to induce age related hearing loss-like pathology was *ahl* in C57 mice (Willott et al, 1998; Hequembourg & Liberman, 2001). It was revealed this *ahl* gene codes for cadherin 23, a protein part of the tip link in the stereocilia of hair cells (Di Palma et al, 2001). It was later shown to be a primary determinant of presbycusis (Noben-Trauth et al, 2003). However, it was shown only to increase susceptibility and not be the only cause as other genetic factors are believed to be involved. If a person's genes may predispose them to presbycusis it suggests a model that can be explored using cell-based therapies.

The development and differentiation of hair cells in the developing cochlea is regulated by the expression of a gene called *Atoh1*. Knockout mice lacking this gene fail to produce hair cells

during development (Chen et al, 2002). It was found that cellular and functional repair of the organ of Corti in a mature deaf mammal occurred following the delivery of the *Atoh1* gene to the inner ear by virus-mediated gene therapy (Izumikawa et al, 2005). This technique provides the ability of a virus carrying a gene to attach and enter a target cell, successful transfer to the nucleus, enabling stable expression in the nucleus, and a lack of toxicity (Izumikawa et al, 2005). Their findings showed that treatment with *Atoh1* results in the generation of new hair cells and significant improvement of auditory brain stem responses by restoring their functional thresholds.

However, one of the major limitations of virus-mediated gene therapy is the delivery of the virus to all cochlear spiral regions as this would require multiple injections at many different locations and increase the risk of additional damage. Also other supporting cells outside of the organ of Corti took up the *Atoh1* gene causing ectopic hair cells to develop which would not be effective in re-establishing auditory function (reviewed in Cotanche, 2008).

The presence of ectopic hair cells has been found to be associated with severe hearing loss (Chen et al, 2003). Overall, this delivery of Atoh1 in an adenovirus to the adult damaged cochlea revealed some hair cell differentiation, but the number of was unclear and the new hair cells could not be traced from their precursors which caused difficulty in identifying "new" hair cells and those recovered from damage due to toxin or noise.

Later, significant hair cell regeneration was demonstrated in a mammal by y-secretase inhibitor treatment in a damaged cochlea (Mizutari et al, 2013). Their approach of a caspase-3 mouse allowed a model in which hair cells could be killed without damaging other cells so new hair cells could be quantified. This *in vivo* treatment produced partial recovery after noise-induced hearing loss. Labelling revealed hair cell regeneration that resulted from transdifferentation of supporting cells. This finding of transdifferentation has led to the

development of a gene therapy consisting of virus-delivered *Atoh1*, tested in a clinical trial, the goal being to assess if inner ear fusion of CGF166 is safe and effective as a treatment for hearing loss. This therapy will not help those with inherited hearing loss where there is damage to the auditory nerve or missing structures, but it might help those with acquired hearing loss through drug and noise damage and aging (Actiononhearingloss.org.uk).

1.8.3 Stem Cell Therapy

Another experimental approach for inducing regeneration in the mammalian cochlea is to introduce cells to replace dead or dysfunctional ones and integrate them into the damaged sensory epithelium (reviewed in Cotanche, 2008). Using stem cells to replace hair cells or spiral ganglion neurons is less advanced, though it is still being explored (Liu et al, 2012; Su et al, 2014; Atkinson et al, 2015; Burns & Stone, 2017; Samarajeewa et al, 2018). Although work on the development of stem cell replacement has been significant, the research is still in its infancy and strategies to examine longer survival times or ways to direct stem cells to the cochlea still need to be determined. The main obstacles related to the use of stem cells are: 1) finding a suitable area of the cochlea to access; 2) ensuring that the transplanted cells survive, integrate and mature properly; and 3) finding ways to ensure that the stem cells do not become tumours (Oshima et al, 2010). The superficial location of fibrocytes within the lateral wall makes them suitable to replacement by cellular transplantation

Transplanted neural stem cells into the *scala tympani* of mice and guinea pigs 2 days after noise exposure produced fewer stem cells in the cochlea than in the nerve (Parker et al, 2007). Interestingly, cells that penetrated the cochlear lateral wall showed morphological, protein and genetic characteristics of cochlear-specific cells, such as IHCs and OHCs, pillar cells, Deiter's cells, fibrocytes and *stria vascularis* cells. Neural stem cells normally express myosin 7a (a mechanochemical protein and specific cochlear hair cell marker) when they are cultured in

differentiating conditions *in vitro*. Neural stem cells localised to the spiral ganglion, spiral ligament and spiral limbus expressed myosin 7a, while in these areas endogenous cells do not express it. This could be due to the limited ability of the neural stem cells to completely differentiate into cochlear-specific cells types and therefore form ectopic cells.

Since then, human embryonic stem cells (hESCs) have been used to develop a cell-based therapy for deafness (Chen et al, 2012). Two types of otic progenitors were attained, capable of differentiating into hair cells and auditory neurons *in vitro* that exhibited the electrophysiological properties expected. The differentiation potential of otic epithelial progenitors (OEPs) and otic neural progenitors (ONPs) were tested using 'neutralising' and 'hair-cell' culture conditions. The OEPs produced hair-cell-like cells which expressed an outward K^+ current, inwardly rectifying K^+ current and inward Ca^{2+} current. The ONPs produced neurons showing a delayed-rectifier K^+ current and Na^+ current and provoked single action potentials. To explore properties of ONPs *in vivo* a toxic model of neuropathic deafness was used where these cells were transplanted into ouabain-treated gerbils (Chen et al, 2012). Ouabain was applied directly to the round window which selectively damages type 1 spiral ganglion neurons and preserves hair cells and the organ of Corti. Once the ONPs were transplanted, after 2-3 weeks, five out of six animals had surviving transplanted cells grafted in the modiolus, forming an ectopic spiral ganglion and after 10 weeks it was still present but cells had also migrated into the Rosenthal's canal. The projections reaching the organ of Corti were targeting hair cells and in the transplanted animals there was a significant functional improvement in ABR thresholds of 46%. The cells were able to survive at least 3 weeks after transplantation; however, their impact on hearing was not assessed. The replacement of hair cells may not be an effective method for combating presbycusis. Despite the findings described, it was suggested that even though hair cells are functional, age-related metabolic

degenerations in the cochlear lateral wall can result in significant declines in cochlear responses (Saremi & Stenfelt, 2013).

A rat animal model of hearing loss caused by cochlear energy failure through the application of the mitochondrial toxin 3-nitropropionic acid (3NP-an inhibitor of an enzyme of the mitochondrial electron transport chain) revealed pathological changes in fibrocytes in the lateral wall and spiral limbus initially (Kamiya et al, 2007). There were no signs of significant organ or Corti or spiral ganglion damage, indicating pathology of metabolic hearing loss. They used levels of 3NP that would induce a temporary threshold shift to explore the result of transplanted mesenchymal stem cells (MSCs) into the semi-circular canals and revealed significantly enhanced hearing recovery. The outcome was complete hearing recovery at low frequencies, but residual hearing loss remained at higher frequencies. The MSC in the cochlear lateral wall showed connexin 26 and connexin 30 immunostaining indicative of gap junctions; however, connexin 30 staining was very weak in the apical region of the lateral wall and the cells did not show the staining pattern at contact sites with neighbouring fibrocytes that would indicate gap junction connections. This contact site staining pattern was also not clearly seen in connexin26 staining (Kamiya et al, 2007).

Moreover, the nuclei of some of the MSCs were small and irregular, and the cells were found to express connexins in the nucleus and cytoplasm as well as in the cell membrane. These connexin proteins were not expressed in the nuclei of normal cochlear fibrocytes which suggest they were not completely differentiated as cochlear fibrocytes or were an artefact due to the procedure or mitochondrial toxin model. This toxin model represents *artificial* damage to the lateral wall and does not represent any known ageing cochlear pathologies. This may mean that the hearing recovery could be due to the natural regeneration capacity of fibrocytes and not the MSCs, therefore it is questionable whether this model represents the natural ageing process of fibrocyte loss.

Additionally, the uptake of these cells was limited and they were dispersed throughout multiple locations and were not contained within the spiral ligament as they would be natively. More recently a study examined MSC transplantation into the semi-circular canals in mice with the intention to stop/delay hearing loss by transplanting before hearing ability and auditory pathways are fully mature (Kasagi et al, 2013). They found through the use of immunofluorescence for connexin26 that in young mice (of 2 to 3 weeks), engrafted MSCs migrated towards the cochlear lateral wall and differentiated into suspected type II and V fibrocyte-like cells due to the intense connexin26 labelling in the regions of the spiral ligament where these fibrocyte types reside (fig. 1.6). Interestingly this had no effect on auditory function. Moreover, in the adult mice (24-26 weeks) there was no detected migration or differentiation in transplanted cells (fig. 1.6).

This was the first time 'types' of fibrocytes differentiated from MSCs transplantation were identified. However, major a limitation of these studies is that the immunostaining for connexins (26 and 30) were the only markers used which they believed to represent SLFs. Although Connexin 26 is expressed mainly by type I fibrocytes in the cochlear lateral wall (Kikuchi et al, 1995) both connexin26 and connexin30 are widely expressed in the supporting cells of the sensory epithelium as well as fibrocytes of the SL, spiral limbus and *stria vascularis* (Kikuchi et al, 1995; Lauterman et al, 1998; Ahmad et al, 2003). This means the staining found in this study may not only represent SLFs but cells of the organ of Corti. Additionally, the immunostaining for these connexins were mainly detected in the cytoplasm and surrounding cells where MSCs attached to the cochlea, therefore where not detected in the membrane of the cells as they would be natively. Collectively, these findings are not conclusive in the differentiation of MSCs into SLFs after transplantation into the semi-circular canals due to an inaccurate representation of cochlear degeneration pathology or indefinite detection of SLFs due to unspecific immunostaining.

Figure 1. 6 Immunohistochemistry of the connexin26 gap junction protein.

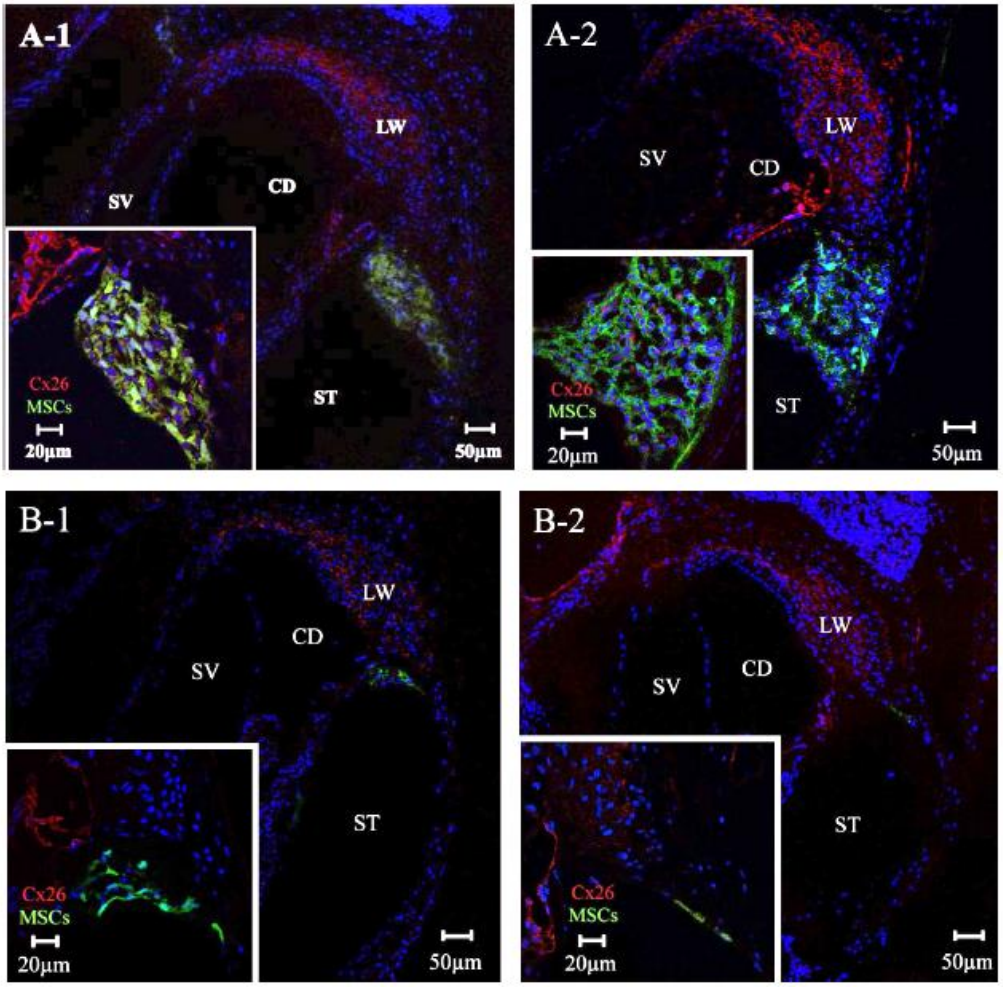

Figure 1.6 Immunohistochemical analysis of gap junction protein Cx26. (A-1) one week after transplantation Cx26 was expressed in the cytoplasm and surrounding cells, where MSCs attached to the cochlea in the young group. (A-2) 2 weeks after transplantation Cx26 was expressed in the cytoplasm and surrounding cells, where MSCs attached to the cochlea in the young group. (B) Cx26 was not detected in the adult group. *Stria vascularis*: *scala vestibuli*; CD: cochlear duct; ST: *scala tympani*; LW: lateral wall. Taken from Kasagi et al (2013).

To identify the mechanism of SLF repair and the impact of transplanted MSCs the mutual effects on differentiation and proliferation between the two in a co-culture system was examined (Sun et al, 2012). Under typical culture conditions MSCs did not express markers for SLFs, but when they were plated on collagen-coated dishes a small group of the MSCs differentiated into SLF-like cells. In the initial MSC cultures, no cells were positive for Na^+

K^+ ATPase β1 expression. When the cells were plated on collagen-coated dishes, SLF condition medium addition increased this Na^+ K^+ ATPase β1 expression compared to cultures without the conditioned medium.

This suggests that transplanted MSCs in the damaged spiral ligament may induce regeneration of SLFs, and consequently promote hearing recovery (Sun et al, 2012). Whilst it has yet to be shown whether transplanted MSCs *in vivo* transdifferentiate into SLF-like cells, the results suggest hearing recovery following inner ear MSCs transplantation occurs by two mechanisms which contribute to damaged SLF functional recovery. Firstly MSCs transdifferentiate into SLF-like cells that attempt to replace the lost SLFs and secondly transplanted MSCs induce the proliferation and regeneration of host SLFs.

1.9 Problems with Cell Replacement Strategies

Cell therapies such as stem cell replacement have many advantages over drug and gene therapies. It is generally understood that replacement, repair and restoration of function is achieved best by cells that fulfil the most appropriate physiological/metabolic role better than any mechanical device, recombinant protein therapeutic or chemical compound (reviewed in Fodor, 2003). The most advanced and successful cell replacement strategies are autologous cell therapies such as those involved in the treatment of burns with autologous cultured keratinocytes (Carsin et al, 2000). Use of autologous retinal pigment epithelial cells for treating age-related macular degeneration is an area explored and it has been demonstrated that transplantation of these cells improved visual acuity in 57% of patients with age-related macular degeneration (Binder et al, 2002; Semkova et al, 2002). Such success provides proof-of-principle of cell replacement therapies in age-related cellular degeneration processes.

Although cell replacement strategies- at least superficially- seem very persuasive they still have limitations, the obvious one being that a surgical procedure is required to collect host

cells, and this introduces the possibility of secondary complications. Ideally this damage would be minimal or reduced to a much lesser extent than the pre-intervention disorder (reviewed in Fodor, 2003). In a clinical setting these cells could be taken from the same patient avoiding the rejection of the foreign cells after transplantation. In other models of hearing loss, transplantation has accelerated natural repair after ototoxic insult (Kamiya et al, 2007; Sullivan et al, 2011), but this has not been done in models of presbycusis.

Many studies have shown viability and survival of ESC cells in the inner ear, but few demonstrate the differentiation and regeneration of endogenous cell types. It has been found that the survival rate of pre-differentiated cells (13.6%) was greater than that of undifferentiated cell types, suggesting the pre-differentiation and targeted delivery of progenitor cells is a more successful cell-based therapy for treating hearing loss (Corrales et al, 2006).

Moreover, during the initial cell culture period, some cultured cells can become senescent or even de-differentiated (reviewed in Fodor, 2003). But since fibrocytes are mesenchymal in origin and possess the innate ability to differentiate, this allows the functional characteristics of fibrocytes to be identified in order to determine whether they would be suitable candidates for transplantation.

For a cell replacement therapy to achieve functional restoration a number of criteria needs to be fulfilled: generation of a sufficient number of cells to reverse the defect; the correct differentiation of cell phenotype; three-dimensional structure formation; cells produced that are mechanically and structurally the same as the native cells; and transplanted tissue integration with native tissue without rejection (Vats et al, 2002). Fibrocytes are ideal for cell replacement strategies given their critical role in the hearing process by maintaining the EP. In order for hearing restoration to be possible, the transplanted cells need to possess all of the

functional characteristics of the native cells they will replace, specifically, transplanted cells must mimic native fibrocytes.

1.10 Established spiral ligament fibrocyte cultures

In vitro culture studying is a useful and effective technique in the search for factors that cause disruption of SLFs. Critically inner ear spiral ligament cells can be isolated and maintained in secondary culture whilst retaining many of their *in vivo* characteristics (Gratton et al, 1996). Cochlear fibrocytes can be successfully cultured *in vitro* where the most common fibrocyte type to be identified in culture is type I (Gratton et al, 1996; Suko et al, 2000; Ichimiya et al, 2000; Liang et al, 2003; Shen et al, 2004) enabling the exploration of certain protein expression and ion channel physiology (Liang et al, 2004; Shen et al, 2004; Liang et al, 2005). Also cultures of type III (Kelly et al, 2012) and type IV (Qu et al, 2007) fibrocytes have been identified. However, issues related to the identity of the type I cultures have surfaced from Gratton et al's (1996) initial characterisation of fibrocytes grown in culture. Many researchers based their identification of type I fibrocyte-containing cultures on these early observations and incorrectly showed negative labelling for the Na^+ K^+ ATPase. Indeed, the presence of the Na^+ K^+ ATPase is now believed to be a characteristic of type I fibrocytes, though not to as great an extent as type II fibrocytes (Mahendrasingam et al, 2011a).

There are a range of proteins that have been identified in cultured fibrocytes, including gap junction connexins (Kasagi et al, 2013; Yamaguchi et al, 2015), BK channels (Liang et al, 2003; Shen et al, 2004), Ca1.2 calcium channels (Liang et al, 2004), chloride channels (Que et al, 2007), glutamate-aspartate transporters (Furness & Mahendrasingam, unpublished) and otospiralins (Zhuo et al, 2008). However, there is some discrepancy between the complement of proteins expressed in native SLFs and those expressed in cultured fibrocytes, as well as the

ionic conductance properties involved in potassium recycling in the cochlea that require these key proteins.

1.10.1 Expression profile

Numerous proteins and transporters have been identified in native and cultured SLFs. Otospiralin (*Otos*) is found to be involved in the functionality of fibrocytes (Delprat *et al*, 2005), using a mouse model with *Otos* deletion indicated that a lack of otospiralin causes fibrocyte alterations and hearing impairment. Damage to the mesenchymal spiral ligament and spiral limbus fibrocytes was the only histological abnormality observed in the 21 day old *Otos*-/-mice as histopathology revealed degeneration of type II and IV fibrocytes, whilst the hair cells and *stria vascularis* appeared normal establishing that fibrocyte degeneration precedes hair cell degeneration (Delprat et al, 2005). Also since cytoplasmic alterations predominate in the fibrocytes that produce otospiralin, being type II in the spiral ligament and some spiral limbus fibrocytes, this suggests the lack of otospiralin has a direct effect on these fibrocytes, and consequently cochlear physiology contributing to age-related hearing loss.

GLAST (glutamate aspartate transporter) is a transporter protein found to be localised in lateral wall fibrocytes and has been localised to types of fibrocytes (Hakuba et al, 2000; Jin et al, 2003). *In vivo* GLAST undertakes the function of transport of glutamic and aspartic acid. Type II and V are involved in cochlear glutamate homeostasis with type V containing the most glutamate in the lateral wall. The lateral wall of a CD/1 mouse expressed most GLAST (38%) compared to the SG (35%) and organ of Corti (27%) (Furness et al, 2009). These findings suggest that a functional mechanism for glutamate transport exists in lateral wall fibrocytes (Furness et al, 2009). Immunocytochemistry and electrophysiology was used to assesses D-aspartate (a glutamate analogue) uptake and GLAST expression where D-Aspartate accumulated into GLAST expressing fibrocytes *in vitro* and evoked currents blockable by the

GLAST inhibitor D,L-threo-β-benzyloxyaspartate (TBOA, Furness et al, 2009). The currents were strongest in spiral limbus fibrocytes, lower in type V and type II, and negligible in type I fibrocytes consistent with GLAST expression levels. Hair cells are sensitive to glutamate induced damage therefore the importance of the role of fibrocytes in the transport of glutamate is crucial to cochlear functioning. Since then, the presence of GLAST in the human cochlea has been demonstrated in SLFs (Ahmed et al, 2013).

Cultured SLFs have also been found to express connexins, gap junction proteins, as do native SLFs. Connexin26 (Kasagi et al, 2013), connexin30, and connexin43 have been detected in cultures, with connexin43 having the highest level (Yamaguchi et al, 2015).

Moreover, potassium channels have been identified in cultured SLFs as it has been reported that cultured type I SLFs have a dominant K^+ membrane conduction mediated by BK channels (Shen et al, 2004). They reported that the averaged half-maximal voltage-dependent membrane potential for whole-cell currents was 70+/-1.2mV at 1nM intracellular free Ca^{2+} and shifted to 38+/-0.2mV at 20 mM intracellular free Ca^{2+}. This BK channels activity imparts to neurons biophysical properties similar to those of potassium inward rectifiers in cardiac myocytes, enabling the cells to maintain their membrane potential whilst conserving intracellular K^+ (McManus et al, 1995; Wallner et al, 1999; Brenner et al, 2000). This suggests that BK channels are involved in the maintenance of the membrane potential of type I SLFs and points towards them possessing a crucial role in the generation and regulation of the electrochemical gradient in the lateral wall, known to be vital to K^+ recycling (Wangemann, 2002).

Intracellular free Ca^{2+} levels are critical to the activity of BK channels in type I SLFs of the inner ear. The voltage dependent L-type Ca channel present in type I SLFs (Cav1.2 channel) has also been found in type I SLF cultures using the patch-clamp technique with the peak

current ranging from 50 to 274 pA and average of 132.4±76.2 pA (Liang et al, 2004). Steady inward currents were elicited with little inactivation of membrane depolarization and turned off quickly with membrane repolarisation (Liang et al, 2004).

Another potassium channel found in native SLFs is the Kir5.1 channel. Kir5.1 is an inwardly rectifying potassium channel (Hibino et al, 2004; Pan et al, 2016) and this channel was found to be expressed in type II and IV SLFs in C57/BL/6J mice but not in type I or III where its expression is downregulated in the ageing cochlea (Pan et al, 2016). The Kir5.1 channel has not yet been detected in cultured SLFs.

Moreover, ClC-2 and ClC-K2 chloride channels have been identified in cultured rat type IV SLFs (Qu et al, 2007). The presence of these channels was confirmed through reverse transcriptase -PCR and western blot analysis. For the recording of the ClC-K2-like and ClC-2 like whole cell Cl^- currents in cultured cells, tetraethylammonium (TEA) was used to block simultaneous K^+ activity and to study Cl^- currents in isolation. The recordings identified two Cl^- currents in cultured cells; an inwardly rectifying Cl^- current activated by hyperpolarisation or decreased extracellular pH, which resembles ClC-2. The second, a weak outwardly rectifying Cl^- current regulated by extracellular pH, Cl^- and Ca^{2+} indicating ClC-K2 characteristics. The findings suggest two functionally distinct Cl^- channels are involved in the regulation of membrane anion conductance in cultured type IV SLFs. Due to the low and variable level of ClC-2 expression; it seems ClC-K2 is the dominant Cl channel in cultured type IV fibrocytes. However, it cannot be ruled out that a small portion of the current could be carried by the ClC-2, suggested by opposite regulatory effects of extracellular pH. Moreover, even though ClC-2 and ClC-K2 are likely co-expressed, there was difficulty in recording ClC-2 currents in this study as a result of the experimental conditions.

Table 1.1 summarises the properties used to distinguish between the various types of fibrocytes that enable them to carry out their highly-specialised cochlear functions involved with maintenance of the EP and hearing function.

1.11 Electrophysiological properties of spiral ligament fibrocytes

In vivo, fibrocyte membranes have been found to have a positive potential of +5 to +12 mV relative to the perilymph (Nin et al, 2008; Adachi et al, 2013; Yoshida et al, 2015). A recent study has shown that the resting membrane potential of fibrocytes is around +9 mV, *in vivo* (Yoshida et al, 2016). The experiments involved the simultaneous insertion of electrodes into the cochlea, as well as the use of a potassium-sensitive microelectrode inserted from the perilymph towards the endolymph to record the potential and the concentration of potassium of the lateral cochlear wall in guinea pigs. Results showed that fibrocyte membranes are significantly more permeable to sodium than to either potassium or chloride. They concluded that this unique profile and sodium concentration gradient contributes to the positive resting membrane potential of fibrocytes (Yoshida et al, 2016).

Table 1. 1 Characteristics of types of SLFs

Fibrocyte type	Location (Mahendrasingam et al, 2011a)	Morphology (Mahendrasingam et al, 2011a)	Marker proteins	$Na^+K^+Cl^-$ cotransporter	Kir5.1	BK	ClC-2/ClC-K2	Connexin26	Connexin31	GLAST	Otospiralin
I	Upper central ligament adjacent to the *stria vascularis*	Elongated with few fine processes, light cytoplasm & few cytoplasmic organelles				Liang et al (2004)		Kasagi et al (2013)	Xia et al (1998; 2000)		
II	Below type I cells	Less elongated, darker, with more cytoplasmic organelles & many fine processes	S-100, αNa^+K^+ ATPase (Mahendrasingam et al, 2011a)	Crouch et al (1997)	Hibino et al (2004); Pan et al (2016)		Qu et al (2006)	Kasagi et al (2013)	Xia et al (1998; 2000)	Jin et al (2003); Furness et al (2009)	Delprat et al (2005)
III	Line the boundary of the ligament with the bony out covering the of the cochlear	Flattened with honey-comb-like processes and narrow cytoplasm	AQP1 (Mahendrasingam et al, 2011a)								
IV	Below type II cells	Round and dense with few fine processes & narrow cytoplasm	S-100 (Mahendrasingam et al, 2011a)	Adams (2009)	Hibino et al (2004); Pan et al (2016)		Qu et al (2006)		Xia et al (1998; 2000)		Delprat et al (2005)
V	Above Reissner membrane	Closely resemble type II with dark cytoplasm, organelles & many fine and coarse processes	S-100, αNa^+K^+ ATPase (Mahendrasingam et al, 2011a)	Crouch et al (1997)	Hibino et al (2004)		Qu et al (2006)	Kasagi et al (2013)		Furness et al (2009)	
Cultures			AQP1- Type III (Kelly et al, 2012)			Type I (Liang et al, 2003; 2004; 2005 Shen et al, 2004)	Type IV (Que et al, 2007)			Furness & Mahendrasingam (unpublished)	Zhuo et al (2008)

Table 1.1 Detailing all the functional characteristics possessed by SLFs from location and morphology to protein expression.

The atypical characteristics of fibrocytes are believed to be crucial for maintaining the EP. Both the EP and hair cell membrane potentials are driving forces in sensory transduction as the EP is essentially a potassium equilibrium potential generated by the potassium channel, Kir4.1, in the intermediate cells of the *stria vascularis* in conjunction with the low concentration of potassium of the intrastrial fluid and high concentration in the intermediate cells (Takeuchi et al, 2000; Marcus et al, 2002). SLFs, containing potassium uptake mechanisms, assist with the EP generation by the maintenance of a high concentration of potassium inside the intermediate cells (Schulte & Adams, 1989; Crouch et al, 1997; Mizuta et al, 1997). Therefore, these K^+ uptake mechanisms are critical to the functioning of the cochlea and should be a focus for a potential treatment for metabolic age-related hearing loss.

1.12 Study objectives

A way to prevent presbycusis is to maintain the EP well into old age in order to preserve sensitive hearing. In principle, this could be accomplished by replacing dysfunctional fibrocytes as a means of maintaining optimal potassium recycling. Since fibrocytes are mesenchymal, it is possible that the re-introduction of healthy fibrocytes into the spiral ligament using a cell replacement therapy may ameliorate the symptoms of presbycusis. The general premise of a transplantation therapy like this would be to restore the function lost as a result of the normal aging process by replacing dysfunctional cells with new healthy ones that possess the same specialised features and characteristics (Lindvall & Björklund, 2004). Previous inner ear transplantation strategies have involved injecting stem cells directly into the semi-circular canals in order to promote migration to functional sites in the cochlea, including the cochlear lateral wall. Whether these stem cells differentiate sufficiently to become highly specialised or 'fibrocyte-like' is uncertain. Such differentiation is essential to

the success of any possible functional restoration. An exciting alternative would be to transplant cells that are already specialised and differentiated; “designer” cells grown solely to fulfil a specific function in a specific structure. If the cultured fibrocytes mimic the native by showing similarities in their morphology, protein expression and ionic conductance then this would strengthen the argument for their transplantation as they would possess the features that would enable their potassium recycling capacity. Indeed, if fibrocytes can be cultured to show the functional characteristics as the native cells they intend to replace then this would make them a more robust cell group to transplant compared to stem cells whose fate is uncertain following transplantation in terms of migration and differentiation. It may also be possible to identify critical factors to direct the fate of cultured cells from one type to another and grow a specific kind of fibrocyte. Most of the cell replacement therapies or cell regeneration strategies in this area have focused on the regeneration of hair cells or spiral ganglion neurons, but as discussed above loss of SLFs precedes the loss of hair cells in some circumstances (Hequembourg & Liberman, 2001; Mahendrasingam et al, 2011b).

The aim of this research is to attempt to grow fully-functional “designer” fibrocytes in culture, as well as to develop a method to transplant these cultured fibrocytes into the inner ear in an attempt to prevent some forms of presbycusis. Fibrocytes are ideal targets for transplantation because the lateral wall is easily accessible when compared to deeper internal targets within the cochlea. It is believed that cells transplanted into the lateral wall are more likely to survive transplantation due to the abundance of tissue and vascular irrigation in the structure, as well as a low likelihood of infiltration into other cochlear regions (Zhang et al, 2013). Fibrocyte transplantation has not been explored as a potential treatment for presbycusis and it may represent an exciting new therapeutic approach to help individuals suffering from age-related hearing loss.

1.12.1 Comparison of the morphology of native and cultured fibrocytes

The gross morphology of cultured and native fibrocytes was assessed and classification of various fibrocyte types in culture. Growing fibrocytes in 3-D transplantable collagen gel matrices provides an optimal environment for the fibrocytes to develop their morphology in a manner that mimics conditions *in vivo*. Specifically, the gel is permissive in allowing the cultured cells to grow in more spatial planes and interact with other cells and their surroundings when compared to 2-D growth. Cells grown in 3-D matrices display marked improvements in overall cell numbers, viability, morphology, proliferation, differentiation, response to stimuli, migration, general cell function and *in vivo* relevance meaning that they function as they would in the *in vivo* environment (Antoni et al, 2015).

1.12.2 Comparison of the electrophysiological properties of cultured and native fibrocytes

The electrophysiological signature of native and cultured fibrocytes was assessed using the whole-cell voltage-patch clamp technique to measure the intrinsic conductances involved in the generation of the EP. Pharmacological agents were applied to both cultured and native SLFs to isolate and characterise the contributions of potassium channels.

1.12.3 Comparison of the expression of key proteins in native and cultured fibrocytes

The project utilises immunolabelling methods, which enable further identification of fibrocyte types and their key protein expression profiles, including targets such as S-100, AQP1 and the

α1Na^+ K^+ pump. By labelling with combinations of these antibodies, this technique distinguished between each type of fibrocyte except type II and type V fibrocytes. It is therefore feasible to apply this technique to characterise cultured or native fibrocytes, or cells that have been transplanted into the lateral wall where multiple comparisons can be made to distinguish the fibrocyte types (Mahendrasingam, et al, 2011a). Also, immunocytochemistry was used to identify other channels or transporters involved in potassium transport and the generation of the EP in fibrocyte cultures.

1.12.4 Development and validation of a novel cell replacement therapy

The three methodological approaches described above were performed on fibrocytes grown in culture, as well as in native fibrocytes prepared from cochlear slices obtained from CD/1 mice. Such a comparative analysis enabled the determination of whether the "designer" fibrocytes grown in 3-D collagen matrices possess the key physiological characteristics of native fibrocytes. As noted above, the unique morphology, complement of membrane proteins and electrophysiological features inherent in lateral wall fibrocytes are crucial to their involvement in potassium recycling and in the maintenance of the EP, and thus general cochlear function. If the cultured fibrocytes display similar features to those of native fibrocytes then this would provide significant justification for their use in transplantation experiments as opposed to more traditional approaches, such as the use of stem cells. Transplantation strategies and spiral ligament repopulation experiments will be another aspect explored in this research project.

It is hypothesised that the fibrocytes cultured in 3-D collagen gels will retain their native-like morphology; it is further hypothesised that they will possess a similar protein expression profile as certain types of native fibrocytes; and they will also show a similar electrophysiological signature to native fibrocytes. This will then provide suitable justification

supporting the use of these cultured fibrocytes as a potential cell replacement strategy to inject them directly into the lateral wall of experimental animals *in vivo* and assess whether they have a restorative affect upon ABR thresholds in the CD/1 mouse model of presbycusis. This project utilises a combination of powerful techniques made possible at Keele University such as cell culture, intracellular electrophysiology and immunocytochemistry. These approaches complement each other and will be used here in an innovative attempt to develop a possible cell replacement strategy to treat age-related hearing loss.

Chapter 2

Culturing of Spiral Ligament Fibrocytes

2. Chapter 2- Culturing of Spiral Ligament Fibrocytes

2.1 Introduction

The majority of cell culture methods use traditional two-dimensional (2-D) monolayer cells cultured flat on rigid substrates. Although this 2-D approach has been a valuable method for cell-based studies, limitations of this approach have been noted. In the *in vivo* environment cells are surrounded by other cells and extracellular matrix in a 3-D setting, therefore 2-D cell culture does not entirely take the natural 3-D environment of cells into account. This sometimes means tests involving 2-D cell cultures can provide misleading data for *in vivo* cell characteristics due to their unnatural microenvironment (Birgersdotter et al, 2005). It has been shown that 3-D extracellular matrix and its receptors can dictate the phenotype of mammary epithelial cells (Weaver et al, 1997).

It has been found that 3-D culture cells express different morphologies and physiology from 2-D culture cells and 3-D cell responses are more similar to *in vivo* behaviour than 2-D culture cells (Langer & Peppas, 2003; Baharvand et al, 2006; Shield et al, 2009). A study examining the differentiating potential of hESCs into hepatocytes in 2-D and 3-D culture systems found the embryonic body of hESCs cultured in a 2-D environment displayed morphological characteristics of hepatocyte-like cells, binuclei and polyhedral contours. Cells in the 3-D culture system migrated out of aggregates and formed cordlike and multilayer structures which were not observed in the 2-D cultures (Baharvand et al, 2006). Moreover, cells in the 3-D environment showed *in vivo*-like ultrastructure with numerous mitochondria, lysosomes, prominent nucleoli, well-developed Golgi apparatus and rough and smooth endoplasmic reticuli (Baharvand et al, 2006). The differentiation of hESCs into hepatocyte-like cells within the 3-D collagen scaffolds in comparison with 2-D culture also gave rise to cells displaying earlier and higher levels of gene expression patterns and metabolic activities

of hepatocytes (Baharvand et al, 2006). Another example is the transformation process of embryonic sensory neurons which, *in vivo,* express a bipolar morphology with two-opposite neurites, and then transform to pseudo-unipolar axonal arbour (Langer & Peppas, 2003). This transformation of these cells is delayed or disappears in cells cultured on flat 2-D substrates (Langer & Peppas, 2003). This suggests 3-D culture systems provide a microenvironment that is conducive to normal progenitor cell kinetics and enhanced cell differentiation.

It is the dimensionality of the cultures that results in different cellular responses as it affects the spatial organisation of the cell surface receptors that engage with the surrounding cells, but also induces physical constraints to cells. This in turn affects the signal transduction from the inside to the outside of a cell, consequently influencing gene expression and cellular behaviour (Bettinger et al, 2009). It has been found that there is a significant variation between cell cultured as 2-D monolayers and those in 3-D constructs in mammalian cell responses including cell polarity and migration, cytoskeleton structure, distribution of receptors, hormone responses, growth factors and apoptotic factors (Tibbitt & Anseth, 2009; Kim et al, 2012). Cellular responses to pharmaceutical drugs in 3-D cultures from cells lines from malignant ovarian tumours have been demonstrated to be more similar to that *in vivo* than 2-D (Shield et al, 2009; Zietarska et al, 2007; Lee et al, 2008). Work has gone into developing 3-D culture systems in areas of drug discovery, cancer cell biology, stem cells and implantation strategies where the 3-D culture systems allow exploration of *in vitro* models resembling *in vivo* environments (Baharvand et al, 2006; Justice et al, 2009; Reininger-Mack et al, 2002; Sun et al, 2006).

As stated, cells in a 3-D environment differ from 2-D cultures in terms of gene, protein, and cell receptor expression (Baharvand et al, 2006).This difference in gene and protein expression explains why cells cultured in 3-D behave differently in many cellular processes, including growth and proliferation, migration and invasion, and morphology (Gurski et al,

2010). A lot of the genes that promote rapid growth and proliferation, as well as those responding to factors in culture medium, are usually upregulated in cells in 2-D culture environments. In 2-D cell cultures the expression of genes that limit growth and proliferation are repressed when compared to tissue (Birgersdotter et al, 2005). This is consistent with the fact that 2-D cultured cells proliferate more rapidly than cells cultured in 3-D models. Therefore, 3-D models are crucial in maintaining gene and protein expression profiles and functions of cells ultimately making them behave similarly to how they would *in vivo*.

Common cell culture techniques are traditional 2-D cultures (fig. 2.1a); and two typical 3-D cultures where cells are either grown on a scaffold/matrix (fig. 2.1b); or grown in a scaffold/matrix (fig. 2.1c). Most hydrogel-based scaffolds do not naturally adhere cells nor promote cell function. Collagen is an exception as it is rich in integrin-binding domains that enhance cell attachment and growth. The collagen molecule is a three-stranded structure which consists of three polypeptide chains twined around one another, with each chain having an individual twist in opposite directions (Lee et al, 2001). In the lattice structure the strands are held together by hydrogen and covalent bonds. Type I collagen is the most favourable for tissue engineering because it is a major extracellular matrix protein and fibroblasts naturally reside in collagen-rich matrices. Cells delivered in 3-D collagen gels have been used as a potential and promising treatment for neurons damaged due to injury/ disease (Lindvall et al, 2004; Thompson & Björklund, 2015).

SLFs (specifically type I and IV) have previously been cultured primarily in 2-D monolayers (Gratton et al, 1996; Suko et al, 2000; Ichimiya et al, 2000; Liang et al, 2003; 2005; Shen et al, 2004; Qu et al, 2007). However, one study has demonstrated 3-D culturing of type III 'tension' SLFs within a type I collagen gel demonstrating that these fibrocytes can impart myosin-dependent contractile force on a collagenous substrate (Kelly et al, 2012). This work

provided support for the tension regulation function hypothesis in the spiral ligament-basilar membrane, and therefore their role in determining auditory sensitivity (Kelly et al, 2012). In this present study a successful culture of SLFs was established and cultured on a collagen matrix, providing not only a representative environment that more closely mimics the *in vivo* environment in terms of cells morphology, proliferation rates and gene/protein expression but also made it feasible to perform electrophysiology in the cells as they could be accessed at the top of the gels.

In vivo, SLFs are typically spindle-shaped with long parallel processes (Liang et al, 2003). The significance of fibrocyte morphology to hearing is that their characteristic spindle-like shape and long processes may be a key factor in the transport of potassium as these processes/projections enable the formation of gap junctions between other cells which utilise this transport system. Without these features their ability to participate in potassium recycling would be affected and thus so would the EP. Fibrocyte ultrastructure is shown to be crucial to hearing since the severe ultrastructural alterations in knockout mice lacking the *Brn-4* transcription factor has been shown to result in severe deafness (Minowa et al, 1999). *Brn-4* is the gene responsible for human DFN3, an X chromosome linked non-syndromic hearing loss (de Kok et al, 1995). *Brn-4* deficient mice exhibit a reduced EP and hearing loss, as well as markedly fewer cytoplasmic extensions and a dramatically reduced volume of cytoplasm and number of mitochondria (Minowa et al, 1999). The purpose here is that if the cells are grown in a 3-D matrix as opposed to a monolayer, the morphology and associated functions in hearing may possibly provide a restorative effect if transplanted.

Figure 2. 1 Schematic of cell culture systems

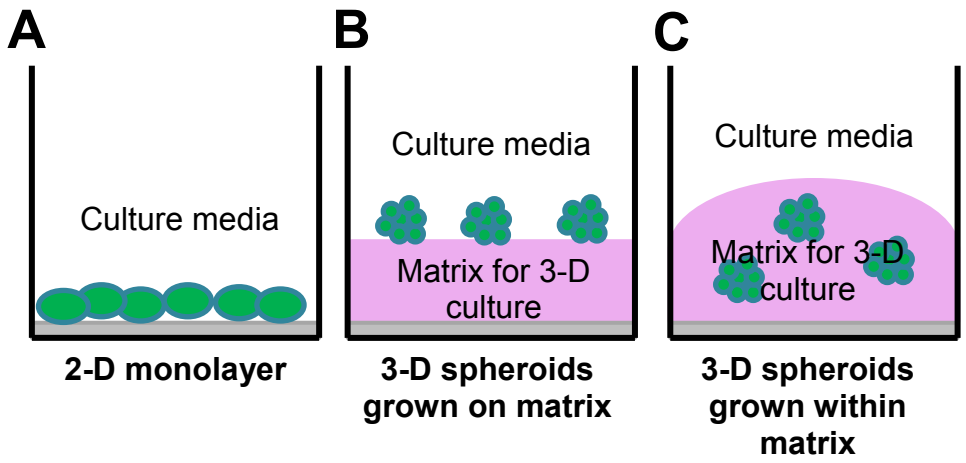

Figure 2.1 Traditional 2-D monolayer culture (A) and typical 3-D cell culture systems: cell spheroids/aggregates grown on matrix (B) or cell embedded within matrix (C). (Modified from Edmondson et al, 2014).

There have been previous attempts for transplantation to restore degenerated SLFs using mesenchymal stem cells which were met with partial success however suffered issues with migration and differentiation of the transplanted cells (Kamiya et al, 2007; Kasagi et al, 2013). Alternative strategies for repopulating the spiral ligament would be either transplanting a cell-laden gel or a decelluarised tissue which has been re-cellularised.

A particularly appealing approach to engineer tissues or organs uses a combination of a patient's own cells combined with polymer scaffolds. The cells are harvested and incorporated into 3-D polymer scaffolds which act as the extracellular matrices found in tissues and enable delivery of the cells to the desired site in the body, provide space for new tissue formation, and potentially control the structure and function of the engineered tissue (Chen & Chen, 2019; Nishimure et al, 2019). Hydrogels have been successfully used to improve post-transplantation survival of encapsulated stem and progenitor cells (Chang et al, 2012; Ballios et al, 2015; Jha et al, 2015).

Another process is decellularisation, by which cells are discharged from tissues/organs, but all of the essential cues for cell preservation and homeostasis are retained in a three-dimensional structure of the organ and its extracellular matrix components (Badylak, 2007). For the recellularisation, the scaffold/matrix is seeded with cells with the goal being to form a practical organ/functioning tissue. This technique has been used in numerous other studies using different tissue and cell types providing successful approaches for insights into repopulation of decelluarised tissue for heart valve engineering and kidney regeneration (Roosens et al, 2017; Chani et al, 2017; Destefani et al, 2017). This could be a potential route for research into the degeneration of fibrocytes in the cochlea spiral ligament.

The aim of this study was to develop from an initial 2-D culture system of SLF to a subsequent 3-D culture environment in which the cells can grow in a way that enables them to possess a native-like morphology, genetic and physiological functions that are crucial to their potassium recycling function, maintenance of the EP and ultimately hearing. The development of this 3-D transplantable matrix or scaffold could provide a potential cell replacement therapy to treat metabolic age-related hearing loss.

2.2 Methods

2.2.1 The experimental animal

An outbred strain of CD/1 mice (Mahendrasingam et al, 2011) aged P9-30 was used for the experimental work outlined below. CD/1 mice were selected for use in this study because they show accelerated age-related hearing loss and can be used for ageing studies for comparison with other rodent strains.

2.2.2 Preparation of the experimental animal

CD/1 mice were bred and maintained in the Central Animal Facility at Keele University. All animals were treated in accordance with the UK Animal (Scientific Procedures) Act of 1986, and approved by the Animal Welfare and Ethical Review Board at Keele University. 4 to 5 week old CD/1 mice were deeply anesthetized with sodium pentobarbitone (Vetalar) injected intraperitoneally at a dose of 0.1 ml for a 30 g mouse. After loss of the pedal withdrawal reflex, animals were decapitated. Pups were decapitated following schedule 1 killing guidelines.

2.2.3 Cell culture

2.2.3.1 Collagen I coating

Before initiating any cell culture within plastic wells or flasks for monolayer cultures the bottom of these had to be coated with a dilute collagen I solution to better enable any future cells to adhere more efficiently. Stocks of rat tail collagen I (Corning, fisher scientific, UK) solutions were diluted to a 0.01% working solution using sterile tissue culture grade water. When coating coverslips within wells the coverslips were sterilised in 100% ethanol and dried in a laminar flow cabinet before use. The 0.01% collagen solution was added to the well or flask (200uL per $1cm^2$) and removed after 5-6 h and were incubated to dry out overnight @37.5ºC. Rinse with sterile tissue culture grade water twice before introducing cells (table 2.1).

Table 2. 1 Collagen coating of culture dishes

Cell culture plate	Area/well	Volume	Concentration	Time todry
24 well plate	2 cm^2	200 µL	0.01%	Overnight
6 well plate	10cm^2	2 mL	0.01%	Overnight
T25 flask	25 cm^2	5 mL	0.01%	Overnight

Table 2.1 Scheme of pipetting for coating of culture dishes for monolayer culture with collagen I solution.

2.2.3.2 Reagents for cell culture

Minimal Essential Media-α (MEM-α, Fisher scientific, UK), Antibiotic-Antimycotic (PSF, Sigma Aldrich, UK), 10% foetal calf serum (FCS, Fisher scientific, UK) and 1% Insulin-Transferrin-Selenium-G Supplement (ITS-G, Fisher scientific, UK) were combined to make medium for cell culture. Each 5 ml of medium consisted of 4.4 ml of MEM-α, 500 µl FCS, 50 µl ITS-G, 50 µL PSF. Phosphate-buffered saline (PBS, Fisher scientific, UK) and PSF were combined to make the sterile wash used between medium changes. Each 5 ml of the wash solution contained 4.95 ml of PBS and 50 µl PSF. Trypsin-EDTA (Fisher scientific, UK) was used for the dissociation of cells for passaging.

2.2.3.3 Tissue preparation and cell culture

The cochlea was carefully and quickly dissected from the skull. With the skull facing up, the head was bisected, bullae removed and opened to reveal the cochlea beneath the otic capsule (the temporal bone is harder the older the animal). Surrounding bones were dissected away and the cochlea was then removed and placed into a petri dish in cold culture medium (4 ^oC) until micro-dissection.

The lateral wall was dissected under a dissecting microscope using aseptic techniques (using forceps soaked in 100% ETOH) whilst immersed in 4 ^{o}C MEM-α with PSF. A small hole was chipped through the bone at the apex of the cochlea using a sterile needle; sterile forceps were used to chip away the outer bone to reveal the turns of the inner spiral. Lengths of the lateral wall were detached and pulled away, the *stria vascularis* was then removed from the section of lateral wall leaving the spiral ligament remaining. These lengths of the spiral ligament were broken up into shorter length to then be used to initiate cultures,

To increase the likelihood of attachment of the tissue to the collagen coated wells, 50 µl of culture medium consisting of MEM-α supplemented with 10% FCS, 1x PSF and 1% ITS-G supplement was added onto the collagen-coated 10 cm^2 well (6-well plate). The spiral ligament tissue fragments were placed into the 50 µl of medium (*strial* side downwards) and covered with a 22mm x 22mm ½ oz. glass cover slip (smaller coverslips failed to generate cultures). A few drops of culture medium were added to the edges of the coverslips to prevent drying out. The well plates containing the ligament were placed in an incubator at 37 ^{o}C (5% CO_2, 95% O_2, BOC, UK) for 24 hours.

Culture medium was then added to cause the coverslip to float and facilitate its removal. Once removed, 2 ml of culture medium was then slowly added to the wells containing the ligaments which were incubated further. The culture medium was changed every 2 to 3 days after rinsing twice with the washing buffer (sPBS with 1x Antibiotic-Antimycotic).

2.2.3.4 Passaging and freezing of cells

Once cells in the primary culture had reached confluence (~2 weeks) they were passaged into T25 flasks. The cells were washed with sterile PBS (sPBS) and detached by the addition of 0.02% trypsin/EDTA (1mL for $10cm^2$) being placed back into the incubator for ~10-15m. The action of trypsin was halted by the addition of medium to make a total volume of 10 ml. The detached cells were then centrifuged @270.5 G-force (1200 rpm) for 5 min, the supernatant was removed and the cell pellet was re-suspended in new culture medium and either seeded onto collagen coated T25 flasks and grown until confluence or the cells were then harvested and seeded onto gels. The medium was changed the next day after being passaged. Seeding densities guides are shown in table 2.2.

Table 2. 2 Seeding density and volumes for culture dishes

Cell culture plate	Seeding density	Volume	Cells at confluency
24 well plates	$0.05x10^6$	200 µL	$0.24x10^6$
6 well plates	$0.3x10^6$	2 mL	$1.2x10^6$
T25 flask	$0.7x10^6$	5 mL	$2.8x10^6$

Table 2.2 The media volumes and density of cells for seeding.

To freeze the cells the same protocol as passaging was followed, then once the cell pellet had been produced it was re-suspended in MEM medium with 10% DMSO (Sigma Aldrich, UK). Then this was transferred to a freezing tube and stored at -80ºC. To defrost and re-seed these cells the frozen tubes were slowly defrosted in hands and then 100µL of warmed medium added and re-suspended. The re-suspended cells were added to fresh medium in either a T25 flask or 6-well plate, re-suspended and incubated at 37ºC for 24 hours. A medium change took place the following day to remove any dead cells.

2.2.3.5 Trypan blue live-dead test

Cell viability and cell number of spiral ligament fibrocytes were assessed by the trypan blue exclusion test. This is based on the principle that live cells possess intact cell membranes and therefore exclude trypan blue as it cannot enter the cell (the live cells then appear golden), whereas dead cells do not as they lack intact cell membranes so the dye is able to penetrate causing the cells to appear blue.

A haemocytometer was cleaned using 70% ethanol, and coverslip added using small volumes of sterile water to adhere it down. Before the cell suspension settled 10µL was taken out and added to an Eppendorf tube and incubated with 10µL of trypan blue solution (Thermofisher Scientific, UK) for 1 min at RT after being gently mixed. 10µL of the cell mixture was added to the haemocytometer by placing the tip at the end of the cover slip and expelling the solution until it filled the chamber. After, viable and dead cells were counted using a Fuch-Rosenthal-Chamber by counting the cells within 16 square each (4x4) in each corner of the grid using X10 magnification and taking the average. The numbers of living and dead cells were used to calculate the viability, as well as the total number of cells. The total count from 4 sets of 16 corners was divided by 4 (to get the average), and then multiplied by 2 to adjust for the 1:2 dilution in trypan blue (the two steps are equivalent to dividing the cell count by 2). The viability had to be greater than 85% for the cells to be used for further studies.

$$Cells \times 10^4 / mL = Cells_{Viable} / 2 \qquad \%_{(Viability)} = \frac{Cells_{Viable}}{Cells_{Viable} + Cells_{Dead}} \cdot 100$$

2.2.3.6 Preparation of collagen I gels

Gels were made as instructed on Thermofisher Scientific, UK, website, a few hours prior to being seeded with cells (the gels set 30 min after preparation). The 3-D gels were made at a final concentration of 3 mg/mL collagen I from a stock solution of 9 mg/ml. A total volume of 1 ml was made using 330 µL of the 9 mg/mL collagen solution, 100 µL 10XDMEM (Thermofisher scientific, UK, polymerised by addition of 18 µL 1N NaOH, and 552 µL of sterile H_2O. All solutions were kept on ice and tubes were wiped with ethanol sprayed blue roll. In one chilled tube the 10XDMEM, NaOH and H_2O were gently mixed using a pipette tip avoiding air bubbles. The collagen was transferred gently into another chilled vial to reduce air bubbles. Both tubes were transferred to the ice for 5 min. The 10XDMEM, NaOH + H_2O mixture was transferred into the collagen aliquot and stirred using a pipette tip until homogeneous and transferred to the ice until use. Initially 250 µL volumes were placed into 4 wells of a 24 well plate; however this caused issues for electrode access during electrophysiology experiments. Thus, 250 µL was instead added to the centre of a 30 x 11 mm sterile petri dish, with the gels having a diameter of approximately 15.6 mm, and incubated at 37 ^{o}C for a minimum of 30 min (fig. 2.2).

Cells were seeded directly on top of the gels using 50µl of cell suspension containing a density of approximately $5x10^4$ cells per sample where they were left to settle for ~2 h after which fresh culture medium (MEM-α supplemented with 10% FCS, 1% ITS-G and PSF) was gently added to cover them overnight. The gels containing the cells were then used for electrophysiological experiments over the following few days and finally fixed for later immunocytochemistry.

2.2.3.7 Fixation of cells or gels for immunolabelling

Cells on coverslips or on gels were fixed in 4% paraformaldehyde (PFA) for 2 h for immunocytochemistry. 4% PFA was made using 2g PFA dissolved in 25mL of filtered H_2O in a fume cupboard, whilst being stirred at 60ºC. 1 pellet of NaOH was added to aid this. The solution was then taken off the heat and 25mL of 0.2M PB was added and the pH of the solution was checked and amended to pH7.4. After the 2 h of fixation in 4% PFA the gels were kept in 0.4% PFA for longer storage.

2.2.3.8 Trouble shooting and optimisation

In the early trouble shooting period of the project, the cells (after initially being cultured in a 2-D 6-well plate) were seeded onto collagen gels set within the wells of a 24-well plate. This caused numerous problems later on when it came to electrophysiology as the electrodes could not reach the cells due to the sides of the wells. It was then attempted to remove the gel and place it into the lip of a petri dish, this also raised problems of its own as it was very tricky to remove the gel and meant the gel was often damaged and mangled making it hard to locate and access the cells on the surface. Therefore it was established that the gels could be made directly onto the inside lid of a 30x11mm sterile petri dish. Once the solution for the gel was mixed, it was pipetted straight onto the petri dish in a central convex mass where it held its shape and set (fig. 2.2). This then enabled the cells that would later be seeded directly on top to be easily accessed by the electrodes to undertake the electrophysiology.

Figure 2. 2 Schematic of collagen gel

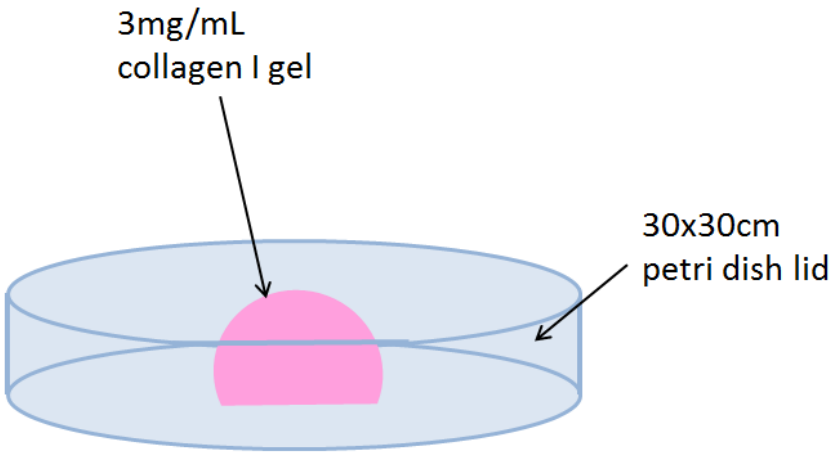

Figure 2.2 Collagen gel set up (not to scale). Gel pipetted into the centre of a sterile petri dish lid where it sets. Once set it was seeded with the cultured SLFs before being covered by medium.

2.2.3.9 Making antifade mountant

Anti-bleaching agents are widely used for preserving signal for fluorescent dyes. Antifade is a custom made reagent used in our laboratory. It was freshly prepared just before the samples were ready to view on the confocal microscope. However the PVA/glycerol component of the antifade solution had to be made up in advance. The PVA/glycerol was made by dissolving 1g of polyvinyl alcohol (PVA) in 40mL of 0.1M PB (pH 8) @RT (stirred for 16 h). After this period 20mL of H_2O free glycerol was added to the PVA solution and stirred for another 16 h. The PVA/glycerol mixture was then stored at 4ºC.

The antifade was then freshly prepared by centrifuging the PVA/glycerol mixture for 15 min. 0.01g of para-phenyldiamine (pPD) was dissolved in 1mL of 0.1M PB (pH8). The freshly dissolved pPD was diluted with the centrifuged PVA/glycerol mixture (1:10) before use.

2.2.3.10 Immunocytochemical labelling for cells on collagen gels

For immunofluorescent labelling of the cultured cells, the gels were fixed in 4% paraformaldehyde for 2 h as described above, washed with PB X3 and PBS X1 before following similar immunolabelling procedures used previously (Mahendrasingam et al, 2011a). In brief they were permeabilised with 0.25% Triton-X-100 in PBS with 1% goat-serum for 30 min. The gel was then washed with PBS X3 and pre-blocked with 10% goat-serum PBS for 30 min. Samples were then incubated overnight at 4 ^{o}C on a rotator with primary antibody (table 2.3). The following day the gel was washed with 1% goat-serum PBS X3 followed by application of the appropriate conjugated secondary antibodies (AlexaFluor 488 green and 568 red) for 2 h at room temperature (table 2.3). After this the gels were washed in PBS X3 and mounted in antifade just prior to being observed using a confocal system (1024 two-photon, MRC-BioRad, UK).

Trials of antibody concentrations were done using guides from the data sheet and other research using the antibody. Initial concentrations were used and modified until optimal labelling was achieved.

Table 2. 3 Antibody table

Protein	Primary antibody species and dilution	Secondary antibody species and dilution
AQP1	Rabbit 1:100 (MilliporeSigma, UK)	Goat anti-rabbit 1:50 (Invitrogen Thermofisher Scientific, USA)
S-100	Goat 1:100 (Santa Cruz, USA)	Donkey anti-goat 1:50(Invitrogen Thermofisher Scientific, UK)
Phalloidin	1:250 (Thermofisher Scientific, UK)	

Table 2.3 A summary of the marker proteins with primary and secondary antibodies used with their dilution ratio.

2.2.3.11 Seeding of cultured SLFs onto dissected decellularised spiral ligament

In this preliminary experiment the cochlea of a P29 CD/1 mouse was isolated and incubated for 5 days with the culture medium being changed every 2 to 3 days, so that the spiral ligament degeneration could occur (Kubikova & Furness, unpublished observations). The spiral ligament was micro-dissected after 5 days in culture and placed into 50µL of culture medium. The 50µL of medium was then replaced in the experimental samples with 50µL of cell suspension from cultures from a P9 mouse, cell count $8x10^5$ live cells/mL. They were then placed back into the incubator for 24 h.

After 24 h of incubation the cell suspension of medium was removed from surrounding the ligaments which were then fixed in 4% paraformaldehyde for 1 h and incubated with a fluorescent phalloidin and a goat-anti-rabbit TRITC antibody for background, before being prepared for confocal viewing with antifade to preserve fluorescence's (a custom made solution not commercially available).

2.2.4 Confocal fluorescence microscopy imaging

A confocal laser scanning microscope (1024 two-photon, MRC-BioRad, UK) was used to observe cultured fibrocytes throughout collagen I gel construct. Fluorescence was detected using in-line filters for 510-530nm (green) and 565-600nm (red). Images were captured using either x20, x40 or x60 magnification. Three individual fluorescent images over the full z-axis range were captured with Lasersharp2000 software and merged into a single representative image using Adobe Photoshop (version 7.0).

2.2.5 Statistics

Data were analysed using GraphPad Prism statistical analysis software (version 5.0). All data are expressed as mean ± standard error of the mean (S.E.M.). Tests for normal distribution and equal variance were conducted to determine the suitable parametric or un-parametric test to be used. The analysis of variance and t-tests used to examine the significance of these data were calculated using GraphPad prism. Cell counts graphs used number of cells in 10 random areas within each well for each condition. Unless otherwise stated, significance was assessed at the 5% level ($p< 0.05$*); $p<0.01$**; $p<0.001$***; $p<0.0001$ indicate significance, shown across groups by bars.

2.3 Results

2.3.1 Establishment of SLF culture

2.3.1.1 Two Dimensional (monolayer) culturing

In order to establish an isolated primary culture of SLFs, the spiral ligament from the cochlea of CD/1 mice was dissected using the approach described previously and stuck down on collagen coated 6-well plates where cells could then begin to grow. The cells were successfully cultured as they were seen to begin 'crawling' out of the pieces of ligament a day after being stuck down (fig. 2.3a & d). At this point the ligament was removed to allow the cells to grow until confluent (fig. 2.3c & f). After around 2 weeks of culturing the cells became confluent and were then either passaged into T25 flask to continue growing or seeded onto collagen gels. Cell viability was assessed by trypan blue dye and fibrocytes with >85% viability were seeded as described previously.

The success rate of this was often quite low (usually less than 50%) therefore only 2 or 3 out of the 6 wells would grow cells. A way to improve this was to be rather 'rough' when dissecting the spiral ligament and break it up into smaller pieces. This was to allow the cells to be more exposed for culture initiation.

Figure 2.3 Cells crawled out of ligament from day 1 to 5.

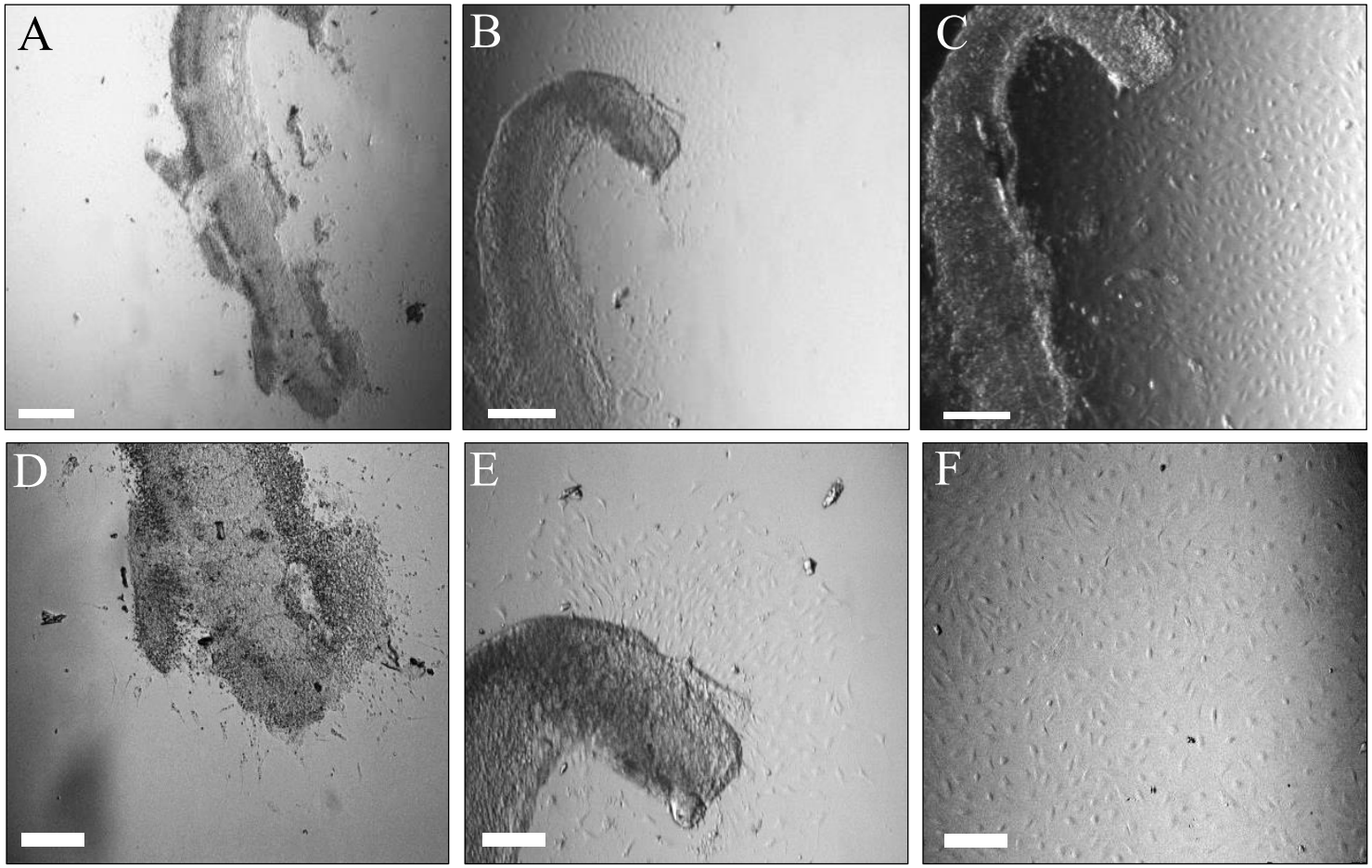

Figure 2.3. Light microscope images of a piece of spiral ligament cultured from P9 mouse starting a culture of SLFs on day 1 (A & D), 3 (B & E) and day 5 (C & F) after initial dissection. Cells shown to be crawling out of ligament by the first day after dissection and the density of cells increases from day 1 to day 5 until becoming confluent. Images A, B & C taken at x4 magnification and scale bar represents 50µm, and D, E & F at x10 magnification and scale bar represents 25um.

After becoming confluent in the 6-well plates the cells were either seeded onto 3-D collagen gels or passaged and split into T25 flasks to continuing growing. The cells seeded into and growing in T25 flasks in the 2-D environment appeared quickly and from day 3 to 9 (fig. 2.4) the density of cells significantly increased over time. Confluency was reached around day 10-14 in culture. Figure 2.5 shows the density of cells at day 3 in the cultures from P22 mice was significantly different from the density of cells at day 6 (12.22cells per mm^2±3.894, *n=3*, verses 80.22 cells per mm^2±12.64, *n=3*, respectively; *p=0.0217*). Moreover, the density of cells at day 6 in the cultures from P22 mice was significantly different to the density of cells at day 9 (257.2 cells per mm^2±45.22, *n=3*; *p=0.0441*). The density of cells at day 3 in the cultures from P22 mice was also significantly different to the density of cells at day 9 *(p=0.0273*).

Figure 2.4 Cells cultured on 2-D (monolayer) plastic collagen coated surface of T25 flasks on day 3, 6 and 9.

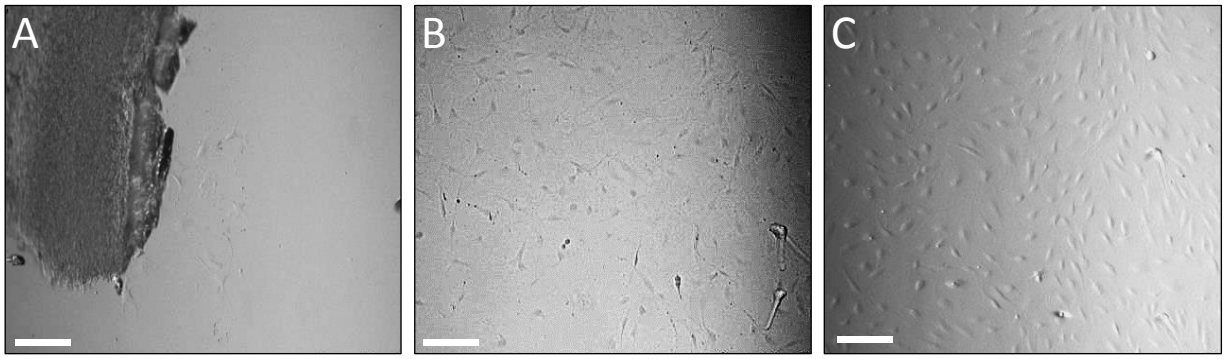

Figure 2.4 Light microscope images of cultured SLFs from P22 mouse on day 3 (A), 6 (B) and day 9 (C) after seeding into T25 flask. Density of cells increases from day 3 to day 9 until the cells in the T25 flask are confluent. Image A, B & C taken at x10 magnification. Scale bar represents 25µm.

Figure 2.5 SLFs cultured in monolayer environment on day 3, 6 and 9.

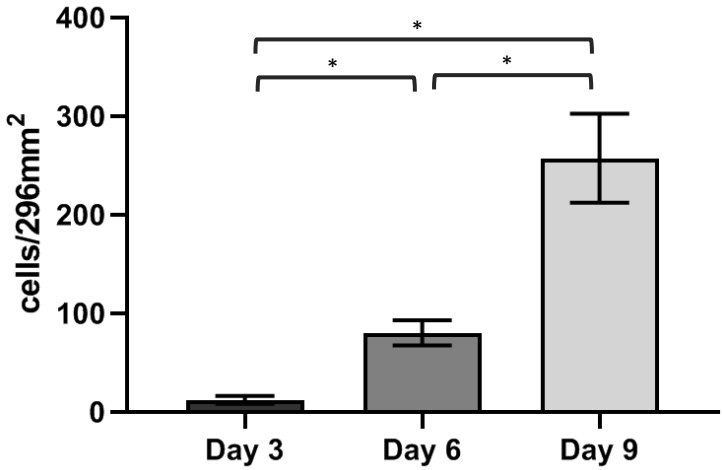

Figure 2.5 Bar graph showing the density of cells in a 2-D T25 flask on day 3, 6 and 9. Density of cells increase over time.

2.3.1.2 Preparation and use of collagen gel

The collagen hydrogel was a critical factor to the quality and reproducibility of the assembled gels. Incorrectly measured components resulted in hydrogels that were too structurally weak to produce constructs after curing and not suitable to use in fluorescence microscopy. In this context, stock collagen concentrations at 3.5 mg/mL were used, which had a relatively low viscosity compared to higher concentration solutions at 10.2 mg/mL and were easier to accurately measure volumes and mix with the other hydrogel components. Additionally, the added handling difficulties inherent with the higher stock concentration resulted in the introduction of bubbles into the final collagen solution, which were transferred into the produced constructs and further impacted on the visualisation of cells. Thus the lower stock concentration was used to produce the solution. Furthermore, a rise in solution temperature increased the time constraints during production because the solution began to cure. Using compacted ice to chill both the hydrogel components and the neutralised hydrogel prevented the accumulation of air pockets within as it solidified over time and maintained the solution at

a constant temperature. The effects of high ambient laboratory temperature were overcome by restricting the length of time the solution was out of ice to a maximum of five min and the effects of body heat mitigated by using a rack to place the final hydrogel (and the components during production) in the culture hood.

The initial design of the gel later created more challenging methodological steps as gels were made within 24-well plates where electrode access was impossible and if the gel was removed it would become twisted and would break apart, again making later electrophysiology and labelling difficult. The new design of the gel set up in the petri dish enabled more optimal further assessment of the SLFs as electrodes could access the cells for electrophysiology. Moreover, seeding the SLFs on top of the collagen gels as opposed to within the gels made patch clamp electrophysiology possible as the patch electrode does not effectively penetrate the collagen matrix.

2.3.1.3 Three-dimensional cultures of SLFs

Once the cultured spiral ligament fibrocytes were confluent they were seeded onto collagen I gels, covered with medium and cultured for up to1 week. After the initial seeding onto the gels, the cells appeared very round and isolated (fig. 2.6a & e) before beginning to move around, spread out and make connections within an hour after seeding (fig. 2.6). Within the first 24 h the cells appeared much fatter, elongated and interconnected. This continues over the next 4 days with the cells becoming more connected and cell clusters forming (fig. 2.6d & h, appendix 1).

The numbers of cells appeared to slowly decrease over time period of 4 days and therefore seemed to have a cell death rate greater than the proliferation rate. Cells grown in a 3-D culturing environment seemed to have a lesser proliferation capacity. It could also be that the cells clumped together in large clusters so the cell density appears reduced.

Figure 2. 6 SLFs cultured on a 3-D collagen I gel from day 1 to 4.

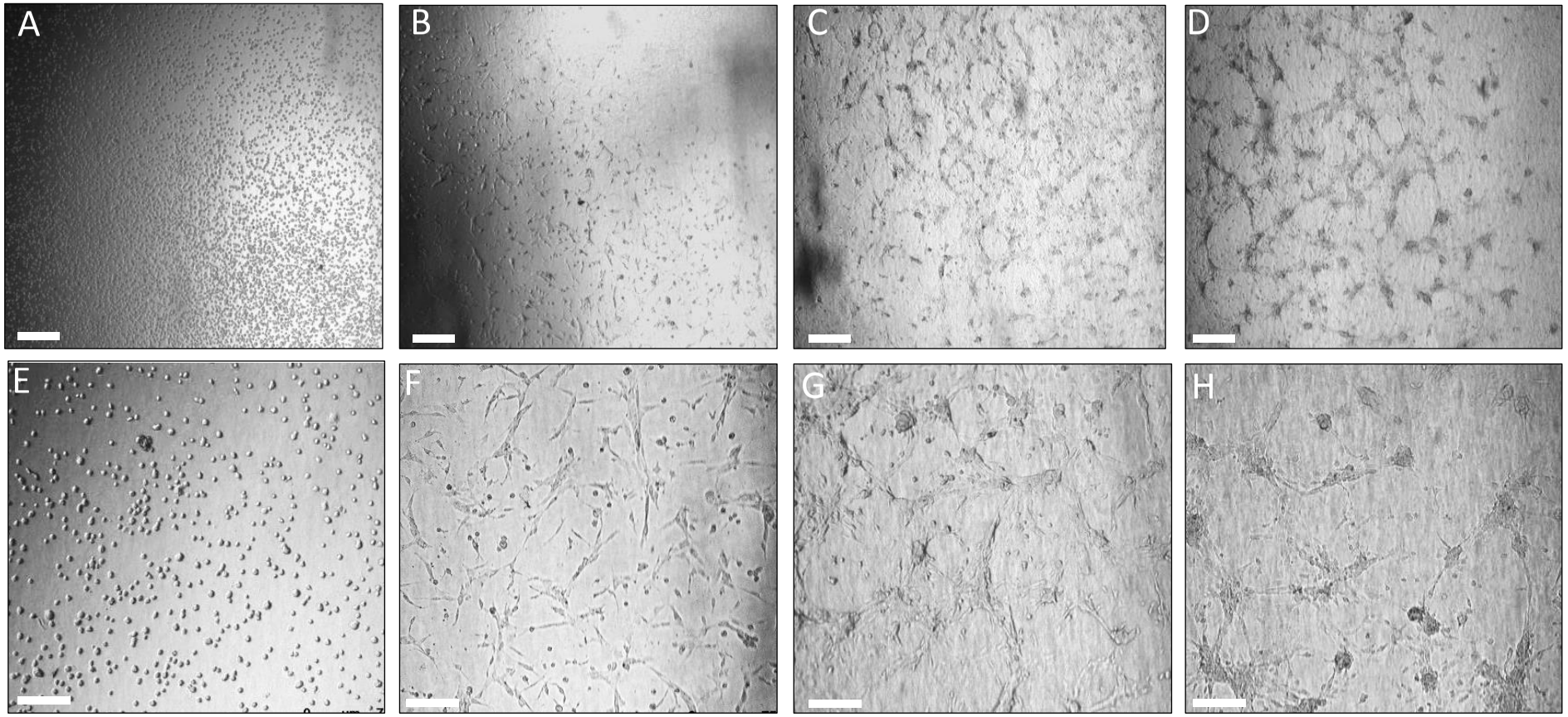

Figure 2.6. Light microscope images of cultured SLFs from P10 mouse on day 1 (A & E), 2 (B & F), day 3 (C & G), and day 4 (D & H) after seeding onto collagen gels. Density of cells slowly decrease from day 1 to day 4. Images A, B, C & D taken at x4 magnification and scale bar represents 50µm, and E, F, G & H at x10 magnification and scale bar represents 25µm.

2.3.2 Morphological characterisation of primary mice spiral ligament fibrocytes

2.3.2.1 Morphological examinations of 2-D (monolayer) and 3-D cultures

To mimic the spiral ligament environment, the cells where seeded onto collagen I gels in order to allow them to grown in a 3-D native-like environment. We examined the morphology of SLFs grown for up to 4 days in culture in 3mg/mL collagen gels. Light microscope images and time-lapse video microscopy (appendix 1) show that as cells proliferate in the hydrogels, they form connections and multicellular clusters (fig. 2.6). These resemble the morphology of fibrocytes within the spiral ligament. In comparison to the monolayer culturing where the cells remained more spherical and isolated. The cells in the monolayer were more spread out and had a more flattened morphology even when confluent, accompanied by an increase in the size of the nucleus (fig. 2.6b).

After initial seeding, after trypsinization, the fibrocytes appeared very rounded with no processes or connections. Once the cells were settled on the 3-D collagen I gels compared to 2-D collagen coated surfaces, the cells were more interconnected and rounder in terms of their 3-D appearance (fig. 2.7). Cells were examined for morphological changes after seeding onto the gels, and within an hour after seeding the cells had already regained their polygonal shape and appeared to move around the gel starting to establish extensive cell-cell contacts with their processes appearing to form a network and also showing a decrease in cell size relative to the monolayer cells.

Figure 2. 7 2-D monolayer and 3-D cultured spiral ligament fibrocytes

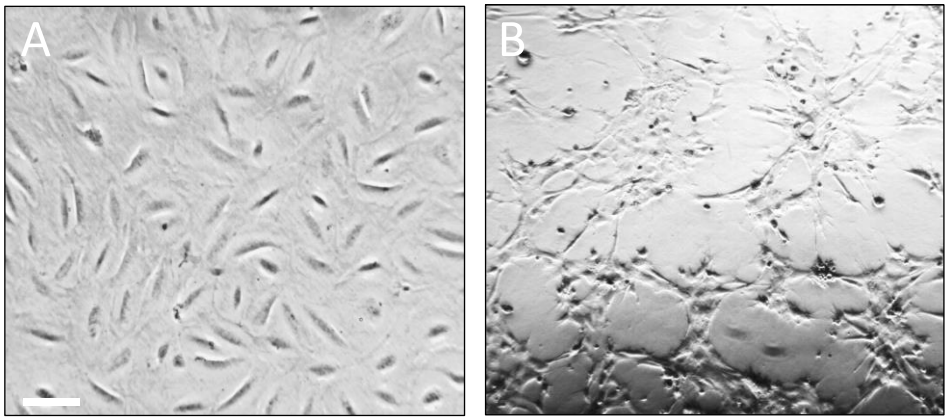

Figure 2.7 Culturing lateral wall fibrocytes on 3-D collagen hydrogels. 2-D cultured fibrocytes appear flatter (a). Fibrocytes exhibit a rounder morphology and have processes forming a network when on a 3-D collagen gel (b). Scale bar represents 25μm.

The 3-D cultured fibrocytes moved towards each other and built clusters of cells (shown and fig. 2.9 and appendix 1), expressing a more fibrocyte-like morphology by initially forming connections with the projections from the cell bodies before grouping together, shown in more detail through actin fibre labelling (fig. 2.7a & 2.8). In the time-lapse video (appendix 1) cells can be seed becoming more spindle-shaped from their initial circular appearance after seeding (fig. 2.9a). The cells begin to form processes and make connections with surrounding cells before forming clumps of cell bodies. Stills taken from different time-points of the 24-h time-lapse (fig. 2.9) show that after only 1 h after seeding onto the collagen gels the cells already appear to be forming processes and connections (fig. 2.9b) and by 6 h there is a large network between the cells (fig. 2.9c). At some point after this the cells begin to join and form clusters with the projections appearing to retract (fig 2.9d) and by 18-24 h there are just clumps of cells remaining (fig 2.9e & f). An individual cell can be seen (indicated by an arrow) forming connections and joining the masses of cell bodies and another cell can be seen dividing in figure 2.9b indicated by a circle. It also appears that the density of cells decrease

over time- this may be due to the cells joining the cell clumps or dying over longer time periods on the gels.

Figure 2. 8 Phalloidin (actin) labelling in 3-D cultures

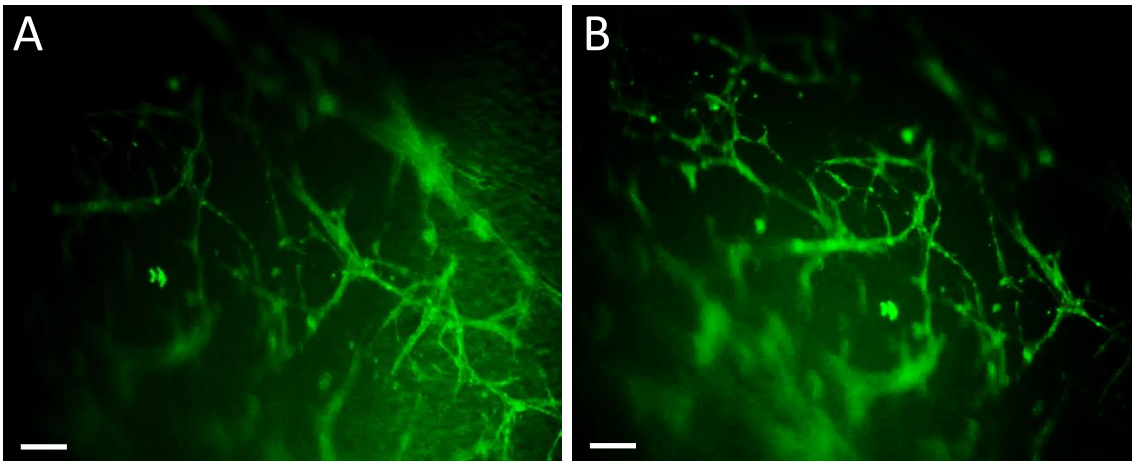

Figure 2.8 Actin labelling from a fluorescent microscope showing confocal stack images of cultured SLFs in a collagen I gel from P21 mouse one day after seeding. Images A & B at X10 magnification. Scale bar represents 20µm.

Figure 2. 9 Still images from 24-h time-lapse of SLFs seeded onto 3-D collagen.

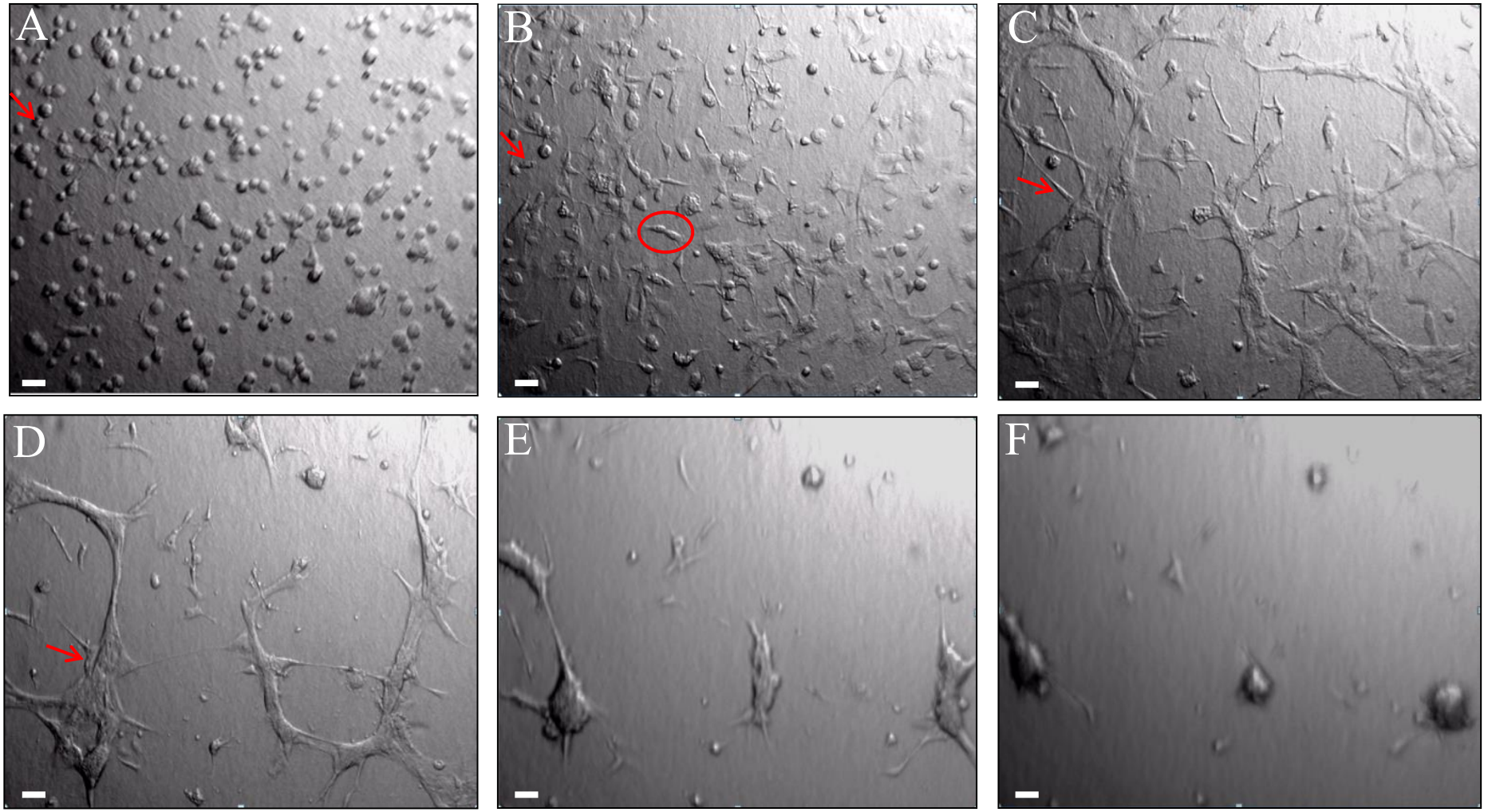

Figure 2.9 Still images from 24 hour time-lapse of SLFs seeded onto a 3-D collagen gel. Images taken just after seeding (A) at 1 hour (B) 6 hours (C) 12 hours (D) 18 hours (E) and 24 hours (F). Arrows highlights a specific cell forming connections and the circular highlights a dividing cell. Scale bar represents 50µm.

2.3.3 Age-dependent differences in growth rates

When comparing different ages to initiate 2-D cultures; the speed of growth was significantly greater in the younger (P10) mice when compared to the older mice (P22, fig. 2.10). Cells are seen growing from the ligament by day 3 in cultures derived from both P22 (fig. 2.10a) and P10 (fig. 2.10c). By day 6 there are significantly more cells in the cultures derived from P10 mice (fig. 2.10d) than those from P22 mice (fig. 2.10c).

Figure 2. 10 Comparison of growth of spiral ligament fibrocytes from a P22 and P10 mouse.

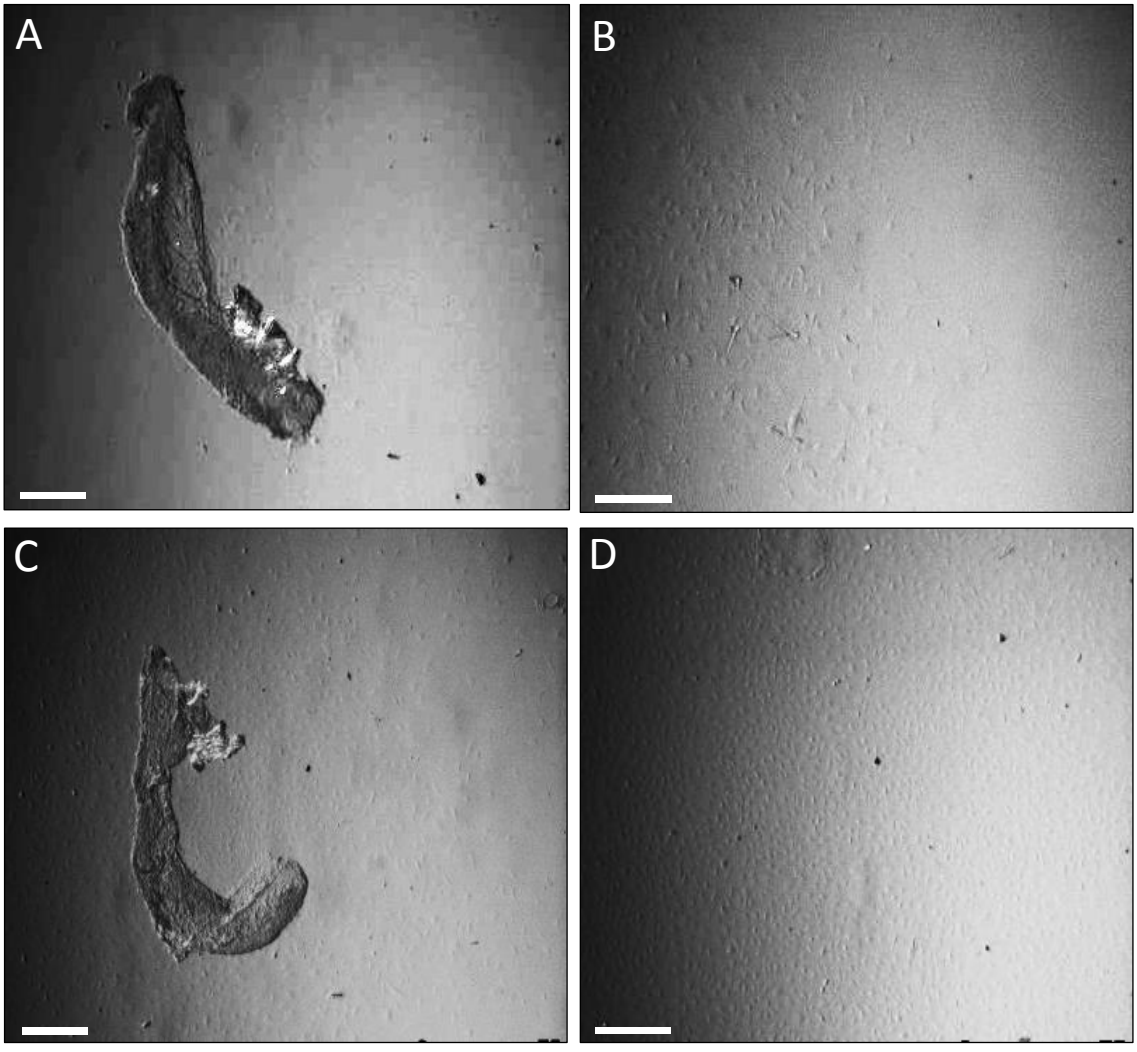

Figure 2.10 The initiation of cultures of spiral ligament fibrocytes from P10 and P22 CD/1 mice. Images taken of the same wells at day 3 and 6. Images A (P22 culture) & C (P10 culture) at day 3 with the corresponding image of the same wells at day 6 in B & D. All images taken at X4 magnification and scale bar represents 50µm.

As shown in the fig. 2.11 there was a significantly greater density of cells at both day 3 and 6 from P10 mice when compared to day 3 and 6 from P22 mice. By day 6 the P10 mice cultures are almost confluent, halving the confluency time of the older mouse cultures. The density of cells at day 3 in the cultures from P10 mice was significantly greater than the density of cells at day 3 from P22 mice (189.8 cells per mm^2±29.79, *n=3* verses 12.22 cells per mm^2±3.894, *n=3*, respectively; *p=0.0041*). The density of cells at day 6 in the cultures from P10 mice was significantly different to the density of cells at day 6 from P22 mice (400.4 cells per mm^2±98.29 verses 80.22 cells per mm^2±12.64, respectively; *p=0.0319*). There was no significant difference in the density of cells from the P10 mice at day 3 and day 6 (*p=0.1497*), however, there was a significant difference in the density of cells from the P22 mice at day 3 and day 6 (*p<0.0217*).

Figure 2. 11 Cell seeding/cell count graph for P10 and P22 mice cultures

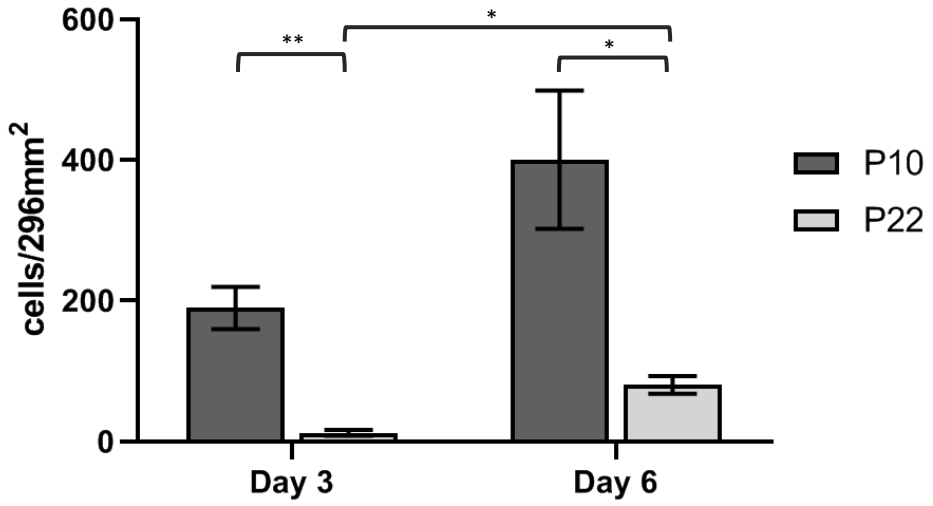

Figure 2.11 Bar graph showing difference in cell proliferation rates between cultures derived from P10 and P22 mice at day 3 (*n=3*) and day 6 (*n=3*). (Mean ± SEM).

2.3.4 Aquaporin (AQP1) and S-100 spiral ligament fibrocyte marker labelling

Results of immunolabelling experiments conducted on cultured fibrocytes in 2-D monolayers and 3-D gels (bright field of stained cells shown in fig. 2.12-D & 2.13-D) using antibodies against AQP1 and S-100 show expression of the water regulating membrane channel protein, AQP1 (fig. 2.12a & 2.13a) and the cytoplasmic calcium regulating protein, S-100 (fig. 2.12b & 2.13b). Merged confocal microscopic images show the cells expressing both AQP1 and S-100 (fig. 2.12c & 2.13b). These images clearly show that AQP1 and S-100 proteins are expressed in these cultured fibrocytes and it appears that the AQP1 seems to be most concentrated in the cell bodies and nucleus and the S100 more so punctate and cytoplasmic.

Figure 2. 12 AQP1 and S-100 marker protein expression in a monolayer culture of SLFs.

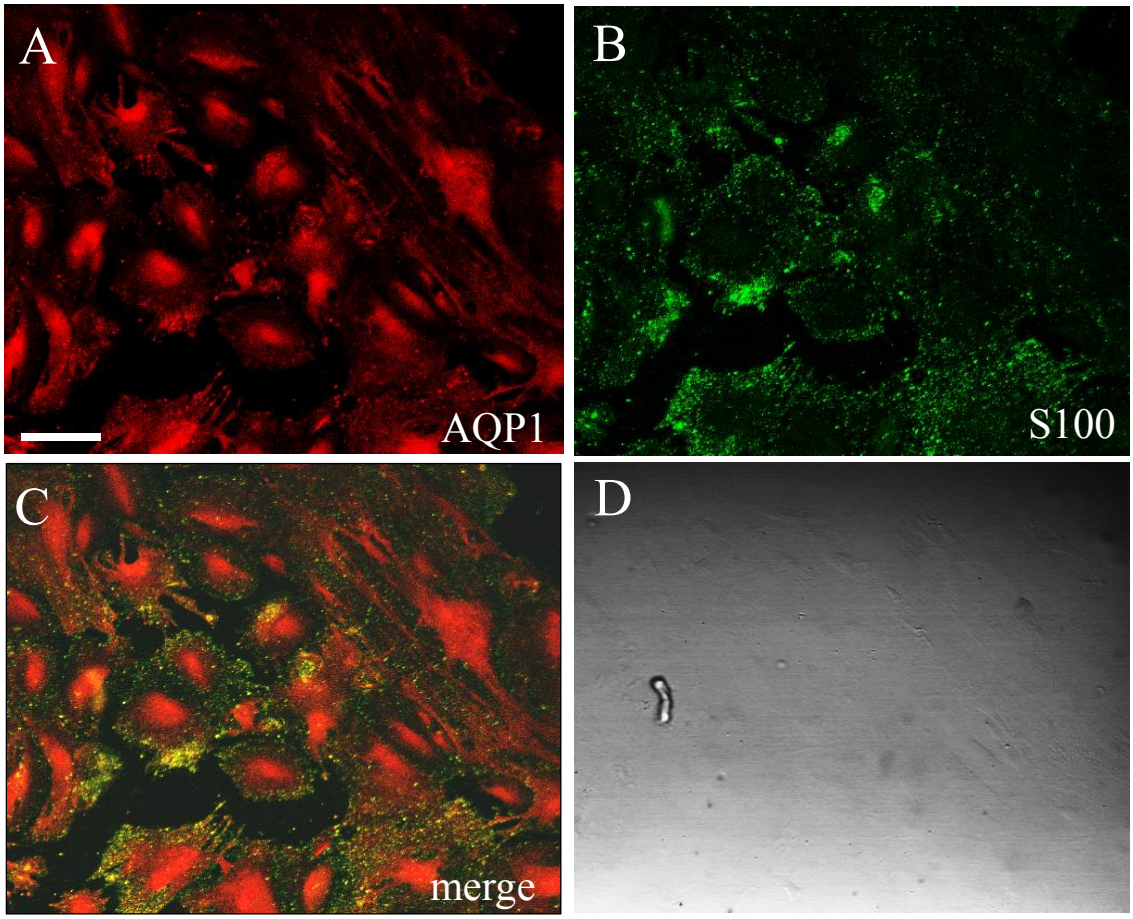

Figure 2.12 2-D cultured SLFs express marker proteins. Immunolabelling for the water channel, aquaporin (AQP1; a), and for the calcium binding protein, S-100 (b), is high in the monolayer cultured fibrocytes. The merged image in c shows that AQP1 and S-100 are both expressed in the same fibrocytes. A bright field image of the cultured fibrocytes is shown in d. Scale bar represents 10µm.

2.3.5 Repopulation of degenerated spiral ligament using cultured fibrocytes

As this was a preliminary study only two cochleae were used so labelling was conducted for the experimental and control conditions on pieces of ligament tissue from each. Nevertheless, the confocal results found through phalloidin labelling that the cultured SLFs were present in the decelluarised section of both ligament 1 and 2 from the experimental group seeded with a cell suspension of cultured SLFs (fig. 2.14a & e show light image and fig. 2.14b & f show corresponding confocal image) compared to the control group which was incubated with medium only where no cellular phalloidin labelling was present (fig. 2.14c & g show light image and fig. 2.14d & h show corresponding confocal image). Clear distinctive cell bodies can be seen in figure 2.14b& f with the morphology of the cells showing projections from the cell bodies making connections with other cells. In the control images (fig.2.14d& h) it appears fibrocytes are not present, however, blood vessels can be seen within the piece of spiral ligament with red blood cells in them.

Figure 2. 13 AQP1 and S-100 marker protein expression in cultured SLFs on 3-D collagen I gels

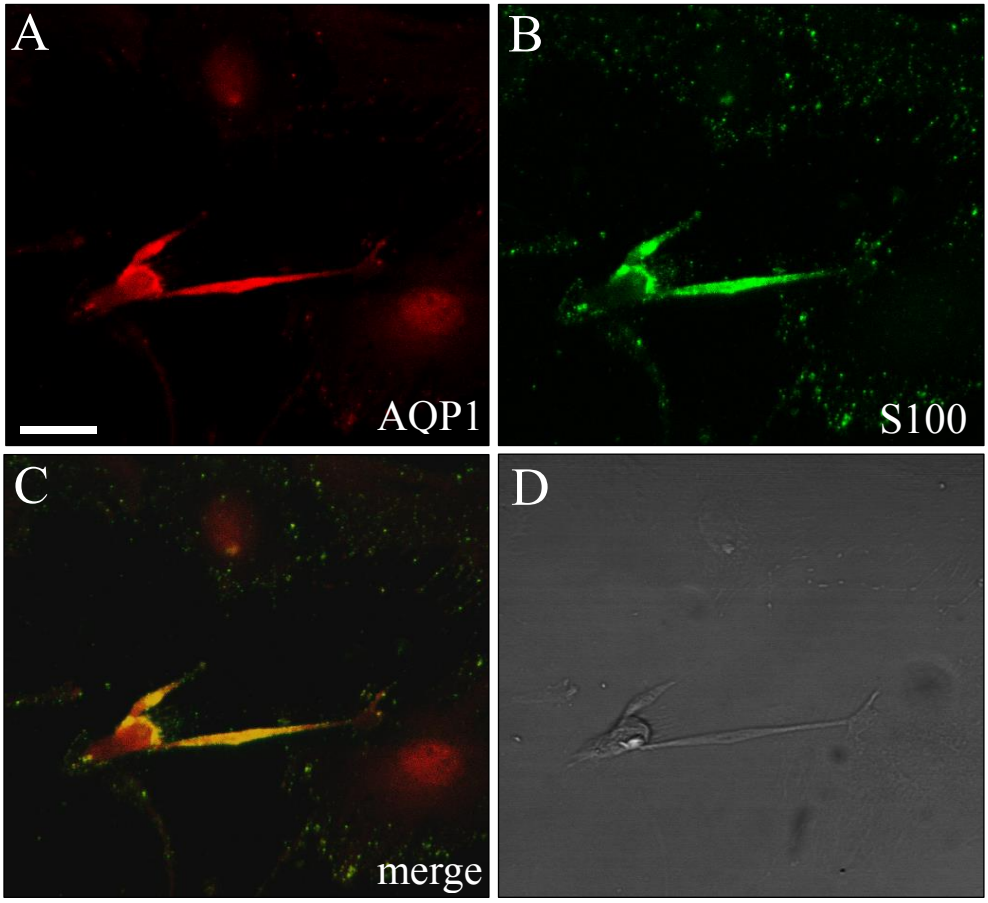

Figure 2.13 3-D cultured SLFs express marker proteins. Immunolabelling for the water channel, aquaporin (AQP1; a), and for the calcium binding protein, S-100 (b), is high in cultured fibrocytes. The merged image in c shows that AQP1 and S-100 are both expressed in the same fibrocytes. A bright field image of the cultured fibrocytes is shown in d. Scale bar represents 10µm.

Figure 2. 14 Actin labelling for cultured spiral ligament fibrocytes in two depopulated spiral ligaments.

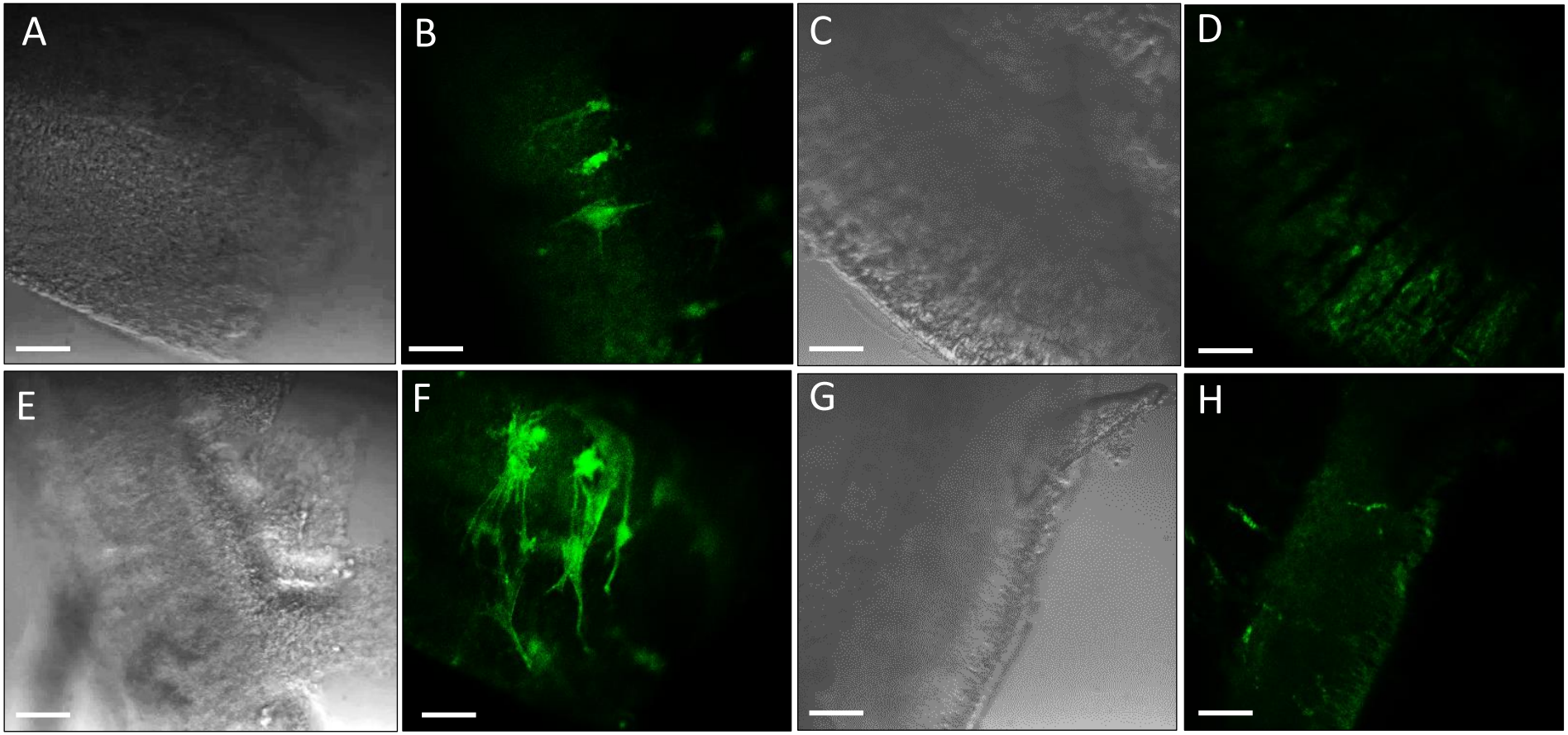

Figure 2.14 Confocal images showing actin labelling of cultured spiral ligament fibrocytes in two depopulated spiral ligaments, ligament 1 A to D and ligament 2 E to H. A, B, E, F show light microscope and confocal of spiral ligament incubated with spiral ligament fibrocyte cell suspension (experimental). C, D, G, H show light microscope and confocal of spiral ligament incubated with cell medium containing no cells (control). Scale bar represents 50µm.

2.4 Discussion

When trying to determine the mechanisms underlying cochlear homeostasis the spiral ligament presents a significant challenge. The complexity in the cell types within the ligaments limits the access of investigation though recording techniques, such as patch clamp electrophysiology. Cultured-cell lines offer a more accessible approach to characterise these cells. Here, using an alternative approach, SLFs were successfully derived and cultured in a 2-D and 3-D environment, to determine their characteristics as a prelude for supporting evidence in a potential cell replacement therapy. The cells in the 3-D environment were cultured within collagen as to mimic better the natural 3-D environment in which SLFs reside *in vivo*.

The expression of collagen types I, II, III, IV, V, IX, and XI in the inner ear has been reported (Cosgrove et al, 1996; Tsuprun & Santi, 1997; Asamura et al, 2005). Among these, collagen II has been detected in the spiral ligament (Thalmann, 1993; Dreiling et al, 2002; Asamura et al, 2005). Here, collagen I was used instead of collagen II due to difficulty getting collagen II to set, therefore trial experiments were conducted mixing collagen I and II.

Changes in substrate stiffness have been reported to cause a change in cell shape, where cells on compliant substrate retain a more rounded morphology and on a stiff substrate a flattened shaped, such as cells cultured on hard plastic in traditional 2-D techniques (Chen et al, 2008). Also, a compliant substrate directly reduces the stress at cell-matrix adhesions in an contracting cell which suppresses the normal maturation of focal adhesions and provides evidence that compliant substrates most likely supress certain types of signal while promoting others. Gel studies suggest that substrate stiffness can alter cellular functions such as migration, proliferation and differentiation (Lo et al, 2000; Peyton & Putnam, 2005; Leach et al, 2007; Li et al, 2007). Increasing substrate stiffness also appears to enhance proliferation of

cells and facilitates tumour progression (Paszek & Weaver, 2004; Wozniak et al., 2003; Georges & Janmey, 2005). MSCs differentiate into different lineage fates as a function of material stiffness, in a way that would promote tissue-specific healing (Engler et al., 2006).

Preliminary attempts to introduce suspensions of fibrocytes in isolated cochleae were not very effective (Mahendrasingam & Furness, unpublished observations). The results of the study thus far indicate that it is possible to culture SLFs on a 3-D collagen matrix thus enabling them to have a more 3-D morphology compared to 2-D cultures. This allows the cells to possess an *in vivo*- like morphology do to the cells exhibiting a rounded cell body and a more interconnected network of cells as opposed to a flatter cell within the 2-D culture within no obvious processes forming connections. This then indicates the 3-D environment makes the cultures SLFs more suitable for transplantation than 2-D cultured SLFs.

2.4.1 Optimisation of hydrogel construct for spiral ligament fibrocyte culture

The new design of the gel enabled a middle ground where a comprehensive study could be undertaken as cells seeded on top of collagen I gels could be accessed for patch-clamp electrophysiology performed whilst still providing the cells a 3-D environment. It has previously been shown that it is possible to make patch clamp recordings from isolated neurons at or near the surface of collagen gels (Coates & Nathan 1987; O'Shaughnessy et al, 2003).

2.4.2 Characterisation of 2-D monolayer cultured SLFs compared to 3-D gel cultured SLFs

The interactions in 3-D spatial arrangement affect a range of cellular functions, such as cell proliferation, differentiation, morphology, gene and protein expression, and cellular responses to external stimuli (Baharvand et al, 2006; Gurski et al, 2010; Szot et al, 2011; Baker & Chen, 2012; Price et al, 2012; Xu et al, 2012; Huang et al, 2013). The cell culture techniques in this study show that SLFs grown in a 3-D collagen environment possess a similar morphology to SLFs *in vivo* which, from *in situ* filled patch recordings in rat cochlea slice preparations, appear to be elongated with processes (Furness et al, 2009; Kelly et al, 2012). In contrast, those grown in a 2-D environment express a more flat and stretched out morphology as opposed to a more rounded 3-D appearance. The 3-D culture cells display processes appearing to form a network environment, therefore the 3-D environment enables the cells to make projections and cell-cell connections which more closely represents the native environment networks of cells forming gap junctions. It could be that putting the cells back into a 3-D environment, from the initial monolayer cultures, enables the cells to revert back to a more native-like morphology. If these 3-D cultured cells were used for transplantation back into the spiral ligament they would already possess the morphology require for function in addition to being embedded within a matrix that holds the cells within the specific area, where they can integrate back into the ligament.

The growth rates of 3-D cultures are more consistent with that of cells *in vivo* than 2-D culture environments as findings show tumour cells cultured in the 3-D environments grow more compared to the same cells cultures in 2-D environments (Gorlach et al, 1994) and the growth rates in 3-D more closely reflects the mathematical models of tumours *in vivo* than the growth rates of the cells in 2-D (Chignola et al, 2000; Gurski et al, 2010; Chitcholtan et al,

2012). In traditional 2-D monolayer culture, cells adhere and grow on a flat surface enabling these cells to receive a homogenous amount of medium during growth (containing nutrients and growth factors; Huang et al, 2013). This monolayer mostly contains proliferating cells, as necrotic cells are usually detached and removed during medium changes. This is consistent with the unpublished findings by Furness *et al* that the endoplasmic reticulum of 2-D cultured SLFs appear like immature SLFs meaning they could have a faster proliferation capacity, then at P14 begin to look distinct and mature-like. The slower proliferation rates and slower decrease in density of SLFs in the 3-D environment could be due to the medium not being able to penetrate the clumps of cells that form after a period of days grown on the gels and therefore nutrients, oxygen and growth factors may not reach the cells inside the core causing them to become quiescent or hypoxic, whereas those in the outer layers are more exposed to the medium so are less challenged by the conditions. Current 3-D constructs still lack the complex *in vivo* vascular system that provides the tissues with oxygen, nutrients and waste removal. In the 3-D cultured cells these processes are only possible through diffusion.

2.4.3 Faster growth of SLF cultures from younger aged mice

The difference here between the growth rates of the P10 and P22 cultures show that the SLFs cultured from the younger mice grow at a significantly greater speed than the older mice cultures. It may be that the younger mouse and younger/immature fibrocytes have a greater regeneration capacity and thus may be more useful as a cell replacement when compared to older cultures. This finding in consistent with studies showing adult hematopoietic stem cells (HSCs) and adult MSCs which have a decreased ability to self-renew and differentiate (Lang et al, 2003; Roobrouck et al, 2008).

A decrease in fibrocyte proliferation was found in the spiral ligament of an aged gerbil cochlea (35-37 month, when compared to a 6 month old young gerbil), significantly only in

type II and IV fibrocytes (Lang et al, 2003). This decrease in the turnover of type II and IV spiral ligament fibrocytes in aged cochleas may be related to the decrease of ion-transport enzymes found in the lateral wall of aged animals. For instance immunostaining of Na^+K^+ATPase is significantly reduced in type II and IV fibrocytes in aged cochleas (Schulte & Schmiedt, 1992; Spicer et al, 1997; Lang et al, 2003). A decreased cell turnover in type I and IV fibrocytes may lead to fewer surviving cells and potentially be responsible for the reduced immunostaining of Na^+K^+ATPase. Moreover, recently it has been found that most dividing cells in the lateral wall are located in the spiral ligament before P28 and cycle slowly as long as P72 days, and the number of dividing cells declines as the mice aged (from P13 to P72; Li et al, 2017; 2018). Therefore, this age-related decrease in cell proliferation may well be a causal factor in the loss of EP due to loss of function in the potassium recycling within the cochlea, and consequently a cause of associated metabolic presbyacusis.

2.4.4 Marker protein expression in 2-D monolayer and 3-D cultured fibrocytes

The identity of these 2-D monolayer and 3-D cultured cells could be verified immunocytochemically with marker proteins known to be expressed in different types of fibrocytes. The positive immunolabelling in both the 2-D and 3-D for AQP1 and S-100 show that in these cultures labelled for both but predominantly for AQP1. It therefore may be possible that these cultures are of a mixed phenotype with partial type III properties. AQP1is a marker for type III fibrocytes in mice (Li & Verkman 2001; Huang et al, 2002; Carbey & Age, 2009; Kelly et al, 2012) and the calcium binding protein S-100 (Donato, 2001) is strongly expressed in types I, II and V fibrocytes (Mahendrasingam et al, 2011a). The positive labelling for AQP1 and S-100 implies that the cultured cells still retain their functions of water regulation and calcium regulation. Aquaporins are proteins that facilitate water permeability for osmotic movement which is essential for fluid ionic transport and

homeostasis at their expression sites (Stankovic et al, 1995). It may also function in type III fibrocytes to regulate hydrostatic pressure within the spiral ligament, alongside its tension regulation of basilar membrane (Kelly et al, 2012).

Additionally, type III fibrocytes have recently been found to possess a stem cell proliferation capacity as well as a protective capacity from degeneration that compensates for the other degenerating fibrocyte types. This aligns with the findings of a predominantly type III mixed phenotype culture as they may 'take over' as the other types die out and this characteristic may contribute to the endogenous regeneration of the lateral wall *in vivo* (Li et al, 2017; 2018). It is possible that there may be redundant systems in the lateral wall for K^+ recycling and EP generation, so that other fibrocyte subtypes can take over functionally when certain fibrocytes are damaged or degenerated. Thus type III fibrocytes may be the key target for future regenerative therapies to combat age related hearing loss alongside their established contractility function of regulating the tension of the basilar membrane (Kelly et al, 2012).

2.4.5 Spiral ligament repopulated with cultured SLFs after decellularisation *in vitro*

In this preliminary study we demonstrated that a decellularised spiral ligament could be repopulated with a cell suspension of cultured SLFs. The purpose of this was to investigate whether it is feasible to regenerate the ligament with these cultures as an approach to a cell replacement therapy. The cultured SLFs found to be present by actin labelling appeared to have migrated into the dissected spiral ligament. This confirms the repopulation and migration properties of these SLFs cultures strengthening the idea that they could be suitable for a cell-replacement therapy to treat age-related hearing loss. Previous *in vivo* studies have used toxin models to repopulate the spiral ligament by transplanting mesenchymal stem cells into the semi-circular canal of which a number where detected in the injured area of the lateral

wall (Kamiya et al, 2007; Kasagi et al, 2013). One group found significantly higher hearing recovery in the transplanted group compared to controls (Kamiya et al, 2007). However, firstly these models were toxin models that do not reflect the process of natural circumstances of SLFs loss. Secondly, there were problems of migration and differentiation of the transplanted stem cells as some grew ectopically. Moreover, the differentiation of the MSCs into fibrocyte-like cells was demonstrated by connexin26 labelling, which although is expressed in SLFs, is also expressed in other cells in the inner ear, therefore is not a specific marker of SLFs.

Although these studies were more developed than this preliminary experiment, it highlights the potential for using this decellularisation and recellularisation technique. This technique has been successful in the repopulation of decellularised tissue for heart valve engineering and kidney repopulation (Chani et al, 2017; Destefani et al, 2017; Roosens et al, 2017). Using differentiated cultured SLFs and transplanting them directly into their native area of the spiral ligament may be an optimal approach, thus removing any issues of migration or differentiation enabling maximal opportunity for them to fulfil their function in the maintenance of hearing.

2.4.6 Conclusion

To conclude, a mixed phenotype SLF culture with properties of partial type III has been successfully established and grown in a 3-D collagen I gel environment provides a native-like environment where SLFs develop a degree of native morphology and characteristics. The proliferation of these SLFs is faster in younger mice cultures compared to older mice cultures. The collagen gel 3-D environment here provides a transplantable matrix environment where

they could be easily manipulated and placed directly into the spiral ligament *in vivo*. The preliminary recellularisation experiment indicates it may be possible repopulate a degenerated ligament with cultures SLFs. These predominantly type III SLFs cultures can be used to be assessed further to determine whether they can be used as a therapeutic target for a cell replacement therapy to treat metabolic age-related hearing loss. The next chapters will build upon and explore further assessments of these cells to determine their functionality. To acquire deeper insights into the functionality of cultured spiral ligament fibrocytes, their protein profile and electrophysiological signature will be explored in the following chapters.

.

Keele UNIVERSITY

Chapter 3

Characterisation of Spiral Ligament Fibrocytes by Immunolabelling

3. Chapter 3- Immunolabelling of Spiral Ligament Fibrocytes

3.1 Introduction

SLFs function in cochlear homeostasis and in the maintenance of the EP through their involvement in K^+ recycling. The degeneration of fibrocytes contributes to hearing loss (Okamoto et al, 2005; Antje et al, 2019), perhaps through loss of the EP. The functional characterisation of cochlear fibrocytes has been achieved by the discovery of the expression of proteins in the nonsensory regions in the cochlea involved in K^+ transport in the lateral wall (Liang et al, 2003; 2004; Shen et al, 2004; Hibino et al, 2004; Pan et al, 2016). Fibrocytes express different combinations of water and ion channels, carbonic anhydrases II and III (Stankovic et al, 1995; Sakaguchi et al, 1998; Liang et al, 2003; Hibino et al, 2004; Shen et al, 2004; Pan et al, 2016), and gap junction connexins 26, 30, 31 (Forge et al, 1999; Xia et al, 2000), depending on their role in water and ionic transport.

The inwardly rectifying K^+ channel, Kir4.1 is distributed in the *stria vascularis* and critically contributes to the formation of a positive EP (Hibino et al, 1997; 2010; Marcus et al, 2002). In renal epithelia (Tucker et al, 2000; Lourdel et al, 2002) and retinal Müller cells (Ishii et al, 2003), heteromeric assembly of Kir4.1 and a Kir channel subunit, Kir5.1, occurs and forms a functional channel. It has previously been found that the Kir5.1 subunit is strongly expressed in type II, IV and V fibrocytes in the spiral ligament, whilst in the lateral wall Kir4.1 is expressed in the *stria vascularis*, the spiral ganglion area, and supporting cells in the organ of Corti (Hibino et al, 1997; Hibino et al, 1999; Ando & Takeuchi, 1999; Takeuchi et al, 2001).

A difference in the time-course of developmental expression between Kir5.1 and Kir4.1 has also observed as well as a decrease in Kir5.1 expression levels in cochlea of ageing C57BL/6J mice (Hibino et al, 2004; Pan et al, 2016), suggesting distinct and unique roles in

the K^+ movement within the cochlea. In the spiral ligament, fibrocytes are bathed in perilymph and express Kir5.1 homomeric channels predominantly in the cytoplasm where it is believed not to form functional channels on the membrane surface of the cell (Grosse et al, 2003; Hibino et al, 2004; 2010). Most of these channels appear to be localised in intracellular compartments. However, since perilymphatic perfusion of Ba^{2+} (Barium) slightly increases the EP, it is possible that a small number of the Kir5.1 homomers on the ligament plasma membrane could negatively regulate K^+ circulation and prevent the cochleas overshoot, as with the exit of K^+ the cell overshoots the membrane potential and hyperpolarises (Hibino et al, 2004; Marcus, 1984).

As opposed to a heteromeric Kir4.1/Kir5.1 channel that is stable and functional on the plasma membrane of various cells, homomeric Kir5.1 subunits believed to be endocytosed and internalised through the membrane surface and do not carry any current (Tanemoto et al, 2002). It is reported in PC12 cells, that high K^+ solution activates protein-kinase A (Salvatore et al, 2001), the concentration of K^+ in the extracellular solution surrounding fibrocytes could be a controlling factor in the functional expression of Kir5.1 on the plasma membrane. After cessation of the protein-kinase A-mediated signalling, unphosphorylated Kir5.1 in the cytoplasm would be recruited to the plasma membrane, where binding to the anchoring proteins could restore the negative control mechanism. The cochlea may use the two distinct Kir channel subunits, Kir4.1 and Kir5.1, in different ways to attain adequate K^+ circulation for the EP formation in the lateral wall.

Another potassium channel is the BK channel, a universally expressed large conductance calcium- and voltage-activated K^+ channel (Meera et a, 1997) with the ability to integrate changes in intracellular calcium and membrane potential (Butler et al, 1993; Pallanck & Ganetzky, 1994). This makes the BK channel an important negative feedback system linking increases in intracellular calcium to outward hyperpolarizing potassium currents. Thus, the

channel has many important roles, including regulation of neurotransmitter release, neuronal excitability and smooth muscle tone (Salkoff et al, 2006). It has been shown that BK channels are also present in inner hair cells (Pattillo et al, 2001), the hair cells responsible for transducing sound to electrical impulses used in signaling to the central nervous system. These hair cells express a potassium current pharmacologically similar to BK channels, showing sensitivity to TEA (Kros & Crawford, 1990; Kros et al, 1998; Pyott et al, 2004; Skinner et al, 2003; Hafidi et al, 2005).

The BK channel has been identified and characterised in cultured type I SLFs and freshly isolated type I SLFs, and these fibrocytes have been found to have a dominant K^+ membrane conductance mediated by these BK channels (Liang et al, 2003; Shen et al, 2004). This, therefore, suggests that the cells have a crucial role in the K^+ recycling and regulation of the electrochemical gradient in the lateral wall (Wangemann, 2002).

Gap junction mediated intercellular communication is important in the maintenance of the unique ionic composition of the endolymph and intracellular ion content, both of which are essential for cochlear function. Connexins are transmembrane proteins which form the channels that enable transport of ions between cells, called gap junction proteins (reviewed in Kikuchi et al, 2000). Connexin26 is involved in anionic permeability and is key in intercellular signalling (Yamaguchi et al, 2014). It is associated with hereditary deafness in humans and hearing impairment in mice (Cohen-Salmon et al, 2002), and a mutation in the connexin26-encoding (GJB2) gene is predicted to cause 20-50% of human non-syndromic hereditary deafness cases (Yamaguchi et al, 2014). The proteins disruption in the spiral ligament is linked to be a causal and significant factor of presbycusis (Ichimiya et al, 2000).

The expression pattern of connexin31 is detected in type I, III and IV SLFs and coincides with hearing loss mainly of higher frequencies (Xia et al, 1998; 2000; Lòpez-Bigas et al,

2002). Connexin30 is present in the lateral wall and connexin26 is observed in type I, II and V fibrocytes, and connexin30 detection is especially high in type II fibrocytes at the spiral prominence, and in type V fibrocytes at the apical tip of the spiral ligament (Kasagi et al, 2013). It has also been found in an adult guinea pig that type III fibrocytes express connexin43, which are involved in the ion trafficking pathway (Kelly et al, 2012).

Disruption of the connexin26 gap junction system complex adversely affects K^+ recycling from the hair cells base through the supporting cells and cochlear SLFs (Lefebvre et al, 2002). Research using an *in vivo* model of hearing loss caused by intense noise exposure, as well as an *in vitro* system of SLF primary cultures, found that the prolonged decrease in levels of the gap junction proteins, connexin26 (in type I SLFs), connexin30, and Na^+ K^+- ATPase activity occurred in structures of the lateral wall prior to hearing loss caused by acoustic overstimulation. This also resulted in the dysfunction of the intracellular communication between SLFs. Therefore a decrease in connexins and Na^+ K^+- ATPase activity causes a disruption of the ion-trafficking system in cochlear SLFs. Moreover it has also been found spiral ligament connexin26 density reduces with age despite no strial atrophy or Na-K-ATPase reduction being detected (Ichimiya et al, 2000), which suggests that spiral ligament gap junction dysfunction could take place prior to *stria vascularis* dysfunction in an ageing organism.

The aim of this part of the project was to identify and compare some of the relevant protein channels and transporters involved in the K^+ transport function in the cultured and native SLFs, specifically connexin gap junction proteins, and specific potassium channel proteins. Building this protein profile will help to strengthen the case as to whether these cultured SLFs express the same proteins as native SLFs and therefore may be a potential cell replacement therapy to treat age-related hearing loss.

3.2 Methods

3.2.1 Immunocytochemical labelling for cells on collagen gels

Cells cultured on 3-D collagen I gels and native cells in cochlear wax sections were labelled for various channels following the protocol described in section 2.2.3.10 using the antibodies shown in table 3.1 below.

Table 3. 1Antibody table

Protein	Primary antibody species and dilution	Secondary antibody species and dilution
Kir5.1 (Abcam, UK)	Rabbit 1:100	Goat anti-rabbit 1:50
BK (Alomone labs, Israel)	Rabbit 1:100	Goat anti-rabbit 1:50
Connexin26 (Abcam, UK)	Goat 1:100	Donkey anti-goat 1:50
Connexin31 (Alpha diagnostics, USA)	Rabbit 1:100	Goat anti-rabbit 1:50

Table 3.1 A summary of the marker proteins with primary and secondary antibodies used with their species and dilutions.

3.2.2 Cochlear fixation and embedding in paraffin wax for sectioning

The cochlea was embedded in paraffin wax to allow sectioning to improve the access of dyes and antibodies and reduce the overlay of different cell layers. Wax embedding was also used due to it being the most optimal way to retrieve intact sections of the cochlea, as this bony structure would experience structural difficulties (crumbling) without embedding. CD/1 mice were deeply anesthetised following the same procedure as stated earlier (in section 2.2.2) in tissue preparation and cell culture. The bullae were opened and each cochlea was perfusion-fixed in 4% paraformaldehyde in 0.1 M sodium phosphate buffer (PB), pH 7.4, through a small whole made in the apex and base of the cochlea, then immersed in the same fixative for 2 h at room temperature. Next, the cochleae were washed in distilled water X3 for 10 min before being immersed and decalcified in 5.5% (5 mM) ethylene diamine tetra acetic acid

(EDTA) in 0.1% PFA solution for a minimum of 72 h. They were then dehydrated in a graded series of ethanol concentrations for 1.5 h each (50%, 70%, 80%, 90%, 100% and dry 100%). Each cochlea was then left in xylene for 1 h and again in fresh xylene for a further hour. The cochleae were then infiltrated through four changes of fresh molten paraffin wax (Agar Scientific, Stansted, UK) for 2 h each time at 75 ^{o}C before being mounted in a mould and embedded in fresh molten wax solidified by cooling in a refrigerator. The wax block was trimmed around the cochleae and sectioned at 10 µm using a Reichert-Jung 2040 wax microtome (Vienna, Austria). The sections were then mounted onto drops of water on glass slides and dried on a hot plate.

3.2.3 Histological staining of cochlear wax sections

Toluidine blue staining of wax sections of the section of cochlea were undertaken to review the histology of the spiral ligament before labelling to have an overview of the arrangement in that particular slice. Sections were deparaffinised and then stained. First xylene was used twice for 3 min each time and then slides were rehydrated using decreasing concentrations of ethanol first with xylene: ethanol 1:1 for 3 min, then 100% dry ethanol, 100% ethanol, 95% ethanol, 70%, 50% for 1 min each, then distilled water for 1 min. The sections were stained in toluidine blue 0.1% for 5 min then taken back through the solutions to xylene for the same times with the exception of the 95% ethanol in which they were left for 3 min. DPX (dibutylphthalate polystyrene xylene); a synthetic non-aqueous mounting medium was added followed by a coverslip.

3.2.4 Immunolabelling of cochlear wax sections

For immunofluorescence labelling, the same protocol as for histology staining was followed up to the distilled water step. After this was reached the sections were placed in a moist chamber and labelled using the same procedure as the immunolabelling of the gels.

Quantifying the labelling intensity enabled analysis of labelled protein distribution across different structural compartments and the labelling intensity of those compartments. The samples were analysed using Photoshop 7.0 software on a cochlea section where a fixed circle was used to measure the mean pixel intensity at 5 random areas from each the apical, middle and basal spiral ligament and averaged for each region.

3.2.5 Confocal fluorescence microscopy imaging

Imaging was carried out as described in section 2.2.4.

3.2.6 Statistics

Data were analysed using GraphPad Prism statistical analysis software (version 5.0). All data are expressed as mean ± standard error of the mean (S.E.M.). Tests for normal distribution and equal variance were conducted to determine the suitable parametric or un-parametric test to be used. The analysis of variance and t-tests used to examine the significance of these data were calculated using GraphPad prism. Labelling intensity represents the pixels in 5 random areas within the labelled images. Unless otherwise stated, significance was assessed at the 5% level ($p< 0.05$*); $p<0.01$**; $p<0.001$***; and $p<0.00001$ indicate significance, shown across groups by bars.

3.3 Results

3.3.1 Histological labelling of cochlea wax sections reveals turns of spiral ligament

Whole-mount immunohistochemical examination of an adult mouse cochlea shows the orientation of the cochlea within the slices of wax sections (fig. 3.1). The apical, middle and basal spiral ligaments are easily seen in the turns of the cochlea (fig. 3.1). This histology labelling then set a guide for the following immunolabelling in the cochlea wax sections.

Figure 3. 1 Toluidine blue histology staining

Figure 3.1 Toluidine blue staining of a cochlea wax section clearly shows turns of the cochlea and reveals the apical, middle and basal spiral ligaments. SL- spiral ligament, *SV- stria vascularis,* BM- basilar membrane, TM- tectorial membrane, RM- reissners membrane, oC- organ of Corti. Scale bar represents 50µm.

3.3.2 Kir5.1 channel protein expression in cultures

An antibody was used to examine the expression of the inwardly rectifying Kir5.1 protein channel in mouse cultured fibrocytes on 3-D gels. Immunocytochemistry of the cultured fibrocytes was analysed using a confocal microscope, and revealed positive labelling for the Kir5.1 potassium channel (fig. 3.2). Kir5.1 immunoreactivity was found to be diffusely distributed within each fibrocyte. Expression of Kir5.1 was observed at in the membrane and also in the cell cytoplasm.

Figure 3. 2 Cultured SLFs express the Kir5.1 potassium channel

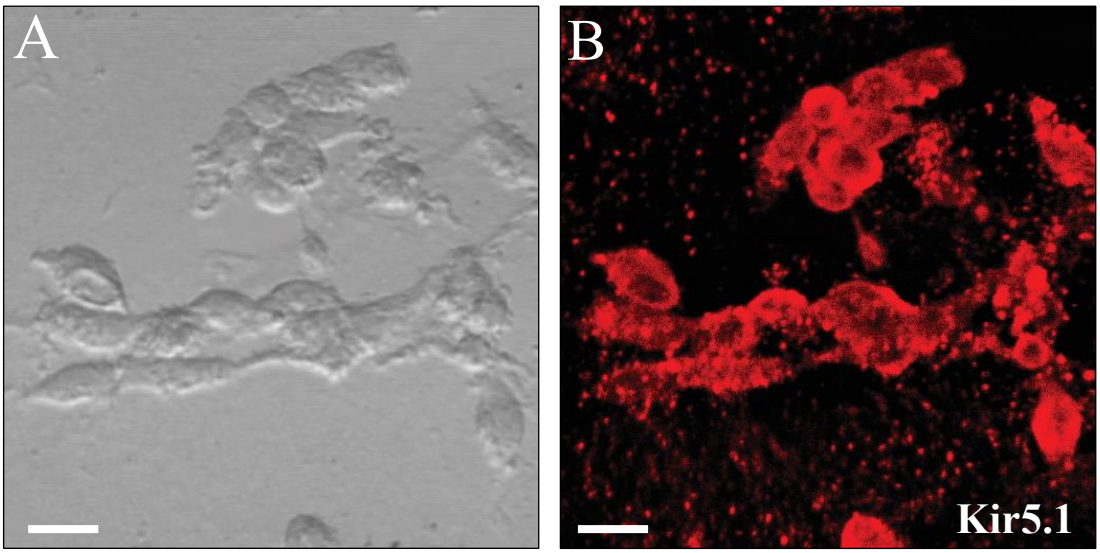

Figure 3.2 Cultured fibrocytes express Kir5.1. Immunolabelling for the potassium channel Kir5.1. Bright field images shown in **a** and **b** shows the confocal image. Scale bars in **a** & **b** represent 10μm.

3.3.3 Kir5.1 channel protein expression in cochlear wax sections

Kir5.1 immunoreactivity was detected in all turns of the cochlear lateral wall. The immunofluorescence technique showed the Kir5.1 immunoreactivity appeared in type III areas, along the back of the spiral ligament in the wax sections of the mouse cochlea (fig.

3.3b). It was expressed in most areas of the ligament indicating moderate expression in all types of fibrocytes. Labelling intensity was significantly greater in the type III area of the ligament compared to any of the other areas containing the other fibrocytes types (fig. 3.4). Pixel intensity was significantly greater in the type III area compared to the type I area (175.3 pixels ±9.776, *n=5 versus* 29.18 pixels ±2.883, *n=5,* respectively, *p<0.0001*). It was also significantly greater compared to the type II area (87.53 pixels±9.983, *n=5*, *p<0.0001*) as well as when compared to type IV (71.30 pixels ±6.714, *n=5*, *p<0.0001*) and type V (44.99pixels± 8.026, *n=5*, *p<0.0001*). Labelling intensity was also significantly greater in the type II area when compared to type I (*p<0.0001*) and to type V (*p=0.0038*). Moreover, labelling intensity in type IV area was significantly greater than in type I area (*p=0.0042*).

Figure 3. 3 Immunohistochemical labelling for cochlea wax sections for Kir5.1 potassium channel.

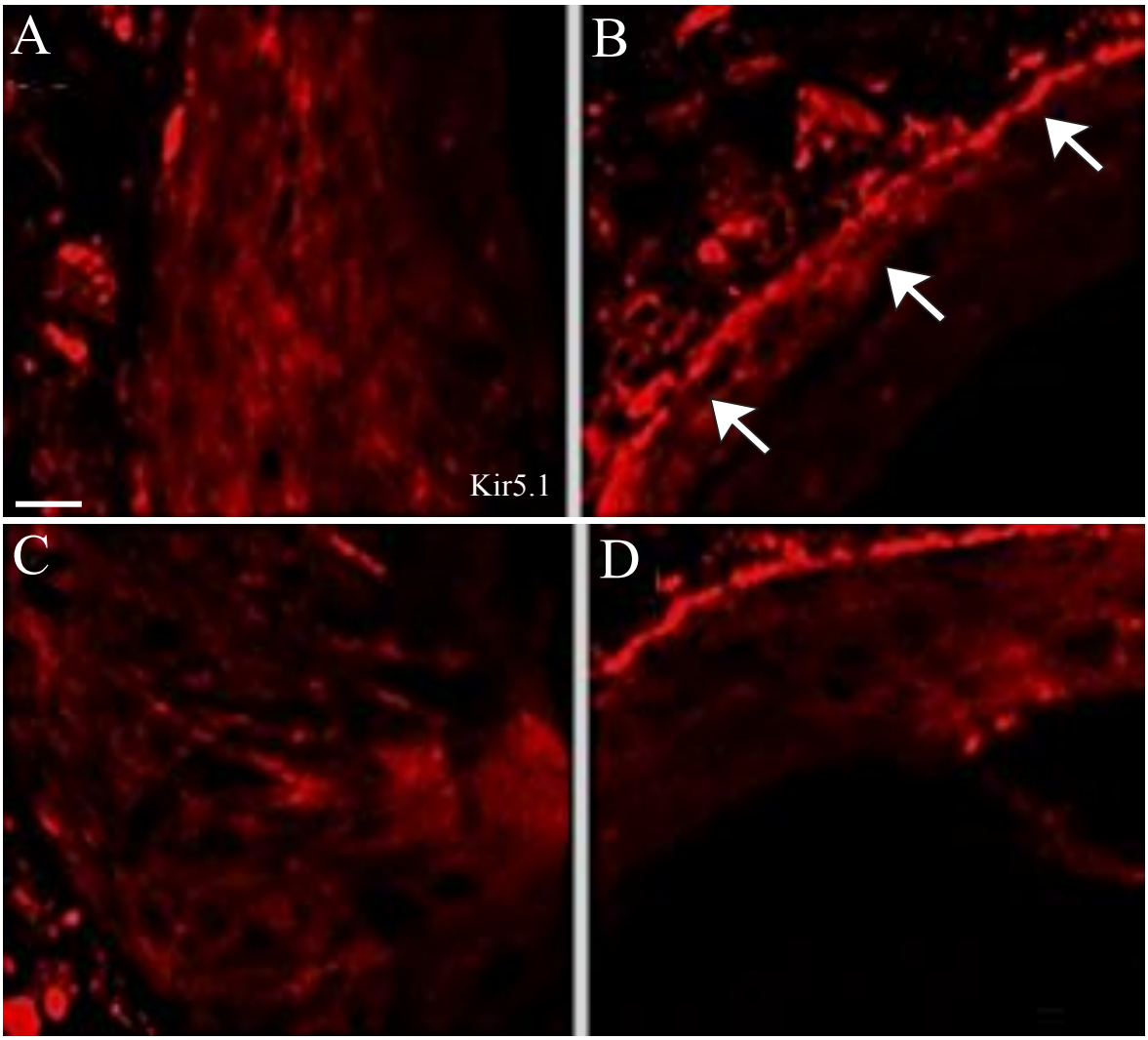

Figure 3.3 Immunohistochemical labelling of a cochlea wax section for Kir5.1. Kir5.1 positively stained in most areas of the spiral ligament. **A** shows labelling in the type II area, **B** in the type III area, **C** in the type IV area and **D** in the type V area. Scale bar represents 30µm.

Figure 3. 4 Cell fluorescence of Kir5.1 labelling in cochlea wax sections.

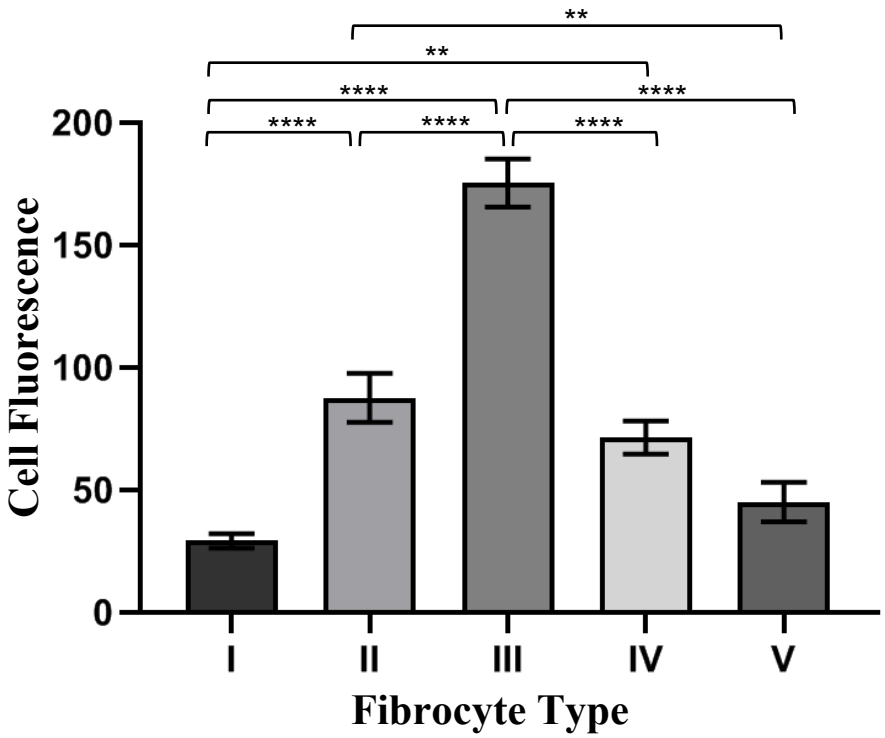

Figure 3.4 Cell fluorescence pixel intensity in the different areas where types I to V fibrocytes reside. Mean ±SEM, *n=5*.

3.3.4 BK protein channel expression in cultured SLFs

A specific antibody against the big conductance voltage-gated BK protein channel was used to examine the expression of BK in cultured fibrocytes in 3-D gels. Immunocytochemistry of cultured fibrocytes obtained with a confocal microscope shows positive labelling for the Ca^{+}-activated potassium channel, BK (fig. 3.5). The expression appears to be more global and cytoplasmic as opposed to membrane specific. The bright spots in figure 3.5a could indicate some form of potential contamination of the gel or could be a reflection of the 'sticky' nature of the gel.

Figure 3. 5 Immunohistochemical labelling for BK potassium channel in cultured SLFs

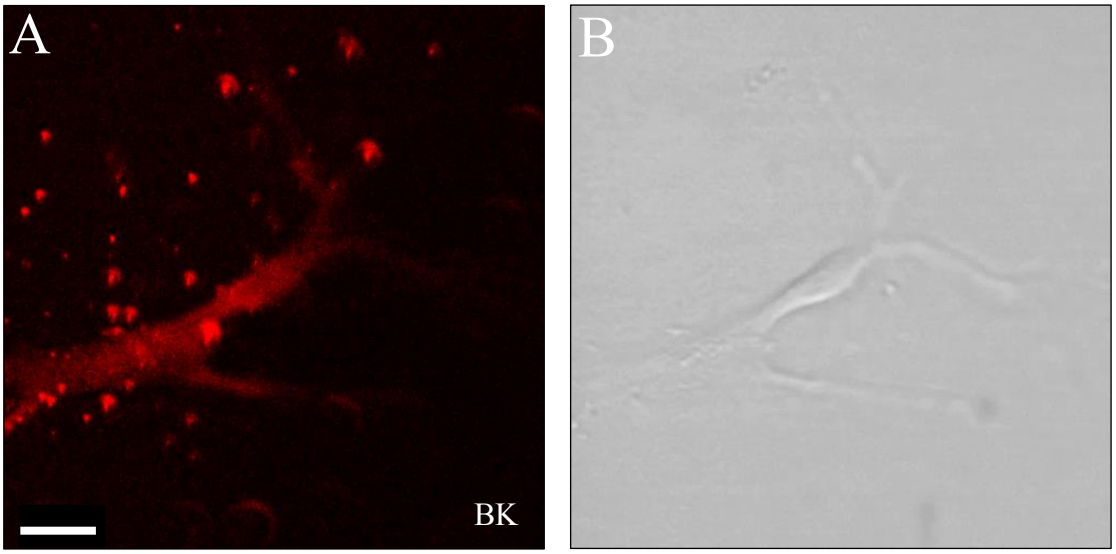

Figure 3.5 Immunolabelling in cultured SLFs for the large conductance calcium-activated potassium channel, BK (a). Bright field image shown in (b). Scale bar represents 10μm.

3.3.5 BK protein channel expression in native cochlea wax sections

Immunolabelling for the Ca^{+} activated potassium channel in the wax sections was inconclusive (fig. 3.6). BK labelling was seen in all areas of the spiral ligament, but it was also observed in the rest of the lateral wall, stronger in the *stria vascularis*, and in all of the organ of Corti (fig. 3.6a).

Figure 3. 6 Immunohistochemical labelling for BK potassium channel in cochlea wax sections

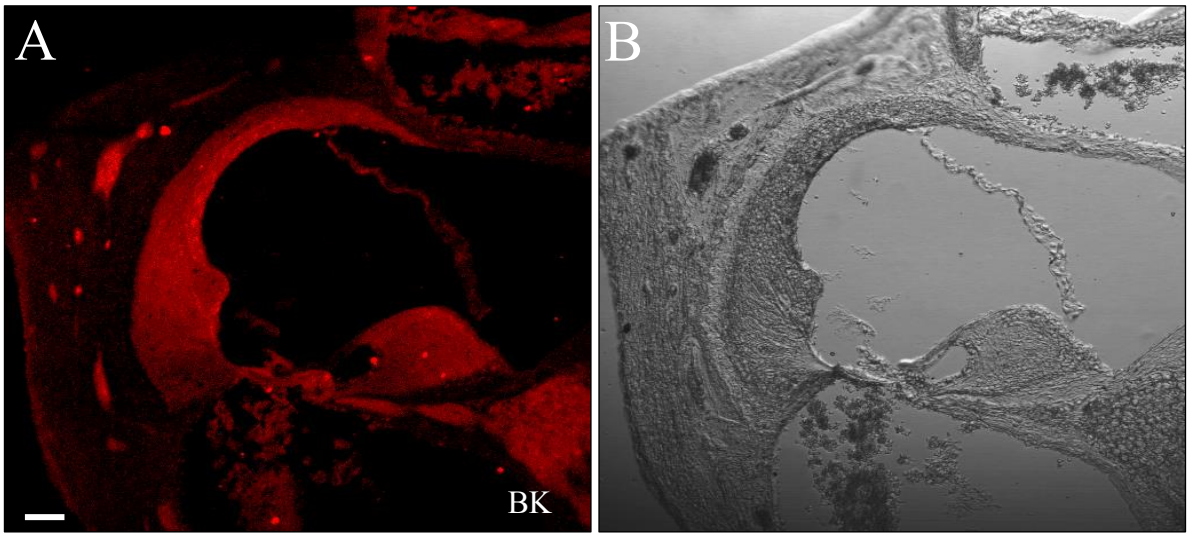

Figure 3.6 Immunolabelling of lateral wall wax cochlea section for the large conductance calcium-activated potassium channel, BK (a). Bright field image shown in (b). Scale bar represents 500μm.

3.3.6 Connexin26 and connexin31 gap junction protein expression in cultures

Positive immunocytochemical labelling for connexin26 and connexin31 was seen in the cultures (fig. 3.7). Some of the cultured cells were found to express both connexin26 and connexin31 (merged image in fig. 3.7c), some areas appeared to express more green fluorescence therefore may possess more connexin26, and some expressed more red fluorescence and may possess more connexin31. There were some cells that were unlabelled, suggesting they expressed neither connexin.

Moreover, the same connexin26 and connexin31 labelling was seen in two cells connected by their projections and this labelling was more intense in this area of potential gap junctions where the cell projections join (fig 3.8). The mean pixel intensity (fig. 3.9) of the labelling of the cell body on the left was significantly different from that along the gap junctional area

(142.5 pixels ±12.27 and 206.9 pixels ±6.201, respectively, *p=0.0016*). The mean pixel intensity of the labelling of the cell body on the left was significantly different from that along the cell body on the right (142.5 pixels ±12.27 and 190.6 pixels ±18.41, respectively, *p=0.0116*). There was no significant difference in the mean pixel intensity between the gap junction area and the right cell body (*p=0.1524*).

Figure 3. 7 Immunocytochemical labelling for gap junction proteins in cultured SLFs.

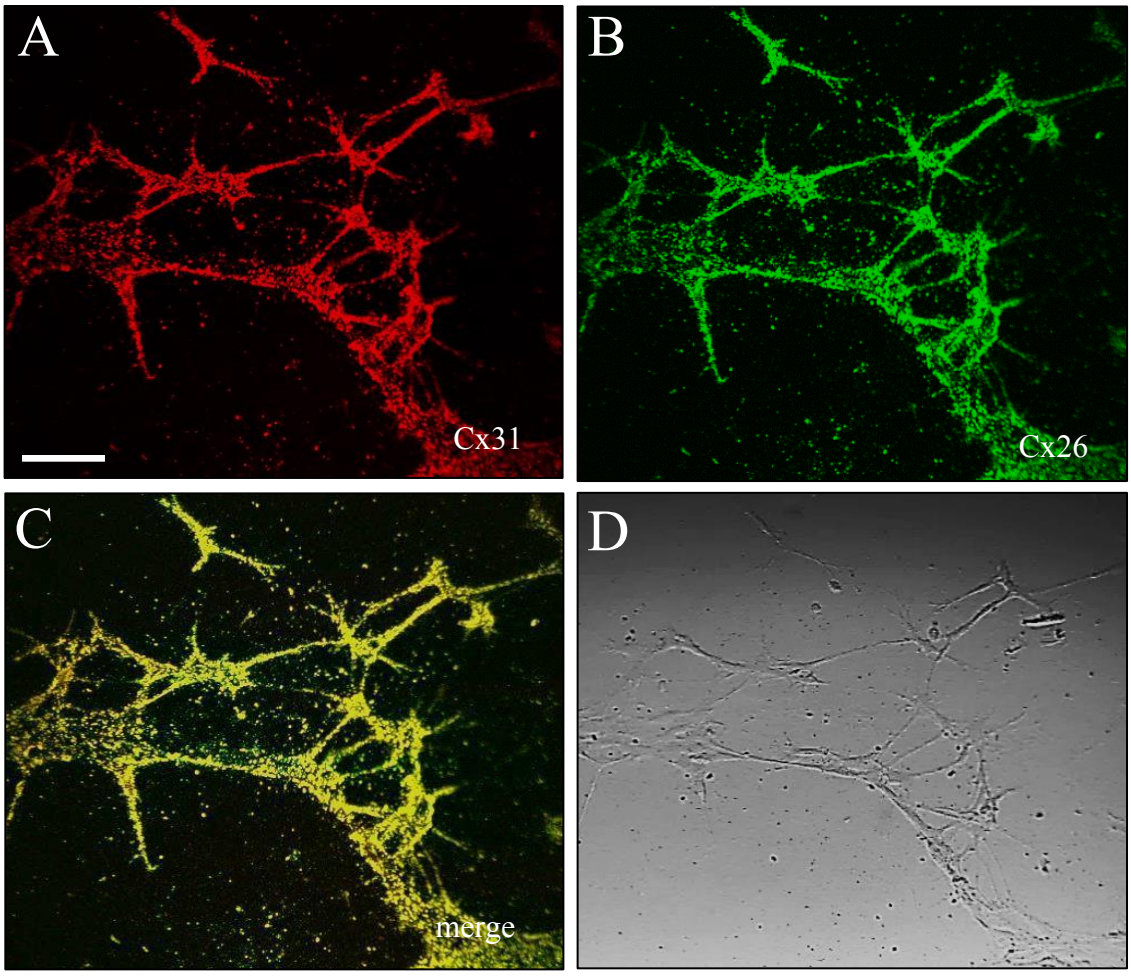

Figure 3.7 Cultured fibrocytes express connexin31 and 26. Immunolabelling for the gap junction proteins, Connexin31 (**a**) and Connexin26 (**b**) is high in cultured fibrocytes. The merged image in **c** shows that Connexin26 and Connexin31 are both expressed in the same fibrocytes. A bright field image of the cultured fibrocytes is shown in **b**. Scale bar indicates 10µm.

Figure 3. 8 Immunocytochemical labelling for gap junction proteins in cultured SLFs

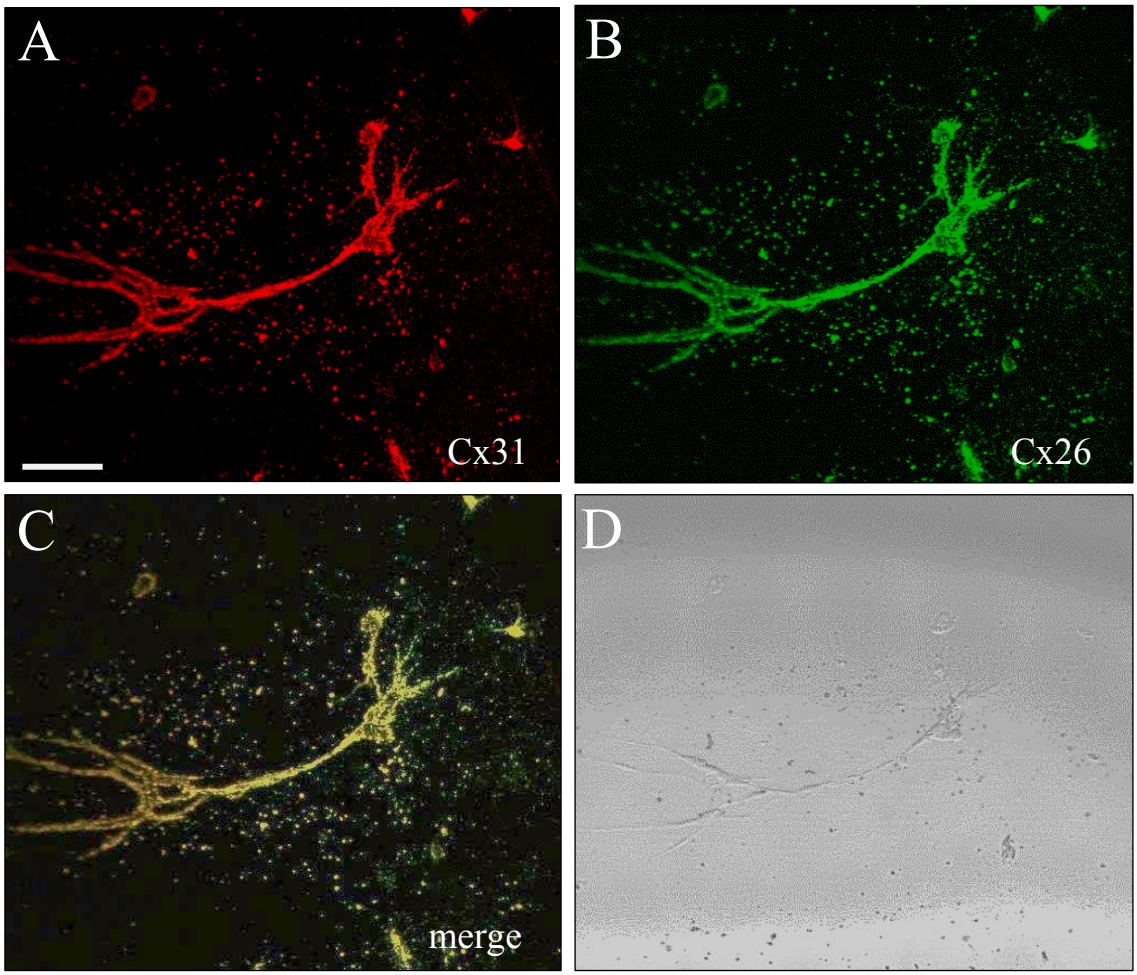

Figure 3.8 Intense gap junction labelling in areas of possible gap junctions between cultured fibrocytes. Immunolabelling for the gap junction proteins, Connexin31 (a) and Connexin26 (**b**) is high in cultured fibrocytes. The merged image in **c** shows that Connexin26 and Connexin31 are both expressed in the same fibrocytes but also show certain areas of more expression of one connexin type than the other indicated by the green and red fluorescence. A bright field image of the cultured fibrocytes is shown in **b**. Scale bar indicates 10µm.

Figure 3. 9 Connexin fluorescent labelling intensity in cultured SLFs

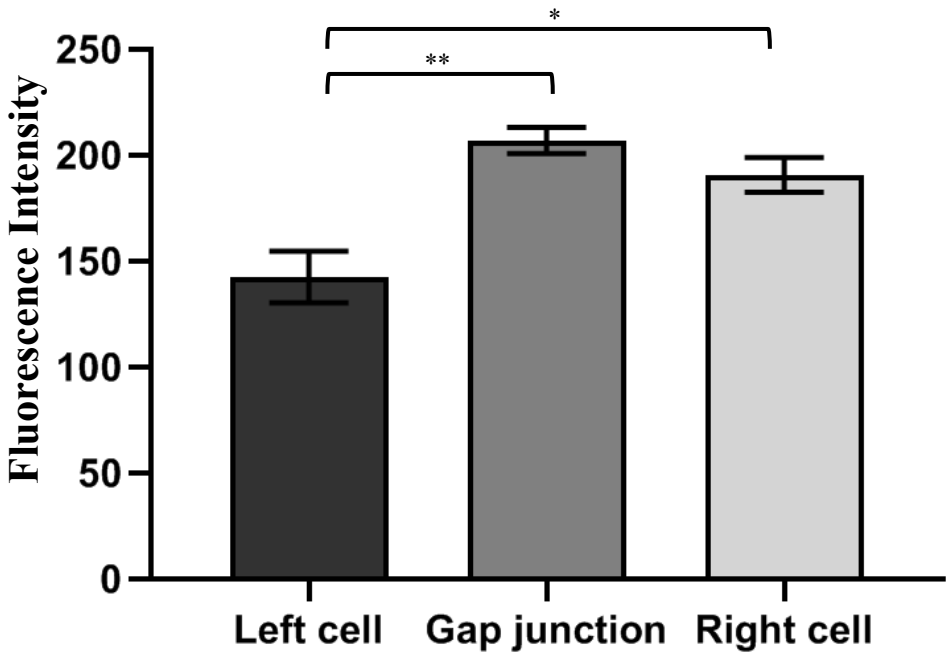

Figure 3. 9 Bar graph showing the merged fluorescent labelling pixel intensity of connexin26 and connexin31 comparing this in a gap junction area to the cell bodies to the left and right of this projection. (mean± SEM, *n=5*).

3.3.7 Connexin26 & connexin31 labelling in cochlear wax sections

Connexin26 and Connexin31 labelling was also found in the spiral ligament of cochlear wax sections (fig. 3.10) and at varying intensities in the different ligaments of the different cochlear turns (apical, middle and basal). Their concentrations appeared greater in the basal turn and decreased towards the apex where the thickness of the ligament decreases. The fluorescence (using the pixel concentration) was compared at the 3 different sites of ligament for both the connexin31 and connexin26 (fig. 3.11). There was no significant difference in the pixel intensity of connexin31 between the apical and middle spiral ligament turn (27.25 pixel ±1.613 and 25.21 pixel ±1.111, respectively, *p=0.3281*). There was no significant difference in the pixel intensity of connexin31 between the middle and basal spiral ligament turn (25.21 pixel ±1.11 and 29.78 pixel ±1.818, respectively, *p=0.064*), or between the apical and basal spiral ligament (*p=0.327*).

In contrast there was a significant difference in the pixel intensity of connexin26 between the middle and basal spiral ligament turn (78.70 pixel ±2.623 and 110.6 pixel ±1.876, respectively, $p<0.0001$) and between the apical and basal spiral ligament turn ($p<0.0001$). However, there was no significant difference in the pixel intensity of connexin26 between the apical and middle spiral ligament turn (72.59pixel ±1.258 and 78.70pixel ±2.623, respectively, $p=0.0689$). Moreover, there was a significant difference in the pixel intensity of connexin31 and connexin26 in the apical turn ($p<0.0001$). Also, there was a significant difference in the pixel intensity of connexin31 and connexin26 in the middle turn ($p<0.0001$). Finally, there was a significant difference in the pixel intensity of connexin31 and connexin26 in the basal turn ($p<0.0001$).

Figure 3. 10 Connexin31 and Connexin26 labelling in turns of the spiral ligament

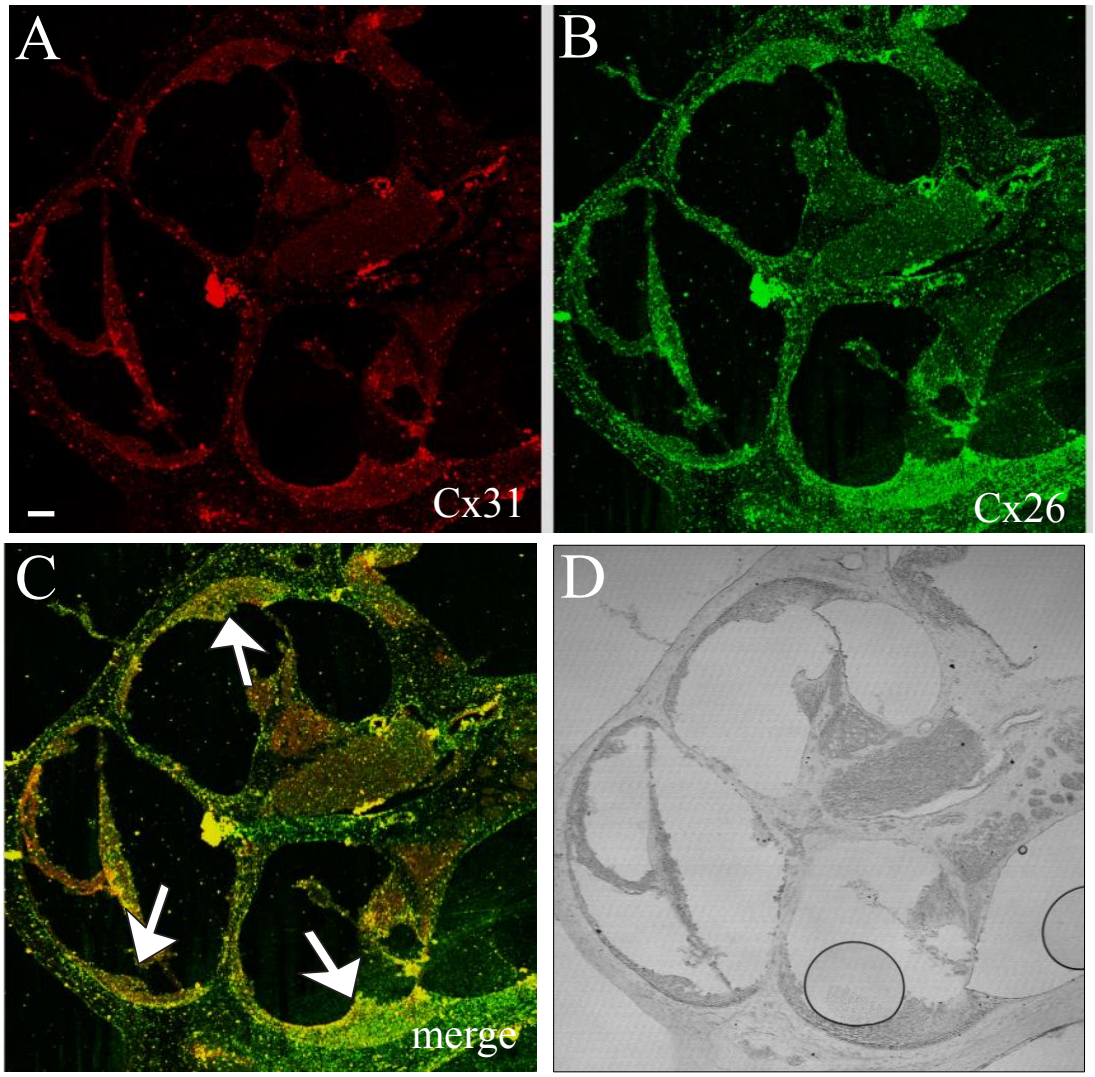

Figure 3.10 Immunohistochemical labelling of a cochlear wax section for Connexin26 and Connexin31. Cross section shows three areas of spiral ligament. Panel **A** shows labelling for Connexin31, **B** Connexin26 and **C** shows a merged panel. In the merged panel (**C**) the left arrow shows the apical, the top arrow indicating the middle turn and the right arrow the basal turn, **D** shows bright field image. Scale bar represents 50µm.

Figure 3. 11 Connexin fluorescent labelling intensity in the native SL

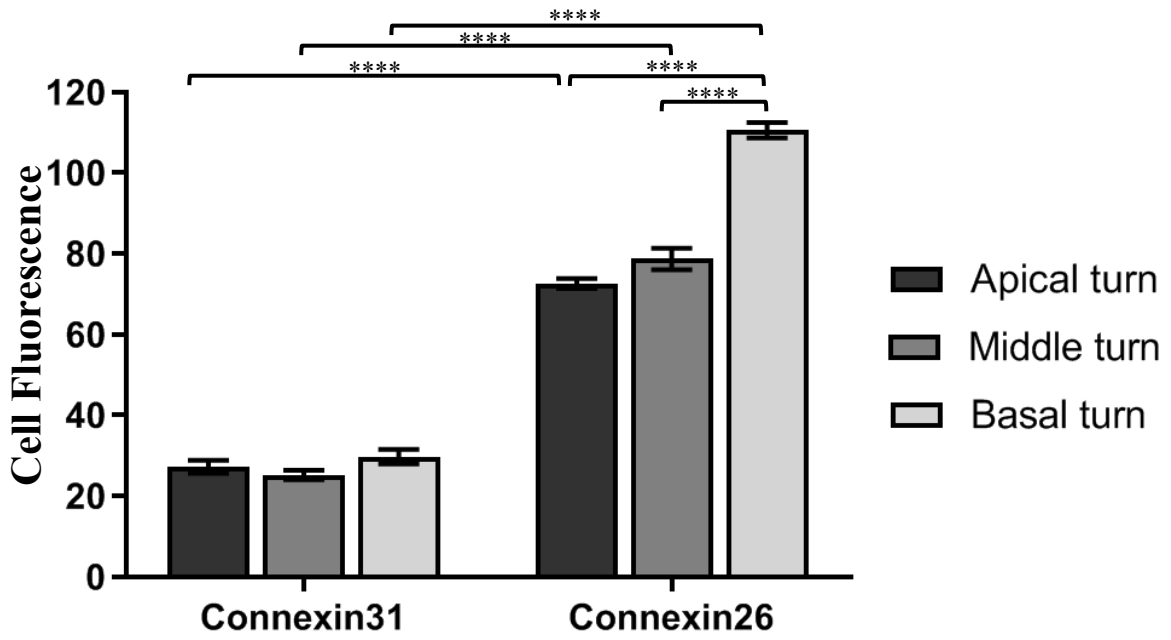

Figure 3.11 Bar graph showing the fluorescent labelling pixel intensity of connexin26 and connexin31 in the spiral ligament comparing this in the ligament in the apical, middle and basal turn. (Mean± SEM, *n=5*).

3.3.8 Immunolabelling controls

Secondary antibody controls were used to show that the labelling observed was due to binding of the secondary antibody to the primary antibody. This was done by eliminating the primary antibodies, therefore with no primary antibody to bind the secondary antibody; no labelling should be seen (fig. 3.12 & 3.13). A very small amount of background labelling can be seen, this could be due to the sticky nature of the collagen gels or interference of the wax.

Figure 3. 12 Immunolabelling controls for cultured SLFs

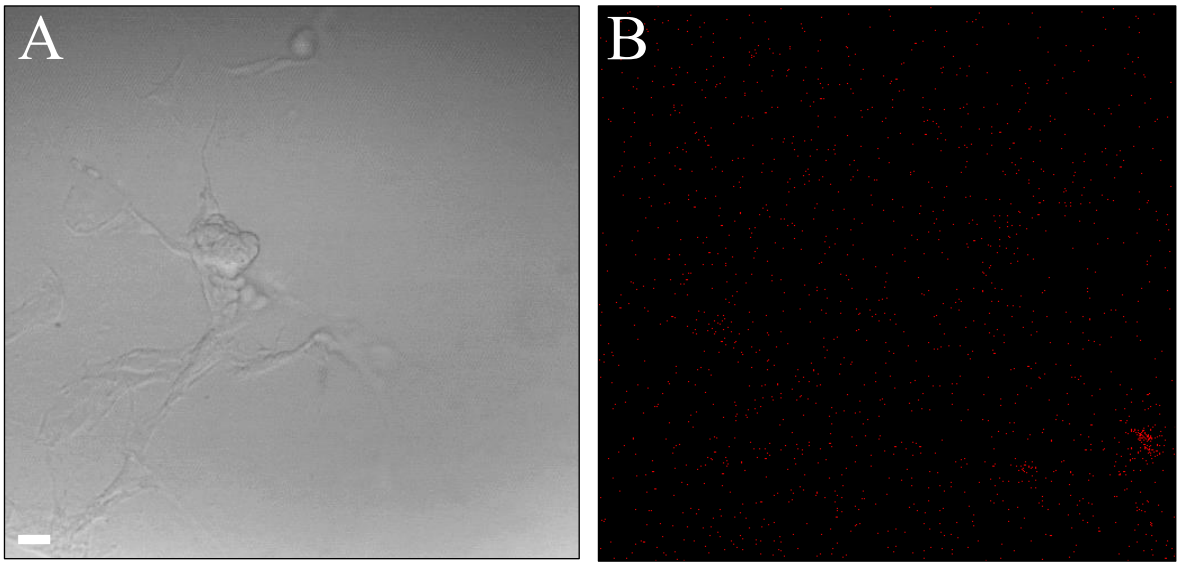

Figure 3.12 Immunolabelling controls for cultured SLFs on gels. (a) shows a bight field of the cells on the gels and (b) shows the confocal image. Scale bar represents 20µm.

Figure 3. 13 Immunolabelling controls for native SLFs

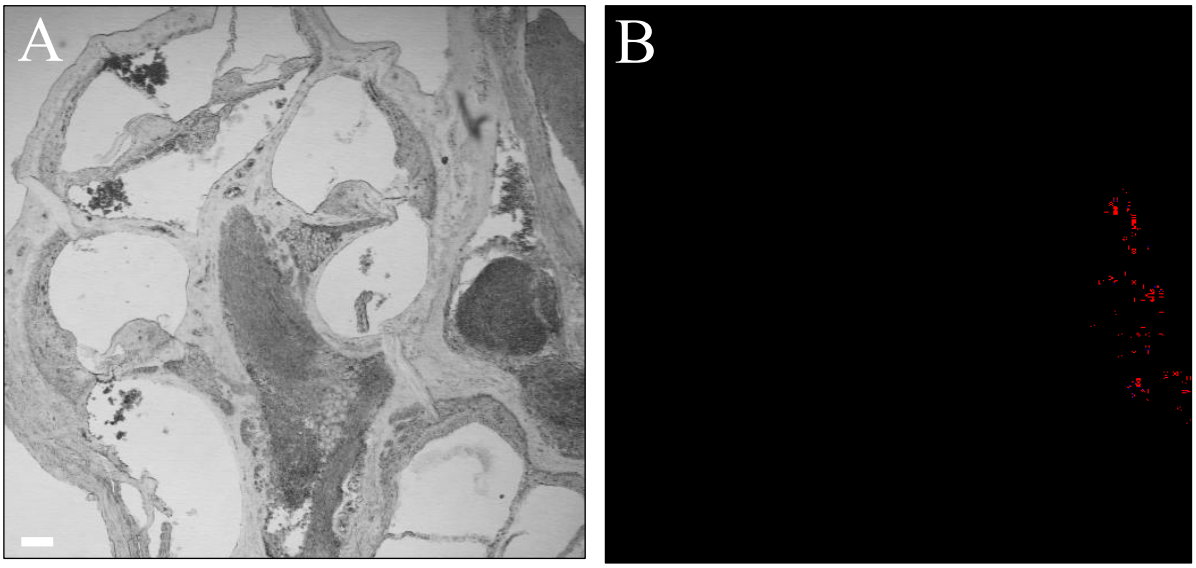

Figure 3.13 Immunolabelling controls for the native wax section slices. (a) shows a bight field of the cochlea slice and turns of the spiral ligament (b) shows the confocal image. Scale bar represents 20µm.

3.4 Discussion

3.4.1 Inwardly-rectifying potassium channels, Kir5.1, expressed in native and cultured SLFs

Findings using immunohistochemistry and immunogold electron microscopy have shown previously that Kir5.1 immunoreactivity was detected in the lower part of the spiral ligament and in the suprastrial zone of the ligament, the location in which type II, IV and V fibrocytes are found (Hibino et al, 2004). Further examination of the lower part of the ligament confirmed this as the cells that showed Kir5.1 labelling were found to be spindle and slender shaped; morphological features indicative of these specific fibrocyte types (Spicer & Schulte, 1996; 2002). This has also been confirmed recently by the discovery that Kir5.1 is expressed in type II and IV SLFs in the cochlea of C57BL/6J mice, but not in type I or III fibrocytes, in which expression is typically downregulated in the aging cochlea (Pan et al, 2016). Type II and IV fibrocytes may play a crucial role in potassium transport as they take up potassium from the perilymph and supply it to the *stria vascularis*. Sodium-potassium pumps and Na^+ K^+ Cl^- cotransporters are also highly expressed in type II and IV fibrocytes and are thought to play an important role assisting in this potassium uptake (Spicer & Schulte, 1996; Xia et al, 1999). Kir5.1 channels are also believed to be involved in potassium transport in the spiral ligament by forming a pathway required for either potassium recycling or potassium extrusion from the spiral ligament to the connective tissue gap junction network.

The EP starts to rise at around P8 and reaches adults levels two weeks after birth (Anniko, 1985). In the *stria vascularis*, Na^+K^+ATPase and $Na^+K^+2Cl^-$ cotransporter are expressed at P1 and increase to adult levels at P10 and P12 (Sakaguchi et al, 1998; Xia et al, 1999). Moreover, Kir5.1 becomes detectable around P10 and its expression increases and plateaus at P15-P16 (Hibino et al, 2004), the time-course for which almost parallels that of the Na^+K^+ATPase,

$Na^+K^+2Cl^-$ cotransporter, and connexin26 in the spiral ligament. Kir4.1 is detected in the *stria vascularis* at P8 as the EP starts to become positive and increases between P10 and P14 (Hibino et al, 1997). Therefore, these molecules might possibly be involved in the rapid phase of elevation of the EP. The two Kir channel subunits, Kir4.1 and Kir5.1, may be used by the cochlea in different ways to efficiently circulate K^+ circulation for the generation of the EP in the cochlea lateral wall. However, this present study is the first finding that cultured SLFs of a predominantly type III mixed phenotype express Kir5.1 suggesting they are possibly involved in the K^+ transport in the cochlea. Type III SLFs line the space between type I and II fibrocytes and the optic capsule, and are more frequent in the basal region of the cochlea (Henson & Henson, 1998), therefore these cells could be connected potentially through connexin channels to the type I and II fibrocytes and involved in potassium recycling through this Kir5.1 expression.

Heteromeric Kir4.1/Kir5.1 channels have been found to be stable and functional on the plasma membrane, and homomeric Kir5.1 subunit channels endocytosed and internalised through the membrane surface whilst generating no current (Tanemoto et al, 2002). Previous findings have found Kir5.1 to be slightly expressed on the membrane surface but abundantly distributed in the cytoplasm, presumably on the transport vesicles (Hibino et al, 2004). A possible explanation for this could be that Kir5.1 is actively recycled between the cytoplasm and membrane surface, and this recycling system could dynamically regulate the activity of Kir5.1 in the fibrocytes. It could also bind to anchoring proteins, to restore the negative regulatory control mechanisms and therefore show expression not only in the membrane. Kir6.1 has been found subcellular in the mitochondria in rat skeletal muscle and liver cells, located on the inner membrane (Suzuki et al, 1997). Also, when Kir2.1 was expressed in cultured cells, it is distributed mainly in the Golgi complex with little expression on the cell

surface (Hofherr et al, 2005). This suggests that Kir subunits might possess functions intracellularly, as well as in the plasma membrane.

Here Kir5.1 expression was detected in native SLFs of cochlear wax sections and in the cultures of SLFs. The native labelling is consistent with previous research of Kir5.1 being expressed in SLFs (Hibino et al, 2004; Pan et al, 2016), although it cannot be confirmed here whether this channel is formed homomerically or heteromerically as Kir4.1 research has clearly shown that Kir5.1 and Kir4.1 subunits are found in different types of cells in the cochlea (Hibino et al, 2004). It is therefore highly possible that Kir5.1 expression in cochlear fibrocytes assembles homomerically. This homomeric assembly could mean this channel subunit could remain non-functional, consistent with a lack of inward rectification in these cells in this study.

Moreover, the detection of Kir5.1 expression in the cultured SLFs is the first of this finding, the cultures of which we believe to be of a predominantly type III mixed phenotype. This is also consistent with the labelling of wax sections which found greater expression in the type III area when compared to other areas. This labelling strongly points towards type III SLFs possessing a potassium transport function, alongside its known established tension regulation function. This fibrocyte type has also been found to possess a regeneration capacity within the spiral ligament (Li et al, 2017; 2018), therefore could be a target for a cell replacement therapy to restore the loss of these cells that occurs in ageing organism, a promising treatment for metabolic presbycusis.

3.4.2 Weak BK potassium channel expression in native and cultured SLFs

Large Ca^{2+}-activated K^{+} channels, BK, have a high unitary conductance and are activated by both membrane depolarisation and intracellular Ca^{2+} (reviewed in Vergara et al, 1998). BK channels are known to play a prominent role in hair cell function in lower vertebrates

(Fettiplace & Fuch, 1999). However, the role of BK channels in mammalian cochlear hair cells remains more obscure since these hair cells do not display electrical resonance. The BK channel has previously only been found in cultured type I SLFs (Liang et al, 2003; Shen et al, 2004). In this current study, the cultured SLFs of a potential type III mixed phenotype, displayed weak expression for the BK channel. The non-specific labelling in the native SLFs could be due to a developmental effect as the sections were from a cochlea of a P7 mouse, whereas the cultures, although from a P9 mouse, may not be a same maturity from age of culture initiation due to the continuation of cell culture over a period of weeks. These cultured cells may have reverted back to immature fibrocytes or fully matured therefore may be a possible cause for limited BK expression. Strong membranous labelling for BK in inner hair cells is not seen until P12 to adult (Hafidi et al, 2005), an age at which the auditory system becomes functional. The age and fibrocyte type could therefore explain the lack of BK expression in the cultures and native SLFs, or alternatively, may not be present in these SLFs, as most of the research in this area has identified this BK channel in cultured type I SLFs. Therefore, differences in initial cell subtypes in addition to differences in unstable characteristics in cells that change over time in continuous culture could explain these differences in findings.

3.4.3 Connexin gap junction protein expressed in native and cultured SLFs

It has been reported previously that connexin26 and connexin31 are expressed in spiral ligament fibrocytes (Xia et al, 2000; López-Bigas et al, 2002). Connexin26 is found in type I, II and V fibrocytes, as expression is especially intense in type II at the spiral prominence and in type V at the apical tip of the spiral ligament (Liu & Zhao, 2008; Kada et al, 2009; Kasagi et al, 2013). Connexin31 has also been found to be expressed in type I, II and IV SLFs of the lateral wall (Xia et al, 2000; 2002; Liu & Zhao, 2008).

In the current study, both native and cultured SLFs expressed the gap junction proteins connexin26 and connexin31. The cultured SLFs showed more intense labelling at connecting processes, however, this level of detail could not be determined in the native SLFs. These proteins were also more concentrated at sites of potential gap junction connections between cell projections, suggesting that the cultured fibrocytes retain gap junctional features provided by these connexins as they do in the native cochlea. Findings that connexin expression labelling appears more intense in areas where cell projections join together further suggest the presence of gap junctions (Kikuchi et al, 2000). The presence of the connective-tissue gap junction network between fibrocytes of the spiral ligament and the basal and intermediate cells of the *stria vascularis* are required for the recycling of potassium ions (Kikuchi et al, 2000; Liu & Zhao, 2008). Further labelling for connexin 43 would have been beneficial as secondary marker to confirm a type III phenotype in the cultures (Kelly et al, 2012).

Moreover, the results from the positive connexin labelling in the cochlear wax sections regarding the difference in expression between the spiral ligaments of the different turns of the cochlear were not found to be significantly different for the connexin31 but was significant for connexin26 when comparing the basal turn to the middle and apical, with basal expressing a greater amount. The apical and middle, in contrast, were not significantly different from each other. It may indicate that there could be more connexin26 per fibrocyte in the basal spiral ligament compared to the apical. This is consistent with the fact that presbycusis is characterised by an initial loss of high frequency sound detection associated with the base of the cochlea and that connexin26 disruption in the spiral ligament is linked to be a causal and most significant factor of presbycusis (Ichimiya et al, 2000).

The use of paraffin wax embedding is a technique that does not come without its weaknesses as the hot temperatures used to melt the wax can have negative impacts on the samples, such as denaturing proteins. These experiments would benefit from being repeated on slices of

cochlea tissue sections where the spiral ligament is dissected and embedded in agarose gel before then being sectioned (Jagger et al, 2000), this may provide the optimal protein expression.

3.4.4 Conclusion

To conclude, Kir5.1 potassium channels are expressed in both native and cultured SLFs, both pointing towards the confirmation of this channel being potentially expressed in type III SLFs, a novel finding. The BK potassium channel was weakly expressed in these cultures and connexin gap junction protein expression was strong in both cultured and native SLFs, especially in the basal turn of the spiral ligament. This expression was intensified at points where gap junction could be more concentrated. Overall, the findings show that these SLF cultures have a similar protein expression profile as native SLFs. Therefore these cultured cells may not experience a loss of function when compared to native SLFs, further building the case of their use in a cell-replacement therapy to treat age-related hearing loss.

Chapter 4

Electrophysiology of Spiral Ligament Fibrocytes

4. Chapter 4- Electrophysiology of Spiral Ligament Fibrocytes

4.1 Introduction

The maintenance of the ionic balance within and between the unique fluids of the cochlea is key to the functioning of the auditory system. The homeostasis of potassium is particularly important as K^+ is the main cation carrying the acoustic transduction MET currents in the sensory hair cells (Corey & Hudspeth, 1979; Zidanic & Brownell, 1990). K^+ concentration is low in the perilymph (~5mM) and high in the endolymph (~150mM) under normal conditions (Smith et al, 1954) and it is this gradient and the highly positive EP (~80mV) that provides the driving force for K^+ influx into the hair cell through the MET channels to mechanoelectrical transduction in the mammalian cochlea. The active secretion of K^+ from the *stria vascularis* maintains the high concentration of K^+ in the endolymph (Wangemann, 2002). However, there is accumulating evidence that non-sensory cells, including highly specialised subpopulations of the spiral ligament fibrocytes, are active in this process (Spicer & Schulte, 1996; Minowa et al, 1999; Steel, 1999). The reason for the lack of information in this area is due to difficulties in establishing pure subpopulations of healthy SLFs, as well as the challenges when attempting to access SLFs *in vivo*. In this study we investigate the electrophysiological and molecular characterisation of voltage-dependent K^+ channels in native and a culture of predominantly type III mixed phenotype SLFs.

The difference in electrical potential between the interior and exterior of the fibrocyte network enables the movement of ions; it has been found *in vivo* this membrane potential difference is maintained between +5 and +12 mV with respect to outside (Nin et al, 2008; Adachi et al, 2013; Yoshida et al, 2015; 2016). Yoshida et al (2016) found that fibrocyte membranes were significantly more permeable to sodium than to potassium or chloride. However, previous findings show type I SLFs cultures have a membrane conductance dominated largely by

potassium and a RMP of ~-40mV (Shen et al, 2004). The variance within these experiments could be due to a variety of reasons such as fibrocyte types, as some work exploring the electrophysiology of SLFs has been conducted on type I cultures specifically, and other work on the spiral ligament as a whole. Another potential reason for variance could be between the environments in terms of cultures or *in vivo* recordings, in addition to the difference in techniques used ranging from single or double-barrelled electrode insertion to whole-cell patch clamping. The inconsistencies may also be related to difference in the efficiency of the perilymphatic perfusion.

A BK channel has been identified and characterised in cultured type I SLFs using both the patch-clamp technique and reverse transcription polymerase chain reaction (Liang et al, 2003). It is thought that this channel significantly influences the cell membrane properties and it was demonstrated that BK channels are the dominant force responsible for regulating membrane conductance in type I SLFs. This suggests they have a critical role in the establishment of a proper electrochemical gradient for the potassium recycling in the cochlea (Liang et al, 2002; 2003; Shen et al, 2002; 2004).

TEA^+ is a small organic cation, about the size of a hydrated K^+ ion that blocks most K^+ channels. Presumably, it occupies a vestibule that is large enough to accept a hydrated K^+ ion, but TEA^+, unlike K^+, cannot pass through a narrower part of the pore and thus blocks rather than permeating. The effects of the non-specific K channel blocker that reversibly blocks most K channels by binding to the K^+- permeable pore, has also been shown to almost completely reduce the current in type I SLFs (Liang et al, 2003; 2005; Shen et al, 2004). It is found intracellular application of 4mM TEA had no effect on single channel activity; however, extracellular application of 1mM TEA inhibited channel activity completely (Liang

et al, 2003). They produced a dose-response curve of the opening probability in response to extracellular TEA showing the opening probability significantly decreased with increasing TEA concentration.

Some fibrocyte types are believed to be involved in the cochlea's inflammatory response to trauma induced by disease, noise and ageing (Hequembourg and Liberman, 2001; Ohlemiller, 2009). The type III SLFs *in vitro* have been suggested to be involved with tension regulation in the spiral ligament-basilar membrane complex as they possess muscle and non-muscle filaments and display a mechanically contractile phenotype by cells inducing contraction of a collagen lattice. Therefore these cells are a crucial component in determining auditory sensitivity (Kelly et al, 2012). However, due to their inaccessibility *in vivo* direct experimental evidence to investigate these cells further is limited.

Here we compare the electrophysiological properties of cell cultures of predominantly type III mixed phenotype SLFs, type III being the 'tension' fibrocytes, obtained from freshly isolated primary spiral ligament explants, to that of native SLFs from freshly sectioned cochlea, revealing an active potassium channel in both. This is the first work directly comparing the physiological properties between a predominantly type III mixed phenotype culture of SLFs and native SLFs, and exploring the K^+ transport in these cultured SLFs which could provide new insight into a way to treat age-related hearing loss. We report the electrophysiological characterisation of voltage-dependent K^+ channels in these cells.

4.2 Methods

4.2.1 Preparation of fresh cochlea sections

Cochlear slices were taken from P7-9 CD/1 mice, as this was the optimal age for slicing of the cochlea and used the technique provided by Jagger et al (2000). The bullae were excised and the cochlear bones exposed. Additional dissection was performed in 4 ^{o}C artificial cerebrospinal fluid (ACSF, table 4.1), bubbled with 5% CO_2 and 95% O_2. The cochlear bone was mounted on a vibratome (Leica VT1000) using superglue and slices were cut horizontally from apical to basal end in a mid-modiolar plane at 300 μm using a vibrating blade at a speed of 1.5 mm/sec and frequency of 8Hz. The slices were then submerged in the cold ASCF and transferred into a recording chamber and positioned in such a way as to expose the spiral ligament to perform electrophysiology on SLFs.

Another technique for the native fibrocytes access for patch clamping was employed when vibratome produced sub-optimal results. Dissection of the spiral ligament was used following the same microdissection procedure as that for the dissection prior to cell culture using a dissection microscope (Leica, Wild M8), however, once a section of spiral ligament was dissected it was held down in the recording chamber by two pieces of teased dental floss (fig. 4.1) to enable the tissue to be held securely and allow access of the recording electrodes to the fibrocytes.

4.2.2 Whole cell recording set up and preparation

The set-up used for the patch clamping utilized a microscope (Upright, Olympus BXWI) supported on a vibration-isolation table. On the left of the patch rig a micromanipulator held the puffer pipette and on the right a second micromanipulator held the patch pipette. The

microscope image was also displayed on the computer screen through a monochromatic video camera (fig. 4.1).

Figure 4. 1Rig set-up

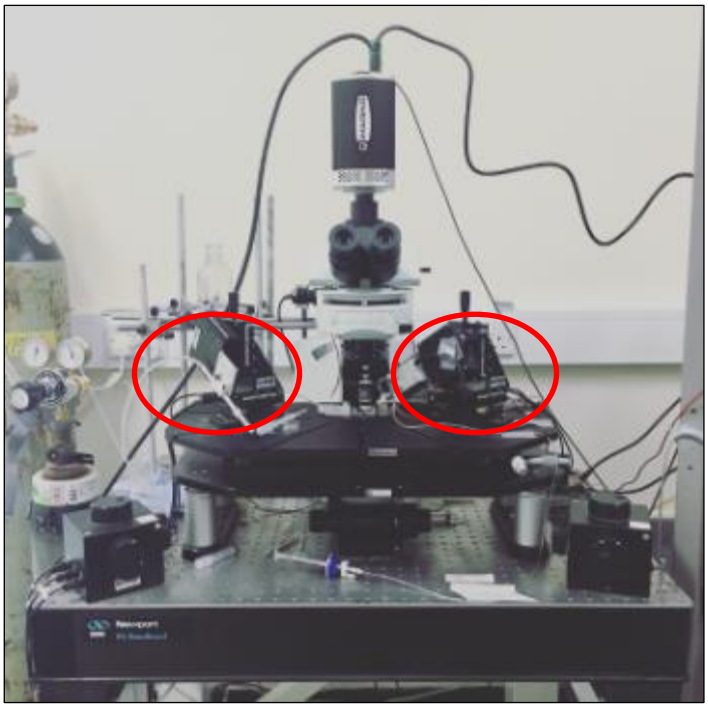

Figure 4.1 Photo of the setup of the rig. At the top of the image the inverted camera can be seen. To the left of the stage the micromanipulator for the puffer can be seen and to the right the recording pipette with the fine manipulators either side and coarse directly on top of the air table.

At the start of the recordings, the pump was set to perfuse artificial perilymph @RT, bubbled with 5% CO_2 95% O_2 (BOC gas), through the recording chamber. The experimental chamber contained a petri dish with the hydrogel central in the recording chamber with the cells facing up (on top of the gel) for the cultured fibrocyte recordings. A set up containing two strings of dental floss in a cross pattern to hold the spiral ligament in place for the native fibrocyte recordings, both could be transferred from the dissection microscope to the patch clamping microscope. A constant supply of ACSF was delivered to one side of the sample set up and this ACSF was removed at an average rate of 0.2mL per min.

A glass capillary puller (Narishige PC-10) was used to make recording electrodes from borosilicate glass capillaries (GC120TF-10, Harvard apparatus) with a ~1µm wide tip and

resistance of around 4 MΩ when filled with intracellular solution (KCl solution, table 4.2) pH adjusted to 7.3 with KOH and tip of electrode dipping in the bath. Prior to filling with intracellular solution, patch pipettes were gently fire polished at the rear end of the recording electrode and then insulated with wax to reduce pipette capacitance (avoiding the very tip of the electrode).

4.2.3 Dextran 3000

The patch pipette was filled with fluorescent Dextran 3000 (Thermofisher, UK) diluted in the intracellular solution to enable the cell to be visualised once whole cell patching was successful. A stock at 10mM dissolved in dH_2O was diluted to a final concentration of 0.1mM.

4.2.4 TEA (potassium channel blocker)

100mM TEA (Sigma Aldrich, UK) stock solution was diluted in the ACSF solution to a final concentration of 10mM in dH_2O. The TEA was applied by pressure ejection (controlled by a PV 820 pneumatic picopump, World Precision Instruments, FL, USA) through a glass pipette electrode (opening diameter 1-3µm) approaching the cell from the left, with a variable pressure of between 14 and 70kPa. Once the pipette was in position the pressure was adjusted to obtain clear solution exchange without producing large movements of the cell body. The pipette was kept about 5 to 10µm from the cell. The TEA was usually applied for 0.6s every 2s approximately, with a pause between each sweep.

4.2.5 Whole cell patch clamp recording

Fibrocytes were identified visually. A syringe linked to a filter and micro-loader tip was used to fill a borosilicate pipette with intracellular solution. Pipettes were 'flicked' gently to remove air bubbles and then placed in a pipette holder attached to the head stage of the patch clamp amplifier. The amplifier was set to voltage-clamp mode and the pipette voltage offset was adjusted so the currents measured 0 pA. The electrode tip was directed towards the chosen isolated fibrocyte using a precision micromanipulator whilst simultaneously monitoring the height of the pipette on the video. Once the cells were in focus the pipette tip was kept just above the focus level of the cells, using the fine manipulator controls when proceeding.

The electrode was directed towards the cell body moving using the axial control until the tip touched the cell and a small dimple was observed in the surface of the membrane. Positive pressure was then released and suction applied to obtain a 1 GΩ seal. The holding command voltage was slowly set to negative (-50mV). To form a seal and break through the membrane, suction pulses were applied using the mouth syringe. Following break-in, voltage steps from different holding potentials were delivered to characterise the membrane currents. Recordings were acquired and analyzed using Signal 2.16 software. Voltages were corrected for the uncompensated series resistance and junction potential before plotting of I–V curves. RMPs were measured in voltage-clamp by reading the voltage value where the current was 0nA. Conductance is $\frac{I}{V}$ (inverse of resistance).

Table 4. 1 Extracellular solution

	mM
KCl	2.5
NaCl	124
$CaCl_2$	1.3
$MgCl_2$	2
NaH_2PO_4	1.25
$NaHCO_3$	26
Glucose	17

Table 4.1 Components of extracellular solution (ACSF) made up with dH_2O and adjusted to pH7.3 with NaOH. Source of components from Sigma, UK.

Table 4. 2 Intracellular solutions

	mM
KCl	140
NaCl	10
$MgCl_2$	2
EGTA	0.5
HEPES	5
Glucose	5

Table 4.2 Components of intracellular solution made up with dH_2O and adjusted to pH7.3 with KOH (as from Kelly et al, 2012). Dextran 3000 diluted in solution at 0.1mM. Source of components from Sigma, UK.

Data were analysed using GraphPad Prism statistical analysis software (version 5.0). All data are expressed as mean ± standard error of the mean (S.E.M.). Tests for normal distribution and equal variance were conducted to determine the suitable parametric or un-parametric test to be used. The number of experiments (*n*) refers to the number of cultured or native SLFs recorded from, with multiple primary cultures established from different mouse litters. The analysis of variance and t-tests used to examine the significance of these data were calculated using GraphPad prism. Unless otherwise stated, significance was assessed at the 5% level ($p< 0.05$*); $p<0.01$**; $p<0.001$***; $p<0.0001$ indicate significance, shown across groups by bars.

4.3 Results

4.3.1 Whole-cell voltage clamp experiments

Cells in cultures derived from spiral ligament explants were grown on 3-D collagen gels and accessed successfully by electrodes from electrophysiology (fig. 4.2). SLFs were grown on a gel (fig 4.2a) and individual cells targeted for patch-clamping the cell was immediately filled with Dextran 3000 which fluoresced (figs 4.2b-g). Native SLFs within the spiral ligament of a cochlear slice were also accessed successfully (fig. 4.3). Turns of the cochlea revealed the lateral wall containing the SLFs (fig 4.3a). Individual SLFs within the spiral ligament were also identified and targeted for patch-clamping and once whole-cell were filled with Dextran 3000 (fig 4.3b-g).

Figure 4. 2 Recording from 3-D cultured SLFs

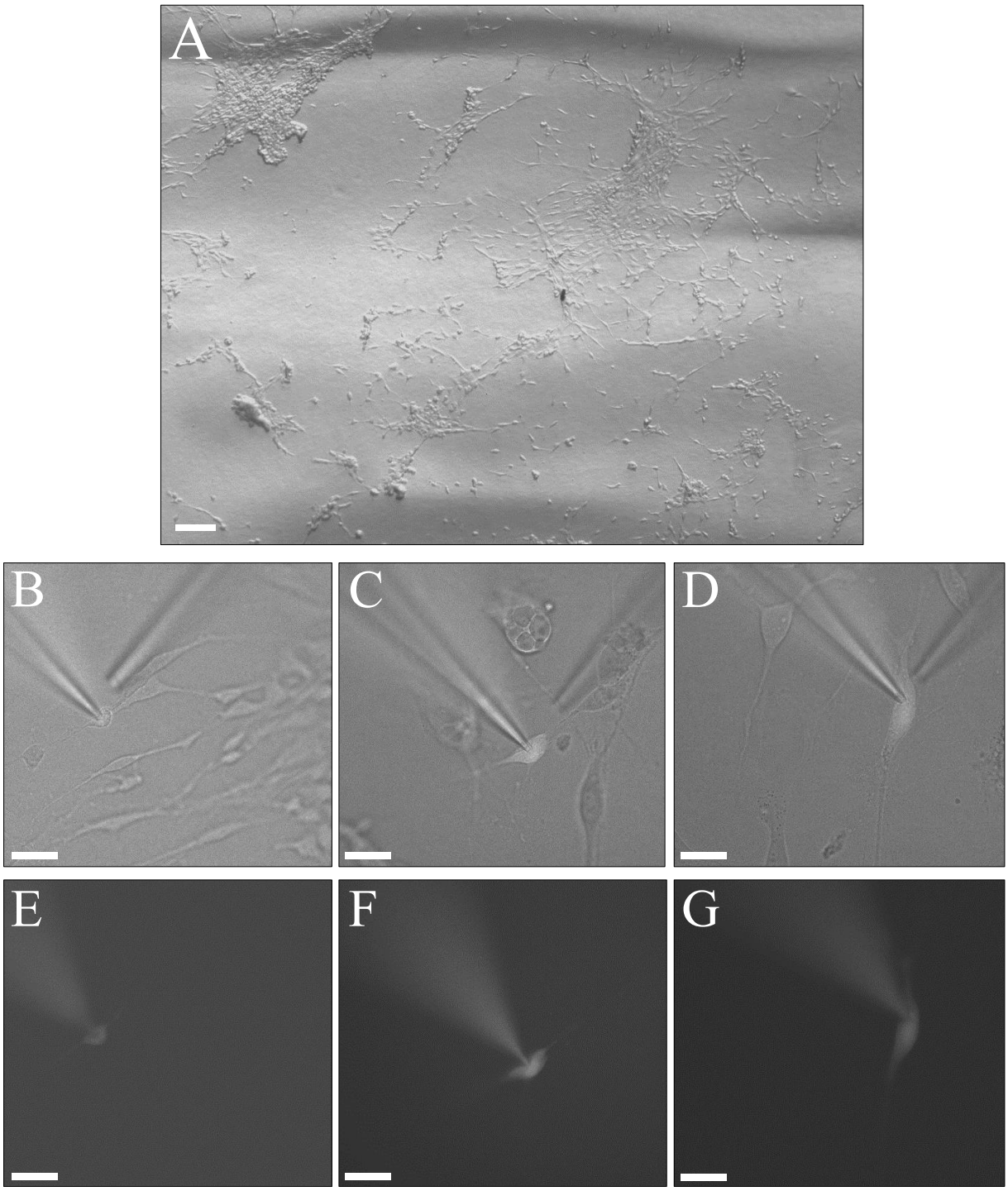

Figure 4.2 Whole-cell recordings of 3-D cultured spiral ligament fibrocytes on a 3-D collagen gel. A shows overview of cells on gel. B-D show light microscope images of SLFs and E-G the corresponding cell filled with Dextran 3000 once whole cell via the recording pipette. Left electrode is recording pipette and right electrode is puffer (filled with 10mM TEA). Scale bar in A indicates 25µm and B-G indicate 10µm.

Figure 4. 3 Recording from native SLF

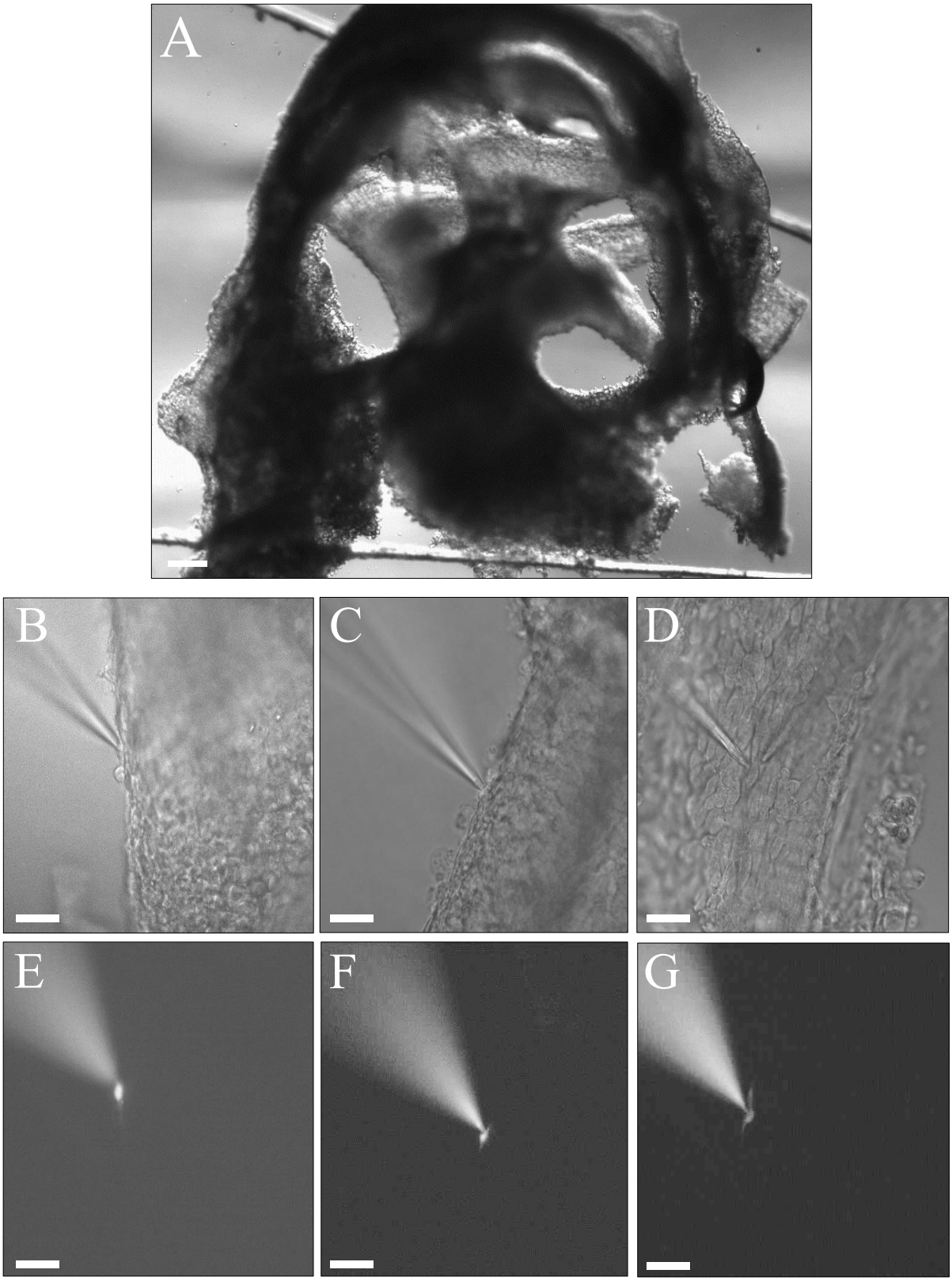

Figure 4.3 Whole-cell recordings of native spiral ligament fibrocytes. A shows cochlea slices revealing spiral ligaments containing the fibrocytes. B-D show light microscope images of SLFs and E-G the corresponding cell filled with Dextran 3000 once whole cell via the recording pipette. Left electrode is recording pipette and right electrode is puffer (filled with 10mM TEA). Scale bar in A indicates 25µm and B-G indicate 10µm.

With a KCl-based pipette solution and a NaCl based bath solution two main characteristic groups arose from the recordings in the cultured and native SLFs, linear responses and outwardly rectifying whole-cell currents induced by depolarising membrane potentials. Cells were filled with the fluorescent dye Dextran 3000 in order to locate and see the exact cells being recorded from. The electrophysiological recordings are shown from SLFs grown in 3-D culture on collagen gels (*n=25*), where whole-cell voltage-clamp recordings of intrinsic membrane conductances were obtained (fig. 4.4). A cultured SLF was filled with Dextran 3000 and exhibited a linear response (non-rectifying) in an *IV* plot (figs 4.4a-c), the average group *IV* plot for linear responses shown in figure 4.4d (*n=17*). A cultured SLF recorded from and immediately filled with Dextran 3000, exhibiting an outwardly rectifying response in an *IV* plot (figs 4.4e-g), the average group *IV* plot for outwardly responses shown in figure 3.3h (*n=8*).

The electrophysiological recordings from native SLFs (*n=38*), where again whole-cell voltage-clamp recordings of intrinsic membrane conductances were obtained. As with the cultured SLFs two main groups arose from the recording responses, linear and outwardly rectifying.

Native SLFs were recorded from and immediately filled with Dextran 3000, exhibiting a linear response (non-rectifying) in an *IV* plot (figs 4.5a-c), the average group *IV* plot for linear responses shown in figure 4.5d (*n=27*). A native SLF was filled with Dextran 3000 and exhibited an outwardly rectifying response in an *IV* plot (figs 4.5e-g), the average group *IV* plot for outwardly responses shown in figure 4.5h (*n=11*). It appears from the trace data shown in figure 4.5e &f that there may be multiple cells contributing to the recording as opposed to a singular cell, the use of tracer dyes could have confirmed this.

Inward current was induced by hyperpolarisation and outward current by depolarisation and in voltage clamp are plotted as negative values and shows downward deflection whilst outward are plotted at positive values and shows upward deflection.

The linear current in both the cultured and native fibrocytes is very similar, however, when comparing the outwardly rectifying groups the current is much greater in the native fibrocytes than the cultured as the total current through the range of voltage steps in the cultured SLFs in the outwardly rectifying group was 0.42 nA, and in native SLFs was 1.77nA, which is x4.2 greater than the current in the cultured SLFs.

4.3.1.1 Resting membrane potential and conductance values in native and cultured fibrocytes

Certain characteristics of the cells (RMP, conductances and reversal potentials values) were deduced from the IV graphs to giving insight into the functions of these cells and the similarities or differences in them between native and cultured fibrocytes. The resting membrane potential tells us the electrical potential when the cell is not stimulated, so the current when there is no voltage injected- what the cell rests at. The RMPs of cultured and native fibrocytes show linear and outwardly rectifying responses (fig. 4.6). In the outwardly rectifying responses the mean RMP was -8.63mV (±4.75, *n=8*) and -16.73mV (±7.01, *n=11*) in the cultured and native fibrocytes respectively; this means the RMP in the native SLFs for the outwardly rectifying group is almost twice as negative than the cultured, however there was no significant difference between the RMPs in the culture and native SLFs. In the mean linear responses the RMP in cultured fibrocytes was -8.13mV (±2.77, *n=17*) and -10.78mV (±3.00, *n=27*) in the native fibrocytes which are relatively similar RMPs and they were not significantly different.

Figure 4. 4 IV plot of responses in 3-D cultured fibrocytes

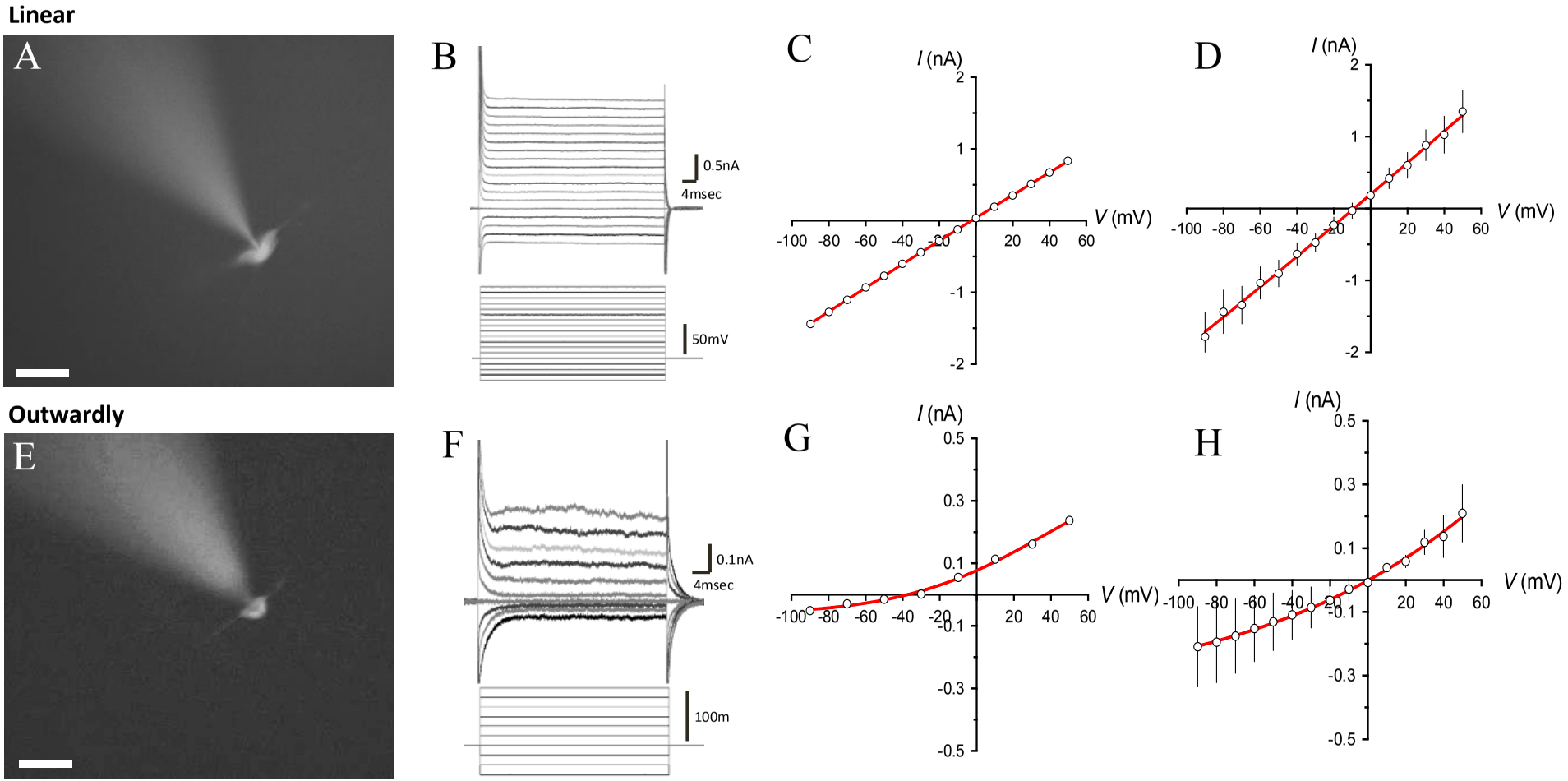

Figure4.4 Whole-cell voltage clamp recordings of membrane currents in 3-D cultured fibrocytes. Electrophysiological recordings showing current-voltage relationships. Images a & e show a recorded cell filled with the fluorescent dye Dextran 3000, c & g IV plots are generated from the data in current traces b & f. IV plots d & h are averages from recordings that show no rectification (d, *n*=17) and outward rectification (h, *n*=8). Scale bars indicate 10µm.

Figure 4. 5 IV plot of responses in native fibrocytes

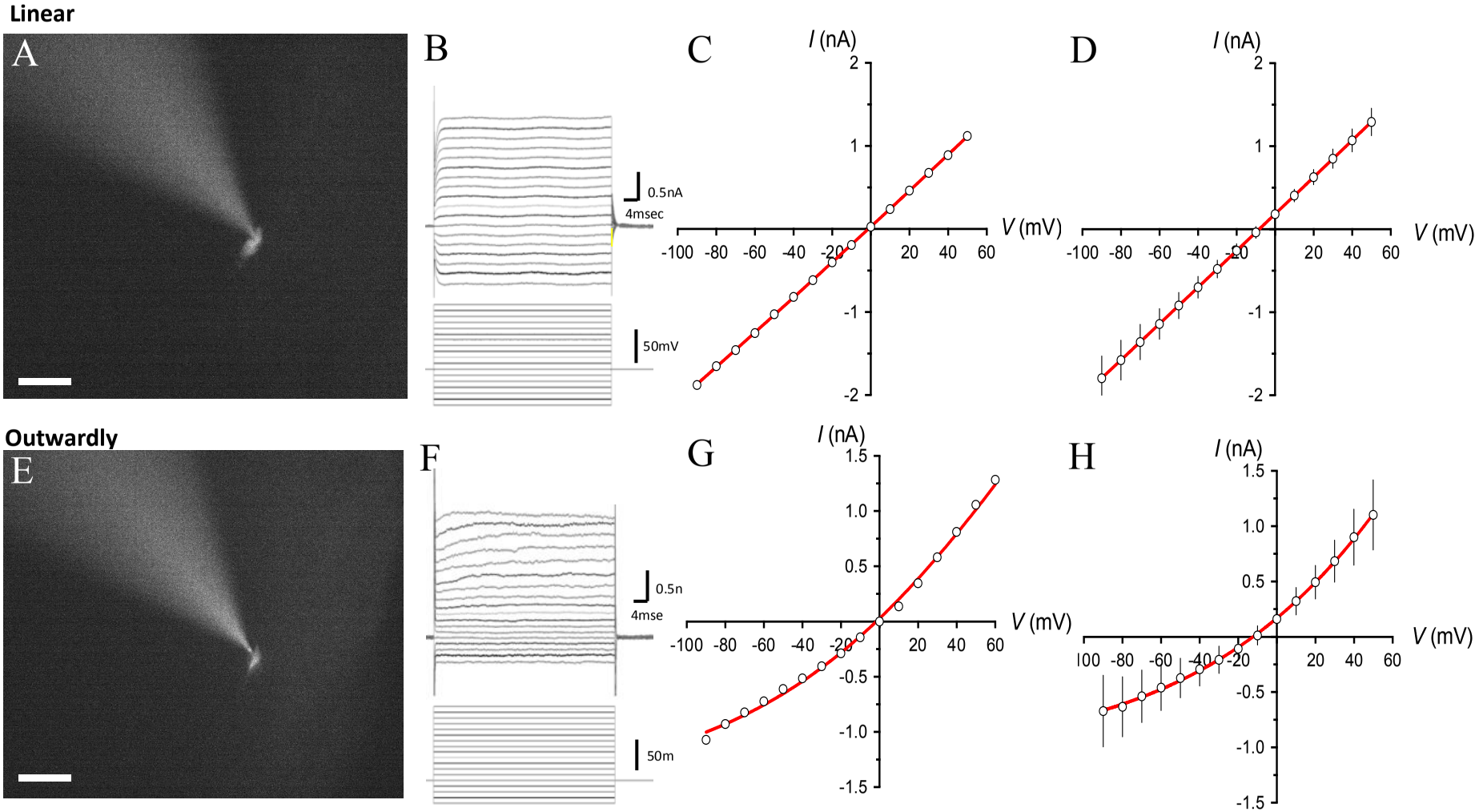

Figure4.5 Whole-cell voltage clamp recordings of membrane currents in native lateral wall fibrocytes. Electrophysiological recordings showing current-voltage relationships. Images a & e show a recorded cell filled with the fluorescent dye Dextran 3000, c & g IV plots are generated from the data in current traces b & f. IV plots d & h are averages from recordings that show no rectification (d, *n*=27) and outward rectification (h, *n*=11). Scale bars indicate 10µm.

Figure 4. 6 RMP of native and 3-D cultured fibrocytes

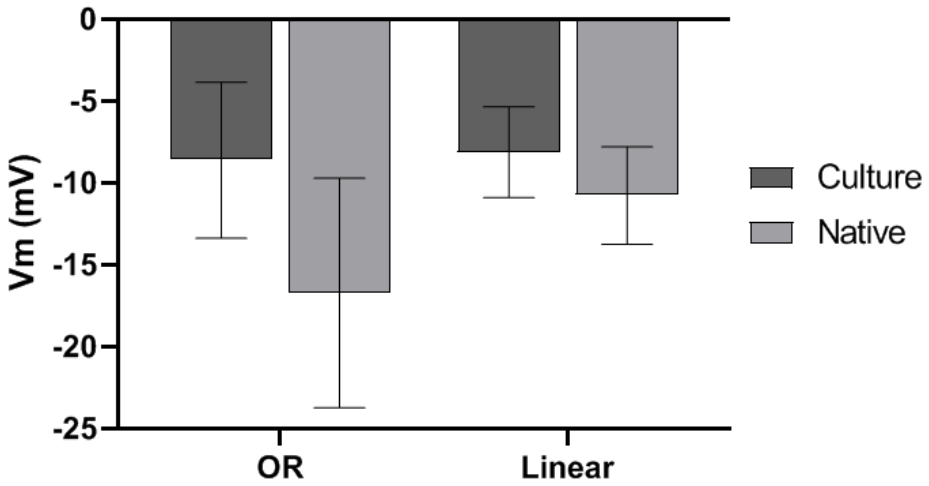

Figure 4.6 Bar graph showing the average resting membrane potentials (RMP) of 3-D cultured fibrocytes (a) and native fibrocytes (b). The two response groups: outwardly rectifying (cultured *n*=8; native *n*=11); and linear (cultured *n*=17; native *n*=27) (mean ± SEM).

The conductance of the membrane to the ion refers to the ratio of the ion's net flow through the cell to the driving force. Figure 4.7 shows the conductance of native and 3-D cultured fibrocytes. The conductance values of cultured and native fibrocytes with linear responses show a very similar mean conductance (0.021µS ±0.004, *n=17*; *versus* 0.023µS ±0.003, *n=27* respectively), therefore there was no significant difference in conductance between the cultured and native fibrocytes showing a linear response. In the outwardly rectifying responses the conductance values at negative voltage steps (-60mV to -80 mV) in cultured fibrocytes was 0.002µS (±0.001, *n=8*) and 0.009µS (±0.003, *n=11*) in native fibrocytes which is X4.5 greater than in cultured SLFs. Despite this there were no significant differences in these values between the native and cultured fibrocytes. There was, however, a significant difference (*p=0.026*) in the conductance values in the outwardly rectifying responses between native and cultured fibrocytes at positive voltage steps (10mV to 20mV), 0.006µS (±0.003, *n=8*) in cultured and 0.02µS (±0.007, *n=11*) in native fibrocytes, over three times greater than in cultured SLFs.

Figure 4. 7 Conductance of native and 3-D cultured fibrocytes

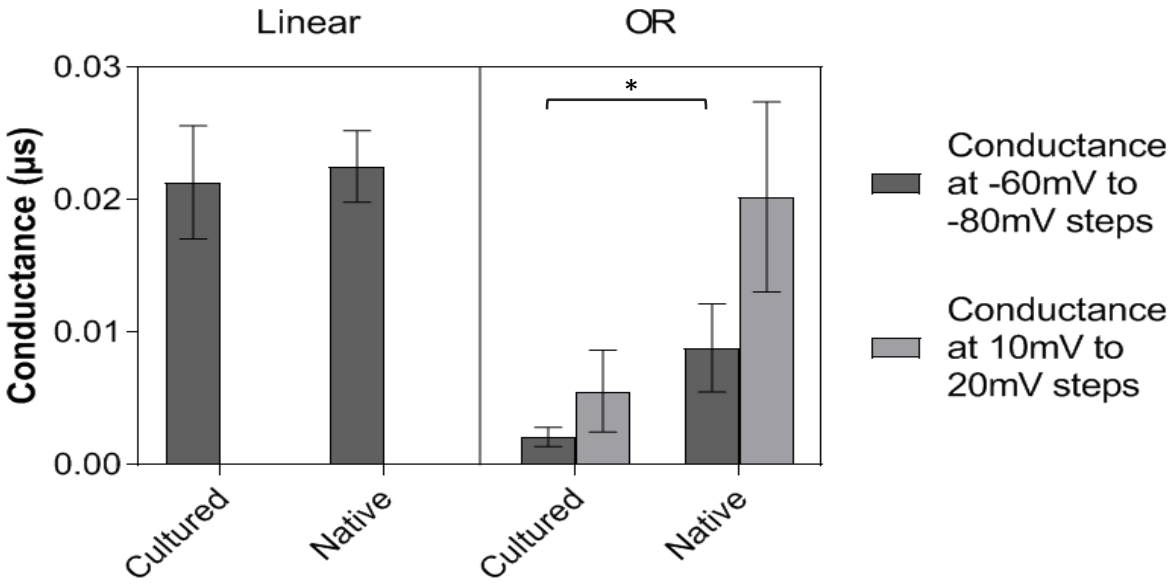

Figure 4.7 Bar graphs showing the average conductance values in 3-D cultured and native fibrocytes. The graph shows the conductance at negative (-80 to -60mV) and positive steps (10 to 20mV) in the linear and outwardly rectifying groups, within the two groups, (mean ± SEM). OR= outwardly rectifying, linear= none rectifying current.

The capacitance of a cell corresponds to the surface area of a cell. The capacitance of 3-D cultured and native SLFs were found to not be significantly different, although higher in cultured fibrocytes (11.67pF±1.424 and 8.225pF±1.272, respectively, *p=0.1329*) (fig. 4.8).

Figure 4. 8 Capacitance of 3-D cultured and native SLFs

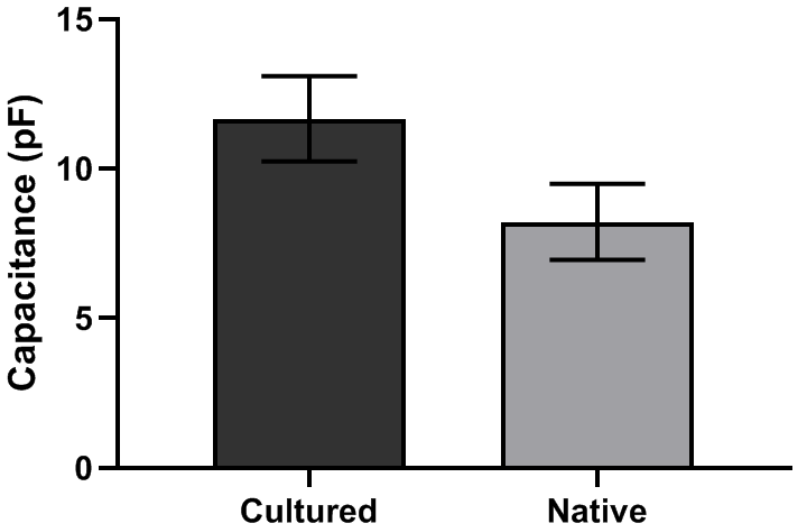

Figure 4.8 Bar graph showing the capacitance of 3-D cultured (*n=3*) and native (*n=4*) SLFs. (mean ± SEM).

4.3.2 TEA experiments/ Effect of TEA on current in 3-D cultured and native spiral ligament fibrocytes

The effect of the non-specific K channel blocker TEA was evaluated with extracellular application. TEA is widely used for reversible blockade of K channels in many preparations and was used in these experiments to assess the presence of potassium currents. It has been shown to reversibly block most K channels by binding to the K^+-permeable pore (Hille, 1991). TEA eliminates the delayed K^+ current measured in voltage clamp experiments. Effect of TEA is almost immediate showing a response after approximately 20msec. Also resistance increases after TEA application as ion channels are closing.

10mM TEA was puffed onto a fibrocyte during a whole-cell recording showing an immediate effect after the TEA puff was applied (fig. 4.9). It then continues to increase resistance where channels have started to close, showing a time dependent block that increases with time. TEA appears to block/reduce the holding current at -50mV, presumably through an effect of an unknown cation channel.

Control TEA experiments were conducted with the puffer electrode to confirm the effect would be due to the TEA itself and not any other confounding variables such as mechanical effects. An example in a native SLFs of the control TEA experiment where ACSF was loaded into the puffer electrode and puffed onto the cell in replacement of TEA (fig. 4.10). TEA has no effect on the current neither in a time dependent of voltage dependent manner (fig. 4.10). Before all experiments the puffer was checked for working by aiming at any lose debris to check if it moved when puffer was released.

Figure 4. 9 Effect of TEA on a current trace response in a native spiral ligament fibrocyte

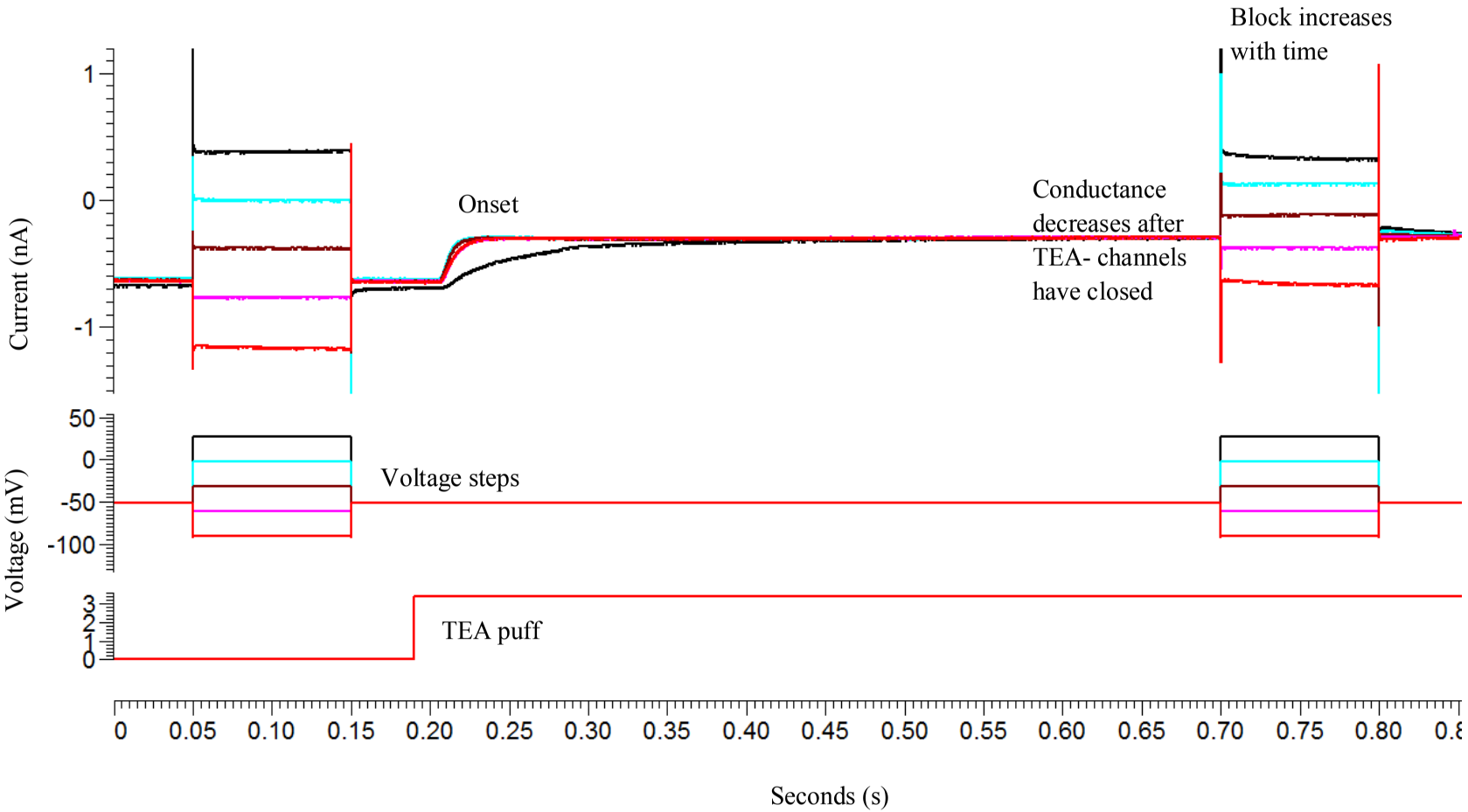

Figure 4.9 An example of a current trace of a native fibrocyte response to 10mM TEA showing the voltage steps and corresponding current traces at each step. It shows the TEA and its immediate effect on the current trace. Also shown are the currents in response to positive and negative voltage steps. Puffer was checked to confirm working.

Figure 4. 10 Effect of ACSF control on a current trace response in a native spiral ligament fibrocyte

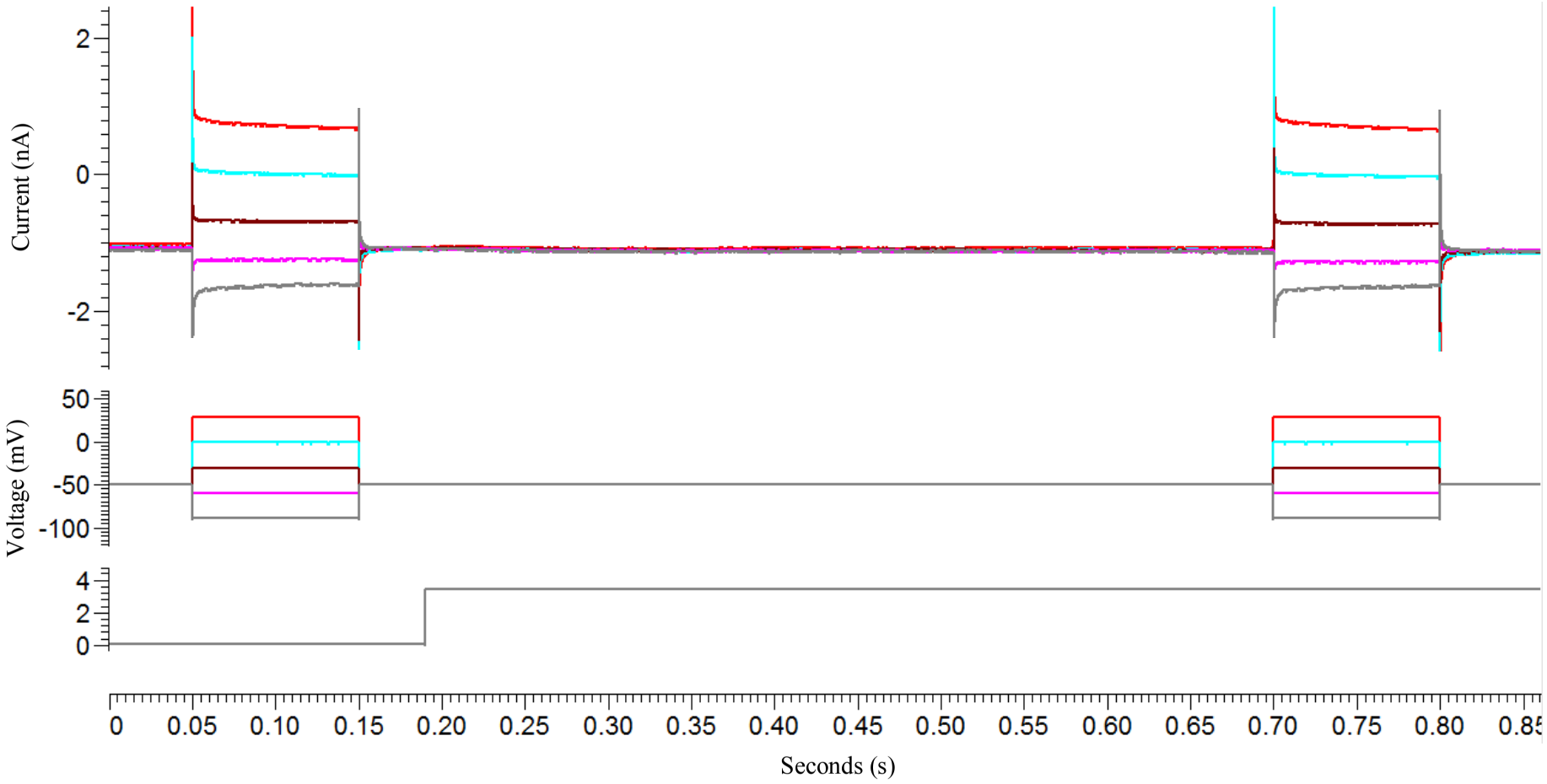

Figure 4.10 Diagram showing an example of a control current trace of a native fibrocyte response to ACSF. Shows the voltage steps and corresponding current traces at each step. It shows the ASCF has no effect on the current trace. Also shown are the currents in response to positive and negative voltage steps. Puffer was checked to confirm working.

The averaged effect of TEA on current is shown in the native SLFs (*n=8*), cultures established from P9 mice (*n=3*) and cultures established from P28 mice (*n=7*) (fig. 4.11). In all cases TEA reduced the current, but produced a greater reduction in native SLFs and cultured SLFs derived from P28 mice. TEA reduced the current in native SLFs by ~1nA (fig. 4.11a) and TEA in the cultures from P9 mice reduced the current to a lesser extent, by ~0.25nA (fig. 4.11b). TEA in cultured SLFs from P28 mice had a similar effect to that of the native SLFs by reducing the current to a similar degree of ~1nA (fig 4.11c). Controls for these experiments in native (a, *n=6*) and cultured (b, *n=6*) SLFs were undertaken by replacing TEA with ACSF in the puffer electrode (fig. 4.11 d & e). ACSF had no effect in either the native or cultured SLFs (fig. 4.11d & e). This means the effect on current was purely due to TEA and not any confounding mechanical stimuli.

The IV plot shown in figure 4.12a shows the effect of TEA on current in native SLFs. TEA had a greater effect at negative voltages than at positive voltages, as the greatest effect of TEA occurred at around -90mV reducing the current by approximately ~1nA (fig. 4.12a). The effect of TEA is reduced as the steps become more positive. An IV plot showing the effect of TEA on the current in cultured SLFs from P9 mice shows TEA had a small effect at negative voltages with the greatest effect reducing the current by approximately ~-0.25nA at around -70mV (fig. 4.12b). An IV plot showing the effect of TEA on the current in cultured SLFs from P28 mice shows TEA has a small effect at around -70mV and 30mV (fig 4.12c).

TEA partially blocked the current in native (fig. 4.12a), cultured fibrocytes from P9 mice (fig. 4.12b) and cultured fibrocytes from P28 mice (fig. 4.12c), but had a greater effect at the negative voltages in native fibrocytes, reducing the current more so. TEA appears to block a non-specific cation channel. Prior to TEA application in this experiment there was generally a greater current in the cultured fibrocytes, contradictory to earlier data, this could be due to

linear and rectifying responses being averaged together or a difference in the protocol due to the application of the TEA.

Figure 4. 11 Effect of TEA on current trace in native and 3-D cultured SLFs

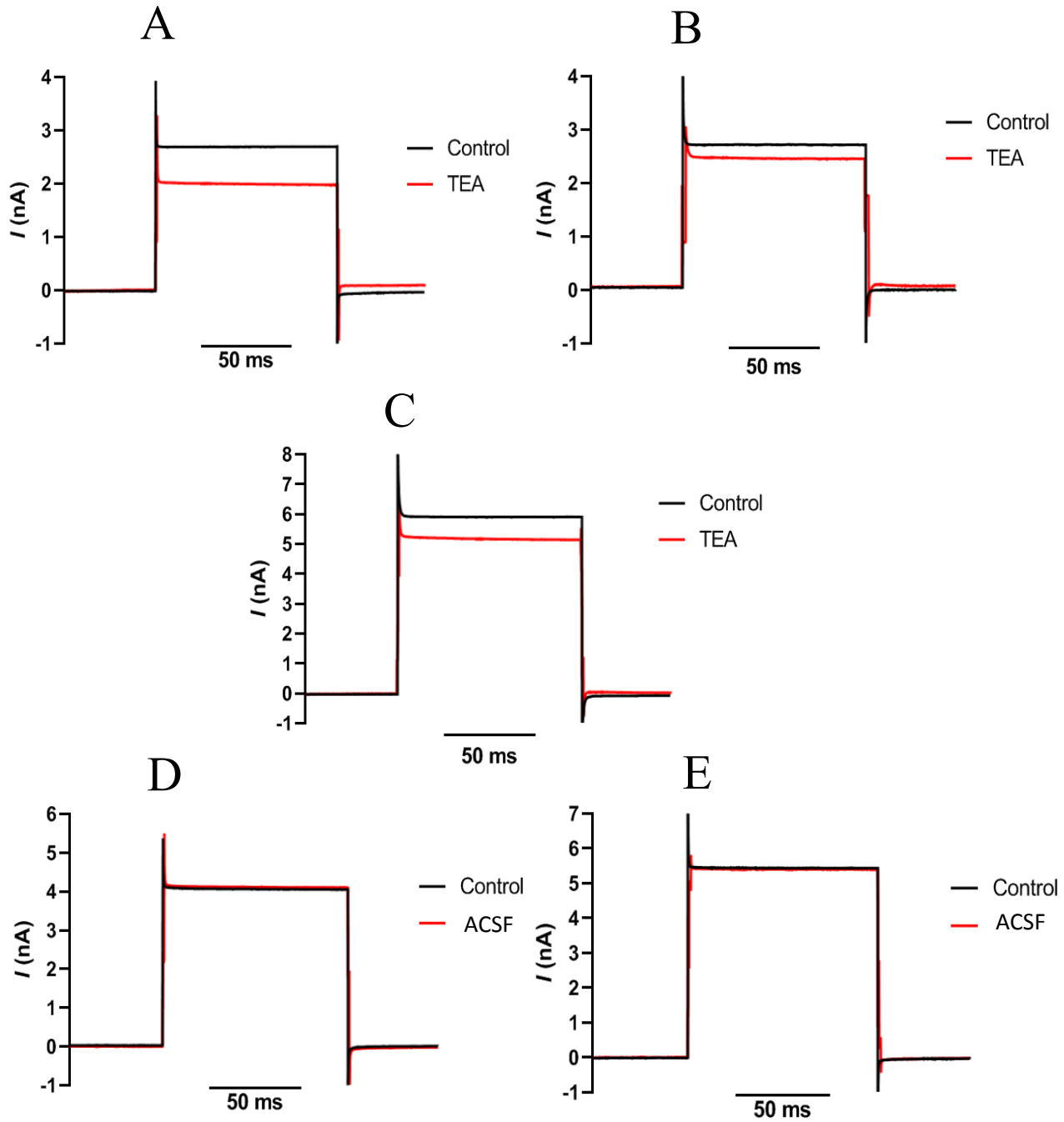

Figure 4.11 Whole-cell currents were inhibited by extracellular TEA, the K channel blocker. Averaged traces showing the current before and after TEA in native (**a**, *n=8*); and 3-D cultured SLFs from P9 mice (**b**, *n=3*); and 3-D cultured SLFs from P28 mice (**c**, *n=7*). Black lines show control, and red lines in **a** to **c** represent the responses after TEA application (10mM) and in **d** & **e** represent responses after TEA wash-off (ACSF application). Control TEA experiments puffing ACSF onto cells in replacement of TEA (**d** & **e**). Averaged traces showing the current before and after ACSF application in native (**d**, *n=6*); and cultured SLFs (**e**, *n=6*). All cells at a holding voltage of -50mV and shown at +30mV step.

Figure 4. 12 Average IV plots of effect of TEA on native and 3-D cultured SLFs

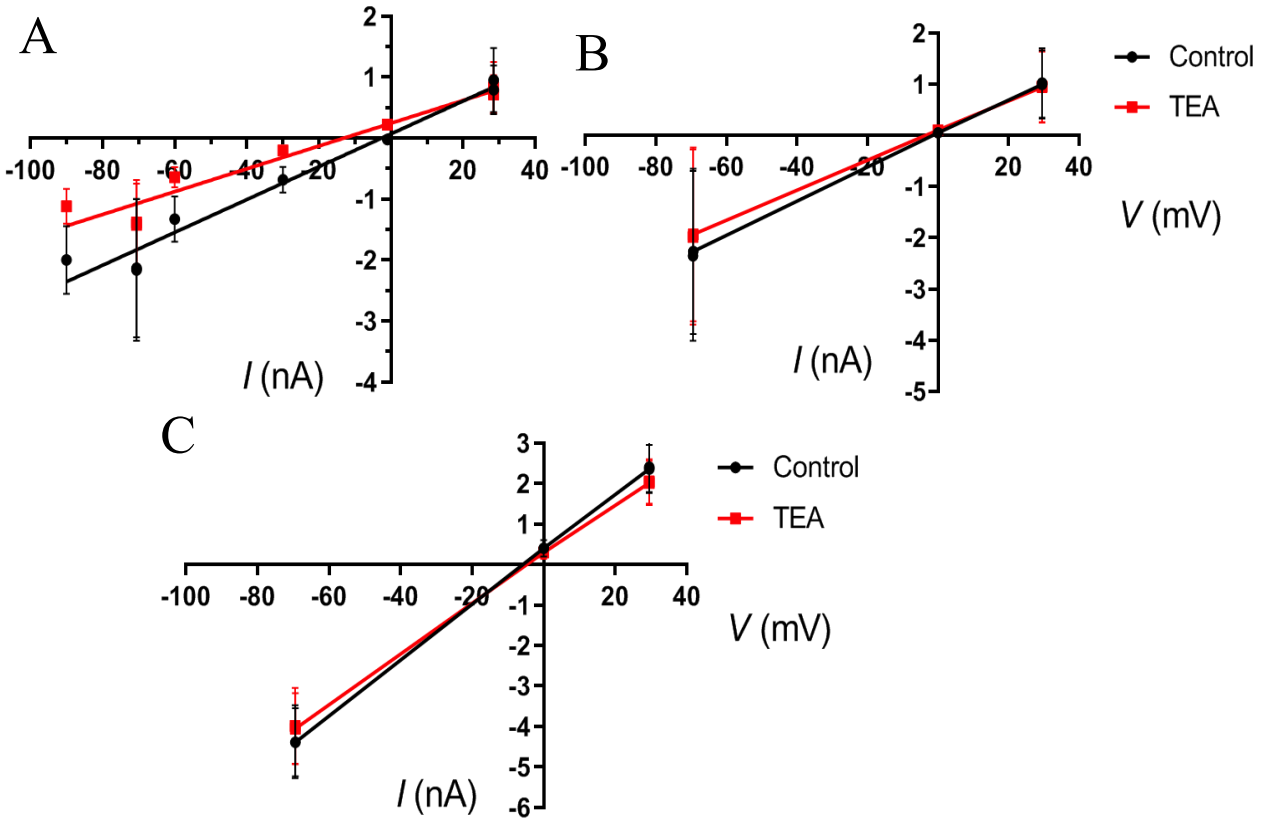

Figure 4.12 Averaged IV plot graphs in native (a, *n=8*); and 3-D cultured SLFs from P9 mice (b, *n=3*); and 3-D cultured SLFs from P28 mice (c, *n=7*). Voltage steps ran from -90mV to 30mV. Black lines show control response (normal current response to different voltage steps), and red lines represent the responses after TEA application (10mM).

4.3.2.1 Effect of TEA on resting membrane potential, conductance and reversal potential values in native and 3-D cultured fibrocytes

Resting membrane potential

In both the native and cultured fibrocytes TEA block results in a more negative RMP (fig. 4.13). In the 3-D culture SLFs TEA experiments were carried out on cultures derived from P9 mice and P28 mice. Both of these groups were compared to native SLFs to see if cultures from one of the ages showed responses similar to the native. There was no significant difference between the RMPs in the control and TEA group in either the P9 *(p=0.214)* or P28 *(p=0.135)* derived culture, however, there was a significant difference between the RMPs in the control group and TEA group in the native SLFs with the effect of TEA on the native SLFs reducing the mean current by over 13 times (-0.85mV ±0.866, *n*=8, *versus,* -11.84mV ±1.84, *n*=8, respectively, *p=0.0012).*

There was no significant difference between the RMPs between native and P9 cultured SLFs in the control group (*p=0.971*) or TEA group (*p=0.195*). There was a significant difference in the RMPs between native and P28 cultured SLFs in the control group (-0.85mV ±0.866, *n*=8, *versus,* -5.62mV ±0.915, *n*=7, respectively, *p=0.0023*) with the RMP being over six times greater in the cultured SLFs, as well as a significant difference in the TEA group (-11.84mV ±1.84, *n*=8, *versus*, -4.00mV ±1.38, *n*=7, respectively, *p=0.0079)* with the RMP being nearly three times greater in the native SLFs. There was also a significant difference in RMP between the P28 and P9 cultures in the control group (-5.62mV ±0.915, *n*=7, *versus*, -0.80mV ± 0.095, *n*=3, respectively, *p=0.0103)*, but not in the TEA group (*p=0.418*).

Figure 4. 13 RMPs in 3-D cultured and native SLFs before and after TEA application

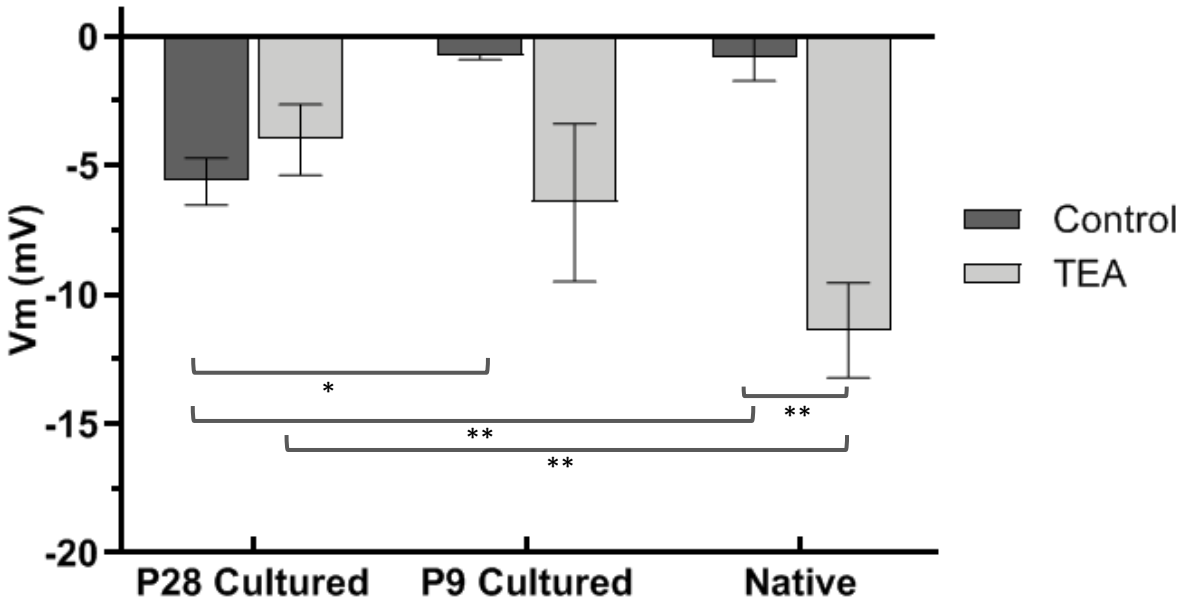

Figure 4.13 Bar graph showing the average resting membrane potentials (RMPs) of 3-D cultured (*n*=10) and native (*n*=8) fibrocytes before and after application of TEA. Groups show cultured SLFs from P9 mice (*n=3*), cultured SLFs from P28 mice (*n=7*), and native SLFs (*n=8*). (mean ± SEM)

Conductance

The effect of TEA on the conductance, as expected, is reduced in both native and cultured fibrocytes (fig. 4.14). In the P9 derived culture there was no significant difference in the conductance between the control and TEA group (*p=0.305*), however, there was a significant difference in conductance between the control and TEA group in the native SLFs (0.0306µs ±0.0142, *n*=8, versus 0.0215µs ±0.0033, *n*=8, respectively, *p=0.0011*), and the P28 cultures (0.0675µs ±0.00529, *n*=7, versus 0.0617µs ±0.0543, *n*=7, respectively, *p=0.0214*).

There was no significant difference in the conductance between P9 cultured and native SLFs in the control group (*p=0.840*), nor the TEA group (*p=0.442*). Furthermore there was a significant difference in the conductance between P28 cultured and native SLFs in the control group (0.0675µs ±0.00529, *n*=7, versus 0.0306µs ±0.0142, *n*=8, *p=0.0002*) as well as in the

TEA group (0.0617µs ±0.0543, *n*=7, versus 0.0215µs ±0.00333, *n*=8, *p<0.0001*). Finally, there was a significant difference in conductance between the cultures from P28 and P9 mice in the control group (0.0675µs ±0.00529, *n*=7, versus 0.0329µs ±0.0134, *n*=3, *p=0.0172*) and in the TEA group (0.0617µs ±0.0543, *n*=7, versus 0.0293µs ±0.00475, *n*=3, versus *p=0.0277*).

Figure 4. 14 Conductance in 3-D cultured and native SLFs before and after TEA application

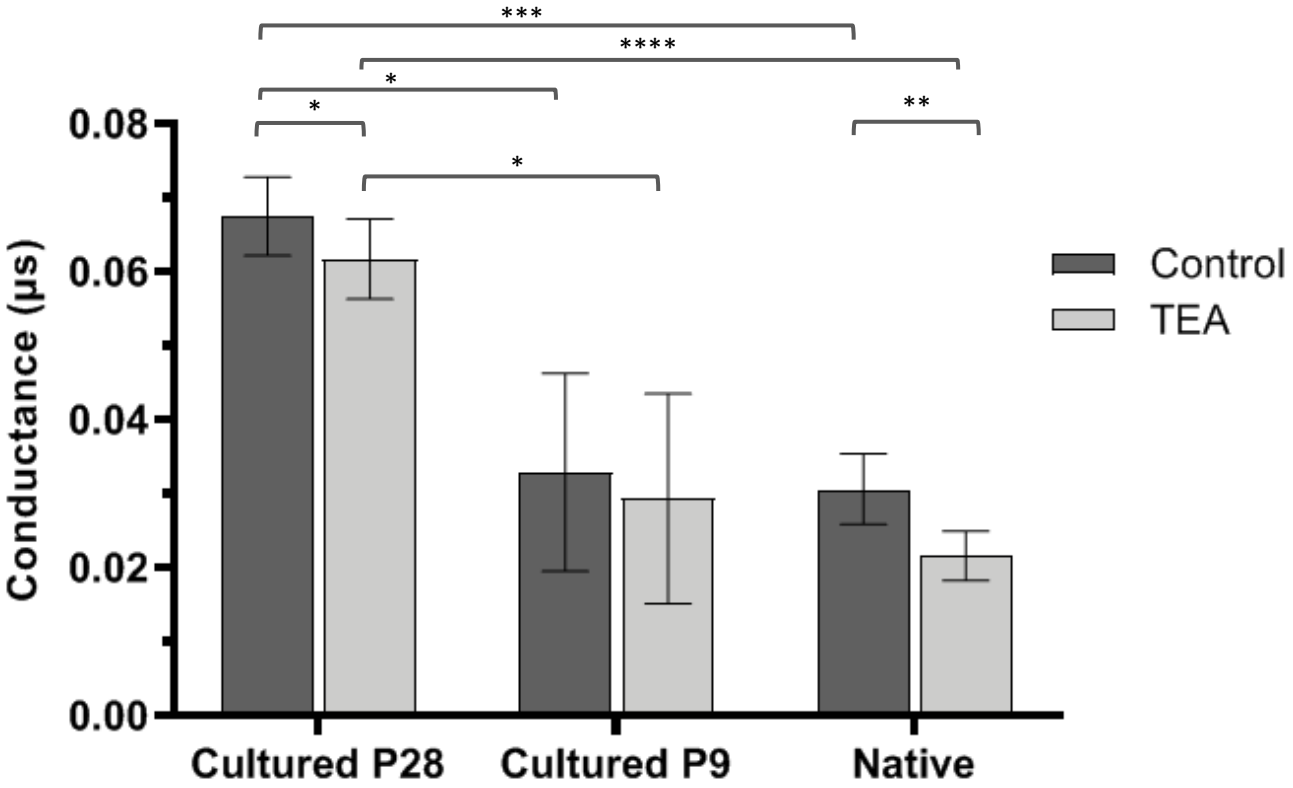

Figure 4.14 Bar graph of the average conductance of 3-D cultured (*n*=10) and native (*n*=8) fibrocytes before and after application of TEA. Groups show cultured SLFs from P9 mice (*n=3*), cultured SLFs from P28 mice (*n=7*), and native SLFs (*n=8*), between steps -20mV to -40mV before and after application of TEA. (mean ± SEM).

Reversal potential

In the apparent reversal potential of TEA in native SLFs and SLFs derived from P9 and P28 mice (fig. 4.15), there was no significant difference between the P9 derived cultured SLFs and native SLFs (-15.72mV±27.32, *n=3 versus* 18.75mV±3.602, *n=8* respectively, *p=0.06*). There was a significant difference in the reversible potential between the P28 derived cultured SLFs and the native (-22.13mV±9.911, *n=7, p=0.0013*). Finally, there was no significant different in the reversal potential between the P28 and P9 cultured SLFs (*p=0.784*).

Figure 4. 15 Reversal potential of TEA- sensitive current in 3-D cultured and native SLFs

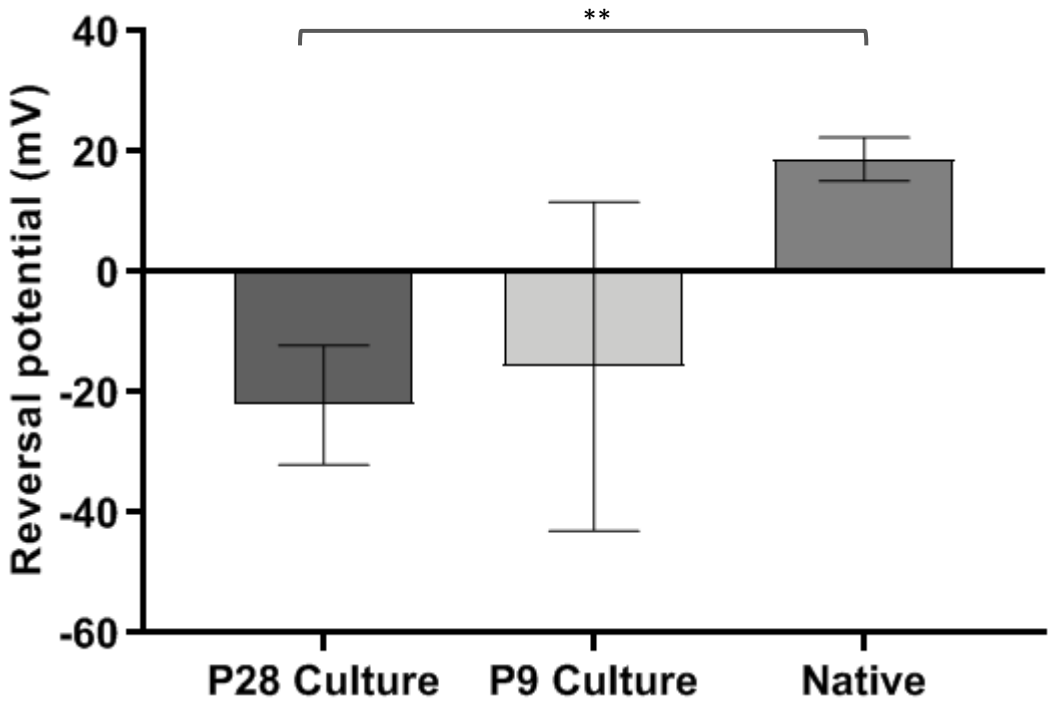

Figure 4.15 Bar graph showing the average reversal potential of native and 3-D cultured SLFs before and after application of TEA. Groups show culture SLFs derived from P9 mice (*n*=3), cultured SLFs derived from P28 mice (*n*=7), and native SLFs (*n=8*). (mean ± SEM).

Overall, the results from the TEA experiments show that the responses to TEA in terms of its effect on the RMP, conductance and reversal potential show that the P9 derived SLFs cultures show more similar trends to native SLFs, when compared to the P28 derived cultures.

4.4 Discussion

There are voltage-gated channels in all living systems and these K^+ channels segregate into at least two main functional groups – hyperpolarised-activated, inwardly rectifying, and depolarised activated, outwardly-rectifying (Riedelsberger et al, 2015). In excitable cells they serve the crucial function of repolarising the membrane to its resting voltage after an action potential.

Indeed, dominant K^+ membrane conductance has been reported in all cell types studied in the lateral wall syncytium (Takeuchi et al, 2000; Liang et al, 2001; 2002). This is consistent with the generation of a concentration gradient enabling the hypothetical movement of K^+ through SLFs to the cells of the *stria vascularis,* as the concentration of extracellular K^+ in perilymph surrounding SLFs (~5 mM) is slightly higher than that in the intrastrial fluid bathing strial basal and intermediate cells (~1.5–3 mM, Salt et al., 1987, Ikeda & Morizono, 1989). The involvement of potassium channels and transporters function in the potassium recycling.

The main findings here that an outwardly rectifying current dominates the voltage-dependent membrane conductance in native and cultured SLFs suggests that they potentially play a major role in generating and regulating the electrochemical gradient inside the lateral wall syncytium, an essential process to K^+ recycling (Kikuchi et al, 1995; 2000; Spicer & Schulte, 1996;1998; Wangermann, 2002). It is also consistent with previous research stating the presence of an outward large conductance voltage-gated potassium current carried by the BK channel in cultured SLFs (Liang et al, 2003; 2004; 2005; Shen et al, 2004).

Additionally, there were a few recordings showing inward rectifying currents (*n=2* in cultured and *n=1* in native, data not shown). The reason, therefore, why not much inward current was detected could be due to the developmental expression of Kir5.1 as it has been seen in mice in the lower part of the spiral ligament at P10 (Hibino et al, 2004). In the cultures the exact

maturity of the cells are unclear due to the lack of external cues that would be present *in vivo* but the native recordings were from mice between P7-9. It may be that at older post P10 ages of the mouse more frequent inward rectification would have been seen, however, this would have made the sectioning of the cochlea much more problematic due to the hardness of the bone as the mouse gets older, causing the slice to crumble.

4.4.1 Similar electrophysiological signature in native and cultured SLFs

The most notable outcome of the electrophysiology work is that both native and cultured showed voltage-dependent potassium currents. This is crucial to the point of cultured SLFs being functional making them a useful target to be used as a cell replacement. Both native and cultured SLFs both show similar responses, they both showed predominantly linear and outwardly rectifying responses. The linear group the current responses were very similar between the native and cultured fibrocytes; however the outwardly rectifying responses in native SLFs were much greater than the outwardly rectifying responses in cultured SLFs. These cultured fibrocytes seemed connected through processes forming a lattice-like structure and label for connexin proteins (data shown in previous chapter) but not connected to the density level as they would be natively. Therefore, these cells possess a greater current as they most likely have more channels for current to pass through.

4.4.2 Similar RMPs and conductance between native and cultured SLFs

In general, the plasma membrane of cells in a resting state is permeable predominantly to K^+ and so their RMPs relative to the neighbouring extracellular solution are negative (-30 to -90mV, Elmslie, 2001; Hille, 2001; Jaye et al, 2010). However, it has been found in microelectrode studies that these fibrocytes *in vivo* show a positive membrane potential of +5 to +12 mV (Nin et al, 2008; Ikeda & Morizono, 1989). It is believed this electrical component is

required for the highly positive EP of around +80mV. It has been demonstrated that the membrane of fibrocytes are more permeable to Na^+ than K^+ or Cl^- and this may explain their positive RMP (Yoshida et al, 2016). It may be that this characteristic accounts for the RMP in type I, II, IV and V SLFs as it is these types that express cation channels that are permeable to Na^+, the Na^+ transporters NKCC and Na^+ K^+ ATPase, whereas type III (and type I) express the K^+ Cl^- transporter (KCC3, Hibino et al, 2004; Mahendrasingam et al, 2011a). Also the native SLFs recordings were mainly from the area of the ligament whereby the type III fibrocytes reside due to them being more easily assessable for patch-clamp recordings then the other types as the previous *in vivo* microelectrode studies would not distinguish between fibrocyte types as it is just known that it is in the fibrocyte region in the spiral ligament. It may be that type I, II, IV and V have a positive RMP and type III slightly negative.

Here native and cultured fibrocytes show similar RMPs as there is no significant difference between any of the RMPs in the linear or outwardly rectifying groups. This means both the native and cultured SLFs share some similar trends in terms of their membrane properties indicating cultured SLFs may be a suitable cell replacement therapy.

Despite research stating the RMP of SLFs is positive, there has been research which has found the membrane potential of fibrocytes to be approximately -5mV (Salt et al, 1987; Von Bekesy, 1951). The average RMP here in this study was around -10mV, therefore, Kir5.1 could stimulate Na^+K^+ATPase and NKCC1 by providing K^+ for their K^+ site in the narrow extracellular space surrounded by the infolded plasma membrane of the fibrocytes. The localised K^+ recycling would reduce the uptake of K^+ released from outer sulcus cells by the K^+ -transport apparatuses as the K^+ is taken up through the hair cells then passed through the epithelial gap junction network to the connective-tissue gap junction network. Thus the K^+-recycling mechanism by Kir5.1 could negatively regulate cochlear K^+ circulation and prevent EP overshoot (Hibino et al, 2006). It is worth noting that Kir5.1 is slightly expressed on the

surface of the membrane but abundantly distributed in the cytoplasm, presumably on the transport vesicles. Therefore, Kir5.1 may be actively recycled between cytoplasm and membrane surface, and this recycling system could dynamically regulate the activity of the Kir5.1 in the fibrocytes, although its regulatory mechanism is still unknown.

Moreover, the conductance in the native and cultured SLFs is similar, particularly in the linear responses and at the negative voltage steps in the outwardly rectifying responses. The native SLFs had a significantly greater conductance compared to cultured fibrocytes at positive steps in the outwardly rectifying responses. This could possibly be due to the cells being more electronically connected natively therefore more channels contributing, compared to the cultured environment where the cells are sparser and more isolated showing fewer connections. It could be that there may be a loss of cell-cell interactions and truncation of projections in the process of acute dissociation and this may alter the electrical activity of the cells. However, the capacity was found to be slightly greater in the cultured SLFs, which is consistent with these cells appearing larger than the native SLFs as shown in the bright field and fluorescent images seen in figures 4.2 and 4.3 with the average cell dimension of cultured fibrocytes being 4.41µm and native 2.01µm. It may be that cells are typically larger in culture, and there may be an association between the size of a cell and the characteristics of those cells. This could be related to cell density as the density of cells *in vivo* is greater than that *in vitro* and it has been found that cells seeding density affects the diameter of the cells as with lower densities the cell diameter was 62-73% larger than those seeded at higher densities (Awad et al, 2000).

4.4.3 TEA reduces potassium currents in native and cultured SLFs

In the TEA experiments the magnitude of the currents are greater in the cultured SLFs derived from the P28 cultures, whereas the currents appear to be similar between the native and P9

derived cultured SLFs. One possible explanation for this is a developmental effect in that the native SLFs (P7-P9 mice) and the cultures derived from P9 mice, the SLFs may not be fully matured and specialised. Even though in this case it is not known how mature the cells are in culture, the fact that they are from a P9 mouse could mean they cells lack in specialisation when compared to the cultured SLFs from the P28 mice. The cultures from the older mice may be more developed for hearing and therefore possess a greater current for K^+ recycling and generation of the EP as in mice it develops between 5 and 17 days after birth (DAB) increasing abruptly 7 DAB and reaches 80mV 14 DAB (Sadanaga & Morimitsu, 1995). This idea is consistent with findings in whole brain slices from mice of varying maturity which found cultures from neonatal mouse tissue survive longer and continuously express progenitor-like cells but do not retain the cellular and cytoarchitectural features of mature tissue cultures (Staal et al, 2011).

Furthermore, TEA has the same effect on the native and cultured SLFs; it decreases the inward holding current ('leak current'). However, it appears to reduce the current more dramatically in native SLFs the more negative the voltage. Reducing the current by ~1nA between around -50mV to -90mV and in P28 mice derived cultures at most positive voltages reducing the current by ~0.5nA between around 20mV to 30mV and also most negative voltages reducing the current by ~0.5nA between around -60mV to -70mV. In comparison the P9 derived cultures current was reduced by ~0.25nA between around -50mV to -70mV but only at the more negative voltages. It is to be expected that TEA would block the current but to a more significant degree as it has been found that extracellular application of 1mM almost completely inhibits channel activity in cultured type I SLFs (Liang et al, 2003; 2005; Shen et al, 2004). It could be that TEA could be blocking a non-specific cation channel.

4.4.4 TEA affects the RMP and conductance of P9 derived cultured and native SLFs similarly

Moreover, TEA affects the RMPs similarly between the native and P9 derived cultures by making them more negative. The RMP prior to TEA in the native and P9 derived cultures are relatively close to zero at -0.85mV and -0.795mV respectively, after TEA application the RMPs becomes more negative -11.38mV and -6.437mV respectively. However, the RMP in the P28 group there was significant difference between the cultured SLFs and native SLFs both before and after TEA application. Also, the RMP in P28 derived SLFs became less negative after TEA application, the opposite effect as to that of the P9 derived cultures and native SLFs. Even though this effect of TEA is the same in both sets of cells, although to different magnitudes, it is unusual for TEA to make the RMP more negative as it blocks the potassium channels so depolarisation would be expected to make the RMP more positive (Barrett et al, 1988). It could be that some channels are insensitive to TEA under these conditions. It seems TEA appears to block current that depolarises the P9 cultured SLFs and native SLFs; this could be a novel finding.

Again the effect of TEA on conductance is similar in native and P9 derived cultured SLFs, as it reduced the conductance in both P9 cultured and native SLFs, significantly so in the native. This is consistent with what would be expected as TEA blocks or reduces the flow of current. However, not only did the TEA significantly reduced the conductance in the P28 cultures and native SLFs but there was a significant difference between the conductance in the cultures and native SLFs both before and after TEA application. Likewise, the reversal potential of TEA in these cells was not significantly different between cultures derived from P9 mice at -15.72 mV and the native SLFs at 18.75 mV; again however, native SLFs was significantly different to that of the cultured SLFs derived from P28 mice at -22.13mV. These results were not due to a change in the relative permeability of the channels to potassium or sodium, but could be

explained by a change in driving force for the permeant intracellular ions (K^+ and/or Cs^+) on their substitution with the impermeant TEA^+ ion.

These results could suggest TEA affects fibrocytes differently depending on age of the mouse, again meaning the older mice cultures may be more mature than that of the P9 mice derived cultures and P7-9 native SLFs which may have less mature cells with a more negative RMP and a greater conductance capacity in order for these cells to fulfil their K^+ recycling function essentials to the maintenance of the EP. It appears in this case the SLFs derived from P9 mice seem to have comparable TEA response characteristics to native SLFs of mice within an age range of P7-9, and different characteristics to that of cultured SLFs derived from older mice of the age P28. Whether these cells are not yet specialised for function *in vitro* is unknown in either cultures so conclusions on this matter cannot be certain, but one would think those in an older mice may be more mature and differentiated with the ready features necessary for maintenance of the EP and function of hearing.

The overall discrepancies between the results found in this study, when compared to previous research, could be accounted for by numerous other factors such as the use of different species as CD/1 mice were used here but many other animals such as rats, gerbils and guinea pigs where used in other studies (Liang et el, 2003; 2005; Shen et al, 2004; Yoshida et al, 2016). CD/1were chosen in this study as they displayed a similar pathology to human age-related hearing loss on an accelerated time period. Additionally, the difference in electrophysiological techniques may also be a variable for consideration as the techniques for establishing the RMP of type I cultured SLFs where microelectrode work compared to the whole-cell patch clamp method used here which could potentially be specific to each fibrocyte type. The use microelectrodes could cast a possible doubt as to whether the area of recording was definitely that of the SLFs.

The fact that here both the cultures and slices used to explore the properties of SLFs are both *in vitro* techniques compared to the *in vivo* work finding positive RMPs could also be a variable in the difference between the results (Yoshida et al, 2016). It could be that the cells are not as they would be naturally *in vivo*; however patch-clamp electrophysiology would be extremely difficult in an *in vivo* setting. It must be remembered here in this case that this is the first attempt at whole-cell voltage clamp recordings from cultured SLFs grown in a 3-D environment and being that of a potentially type III mixed phenotype, as other work exploring the electrophysiological characteristics on these cells has been from possible type I SLFs cultures in a 2-D environmental setting. This again could be another reason for this difference in findings between the cultured SLFs studies as it could be that the different types of SLFs have different properties such as RMPs.

4.4.5 Conclusion

In conclusion, this is the first whole-cell voltage-clamp recordings of and established culture of predominantly a type III mixed phenotype SLF culture grown in a 3-D environment. These recordings were compared to those of native SLFs and in this case functional and comparable potassium currents were found to be present in both the native SLFs and cultured SLFs. Cultures derived from P9 mice responded to TEA more similarly to native SLFs than cultures derived from P28 mice. Overall, this means this could be a unique cell type that may potentially fulfil the functions of the native cells. This is also the first evidence that potentially type III SLFs are involved in K^+ recycling in the spiral ligament additional to their in their tension regulation function of the cochlea lateral wall. In combination, this work strengthens the argument in the case of cultured SLFs being suitable replacement for the degenerating fibrocytes *in vivo* to treat age-related hearing loss.

Chapter 5

General Discussion

5. Chapter 5- General Discussion

It is generally accepted that K^+ is released from cochlear hair cells and cycles from the perilymph, through the cochlea lateral wall, to the endolymph. The lateral wall is made up of the spiral ligament containing SLFs, and the *stria vascularis*. SLFs are one of the crucial components in mediating K^+ circulation.

This study was undertaken to determine if these crucial cells of the spiral ligament could be successfully cultured in a 3-D environment, and investigate whether they possessed the features and characteristics to fulfil the function of native SLFs, building the case for them to be used as a cell replacement therapy to treat age-related hearing loss.

5.1 Successful 3-D cultures of a type III mixed phenotype SLF culture

Firstly, SLFs were successfully cultured in a 3-D collagen gel, enabling the cells to possess a more rounded, interconnected morphology when compared to 2-D cultures which exhibited a more flat, stretched out morphology. The 3-D cultured SLFs were found to be more elongated compared to 2-D cultured cells, and were found to form a network of cell-cell connections. This 3-D environment, potentially, more closely represents the *in vivo* environment of the spiral ligament, and therefore would be a more promising target for a cell replacement as opposed to 2-D cultures. Additionally, these SLFs cultures were found to be that of a type III mixed phenotype culture.

In vivo, type I SLFs are lateral to the *stria vascularis* and are connected via gap junction proteins connexin26 and connexin30 to strial basal cells (Forge et al, 2003; Liu and Zhao, 2008). They are also connected through similar gap junctions to type II SLFs located under the *stria vascularis* and type V above. This connective syncytium is thought to be the main K^+ circulation pathway (Kelly et al, 2011). Type IV SLFs reside underneath type II fibrocytes but

have not been found to express connexin26/connexin30 channels, and consequently are not thought to be contributing to the recirculation pathway (Adams, 2009). However, it is thought they may possibly play crucial roles in perilymphatic Cl^- transport (Que et al, 2007).

Type III SLFs are present at the back lining of the ligament and express connexin31 intracellularly, but do not appear to be connected cytoplasmically to the gap junction network (Kelly et al, 2012). This is consistent with the findings of this study whereby the SLF cultures were observed to be positive for the type III SLF marker (AQP1) and also the connexin 31 and connexin26 gap junction proteins. Type III fibrocytes are also termed 'tension fibrocytes' (Henson et al, 1984; 1985, Henson and Henson, 1988). Analysis of type III fibrocytes *in vitro* has identified a role for these cells in setting basilar membrane tension and auditory sensitivity (Kelly et al, 2012).

Aquaporin labelling in the type III 'bone-lining' cells in all turns of the cochlea (Stankovic et al, 1995) suggests that type III fibrocytes contribute to normal hearing in all tonotopic locations. It is reported that AQP1-null mice retain normal hearing sensitivity (Li & Verkman, 2001), making it unclear as to the role of AQP1 in type III SLFs. Aquaporins facilitate water permeability in sensory and non-sensory tissues, and this may be critical in maintaining the mechanics of tissue and the ionic balance of fluids. In the eye, cells express AQP1 and are associated with regulating volume and pressure of fluids in this network (Verkman , 2003; Lin et al, 2007). It is suggested that additionally to the basilar membrane tensioning in the basal region of the cochlea (Naidu & Mountain, 2007), type III SLFs could regulate hydrostatic pressure within the whole ligament though AQP1.

Mounting evidence suggests that the cochlear fibrocytes may have a regenerative capacity, pointing towards a potential therapeutic target for regeneration of the lateral wall and associated deafness. Cochlear fibrocytes divide continuously until an advanced age where the

proliferation capacity decreases (Lang et al, 2003). This proliferation capacity increases after damage (Roberson & Rubel, 1994; Hirose & Liberman, 2003; Lang et al, 2003). It has further been revealed that the slow cycling, or potential stem cells, is found more often in type III SLFs and that these fibrocytes repopulate the type I area where the most significant decrease in fibrocytes is observed when exposed to intense noise (Li et al, 2017). It is therefore thought that type III SLFs contain the stem cell population in the lateral wall and may be a potential target for a regenerative therapy.

This is consistent with the findings here of a predominantly type III mixed phenotype culture. It may be that this fibrocyte type specifically contains a regenerative capacity that exceeds the other SLF types in culture. It could also be suggested that the cultured cells are of a hybrid phenotype due to the strong labelling for AQP1 and less intense labelling for S-100, indicating the expression of two different markers of fibrocytes in one cell. This could be an effective culture, as expression of two different fibrocyte phenotypes within one cell culture would enable the cells to possess multiple fibrocyte characteristics, thus increasing the likelihood of the cells retaining the ability to function as the fibrocytes of the spiral ligament natively following *in vivo* transplantation.

This study went on to investigate whether this culture of a type III mixed phenotype may also play a part in cochlea K^+ recycling, through determining a protein profile and electrophysiological signature of these cells.

5.2 Cultured SLFs possess potassium transport functions

The immunolabelling and electrophysiology conducted on the 3-D cultured and native SLFs showed similar characteristics. Both showed expression for Kir5.1 and connexin proteins, and showed predominately outward rectifying potassium currents as opposed to inwardly

rectifying. The only discrepancy was the BK labelling as there was weak labelling in the cultured SLFs and inconclusive labelling in the native sections of cochlea.

Kir4.1 and Kir5.1 subunits are expressed in epithelial tissues and glial cells and may form a heteromeric assembly (Tanemoto et al, 2000; Lourdel et al, 2002). Both homomeric Kir4.1channels and heteromeric Kir4.1/Kir5.1 channels can be regarded as the major Kir channels responsible for K^+ transport in glial and epithelial cells. A previous study observed that Kir5.1 and Kir4.1 subunits are expressed in different types of cells in the cochlea (Hibino et al, 2004). This suggests the possibility that Kir5.1 expressed in cochlear fibrocytes is that of a homomeric assembly. Kir5.1 subunit expression has been found specifically in type II and IV fibrocytes in the spiral ligament, and it seems probable that this Kir channel is involved in the control of K^+ transport in this region (Hibino et al, 2004).

In support of this interpretation is the observed developmental time-course of Kir5.1 expression in the ligament. The EP starts to rise at P8 and reaches the adult level at 2 weeks after birth (Anniko, 1985). In the *stria vascularis* the immunoreactivity of Kir4.1 is first observed at P8 when the EP starts to become positive and increases rapidly between P10 and P14 (Hibino et al, 1997). This indicates that Kir4.1- expression may be required for the initiation and establishment of the highly positive EP. This is further supported by a study which demonstrated that the loss of Kir4.1 using Kir4.1 knockout mice resulted in the loss of EP (Marcus et al, 2002). In contrast, Kir5.1 is thought to have an important role in the rapid phase of EP elevation. Kir5.1 is detected in the lower part of the spiral ligament at around P10, and increases to plateaus at P15-P16 (Hibino et al, 2004). During this stage of development EP rises concurrently (Xia et al, 1999), thus suggesting that Kir5.1 plays a role in EP elevation.

Previous studies have also demonstrated that type I SLFs exhibit a dominant BK channel conductance that likely contributes to establishing and maintaining an electrochemical gradient essential for K^+ recycling (Shen et al, 2004). BK channels in type I SLFs have a voltage-dependent incomplete inactivation. This enables the cells to maintain their membrane potential whilst conserving intracellular K^+, a biophysical property similar to that observed in cardiac myocytes (McManus et al, 1995; Wallner et al, 1995; 1999; Brenner et al, 2000). This regulatory mechanism is crucial to the function of type I SLFs, as these cells are believed to transmit K^+ intracellularly through gap junction-coupled SLFs network to return to the *stria vascularis* (Schulte and Steel, 1994; Spicer and Schulte, 1996).

The main findings from the electrophysiology in this study showed that the predominant characteristic groups in both the cultured and native SLFs were linear (non-rectifying) responses and outwardly rectifying responses, whilst there was very little inward rectification seen (some inward rectifying currents can be seen in the current traces in cultured SLFs in fig.3f and native SLFs in fig.4f). However, there was weak labelling for the BK channel in cultured SLFs and inconclusive labelling in the native. This was unexpected as the BK channel is an important negative feedback system linking increases in intracellular calcium to outward hyperpolarizing potassium currents therefore is thought to invoke an outward current in SLFs.

This is also the case for the Kir5.1 labelling as positive labelling for this inward-rectifier was observed in both the cultured and native SLFs, but very little inward rectification was seen in the electrophysiology. The potential homomeric Kir5.1 expression in the cytoplasm and not membrane could explain why little inward rectification was detected in electrophysiology. It could be that the Kir5.1 inward-rectifier may actually impose an outward current due to the resting membrane properties of the SLFs. Outward current through inward rectifier K^+ channels play a vital role in the determination of cells RMP and controlling cell excitability.

Thus, regulation of outward Kir current is important for appropriate physiological functions. It is known that outward Kir currents increase with increasing extracellular K^+ concentration, in a driving force dependent manner (Hagiwara et al, 1976; Lopatin & Nichols, 1996; Matsuda et al, 2010). Previous studies have shown that outward Kir current is increased at higher extracellular K^+ concentrations as a consequence of single channel conductance being elevated at higher extracellular K^+ concentrations.

Despite the discrepancy in the BK labelling between the native and cultured SLFs, in general, the protein expression and electrophysiological results found here are relatively similar between the 3-D cultured and native SLFs. This, therefore, strengthens the case for cultured SLFs being 'fit for function' in a cell replacement therapy to treat age-related metabolic hearing loss, where the SLFs that reside in the ligament *in vivo* degenerate with age.

5.3 Case for transplantation of cultured SLFs

The degeneration and change in cochlear SLFs has been reported to cause hearing loss (Delprat et al, 2005; Minowa et al, 1999). Brain-4 (*Brn-4*) deficient mice, for example, display a reduced EP and hearing loss, and also show ultrastructural alterations, particularly in SLFs such as cellular atrophy and mitochondrial reduction (Minowa et al, 1999; Xia et al, 2002). In mice deficient in otospiralin, type II and IV SLF degeneration is the main pathological change seen, with the appearance of hair cells and the *stria vascularis* being normal (Delprat et al, 2005). It has also been found that age-related degeneration of cochlea SLFs precedes that of any other type of cells within the cochlea, with the most significant pathological changes seen in type II, IV and V fibrocytes, where they have been found to degenerate in aged gerbil models, aged C57BL/6 mice, and aged CD/1 mice (Spicer & Schulte, 2002; Hequembourg & Liberman, 2001; Wu & Marcus, 2003; Mahendrasingam et al, 2011).

MSC transplantation has been used to treat multiple sclerosis and amyotrophic lateral sclerosis (Giordano et al, 2007; Devine, 2002; Karussis et al, 2010; Uccelli et al, 2011). A novel rat model developed for acute sensorineural hearing loss attributable to fibrocyte dysfunction induced by a mitochondrial toxin, found that active regeneration of the cochlear fibrocytes occurred following extreme focal apoptosis, without any changes observed in the Organ of Corti (Kamiya et al, 2007). Moreover, following transplantation of MSCs into the lateral semi-circular canal of the rats some of the MSCs were detected in the injured area of the lateral wall, and those that received MSC transplantation displayed significantly increased hearing recovery compared to the control mice (Kamiya et al, 2007). The MSCs also showed connexin26 and connexin30 immunostaining indicating gap junctions between these cells. This research suggests that regeneration of cells within the spiral ligament of the cochlea leads to hearing recovery after acute sensorineural hearing loss, and that the transplantation of these cells may be a promising therapy.

More recently, a similar study transplanted MSCs into the cochlea in an attempt to explore whether it would be an effective therapy for stopping or delaying the progression of sensorineural hearing loss in childhood (Kasagi et al, 2013). Kasagi *et al* transplanted MSCs into the semi-circular canal of young mice of 2-3 weeks and adult mice of 24-26 weeks. In the young mice they found the transplanted MSCs had differentiated into fibrocyte-like cells and were detected in cochlea tissue. There were no adverse effects on auditory function by the MSC transplantation, and the auditory brain stem responses threshold did not significantly change after surgery. However, no MSC migration or differentiation was observed in the adult mice after transplantation. The problems of migration and differentiation of the MSCs within these studies, where ectopic cells grew and were not completely differentiated into SLFs, highlight the potential of a cell-replacement therapy of those cells that are fully differentiated and 'fit for function'.

The use of collagen gels for transplantation of stem cells is a particularly explored technique for the regeneration of tissues and organs. It has recently been found MSCs seeded collagen gels can be delivered into injured intervertebral discs and maintained safely in live sheep to 6 weeks (Hussain et al, 2019). Another technique when transplanting cells in collagen gels is to use soluble gels or dissolve the gels after transplantation, as it has been found intradermal injection of cells in pepsin-solubilized collagen is a simple and reliable technique for transplanting normal primary cells and preneoplastic cells (Zhang et al, 2002).

The genetic, structural and functional alterations in cochlea SLFs related to deafness signify the importance of these cells in the maintenance of normal hearing. In this study, SLFs displaying a predominantly type III mixed phenotype were successfully cultured on 3-D collagen gels. This technique was found to be advantageous over 2-D culture methods as it resulted in the generation of rounder cells that were more interconnected and formed a network of cells much like those *in vivo*. These cultures also expressed gap junction proteins and potassium channels, as well as having functioning potassium currents. The concept of using the 3-D cultured, fully differentiated SLFs that possess similar characteristics to that of native SLFs, and transplanting them directly into the spiral ligament would avoid the previously experienced problems of migration and differentiation into this area when exploring a cell replacement therapy to treat hearing loss.

5.4 General Conclusion

Overall, the findings from this study support the idea of cultured SLFs being suitable as a cell replacement therapy to treat age-related hearing loss. The cultures generated in this study were found to be that of a type III mixed SLF phenotype as the cells express AQP1 and S-100, with type III believed to possess the regeneration capacity. When grown in a 3-D transplantable collagen matrix these cells were found to display a morphology which

resembles that *in vivo*. The cultured SLFs were demonstrated to express channels found to be expressed in native SLFs, such as the inwardly rectifying Kir5.1 channel, the large conductance BK channel and the gap junction connexin proteins, connexin26 and connexin31. Electrophysiological analysis of the cultured SLFs revealed similarities with that of native SLFs possessing outwardly rectifying potassium currents. Despite some differences in findings to those previously founded by others, the robust techniques such as patch-clamping enabled better access to the inside of cells, and therefore a closer analysis of the characteristics of SLFs when compared to other techniques previously used to explore these cells.

In combination, these findings demonstrated that the cultured SLFs possess active potassium currents and associated protein channels pointing towards the possibility of them being able to fulfil their function as they would *in vivo*. Transplantation strategies should be explored to further these cultured SLFs being used to replace degenerating SLFs in the ageing cochlea, and consequently preventing or restoring associated metabolic hearing loss.

5.5 Future work

Although there were numerous significant challenges experienced throughout the project, such as problems with starting up cultures and testing times trying to retrieve electrophysiological data, the work here uses robust laboratory techniques that have made it possible to conduct a comprehensive comparison of 3-D cultured SLFs to native SLFs. All the work was in aid of investigating whether these cells are fit for transplantation. Reflecting on the project reveals strengths and weakness, as well as areas to explore further which will only benefit the limited knowledge of these cells and their involvement in hearing.

Continuation of this work would involve further investigations into the possibility of using novel cell replacement therapy to treat age-related hearing loss, for example exploring the

viability of the cultured SLFs for long periods on the 3-D gels. The density of SLFs on these gels slowly decline over a 5 day period (data not shown). Long-term survival rates of SLFs cultured of 3-D gels would therefore need to be investigated prior to the implementation of transplantation strategies, as it would be more ideal for the cells to remain viable for a longer period of time. This could involve the use of growth factors such as transforming growth factor beta (TGF-β) and platelet-derived growth factor (PDGF-BB) during cultivation of the cells. This would enable the cells to survive for longer periods of time in the gels so the success rate of cell survival for transplantation would likely be more successful. Future work could also attempt to successfully generate a cell culture containing all of the five SLF types. This is the most desirable and optimal culture as it would more effectively enable regeneration of a degenerated SL, as all the fibrocytes would be present and carry out their individual functions.

Another point for future work is the use of electron microscopy as this was something that was unable to be carried out due to time constraints. This would enable more in-depth look at the morphology and ultrastructure of the cells, giving a more detailed comparison between the native and cultured SLFs. Future work could compare the differences between the density and distribution of labelled membrane proteins between native and cultured fibrocytes using postembedding immunogold labelling for electron microscopy to quantify the levels of these channels and transporter proteins by the number of immunogold particles labelled. This technique would also make it possible to identify whether the protein was localised on the cells membrane or cytoplasm. The use of electron microscopy could also eliminate a potential flaw of the current research, in that it would confirm the target cells in the native ligament to be fibrocytes. These putative fibrocytes of the spiral ligament used for whole-cell recordings were identified by the use of dextran 3000 which enabled the general morphology and

location of the filled cell. However, electron microscopy would make it possible to confirm this by the ultrastructure of the cells.

Furthermore, another area for exploration is the use of more agonists and antagonists as this would allow the ability to distinguish differences in the carrying of the currents. Future work could explore this by applying specific agonists and antagonists to fibrocytes directly in order to isolate and characterise the potassium channels, such as Kir5.1 and the BK channel, and ion pumps, including the Na^+ K^+ ATPase and the Na^+ K^+ Cl^- cotransporter, all of which contribute to the EP.

In this study the predominant phenotype in the established cultures were those of a mixed phenotype with type III properties. Although the type III SLFs have been found to possess a regeneration capacity that enables them repopulate in area where other fibrocyte types have degenerated (Li et al, 2017), a culture population containing a mixture of all five types of SLFs would be most optimal as they could potentially fulfil all of their individual functions.

The next step of future work would involve human work, as although mouse models exhibit a similar morphology to that of a human, there are always differences across species. The accelerated pathology of CD/1 mice is significantly more rapid when compared to humans, and even other animal models. Therefore, this work should be explored in other mice models such as the C57BL/6 strain and other species such as guinea pigs beforehand. To therefore understand the function of SLF in humans, future work in this area should also work towards the exploration of these cells in trial transplantation studies into live CD/1 mice initially to examine the success of cell survival after transplantation into a living organism.

References

Action on Hearing Loss. 2019. Age-related hearing loss. [Online]. [2 July 2019]. Available from: https://www.actiononhearingloss.org.uk/hearing-health/hearing-loss-and-deafness/types-and-causes/age-related-hearing-loss/

Adachi, N., Yoshida, T., Nin, F., Ogata, G., Yamaguchi, S., Suzuki, T., Komune S, Hisa Y, Hibino H, Kurachi Y., 2013. The mechanism underlying maintenance of the endocochlear potential by the K+ transport system in fibrocytes of the inner ear. *Journal of Physiology,* 9, 591(18), pp. 4459-4472.

Adams, J.C., 2009. Immunocytochemical traits of type IV fibrocytes and their possible relations to cochlear function and pathology. *Journal of the Association for Research in Otolaryngology*, *10*(3), pp.369-382.

Adams, J.C., Ichimiya, I. and Kimura, R.S., 1994. Changes in immunostaining of cochleas with experimentally induced endolymphatic hydrops. *Annals of Otology, Rhinology & Laryngology*, *103*(6), pp.457-468.

Ahmad, S., Chen, S., Sun, J. and Lin, X., 2003. Connexins 26 and 30 are co-assembled to form gap junctions in the cochlea of mice. *Biochemical and biophysical research communications*, *307*(2), pp.362-368.

Ahmed, S., Vorasubin, N., Lopez, I.A., Hosokawa, S., Ishiyama, G. and Ishiyama, A., 2013. The expression of glutamate aspartate transporter (GLAST) within the human cochlea and its distribution in various patient populations. *Brain research*, *1529*, pp.134-142.

Alam, S.A., Oshima, T., Suzuki, M., Kawase, T., Taka, T. and Ikeda, K., 2001. The Expression of Apoptosis-Related Proteins in the Aged Cochlea of Mongolian Gerbils. *The Laryngoscope*, *111*(3), pp.528-534.

Anniko, M., 1985. Histochemical, microchemical (microprobe) and organ culture approaches to the study of auditory development. *Acta Oto-Laryngologica*, *99*(sup421), pp.10-18.

Antoni, D., Burckel, H., Josset, E. and Noel, G., 2015. Three-dimensional cell culture: a breakthrough in vivo. *International journal of molecular sciences*, *16*(3), pp.5517-5527.

Asamura, K & Abe, S & Imamura, Yasutada & Aszodi, Attila & Suzuki, N & Hashimoto, S & Takumi, Yutaka & Hayashi, T & Faessler, Raphael & Nakamura, Y & Usami, S., 2005. Type IX collagen is crucial for normal hearing. *Neuroscience,* 132(2), pp. 493-500.

Awad, H.A., Butler, D.L., Harris, M.T., Ibrahim, R.E., Wu, Y., Young, R.G., Kadiyala, S. and Boivin, G.P., 2000. In vitro characterization of mesenchymal stem cell-seeded collagen scaffolds for tendon repair: Effects of initial seeding density on contraction kinetics. *Journal of Biomedical Materials Research: An Official Journal of The Society for Biomaterials, The*

Japanese Society for Biomaterials, and The Australian Society for Biomaterials and the Korean Society for Biomaterials, *51*(2), pp.233-240.

Azarias, G., Kruusmägi, M., Connor, S., Akkuratov, E.E., Liu, X.L., Lyons, D., Brismar, H., Broberger, C. and Aperia, A., 2013. A specific and essential role for Na, K-ATPase α3 in neurons co-expressing α1 and α3. *Journal of Biological Chemistry*, *288*(4), pp.2734-2743.

Baharvand, H., Hashemi, S. M., Ashtiani, S. K. & Farrokhi, A., 2006. Differentiation of human embryonic stem cells into hepatocytes in 2-D and 3-D culture systems in vitro. *International Journal of Developmental Biology,* 50(7), pp. 645-652.

Baker, B. M. & Chen, C. S., 2012. Deconstructing the third dimension – how 3-D culture microenvironments alter cellular cues. *Journal of Cell Science,* 1 7, 125(13), pp. 3015-3024.

Ballios, B.G., Cooke, M.J., Donaldson, L., Coles, B.L., Morshead, C.M., van der Kooy, D. and Shoichet, M.S., 2015. A Hyaluronan-Based Injectable Hydrogel Improves the Survival and Integration of Stem Cell Progeny following Transplantation. *Stem Cell Reports,* 9 6, 4(6), pp. 1031-1045.

Bansal, M., 2012. *Diseases of ear, nose and throat*. JP Medical Ltd.

Barrett, E. F., Morita, K. & Scappaticci, K. A., 1988. Effects of tetraethylammonium on the depolarizing after-potential and passive properties of lizard myelinated axons.. *The Journal of Physiology,* 1 8, 402(1), pp. 65-78.

Bas, E., Dinh, C.T., Garnham, C., Polak, M. and Van de Water, T.R., 2012. Conservation of hearing and protection of hair cells in cochlear implant patients' with residual hearing. *The Anatomical Record*, *295*(11), pp.1909-1927.

Berrocal, J.R.G., Méndez-Benegassi, I., Martín, C. and Camacho, R.R., 2008. Intervention of spiral ligament fibrocytes in the metabolic regulation of the inner ear. *Acta Otorrinolaringologica (English Edition)*, *59*(10), pp.494-499.

Bettinger, C.J., Langer, R. and Borenstein, J.T., 2009. Engineering substrate topography at the micro-and nanoscale to control cell function. *Angewandte Chemie International Edition*, *48*(30), pp.5406-5415.

Binder, S., Stolba, U., Krebs, I., Kellner, L., Jahn, C., Feichtinger, H., Povelka, M., Frohner, U., Kruger, A., Hilgers, R.D. and Krugluger, W., 2002. Transplantation of autologous retinal pigment epithelium in eyes with foveal neovascularization resulting from age-related macular degeneration: a pilot study. *American journal of ophthalmology*, *133*(2), pp.215-225.

Birgersdotter, A., Sandberg, R. & Ernberg, I., 2005. *Gene expression perturbation in vitro - A growing case for three-dimensional (3-D) culture systems.* s.l.:Academic Press.

Boettger, T., Hübner, C.A., Maier, H., Rust, M.B., Beck, F.X. and Jentsch, T.J., 2002. Deafness and renal tubular acidosis in mice lacking the K-Cl co-transporter Kcc4. *Nature*, *416*(6883), pp.874-878.

Boettger, T., Rust, M.B., Maier, H., Seidenbecher, T., Schweizer, M., Keating, D.J., Faulhaber, J., Ehmke, H., Pfeffer, C., Scheel, O. and Lemcke, B., 2003. Loss of K-Cl co-transporter KCC3 causes deafness, neurodegeneration and reduced seizure threshold. *The EMBO Journal*,*22*(20), pp.5422-5434.

Brenner, R., Jegla, T.J., Wickenden, A., Liu, Y. and Aldrich, R.W., 2000. Cloning and functional characterization of novel large conductance calcium-activated potassium channel β subunits, hKCNMB3 and hKCNMB4. *Journal of Biological Chemistry*, *275*(9), pp.6453-6461.

Brenner, R., Peréz, G.J., Bonev, A.D., Eckman, D.M., Kosek, J.C., Wiler, S.W., Patterson, A.J., Nelson, M.T. and Aldrich, R.W., 2000. Vasoregulation by the β1 subunit of the calcium-activated potassium channel. *Nature,* 19 10, 407(6806), pp. 870-876.

Brown, C.J., Abbas, P.J. and Gantz, B., 1990. Electrically evoked whole-nerve action potentials: Data from human cochlear implant users. *The Journal of the Acoustical Society of America*, *88*(3), pp.1385-1391.

Butler, A. et al., 1993. mSlo, a complex mouse gene encoding "maxi" calcium-activated potassium channels. *Science,* 9 7, 261(5118), pp. 221-224.

Carbrey, J. M. & Agre, P., 2009. Discovery of the aquaporins and development of the field. In *Aquaporins* (pp. 3-28). Springer, Berlin, Heidelberg.

Carsin, H., Ainaud, P., Le Bever, H., Rives, J.M., Lakhel, A., Stephanazzi, J., Lambert, F. and Perrot, J., 2000. Cultured epithelial autografts in extensive burn coverage of severely traumatized patients: a five year single-center experience with 30 patients. *Burns*, *26*(4), pp.379-387.

Chang, C.Y., Chan, A.T., Armstrong, P.A., Luo, H.C., Higuchi, T., Strehin, I.A., Vakrou, S., Lin, X., Brown, S.N., O'Rourke, B. and Abraham, T.P., 2012. Hyaluronic acid-human blood hydrogels for stem cell transplantation. *Biomaterials,* 11, 33(32), pp. 8026-8033.

Chani, B., Puri, V., Sobti, R.C., Jha, V. and Puri, S., 2017. Decellularized scaffold of cryopreserved rat kidney retains its recellularization potential. *PLoS ONE,* 1 3.12(3).

Chen, C. S., 2008. Mechanotransduction - a field pulling together?. *Journal of Cell Science,* 15 10, 121(20), pp. 3285-3292.

Chen, J.-F. & Chen, P., 2019. Pillar[5]arene-Based Resilient Supramolecular Gel with Dual-Stimuli Responses and Self-Healing Properties. *ACS Applied Polymer Materials,* 22 7.p. acsapm.9b00516.

Chen, L., Yan, C. & Zheng, Z., 2018. *Functional polymer surfaces for controlling cell behaviors.* s.l.:Elsevier B.V..

Chen, P. and Segil, N., 1999. p27 (Kip1) links cell proliferation to morphogenesis in the developing organ of Corti. *Development*, *126*(8), pp.1581-1590.

Chen, P., Johnson, J.E., Zoghbi, H.Y. and Segil, N., 2002. The role of Math1 in inner ear development: Uncoupling the establishment of the sensory primordium from hair cell fate determination. *Development*, *129*(10), pp.2495-2505.

Chen, P., Zindy, F., Abdala, C., Liu, F., Li, X., Roussel, M.F. and Segil, N., 2003. Progressive hearing loss in mice lacking the cyclin-dependent kinase inhibitor Ink4d. *Nature cell biology*, *5*(5), pp.422-426.

Chen, W., Jongkamonwiwat, N., Abbas, L., Eshtan, S.J., Johnson, S.L., Kuhn, S., Milo, M., Thurlow, J.K., Andrews, P.W., Marcotti, W. and Moore, H.D., 2012. Restoration of auditory evoked responses by human ES-cell-derived otic progenitors. *Nature,* 11 10, 490(7419), pp. 278-282.

Chen, W., Jongkamonwiwat, N., Abbas, L., Eshtan, S.J., Johnson, S.L., Kuhn, S., Milo, M., Thurlow, J.K., Andrews, P.W., Marcotti, W. and Moore, H.D., 2012. Restoration of auditory evoked responses by human ES-cell-derived otic progenitors. *Nature*, *490*(7419), pp.278-282.

Chen, W., Villa-Diaz, L.G., Sun, Y., Weng, S., Kim, J.K., Lam, R.H., Han, L., Fan, R., Krebsbach, P.H. and Fu, J., 2012. Nanotopography influences adhesion, spreading, and self-renewal of Human embryonic stem cells. *ACS Nano,* 22 5, 6(5), pp. 4094-4103.

Chiba, T. and Marcus, D.C., 2001. Basolateral K+ conductance establishes driving force for cation absorption by outer sulcus epithelial cells. *The Journal of membrane biology*, *184*(2), pp.101-112.

Chignola, R. et al., 2000. Forecasting the growth of multicell tumour spheroids: Implications for the dynamic growth of solid tumours. *Cell Proliferation,* 33(4), pp. 219-229.

Chitcholtan, K., Sykes, P. H. & Evans, J. J., 2012. The resistance of intracellular mediators to doxorubicin and cisplatin are distinct in 3-D and 2-D endometrial cancer. *Journal of Translational Medicine,* 6 3.10(1).

Coates, P. W. & Nathan, R. D., 1987. Feasibility of electrical recordings from unconnected vertebrate CNS neurons cultured in a three-dimensional extracellular matrix. *Journal of Neuroscience Methods,* 20(3), pp. 203-210.

Cohen-Salmon, M., Ott, T., Michel, V., Hardelin, J.P., Perfettini, I., Eybalin, M., Wu, T., Marcus, D.C., Wangemann, P., Willecke, K. and Petit, C., 2002. Targeted ablation of connexin26 in the inner ear epithelial gap junction network causes hearing impairment and cell death. *Current Biology*, *12*(13), pp.1106-1111.

Corey, D. P. & Hudspeth, A. J., 1979. *Ionic basis of the receptor potential in a vertebrate hair cell [12]*. s.l.:s.n.

Corrales, C.E., Pan, L., Li, H., Liberman, M.C., Heller, S. and Edge, A.S., 2006. Engraftment and differentiation of embryonic stem cell–derived neural progenitor cells in the cochlear

nerve trunk: Growth of processes into the organ of corti. *Journal of neurobiology*, *66*(13), pp.1489-1500.

Cosgrove, D., Samuelson, G. & Pinnt, J., 1996. Immunohistochemical localization of basement membrane collagens and associated proteins in the murine cochlea. *Hearing Research,* 8, 97(1-2), pp. 54-65.

Cotanche, D.A., 2008. Genetic and pharmacological intervention for treatment/prevention of hearing loss. *Journal of communication disorders*,*41*(5), pp.421-443.

Crouch, J.J., Sakaguchi, N., Lytle, C. and Schulte, B.A., 1997. Immunohistochemical localization of the Na-K-Cl co-transporter (NKCC1) in the gerbil inner ear. *Journal of Histochemistry & Cytochemistry*, *45*(6), pp.773-778.

Dallas, P., 1992. The active cochlea. *The journal of neuroscience*, *2*(12), pp.4575-4585.

Davis, H., 1983. An active process in cochlear mechanics. *Hearing research*, *9*(1), pp.79-90.

Degen, J., Schütz, M., Dicke, N., Strenzke, N., Jokwitz, M., Moser, T. and Willecke, K., 2011. Connexin32 can restore hearing in connexin26 deficient mice. *European journal of cell biology*, *90*(10), pp.817-824.

Delprat, B., Boulanger, A., Wang, J., Beaudoin, V., Guitton, M.J., Ventéo, S., Dechesne, C.J., Pujol, R., Lavigne-Rebillard, M., Puel, J.L. and Hamel, C.P., 2002. Downregulation of otospiralin, a novel inner ear protein, causes hair cell degeneration and deafness. *The Journal of neuroscience*, *22*(5), pp.1718-1725.

Delprat, B., Ruel, J., Guitton, M.J., Hamard, G., Lenoir, M., Pujol, R., Puel, J.L., Brabet, P. and Hamel, C.P., 2005. Deafness and cochlear fibrocyte alterations in mice deficient for the inner ear protein otospiralin. *Molecular and cellular biology*, *25*(2), pp.847-853.

Destefani, A. C., Sirtoli, G. M. & Nogueira, B. V., 2017. Advances in the Knowledge about Kidney Decellularization and Repopulation. *Frontiers in Bioengineering and Biotechnology,* 1 6.Volume 5.

Devine, S. M., 2002. Mesenchymal stem cells: Will they have a role in the clinic?. *Journal of Cellular Biochemistry,* 85(SUPPL. 38), pp. 73-79.

Di Girolamo, S., Quaranta, N., Picciotti, P., Torsello, A. and Wolf, F., 2001. Age-related Histopathological Changes of the Stria Vascularis: An Experimental Model: Cambios histopatólogicos relacionados con la edad en la estría vascular: Un modelo experimental. *Audiology*, *40*(6), pp.322-326.

Di Palma, F., Holme, R.H., Bryda, E.C., Belyantseva, I.A., Pellegrino, R., Kachar, B., Steel, K.P. and Noben-Trauth, K., 2001. Mutations in Cdh23, encoding a new type of cadherin, cause stereocilia disorganization in waltzer, the mouse model for Usher syndrome type 1D. *Nature genetics*,*27*(1), pp.103-107.

Donato, R., 1986. S-100 proteins. *Cell calcium*, *7*(3), pp.123-145.

Donato, R., 2001. S100: a multigenic family of calcium-modulated proteins of the EF-hand type with intracellular and extracellular functional roles.. *The international journal of biochemistry & cell biology,* 7, 33(7), pp. 637-68.

Dreiling, F. J., Henson, M. M. & Henson, O. W., 2002. The presence and arrangement of type II collagen in the basilar membrane. *Hearing Research,* 166(1-2), pp. 166-180.

Dubno, J.R., Eckert, M.A., Lee, F.S., Matthews, L.J. and Schmiedt, R.A., 2013. Classifying human audiometric phenotypes of age-related hearing loss from animal models. *Journal of the Association for Research in Otolaryngology*, *14*(5), pp.687-701.

Dulon, D., Sugasawa, M., Blanchet, C. & Erostegui, C., 1995. Direct measurements of Ca(2+)-activated K+ currents in inner hair cells of the guinea-pig cochlea using photolabile Ca2+ chelators.. *Pflugers Archiv : European journal of physiology,* 7, 430(3), pp. 365-73.

Eckhard, A., Gleiser, C., Rask-Andersen, H., Arnold, H., Liu, W., Mack, A., Müller, M., Löwenheim, H. and Hirt, B., 2012. Co-localisation of Kir4. 1 and AQP4 in rat and human cochleae reveals a gap in water channel expression at the transduction sites of endocochlear K+ recycling routes. *Cell and tissue research*, *350*(1), pp.27-43.

Edmondson, R., Broglie, J. J., Adcock, A. F. & Yang, L., 2014. Three-Dimensional Cell Culture Systems and Their Applications in Drug Discovery and Cell-Based Biosensors. *ASSAY and Drug Development Technologies,* 15 5, 12(4), pp. 207-218.

Elmslie, K. S., 2001. Action Potential: Ionic Mechanisms. In: *Encyclopedia of Life Sciences.* s.l.:John Wiley & Sons, Ltd.

Engler, A. J., Sen, S., Sweeney, H. L. & Discher, D. E., 2006. Matrix Elasticity Directs Stem Cell Lineage Specification. *Cell,* 25 8, 126(4), pp. 677-689.

Engler, A.J., Griffin, M.A., Sen, S., Bönnemann, C.G., Sweeney, H.L. and Discher, D.E., 2004. Myotubes differentiate optimally on substrates with tissue-like stiffness: pathological implications for soft or stiff microenvironments. *J Cell Biol*, *166*(6), pp.877-887.

Estes, B. T., Gimble, J. M., Janmey, G. F. & Weitz, P. A., 2005. HIGHLIGHTED TOPIC Biomechanics and Mechanotransduction in Cells and Tissues Cell type-specific response to growth on soft materials Downloaded from. *Crit Rev Biomed Eng,* Volume 98, pp. 1547-1553.

Estévez, R., Boettger, T., Stein, V., Birkenhäger, R., Otto, E., Hildebrandt, F. and Jentsch, T.J., 2001. Barttin is a Cl-channel β-subunit crucial for renal Cl-reabsorption and inner ear K+ secretion. *Nature*, *414*(6863), pp.558-561.

Fettiplace, R. & Fuchs, P. A., 1999. Mechanisms of hair cell tuning.. *Annual review of physiology,* Volume 61, pp. 809-34.

Finley, C.C. and Skinner, M.W., 2008. Role of electrode placement as a contributor to variability in cochlear implant outcomes. *Otology & neurotology: official publication of the American Otological Society, American Neurotology Society [and] European Academy of Otology and Neurotology*, *29*(7), p.920.

Fodor, W.L., 2003. Tissue engineering and cell based therapies, from the bench to the clinic: the potential to replace, repair and regenerate. *Reprod Biol Endocrinol*, *1*(1), p.102.

Forge, A., Becker, D., Casalotti, S., Edwards, J., Evans, W.H., Lench, N. and Souter, M., 1999, January. Gap junctions and connexin expression in the inner ear. In *Novartis foundation symposium* (pp. 134-156). Wiley.

Forge, A., Becker, D., Casalotti, S., Edwards, J., Marziano, N. and Nevill, G., 2003. Gap junctions in the inner ear: comparison of distribution patterns in different vertebrates and assessement of connexin composition in mammals. *Journal of Comparative Neurology*, *467*(2), pp.207-231.

Friedmann, I., Fraser, G.R. and Froggatt, P., 1966. Pathology of the ear in the cardio-auditory syndrome of Jervell and Lange-Nielsen (recessive deafness with electrocardiographic abnormalities). *The Journal of Laryngology & Otology*, *80*(05), pp.451-470.

Furness, D.N. and Lehre, K.P., 1997. Immunocytochemical Localization of a High-affinity Glutamate-Aspartate Transporter, GLAST, in the Rat and Guinea-pig Cochlea. *European Journal of Neuroscience*, *9*(9), pp.1961-1969.

Furness, D.N., Hulme, J.A., Lawton, D. and Hackney, C.M., 2002. Distribution of the glutamate/aspartate transporter GLAST in relation to the afferent synapses of outer hair cells in the guinea pig cochlea. *Journal of the Association for Research in Otolaryngology*, *3*(3), pp.234-247.

Furness, David & Lawton, David & Mahendrasingam, Shanthini & Hodierne, Laurence & Jagger, Daniel. (2009). Quantitative analysis of the expression of the glutamate-aspartate transporter and identification of functional glutamate uptake reveal a role for cochlear fibrocytes in glutamate homeostasis. Neuroscience. 162. 1307-21. 10.1016/j.neuroscience.2009.05.036.

Gatehouse, S., Naylor, G. and Elberling, C., 2003. Benefits from hearing aids in relation to the interaction between the user and the environment. *International Journal of Audiology*, *42*(sup1), pp.77-85.

Gates, G.A. and, J.H., 2005. Presbycusis. *The Lancet*, *366*(9491), pp.1111-1120.

Gates, G.A., Mills, D., Nam, B.H., D'Agostino, R. and Rubel, E.W., 2002. Effects of age on the distortion product otoacoustic emission growth functions. *Hearing research*, *163*(1), pp.53-60.

Gilley, P.M., Sharma, A. and Dorman, M.F., 2008. Cortical reorganization in children with cochlear implants. *Brain research*, *1239*, pp.56-65.

Giordano, A., Galderisi, U. & Marino, I. R., 2007. From the laboratory bench to the patient's bedside: An update on clinical trials with Mesenchymal Stem Cells. *Journal of Cellular Physiology,* 4, 211(1), pp. 27-35.

Görlach, A., Herter, P., Hentschel, H., Frosch, P.J. and Acker, H., 1994. Effects of nIFN β and rifn γ on growth and morphology of two human melanoma cell lines: Comparison between two-and three-dimensional culture. *International journal of cancer*, *56*(2), pp.249-254.

Gratton, M.A., Schulte, B.A. and Hazen-Martin, D.J., 1996. Characterization and development of an inner ear type I fibrocyte cell culture. *Hearing research*, *99*(1), pp.71-78.

Gratton, M.A., Smyth, B.J., Lam, C.F., Boettcher, F.A. and Schmiedt, R.A., 1997. Decline in the endocochlear potential corresponds to decreased Na, K-ATPase activity in the lateral wall of quiet-aged gerbils. *Hearing research*,*108*(1), pp.9-16.

Gruber, J., Schaffer, S. and Halliwell, B., 2007. The mitochondrial free radical theory of ageing--where do we stand?. *Frontiers in bioscience: a journal and virtual library*, *13*, pp.6554-6579.

Gubbels, S.P., Woessner, D.W., Mitchell, J.C., Ricci, A.J. and Brigande, J.V., 2008. Functional auditory hair cells produced in the mammalian cochlea by in utero gene transfer. *Nature*, *455*(7212), pp.537-541.

Gulya, A.J., Minor, L.B., Glasscock, M.E. and Poe, D., 2010. *Glasscock-Shambaugh Surgery of the ear*. PMPH-USA.

Gurski, L. A., Petrelli, N. J., Jia, X. & Farach-Carson, M. C., 2017. 3-D Matrices for Anti-Cancer Drug Testing and Development. *Oncology Issues,* 30 11, 25(1), pp. 20-25.

Gurski, L.A., Jha, A.K., Zhang, C., Jia, X. and Farach-Carson, M.C., 2009. Hyaluronic acid-based hydrogels as 3-D matrices for in vitro evaluation of chemotherapeutic drugs using poorly adherent prostate cancer cells. *Biomaterials*, *30*(30), pp.6076-6085.

Hafidi, A., Beurg, M. & Dulon, D., 2005. Localization and developmental expression of BK channels in mammalian cochlear hair cells. *Neuroscience,* 130(2), pp. 475-484.

Hagiwara, S., 1976. Potassium current and the effect of cesium on this current during anomalous rectification of the egg cell membrane of a starfish. *The Journal of General Physiology,* 13 5, 67(6), pp. 621-638.

Haimoto, H. and Kato, K., 1987. S100a0 (αα) Protein, a Calcium-Binding Protein, Is Localized in the Slow-Twitch Muscle Fiber. *Journal of neurochemistry*, *48*(3), pp.917-923.

Hajioff, D., Enever, Y., Quiney, R., Zuckerman, J., Mackermot, K. and Mehta, A., 2003. Hearing loss in Fabry disease: the effect of agalsidase alfa replacement therapy. *Journal of inherited metabolic disease*, *26*(8), pp.787-794.

Hakuba, N., Koga, K., Gyo, K., Usami, S.I. and Tanaka, K., 2000. Exacerbation of noise-induced hearing loss in mice lacking the glutamate transporter GLAST. *The Journal of neuroscience*, *20*(23), pp.8750-8753.

Hakuba, N., Watabe, K., Hyodo, J., Ohashi, T., Eto, Y., Taniguchi, M., Yang, L., Tanaka, J., Hata, R. and Gyo, K., 2003. Adenovirus-mediated overexpression of a gene prevents hearing loss and progressive inner hair cell loss after transient cochlear ischemia in gerbils. *Gene therapy*, *10*(5), pp.426-433.

Hampton, T., 2012. Gene Therapy for Hearing Loss. *JAMA*, *308*(9), pp.853-853.

Henson, M. M. & Henson, O. W., 1988. Tension fibroblasts and the connective tissue matrix of the spiral ligament. *Hearing Research,* 15 9, 35(2-3), pp. 237-258.

Henson, M. M., Henson, O. W. & Jenkins, D. B., 1984. The attachment of the spiral ligament to the cochlear wall: Anchoring cells and the creation of tension. *Hearing Research,* 16(3), pp. 231-242.

Henson, M.M., Burridge, K., Fitzpatrick, D., Jenkins, D.B., Pillsbury, H.C. and Henson Jr, O.W., 1985. Immunocytochemical localization of contractile and contraction associated proteins in the spiral ligament of the cochlea. *Hearing research*, *20*(3), pp.207-214.

Hequembourg, S. and Liberman, M.C., 2001. Spiral ligament pathology: a major aspect of age-related cochlear degeneration in C57BL/6 mice. *JARO-Journal of the Association for Research in Otolaryngology*, *2*(2), pp.118-129.

Hibino, H. and Kurachi, Y., 2006. Molecular and physiological bases of the K+ circulation in the mammalian inner ear. *Physiology*, *21*(5), pp.336-345.

Hibino, H., Higashi-Shingai, K., Fujita, A., Iwai, K., Ishii, M. and Kurachi, Y., 2004. Expression of an inwardly rectifying K+ channel, Kir5. 1, in specific types of fibrocytes in the cochlear lateral wall suggests its functional importance in the establishment of endocochlear potential. *European Journal of Neuroscience*, *19*(1), pp.76-84.

Hibino, H., Higashi-Shingai, K., Fujita, A., Iwai, K., Ishii, M. and Kurachi, Y., 2004. Expression of an inwardly rectifying K+ channel, Kir5. 1, in specific types of fibrocytes in the cochlear lateral wall suggests its functional importance in the establishment of endocochlear potential. *European Journal of Neuroscience*, *19*(1), pp.76-84.

Hildebrand, M.S., Newton, S.S., Gubbels, S.P., Sheffield, A.M., Kochhar, A., de Silva, M.G., Dahl, H.H.M., Rose, S.D., Behlke, M.A. and Smith, R.J., 2008. Advances in molecular and cellular therapies for hearing loss.*Molecular Therapy*, *16*(2), pp.224-236.

Hille, B., 2001. *Ion Channel Excitable Membranes.* 3 ed. Sunderland, Massachusetts: Sinauer Associates, Inc..

Hirose, K. and Liberman, M.C., 2003. Lateral wall histopathology and endocochlear potential in the noise-damaged mouse cochlea. *Journal of the Association for Research in Otolaryngology*, *4*(3), pp.339-352.

Hofherr, A., Fakler, B. and Klöcker, N., 2005. Selective Golgi export of Kir2. 1 controls the stoichiometry of functional Kir2. x channel heteromers. *Journal of cell science*, *118*(9), pp.1935-1943.

Housley, G. D. & Ashmore, J. F., 1992. Ionic currents of outer hair cells isolated from the guinea-pig cochlea.. *The Journal of Physiology,* 1 3, 448(1), pp. 73-98.

Huang, D., Chen, P., Chen, S., Nagura, M., Lim, D.J. and Lin, X., 2002. Expression patterns of aquaporins in the inner ear: evidence for concerted actions of multiple types of aquaporins to facilitate water transport in the cochlea. *Hearing research*, *165*(1), pp.85-95.

Huang, H., Ding, Y., Sun, X. S. & Nguyen, T. A., 2013. Peptide Hydrogelation and Cell Encapsulation for 3-D Culture of MCF-7 Breast Cancer Cells. *PLoS ONE,* 20 3.8(3).

Huang, Q. & Tang, J., 2010. *Age-related hearing loss or presbycusis.* s.l.:s.n.

Huang, Q. and Tang, J., 2010. Age-related hearing loss or presbycusis.*European Archives of Oto-Rhino-Laryngology*, *267*(8), pp.1179-1191.

Hudspeth, A.J., 1989. How the ear's works work. *Nature*, *341*(6241), pp.397-404.

Hudspeth, A.J., 1997. How hearing happens. *Neuron*, *19*(5), pp.947-950.

Hussain, I., Sloan, S.R., Wipplinger, C., Navarro-Ramirez, R., Zubkov, M., Kim, E., Kirnaz, S., Bonassar, L.J. and Härtl, R., 2018. Mesenchymal Stem Cell-Seeded High-Density Collagen Gel for Annular Repair: 6-Week Results From In Vivo Sheep Models. *Neurosurgery*, 1 8, 85(2), pp. E350-E359.

Ichimiya, I., Suzuki, M. & Mogi, G., 2000. Age-related changes in the murine cochlear lateral wall. *Hearing Research,* 1, 139(1-2), pp. 116-122.

Ichimiya, I., Yoshida, K., Hirano, T., Suzuki, M. and Mogi, G., 2000. Significance of spiral ligament fibrocytes with cochlear inflammation.*International journal of pediatric otorhinolaryngology*, *56*(1), pp.45-51.

Ikeda, K. and Morizono, T., 1989. Electrochemical profiles for monovalent ions in the stria vascularis: cellular model of ion transport mechanisms. *Hearing research*, *39*(3), pp.279-286.

Ishii, M., Fujita, A., Iwai, K., Kusaka, S., Higashi, K., Inanobe, A., Hibino, H. and Kurachi, Y., 2003. Differential expression and distribution of Kir5. 1 and Kir4. 1 inwardly rectifying K+ channels in retina. *American Journal of Physiology-Cell Physiology*, *285*(2), pp.C260-C267.

Izumikawa, M., Minoda, R., Kawamoto, K., Abrashkin, K.A., Swiderski, D.L., Dolan, D.F., Brough, D.E. and Raphael, Y., 2005. Auditory hair cell replacement and hearing improvement by Atoh1 gene therapy in deaf mammals. *Nature medicine*, *11*(3), pp.271-276.

Jagger, D.J. and Forge, A., 2015. Connexins and gap junctions in the inner ear–it's not just about K+ recycling. *Cell and tissue research*, *360*(3), pp.633-644.

Jagger, D.J., Robertson, D. and Housley, G.D., 2000. A technique for slicing the rat cochlea around the onset of hearing. *Journal of neuroscience methods*, *104*(1), pp.77-86.

Jaye, D. A., Xiao, Y.-F. & Sigg, D. C., 2010. Basic Cardiac Electrophysiology: Excitable Membranes. In: *Cardiac Electrophysiology Methods and Models.* s.l.:Springer US, pp. 41-51.

Jha, A.K., Tharp, K.M., Ye, J., Santiago-Ortiz, J.L., Jackson, W.M., Stahl, A., Schaffer, D.V., Yeghiazarians, Y. and Healy, K.E., 2015. Enhanced survival and engraftment of transplanted stem cells using growth factor sequestering hydrogels. *Biomaterials*, *47*, pp.1-12.

Jin, Z.H., Kikuchi, T., Tanaka, K. and Kobayashi, T., 2003. Expression of glutamate transporter GLAST in the developing mouse cochlea. *The Tohoku journal of experimental medicine*, *200*(3), pp.137-144.

Jongkamonwiwat, N., Zine, A. and N Rivolta, M., 2010. Stem cell based therapy in the inner ear: appropriate donor cell types and routes for transplantation. *Current drug targets*, *11*(7), pp.888-897.

Justice, B. A., Badr, N. A. & Felder, R. A., 2009. *3-D cell culture opens new dimensions in cell-based assays.* s.l.:s.n.

Kada, S., Nakagawa, T. & Ito, J., 2009. A mouse model for degeneration of the spiral ligament. *JARO - Journal of the Association for Research in Otolaryngology,* 6, 10(2), pp. 161-172.

Kakigi, A., Takeuchi, S., Ando, M., Higashiyama, K., Azuma, H., Sato, T. and Takeda, T., 2002. Reduction in the endocochlear potential caused by Cs+ in the perilymph can be explained by the five-compartment model of the stria vascularis. *Hearing research*, *166*(1), pp.54-61.

Kamiya, K., Fujinami, Y., Hoya, N., Okamoto, Y., Kouike, H., Komatsuzaki, R., Kusano, R., Nakagawa, S., Satoh, H., Fujii, M. and Matsunaga, T., 2007. Mesenchymal stem cell transplantation accelerates hearing recovery through the repair of injured cochlear fibrocytes. *The American journal of pathology*,*171*(1), pp.214-226.

Karussis, D., Karageorgiou, C., Vaknin-Dembinsky, A., Gowda-Kurkalli, B., Gomori, J.M., Kassis, I., Bulte, J.W., Petrou, P., Ben-Hur, T., Abramsky, O. and Slavin, S., 2010. Safety and immunological effects of mesenchymal stem cell transplantation in patients with multiple sclerosis and amyotrophic lateral sclerosis. *Archives of neurology*, *67*(10), pp.1187-1194.

Kasagi, H., Kuhara, T., Okada, H., Sueyoshi, N. and Kurihara, H., 2013. Mesenchymal stem cell transplantation to the mouse cochlea as a treatment for childhood sensorineural hearing loss. *International journal of pediatric otorhinolaryngology*, *77*(6), pp.936-942.

Kelly, J. J., Forge, A. & Jagger, D. J., 2011. Development of gap junctional intercellular communication within the lateral wall of the rat cochlea. *Neuroscience,* 28 4, Volume 180, pp. 360-369.

Kelly, J.J., Forge, A. and Jagger, D.J., 2012. Contractility in type III cochlear fibrocytes is dependent on non-muscle myosin II and intercellular gap junctional coupling. *Journal of the Association for Research in Otolaryngology*, *13*(4), pp.473-484.

Kharkovets, T., Dedek, K., Maier, H., Schweizer, M., Khimich, D., Nouvian, R., Vardanyan, V., Leuwer, R., Moser, T. and Jentsch, T.J., 2006. Mice with altered KCNQ4 K+ channels implicate sensory outer hair cells in human progressive deafness. *The EMBO journal*, *25*(3), pp.642-652.

Kikuchi, T., Adams, J.C., Miyabe, Y., So, E. and Kobayashi, T., 2000. Potassium ion recycling pathway via gap junction systems in the mammalian cochlea and its interruption in hereditary nonsyndromic deafness. *Medical Electron Microscopy*, *33*(2), pp.51-56.

Kikuchi, T., Kimura, R.S., Paul, D.L. and Adams, J.C., 1995. Gap junctions in the rat cochlea: immunohistochemical and ultrastructural analysis. *Anatomy and embryology*, *191*(2), pp.101-118.

Kim, D.H., Provenzano, P.P., Smith, C.L. and Levchenko, A., 2012. Matrix nanotopography as a regulator of cell function. *The Journal of cell biology*, *197*(3), pp.351-360.

Kitao, K., Mizutari, K., Nakagawa, S., Matsunaga, T., Fukuda, S. and Fujii, M., 2016. Recovery of endocochlear potential after severe damage to lateral wall fibrocytes following acute cochlear energy failure. *NeuroReport*, *27*(15), pp.1159-1166.

Kral, A. and Eggermont, J.J., 2007. What's to lose and what's to learn: development under auditory deprivation, cochlear implants and limits of cortical plasticity. *Brain Research Reviews*, *56*(1), pp.259-269.

Kral, A. and O'Donoghue, G.M., 2010. Profound deafness in childhood. *New England Journal of Medicine*, *363*(15), pp.1438-1450.

Kral, A. and Sharma, A., 2012. Developmental neuroplasticity after cochlear implantation. *Trends in neurosciences*, *35*(2), pp.111-122.

Kros, C. J. & Crawford, A. C., 1990. Potassium currents in inner hair cells isolated from the guinea-pig cochlea.. *The Journal of Physiology,* 1 2, 421(1), pp. 263-291.

Kros, C. J., Ruppersberg, J. P. & Rüsch, A., 1998. Expression of a potassium current inner hair cells during development of hearing in mice. *Nature,* 16 7, 394(6690), pp. 281-284.

Kujawa, S.G. and Liberman, M.C., 2009. Adding insult to injury: cochlear nerve degeneration after “temporary” noise-induced hearing loss. *The Journal of Neuroscience*, *29*(45), pp.14077-14085.

Kusunoki, T., Cureoglu, S., Schachern, P.A., Baba, K., Kariya, S. and Paparella, M.M., 2004. Age-related histopathologic changes in the human cochlea: a temporal bone study. *Otolaryngology--Head and Neck Surgery*,*131*(6), pp.897-903.

Lang, H., Ebihara, Y., Schmiedt, R.A., Minamiguchi, H., Zhou, D., Smythe, N., Liu, L., Ogawa, M. and Schulte, B.A., 2006. Contribution of bone marrow hematopoietic stem cells to adult mouse inner ear: mesenchymal cells and fibrocytes. *Journal of Comparative Neurology*, *496*(2), pp.187-201.

Lang, H., Jyothi, V., Smythe, N.M., Dubno, J.R., Schulte, B.A. and Schmiedt, R.A., 2010. Chronic reduction of endocochlear potential reduces auditory nerve activity: further confirmation of an animal model of metabolic presbyacusis. *Journal of the Association for Research in Otolaryngology*,*11*(3), pp.419-434.

Lang, H., Schulte, B. A. & Schmiedt, R. A., 2002. Endocochlear potentials and compound action potential recovery: Functions in the C57BL/6J mouse. *Hearing Research,* 10, 172(1-2), pp. 118-126.

Langer, R. and Peppas, N.A., 2003. Advances in biomaterials, drug delivery, and bionanotechnology. *AIChE Journal*, *49*(12), pp.2990-3006.

Lautermann, J., Wouter-Jan, F., Altenhoff, P., Grümmer, R., Traub, O., Frank, H.G., Jahnke, K. and Winterhager, E., 1998. Expression of the gap-junction connexins 26 and 30 in the rat cochlea. *Cell and tissue research*,*294*(3), pp.415-420.

Leach, J.B., Brown, X.Q., Jacot, J.G., DiMilla, P.A. and Wong, J.Y., 2007. Neurite outgrowth and branching of PC12 cells on very soft substrates sharply decreases below a threshold of substrate rigidity. *Journal of neural engineering*, *4*(2), p.26.

Lecain, E., Sauvaget, E., Crisanti, P., Van Den Abbeele, T. and Huy, P.T.B., 1999. Potassium channel ether a go-go mRNA expression in the spiral ligament of the rat. *Hearing research*, *133*(1), pp.133-138.

Lee, C.H., Singla, A. and Lee, Y., 2001. Biomedical applications of collagen. *International journal of pharmaceutics*, *221*(1-2), pp.1-22.

Lee, J., Cuddihy, M. J. & Kotov, N. A., 2008. Three-Dimensional Cell Culture Matrices: State of the Art. *Tissue Engineering Part B: Reviews,* 2 3, 14(1), pp. 61-86.

Lee, K. Y. & Mooney, D. J., 2001. 2001 Chemical Review-Hydrogel. *Chemical Reviews,* 101(7), pp. 1869-1879.

Lefebvre, P.P. and Staecker, H., 2002. Steroid perfusion of the inner ear for sudden sensorineural hearing loss after failure of conventional therapy: a pilot study. *Acta oto-laryngologica*, *122*(7), pp.698-702.

Li, H., Fan, X. & Houghton, J. M., 2007. *Tumor microenvironment: The role of the tumor stroma in cancer.* s.l.:s.n.

Li, J. & Verkman, A. S., 2001. Impaired Hearing in Mice Lacking Aquaporin-4 Water Channels. *Journal of Biological Chemistry,* 17 8, 276(33), pp. 31233-31237.

Li, J. and Verkman, A.S., 2001. Impaired hearing in mice lacking aquaporin-4 water channels. *Journal of Biological Chemistry*, *276*(33), pp.31233-31237.

Li, Y. et al., 2018. Self-protection of type III fibrocytes against severe 3-nitropropionic-acid-induced cochlear damage in mice. *NeuroReport,* 29(4), pp. 252-258.

Li, Y., Watanabe, K., Fujioka, M. & Ogawa, K., 2017. Characterization of slow-cycling cells in the mouse cochlear lateral wall. *PLoS ONE,* 1 6.12(6).

Liang et al 2002 & F. Liang, B.A. Schulte, Z. S., 2002. The BK channel in spiral ligament fibrocytes is regulated by phosphorylation. *Abstr Assoc Res Otolarygol,* Volume 26, p. p. 616.

Liang, F., Hu, W., Schulte, B.A., Mao, C., Qu, C., Hazen-Martin, D.J. and Shen, Z., 2004. Identification and characterization of an L-type Ca v 1.2 channel in spiral ligament fibrocytes of gerbil inner ear. *Molecular brain research*, *125*(1), pp.40-46.

Liang, F., Niedzielski, A., Schulte, B.A., Spicer, S.S., Hazen-Martin, D.J. and Shen, Z., 2003. A voltage-and Ca2+-dependent big conductance K channel in cochlear spiral ligament fibrocytes. *Pflügers Archiv*, *445*(6), pp.683-692.

Liang, F., Schulte, B.A., Qu, C., Hu, W. and Shen, Z., 2005. Inhibition of the calcium-and voltage-dependent big conductance potassium channel ameliorates cisplatin-induced apoptosis in spiral ligament fibrocytes of the cochlea. *Neuroscience*, *135*(1), pp.263-271.

Liberman, M.C., 2015. Hidden Hearing Loss. *Scientific American*, *313*(2), pp.48-53

Lin, H., Hejtmancik, J. F. & Qi, Y., 2007. A substitution of arginine to lysine at the COOH-terminus of MIP caused a different binocular phenotype in a congenital cataract family.. *Molecular vision,* 30 9, Volume 13, pp. 1822-7.

Lindvall, O. and Björklund, A., 2004. Cell replacement therapy: helping the brain to repair itself. *Neurotherapeutics*, *1*(4), pp.379-381.

Lindvall, O., Kokaia, Z. and Martinez-Serrano, A., 2004. Stem cell therapy for human neurodegenerative disorders–how to make it work. *Nature medicine*, *10*(7s), p.S42.

Liu, Y. P. & Zhao, H. B., 2008. Cellular characterization of Connexin26 and Connnexin30 expression in the cochlear lateral wall. *Cell and Tissue Research,* 9, 333(3), pp. 395-403.

Lo, C. M., Wang, H. B., Dembo, M. & Wang, Y. L., 2000. Cell movement is guided by the rigidity of the substrate. *Biophysical Journal,* 79(1), pp. 144-152.

Lopatin, A. N., 1996. [K+] dependence of polyamine-induced rectification in inward rectifier potassium channels (IRK1, Kir2.1). *The Journal of General Physiology,* 13 5, 108(2), pp. 105-113.

López-Bigas, N., Arbonés, M. L., Estivill, X. & Simonneau, L., 2002. Expression profiles of the connexin genes, Gjb1 and Gjb3, in the developing mouse cochlea.. *Gene expression patterns : GEP,* 11, 2(1-2), pp. 113-7.

Lourdel, S., Paulais, M., Cluzeaud, F., Bens, M., Tanemoto, M., Kurachi, Y., Vandewalle, A. and Teulon, J., 2002. An inward rectifier K+ channel at the basolateral membrane of the mouse distal convoluted tubule: similarities with Kir4-Kir5. 1 heteromeric channels. *The Journal of physiology*, *538*(2), pp.391-404.

Löwenheim, H., Furness, D.N., Kil, J., Zinn, C., Gültig, K., Fero, M.L., Frost, D., Gummer, A.W., Roberts, J.M., Rubel, E.W. and Hackney, C.M., 1999. Gene disruption of p27Kip1 allows cell proliferation in the postnatal and adult organ of Corti. *Proceedings of the National Academy of Sciences*, *96*(7), pp.4084-4088.

Löwenheim, H., Kil, J., Gültig, K. and Zenner, H.P., 1999. Determination of hair cell degeneration and hair cell death in neomycin treated cultures of the neonatal rat cochlea. *Hearing research*, *128*(1), pp.16-26.

Lux, H.D., Heinemann, U. and Dietzel, I., 1985. Ionic changes and alterations in the size of the extracellular space during epileptic activity.*Advances in neurology*, *44*, pp.619-639.

Mahendrasingam, S., Bebb, C., Shepard, E. and Furness, D.N., 2011a. Subcellular distribution and relative expression of fibrocyte markers in the CD/1 mouse cochlea assessed by semiquantitative immunogold electron microscopy. *Journal of Histochemistry & Cytochemistry*, *59*(11), pp.984-1000.

Mahendrasingam, S., MacDonald, J.A. and Furness, D.N., 2011b. Relative time course of degeneration of different cochlear structures in the CD/1 mouse model of accelerated aging. *Journal of the Association for Research in Otolaryngology*, *12*(4), pp.437-453.

Makary, C.A., Shin, J., Kujawa, S.G., Liberman, M.C. and Merchant, S.N., 2011. Age-related primary cochlear neuronal degeneration in human temporal bones. *Journal of the Association for Research in Otolaryngology*, *12*(6), pp.711-717.

Marcus, D.C. and Wangemann, P., 2010. Inner ear fluid homeostasis. *The Oxford handbook of auditory science—the ear. Oxford: Oxford University Press. p*, pp.213-30.

Marcus, D.C., Marcus, N.Y. and Thalmann, R., 1981. Changes in cation contents of stria vascularis with ouabain and potassium-free perfusion.*Hearing research*, *4*(2), pp.149-160.

Marcus, D.C., Wu, T., Wangemann, P. and Kofuji, P., 2002. KCNJ10 (Kir4. 1) potassium channel knockout abolishes endocochlear potential. *American Journal of Physiology-Cell Physiology*, *282*(2), pp.C403-C407.

Marcus, Y., 1984. The effectivity of solvents as electron pair donors. *Journal of Solution Chemistry,* 9, 13(9), pp. 599-624.

Matsuda, N., Sato, S., Shiba, K., Okatsu, K., Saisho, K., Gautier, C.A., Sou, Y.S., Saiki, S., Kawajiri, S., Sato, F. and Kimura, M., 2010. PINK1 stabilized by mitochondrial depolarization recruits Parkin to damaged mitochondria and activates latent Parkin for mitophagy. *The Journal of cell biology*, *189*(2), pp.211-221.

Matsui, J.I., Haque, A., Huss, D., Messana, E.P., Alosi, J.A., Roberson, D.W., Cotanche, D.A., Dickman, J.D. and Warchol, M.E., 2003. Caspase inhibitors promote vestibular hair cell survival and function after aminoglycoside treatment in vivo. *The Journal of neuroscience*, *23*(14), pp.6111-6122.

Matsumura, Y., Uchida, S., Kondo, Y., Miyazaki, H., Ko, S.B., Hayama, A., Morimoto, T., Liu, W., Arisawa, M., Sasaki, S. and Marumo, F., 1999. Overt nephrogenic diabetes insipidus in mice lacking the CLC-K1 chloride channel.*Nature genetics*, *21*(1), pp.95-98.

McCartney-Francis, N.L., Frazier-Jessen, M. and Wahl, S.M., 1998. TGF-β: a balancing act. *International reviews of immunology*, *16*(5-6), pp.553-580.

McGuirt, J.P. and Schulte, B.A., 1994. Distribution of immunoreactive alpha-and beta-subunit isoforms of Na, K-ATPase in the gerbil inner ear. *Journal of Histochemistry & Cytochemistry*, *42*(7), pp.843-853.

McLean, W.J., Smith, K.A., Glowatzki, E. and Pyott, S.J., 2009. Distribution of the Na, K-ATPase α subunit in the rat spiral ganglion and organ of corti.*Journal of the Association for Research in Otolaryngology*, *10*(1), pp.37-49.

McManus, O. B. et al., 1995. Functional role of the beta subunit of high conductance calcium-activated potassium channels.. *Neuron,* 3, 14(3), pp. 645-50.

Meera, P., Wallner, M., Song, M. & Toro, L., 1997. Large conductance voltage- and calcium-dependent K+ channel, a distinct member of voltage-dependent ion channels with seven N-terminal transmembrane segments (S0-S6), an extracellular N terminus, and an intracellular (S9-S10) C terminus. *Proceedings of the National Academy of Sciences,* 9 12, 94(25), pp. 14066-14071.

Meyer Zum Gottesberge, A. M. et al., 2008. Inner ear defects and hearing loss in mice lacking the collagen receptor DDR1. *Laboratory Investigation,* 1, 88(1), pp. 27-37.

Mhatre, A.N., Stern, R.E., Li, J. and Lalwani, A.K., 2002. Aquaporin 4 expression in the mammalian inner ear and its role in hearing. *Biochemical and biophysical research communications*, *297*(4), pp.987-996.

Mhatre, A.N., Weld, E. and Lalwani, A.K., 2003. Mutation analysis of Connexin 31 (GJB3) in sporadic non-syndromic hearing impairment. *Clinical genetics*, *63*(2), pp.154-159.

Mills, J.H. and Weber, P.C., 2001. Anatomy and physiology of hearing. *Head and neck surgery—otolaryngology. 3rd ed. Philadelphia, PA: Lippincott Williams & Wilkins*.

Mills, J.H., Schmiedt, R.A. and Kulish, L.F., 1990. Age-related changes in auditory potentials of Mongolian gerbil. *Hearing research*, *46*(3), pp.201-210.

Minowa, O., Ikeda, K., Sugitani, Y., Oshima, T., Nakai, S., Katori, Y., Suzuki, M., Furukawa, M., Kawase, T., Zheng, Y. and Ogura, M., 1999. Altered cochlear fibrocytes in a mouse model of DFN3 nonsyndromic deafness. *Science*, *285*(5432), pp.1408-1411.

Miyabe, Y., Kikuchi, T. and Kobayashi, T., 2002. Comparative immunohistochemical localizations of aquaporin-1 and aquaporin-4 in the cochleae of three different species of rodents. *The Tohoku journal of experimental medicine*, *196*(4), pp.247-257.

Mizuta, K., Adachi, M. and Iwasa, K.H., 1997. Ultrastructural localization of the Na-K-Cl cotransporter in the lateral wall of the rabbit cochlear duct.*Hearing research*, *106*(1), pp.154-162.

Mizutari, K., 2014. Spontaneous recovery of cochlear fibrocytes after severe degeneration caused by acute energy failure. *Frontiers in Pharmacology,* Volume 5 AUG.

Mizutari, K., Fujioka, M., Hosoya, M., Bramhall, N., Okano, H.J., Okano, H. and Edge, A.S., 2013. Notch inhibition induces cochlear hair cell regeneration and recovery of hearing after acoustic trauma. *Neuron*, *77*(1), pp.58-69.

Mizutari, K., Nakagawa, S., Mutai, H., Fujii, M., Ogawa, K. and Matsunaga, T., 2011. Late-phase recovery in the cochlear lateral wall following severe degeneration by acute energy failure. *Brain research*, *1419*, pp.1-11.

Moon, S.K., Moon, S.K., Park, R., Moon, S.K., Park, R., Lee, H.Y., Nam, G.J., Cha, K., Andalibi, A. and Lim, D.J., 2006. Spiral ligament fibrocytes release chemokines in response to otitis media pathogens. *Acta oto-laryngologica*, *126*(6), pp.564-569.

Mutai, H., Nagashima, R., Fujii, M. and Matsunaga, T., 2009. Mitotic activity and specification of fibrocyte subtypes in the developing rat cochlear lateral wall. *Neuroscience*, *163*(4), pp.1255-1263.

Nadol, J.B., 1997. Patterns of neural degeneration in the human cochlea and auditory nerve: implications for cochlear implantation. *Otolaryngology--Head and Neck Surgery*, *117*(3), pp.220-228.

Nagelhus, E.A., Mathiisen, T.M. and Ottersen, O.P., 2004. Aquaporin-4 in the central nervous system: cellular and subcellular distribution and coexpression with KIR4. 1. *Neuroscience*, *129*(4), pp.905-913.

Naidu, R. C. & Mountain, D. C., 2007. Basilar membrane tension calculations for the gerbil cochlea. *The Journal of the Acoustical Society of America,* 2, 121(2), pp. 994-1002.

Navaratnam, D.S., Bell, T.J., Tu, T.D., Cohen, E.L. and Oberholtzer, J.C., 1997. Differential distribution of Ca 2+-activated K+ channel splice variants among hair cells along the tonotopic axis of the chick cochlea. *Neuron*, *19*(5), pp.1077-1085.

Nin, F., Hibino, H., Doi, K., Suzuki, T., Hisa, Y. and Kurachi, Y., 2008. The endocochlear potential depends on two K+ diffusion potentials and an electrical barrier in the stria vascularis of the inner ear. *Proceedings of the National Academy of Sciences*, *105*(5), pp.1751-1756.

Nishimura, S. N. et al., 2019. Photocleavable Peptide-Poly(2-hydroxyethyl methacrylate) Hybrid Graft Copolymer via Postpolymerization Modification by Click Chemistry to Modulate the Cell Affinities of 2-D and 3-D Materials. *ACS Applied Materials and Interfaces.*

Noben-Trauth, K., Zheng, Q.Y. and Johnson, K.R., 2003. Association of cadherin 23 with polygenic inheritance and genetic modification of sensorineural hearing loss. *Nature genetics*, *35*(1), pp.21-23.

Nouvian, R., Ruel, J., Wang, J., Guitton, M.J., Pujol, R. and Puel, J.L., 2003. Degeneration of sensory outer hair cells following pharmacological blockade of cochlear KCNQ channels in the adult guinea pig. *European Journal of Neuroscience*, *17*(12), pp.2553-2562.

Ohlemiller, K. K., 2009. *Mechanisms and genes in human strial presbycusis from animal models.* s.l.:s.n.

Ohlemiller, K. K., Lett, J. M. & Gagnon, P. M., 2006. Cellular correlates of age-related endocochlear potential reduction in a mouse model. *Hearing Research,* 10, 220(1-2), pp. 10-26.

Ohlemiller, K.K., 2004. Age-related hearing loss: the status of Schuknecht's typology. *Current opinion in otolaryngology & head and neck surgery*, *12*(5), pp.439-443.

Okano, T. & Kelley, M. W., 2012. Stem Cell Therapy for the Inner Ear: Recent Advances and Future Directions. *Trends in Amplification,* 16(1), pp. 4-18.

Oliver, D., Klöcker, N., Schuck, J., Baukrowitz, T., Ruppersberg, J.P. and Fakler, B., 2000. Gating of Ca2+-activated K+ channels controls fast inhibitory synaptic transmission at auditory outer hair cells. *Neuron*, *26*(3), pp.595-601.

Osen, K.K., 1972. Projection of the cochlear nuclei on the inferior colliculus in the cat. *Journal of Comparative Neurology*, *144*(3), pp.355-371.

O'Shaughnessy, T. J., Lin, H. J. & Ma, W., 2003. Functional synapse formation among rat cortical neurons grown on three-dimensional collagen gels. *Neuroscience Letters,* 17 4, 340(3), pp. 169-172.

Oshima, K., Shin, K., Diensthuber, M., Peng, A.W., Ricci, A.J. and Heller, S., 2010. Mechanosensitive hair cell-like cells from embryonic and induced pluripotent stem cells. *Cell*, *141*(4), pp.704-716.

Oshima, K., Suchert, S., Blevins, N.H. and Heller, S., 2010. Curing hearing loss: Patient expectations, health care practitioners, and basic science.*Journal of communication disorders*, *43*(4), pp.311-318.

Pallanck, L. & Ganetzky, B., 1994. Cloning and characterization of human and mouse homologs of the drosophila calcium-activated potassium channel gene, slowpoke. *Human Molecular Genetics,* 8, 3(8), pp. 1239-1243.

Pan, C.C., Chu, H.Q., Lai, Y.B., Sun, Y.B., Du, Z.H., Liu, Y., Chen, J., Tong, T., Chen, Q.G., Zhou, L.Q. and Bing, D., 2016. Downregulation of inwardly rectifying potassium channel 5.1 expression in C57BL/6J cochlear lateral wall. *Journal of Huazhong University of Science and Technology [Medical Sciences]*, *36*(3), pp.406-409.

Park, Y.H., Wilson, K.F., Ueda, Y., Wong, H.T., Beyer, L.A., Swiderski, D.L., Dolan, D.F. and Raphael, Y., 2014. Conditioning the cochlea to facilitate survival and integration of exogenous cells into the auditory epithelium. *Molecular Therapy*, *22*(4), p.873.

Parker, M.A., Corliss, D.A., Gray, B., Anderson, J.K., Bobbin, R.P., Snyder, E.Y. and Cotanche, D.A., 2007. Neural stem cells injected into the sound-damaged cochlea migrate throughout the cochlea and express markers of hair cells, supporting cells, and spiral ganglion cells. *Hearing research*,*232*(1), pp.29-43.

Paszek, M. J. & Weaver, V. M., 2004. *The tension mounts: Mechanics meets morphogenesis and malignancy.* s.l.:s.n.

Pattillo, J.M., Yazejian, B., DiGregorio, D.A., Vergara, J.L., Grinnell, A.D. and Meriney, S.D., 2001. Contribution of presynaptic calcium-activated potassium currents to transmitter release regulation in cultured Xenopus nerve–muscle synapses. *Neuroscience*, *102*(1), pp.229-240.

Pauler, M., Schuknecht, H.F. and White, J.A., 1988. Atrophy of the stria vascularis as a cause of sensorineural hearing loss. *The Laryngoscope*,*98*(7), pp.754-759.

Pavelka, M. and Roth, J., 2015. *Functional ultrastructure: atlas of tissue biology and pathology*. Springer.

Peyton, S. R. & Putnam, A. J., 2005. Extracellular matrix rigidity governs smooth muscle cell motility in a biphasic fashion. *Journal of Cellular Physiology,* 7, 204(1), pp. 198-209.

Price, K. J. et al., 2012. Matrigel Basement Membrane Matrix influences expression of microRNAs in cancer cell lines. *Biochemical and Biophysical Research Communications,* 19 10, 427(2), pp. 343-348.

Pyott, S. J., 2004. Extrasynaptic Localization of Inactivating Calcium-Activated Potassium Channels in Mouse Inner Hair Cells. *Journal of Neuroscience,* 27 10, 24(43), pp. 9469-9474.

Qu, C., Liang, F., Hu, W., Shen, Z., Spicer, S.S. and Schulte, B.A., 2006. Expression of CLC-K chloride channels in the rat cochlea. *Hearing research*,*213*(1), pp.79-87.

Qu, C., Liang, F., Smythe, N.M. and Schulte, B.A., 2007. Identification of ClC-2 and CIC-K2 chloride channels in cultured rat type IV spiral ligament fibrocytes. *Journal for the Association for Research in Otolaryngology*, *8*(2), pp.205-219.

Raufer, S., Guinan, J. J. & Nakajima, H. H., 2019. Cochlear partition anatomy and motion in humans differ from the classic view of mammals. *Proceedings of the National Academy of Sciences of the United States of America,* 116(28), pp. 13977-13982.

Reininger-Mack, A., Thielecke, H. & Robitzki, A. A., 2002. 3-D-biohybrid systems: applications in drug screening.. *Trends in biotechnology,* 2, 20(2), pp. 56-61.

Riedelsberger, J., Dreyer, I. & Gonzalez, W., 2015. Outward rectification of voltage-gated K+ channels evolved at least twice in life history. *PLoS ONE,* 10 9.10(9).

Riva, C., Donadieu, E., Magnan, J. and Lavieille, J.P., 2007. Age-related hearing loss in CD/1 mice is associated to ROS formation and HIF target proteins up-regulation in the cochlea. *Experimental gerontology*, *42*(4), pp.327-336.

Riva, C., Longuet, M., Lucciano, M., Magnan, J. and Lavieille, J.P., 2005. Implication of mitochondrial apoptosis in neural degeneration of cochlea in a murine model for presbycusis. *Revue de laryngologie-otologie-rhinologie*,*126*(2), pp.67-74.

Roberson, D., Otology, E. R. -. A. J. o. & 1994, u., n.d. Cell division in the gerbil cochlea after acoustic trauma. *depts.washington.edu.*

Roobrouck, V. D., Ulloa-Montoya, F. & Verfaillie, C. M., 2008. *Self-renewal and differentiation capacity of young and aged stem cells.* s.l.:Academic Press Inc..

Roosens, A., Asadian, M., De Geyter, N., Somers, P. and Cornelissen, R., 2017. Complete static repopulation of decellularized porcine tissues for heart valve engineering: an in vitro study. *Cells Tissues Organs*, *204*(5-6), pp.270-282.

Ruben, R.J., 1967. Development of the inner ear of the mouse: a radioautographic study of terminal mitoses. *Acta oto-laryngologica*, pp.Suppl-220.

Ruggero, M.A. and Rich, N.C., 1991. Furosemide alters organ of Corti mechanics: evidence for feedback of outer hair cells upon the basilar membrane. *The Journal of neuroscience*, *11*(4), pp.1057-1067.

Rüttiger, L., Sausbier, M., Zimmermann, U., Winter, H., Braig, C., Engel, J., Knirsch, M., Arntz, C., Langer, P., Hirt, B. and Müller, M., 2004. Deletion of the Ca2+-activated

potassium (BK) α-subunit but not the BKβ1-subunit leads to progressive hearing loss. *Proceedings of the National Academy of Sciences of the United States of America*, *101*(35), pp.12922-12927.

Sadanaga, M. & Morimitsu, T., 1995. Development of endocochlear potential and its negative component in mouse cochlea. *Hearing Research,* 89(1-2), pp. 155-161.

Sakaguchi, N., Crouch, J.J., Lytle, C. and Schulte, B.A., 1998. Na-K-Cl cotransporter expression in the developing and senescent gerbil cochlea.*Hearing research*, *118*(1), pp.114-122.

Salkoff, L., Butler, A., Ferreira, G., Santi, C. and Wei, A., 2006. High-conductance potassium channels of the SLO family. *Nature Reviews Neuroscience*, *7*(12), p.921.

Salt, A. N., Melichar, I. & Thalmann, R., 1987. Mechanisms of endocochlear potential generation by stria vascularis.. *The Laryngoscope,* 8, 97(8 Pt 1), pp. 984-91.

Salt, A.N. and Konishi, T., 1979. Effects of noise on cochlear potentials and endolymph potassium concentration recorded with potassium-selective electrodes. *Hearing research*, *1*(4), pp.343-363.

Salvatore, M. F., Waymire, J. C. & Haycock, J. W., 2001. *International Society for Neurochemistry,* s.l.: s.n.

Santos-Sacchi, J., 2000. Cell coupling in Corti's organ. *Brain research reviews*, *32*(1), pp.167-171.

Saremi, A. and Stenfelt, S., 2013. Effect of metabolic presbyacusis on cochlear responses: a simulation approach using a physiologically-based model. *The Journal of the Acoustical Society of America*, *134*(4), pp.2833-2851.

Sawada, S., Takeda, T., Kitano, H., Takeuchi, S., Okada, T., Ando, M., Suzuki, M. and Kakigi, A., 2003. Aquaporin-1 (AQP1) is expressed in the stria vascularis of rat cochlea. *Hearing research*, *181*(1), pp.15-19.

Schaette, R. and McAlpine, D., 2011. Tinnitus with a normal audiogram: physiological evidence for hidden hearing loss and computational model. *The Journal of Neuroscience*, *31*(38), pp.13452-13457.

Schiffmann, R., Kopp, J.B., Austin III, H.A., Sabnis, S., Moore, D.F., Weibel, T., Balow, J.E. and Brady, R.O., 2001. Enzyme replacement therapy in Fabry disease: a randomized controlled trial. *Jama*, *285*(21), pp.2743-2749.

Schmiedt, R.A., 1996. Effects of aging on potassium homeostasis and the endocochlear potential in the gerbil cochlea. *Hearing research*, *102*(1), pp.125-132.

Schmiedt, R.A., 2010. The physiology of cochlear presbycusis. In *The aging auditory system* (pp. 9-38). Springer New York.

Schmiedt, R.A., Lang, H. and Okamura, H., 2000. Model of metabolic presbyacusis: neural response under condition of chronically-low endocochlear potentials induced with furosemide. In *Assoc. Res. Otolaryngol. Abstr* (Vol. 23, p. 282).

Schmiedt, R.A., Lang, H., Okamura, H.O. and Schulte, B.A., 2002. Effects of furosemide applied chronically to the round window: a model of metabolic presbyacusis. *The Journal of neuroscience*, *22*(21), pp.9643-9650.

Schmiedt, R.A., Mills, J.H. and Adams, J.C., 1990. Tuning and suppression in auditory nerve fibers of aged gerbils raised in quiet or noise. *Hearing research*, *45*(3), pp.221-236.

Schuknecht, H. F., 1964. Further Observations on the Pathology of Presbycusis. *Archives of Otolaryngology,* 80(4), pp. 369-382.

Schuknecht, H.F. and Gacek, M.R., 1993. Cochlear pathology in presbycusis. *The Annals of otology, rhinology, and laryngology*, *102*(1 Pt 2), pp.1-16.

Schuknecht, H.F., 1974. Pathology of the EarHarvard University Press.*Cambridge, Mass*, pp.259-261.

Schuknecht, H.F., Watanuki, K., Takahashi, T., Aziz Belal, A., Kimura, R.S., Jones, D.D. and Ota, C.Y., 1974. Atrophy of the stria vascularis, a common cause for hearing loss. *The Laryngoscope*, *84*(10), pp.1777-1821.

Schulte, B.A. and Adams, J.C., 1989. Distribution of immunoreactive Na+, K+-ATPase in gerbil cochlea. *Journal of Histochemistry & Cytochemistry*,*37*(2), pp.127-134.

Schulte, B.A. and Schmiedt, R.A., 1992. Lateral wall Na, K-ATPase and endocochlear potentials decline with age in quiet-reared gerbils. *Hearing research*, *61*(1), pp.35-46.

Schulte, B.A. and Steel, K.P., 1994. Expression of α and β subunit isoforms of Na, K-ATPase in the mouse inner ear and changes with mutations at the Wv or Sld loci. *Hearing research*, *78*(1), pp.65-76.

Schulte, B.A., 1993. Immunohistochemical localization of intracellular Ca-ATPase in outer hair cells, neurons and fibrocytes in the adult and developing inner ear. *Hearing research*, *65*(1), pp.262-273.

Semkova, I., Kreppel, F., Welsandt, G., Luther, T., Kozlowski, J., Janicki, H., Kochanek, S. and Schraermeyer, U., 2002. Autologous transplantation of genetically modified iris pigment epithelial cells: a promising concept for the treatment of age-related macular degeneration and other disorders of the eye. *Proceedings of the National Academy of Sciences*, *99*(20), pp.13090-13095.

Seo, A.Y., Joseph, A.M., Dutta, D., Hwang, J.C., Aris, J.P. and Leeuwenburgh, C., 2010. New insights into the role of mitochondria in aging: mitochondrial dynamics and more. *J Cell Sci*, *123*(15), pp.2533-2542.

Shen, Z., Liang, F., Hazen-Martin, D.J. and Schulte, B.A., 2004. BK channels mediate the voltage-dependent outward current in type I spiral ligament fibrocytes. *Hearing research*, *187*(1), pp.35-43.

Shi, S.R., Tandon, A.K., Coté, C. and Kalra, K.L., 1992. S-100 protein in human inner ear: Use of a novel immunohistochemical technique on routinely processed, celloidin-embedded human temporal bone sections. *The Laryngoscope*, *102*(7), pp.734-738.

Shield, K., Ackland, M. L., Ahmed, N. & Rice, G. E., 2009. *Multicellular spheroids in ovarian cancer metastases: Biology and pathology.* s.l.:s.n.

Shodo, R., Hayatsu, M., Koga, D., Horii, A. and Ushiki, T., 2017. Three-dimensional reconstruction of root cells and interdental cells in the rat inner ear by serial section scanning electron microscopy. *Biomedical Research*, *38*(4), pp.239-248.

Shone, G., Raphael, Y. and Miller, J.M., 1991. Hereditary deafness occurring in cd/1 mice. *Hearing research*, *57*(1), pp.153-156.

Skinner, L.J., Enée, V., Beurg, M., Jung, H.H., Ryan, A.F., Hafidi, A., Aran, J.M. and Dulon, D., 2003. Contribution of BK Ca2+-activated K+ channels to auditory neurotransmission in the Guinea pig cochlea. *Journal of neurophysiology*, *90*(1), pp.320-332.

Slepecky, N.B., 1996. Cochlear structure. *The Cochlea, Springer, New York*, pp.44-129.

Smith, C.A., Lowry, O.H. and Wu, M.L., 1954. The electrolytes of the labyrinthine fluids. *The Laryngoscope*, *64*(3), pp.141-153.

So, E., Kikuchi, T., Ishimaru, K., Miyabe, Y. and Kobayashi, T., 2001. Immunolocalization of voltage-gated potassium channel Kv3. 1b subunit in the cochlea. *Neuroreport*, *12*(12), pp.2761-2765.

Spicer, S. S., Gratton, M. A. & Schulte, B. A., 1997. Expression patterns of ion transport enzymes in spiral ligament fibrocytes change in relation to strial atrophy in the aged gerbil cochlea. *Hearing Research,* 9, 111(1-2), pp. 93-102.

Spicer, S.S. and Schulte, B.A., 1991. Differentiation of inner ear fibrocytes according to their ion transport related activity. *Hearing research*, *56*(1), pp.53-64.

Spicer, S.S. and Schulte, B.A., 1996. The fine structure of spiral ligament cells relates to ion return to the stria and varies with place-frequency. *Hearing research*, *100*(1), pp.80-100.

Spicer, S.S. and Schulte, B.A., 2002. Spiral ligament pathology in quiet-aged gerbils. *Hearing research*, *172*(1), pp.172-185.

Spoendlin, H., 1985. Anatomy of cochlear innervation. *American journal of otolaryngology*, *6*(6), pp.453-467.

Staal, J.A., Alexander, S.R., Liu, Y., Dickson, T.D. and Vickers, J.C., 2011. Characterization of cortical neuronal and glial alterations during culture of organotypic whole brain slices from neonatal and mature mice. *PloS one*, *6*(7), p.e22040.

Stankovic, K.M., Adams, J.C. and Brown, D.E.N.N.I.S., 1995. Immunolocalization of aquaporin CHIP in the guinea pig inner ear. *American Journal of Physiology-Cell Physiology*, *269*(6), pp.C1450-C1456.

Steel, K.P., 1999. Perspectives: biomedicine. The benefits of recycling. *Science (New York, NY)*, *285*(5432), pp.1363-1364.

Suko, T., Ichimiya, I., Yoshida, K., Suzuki, M. and Mogi, G., 2000. Classification and culture of spiral ligament fibrocytes from mice. *Hearing research*, *140*(1), pp.137-144.

Sullivan, J.M., Cohen, M.A., Pandit, S.R., Sahota, R.S., Borecki, A.A. and Oleskevich, S., 2011. Effect of epithelial stem cell transplantation on noise-induced hearing loss in adult mice. *Neurobiology of disease*, *41*(2), pp.552-559.

Sun, G.W., Fujii, M. and Matsunaga, T., 2012. Functional interaction between mesenchymal stem cells and spiral ligament fibrocytes. *Journal of neuroscience research*, *90*(9), pp.1713-1722.

Sun, T., Jackson, S., Haycock, J. W. & MacNeil, S., 2006. Culture of skin cells in 3-D rather than 2-D improves their ability to survive exposure to cytotoxic agents. *Journal of Biotechnology,* 10 4, 122(3), pp. 372-381.

Suzuki, M., Kotake, K., Fujikura, K., Inagaki, N., Suzuki, T., Gonoi, T., Seino, S. and Takata, K., 1997. Kir6. 1: a possible subunit of ATP-sensitive K+ channels in mitochondria. *Biochemical and biophysical research communications*, *241*(3), pp.693-697.

Szot, C. S., Buchanan, C. F., Freeman, J. W. & Rylander, M. N., 2011. 3-D in vitro bioengineered tumors based on collagen I hydrogels. *Biomaterials,* 11, 32(31), pp. 7905-7912.

Takahashi, T., Kimura, R.S. and Ewertson, H.W., 1970. The ultrastructure of the spiral ligament in the Rhesus monkey. *Acta oto-laryngologica*, *69*(1-6), pp.46-60.

Takeuchi, S., Ando, M. and Kakigi, A., 2000. Mechanism generating endocochlear potential: role played by intermediate cells in stria vascularis.*Biophysical Journal*, *79*(5), pp.2572-2582.

Tanemoto, M., Fujita, A., Higashi, K. & Kurachi, Y., 2002. PSD-95 mediates formation of a functional homomeric Kir5.1 channel in the brain. *Neuron,* 25 4, 34(3), pp. 387-397.

Thalmann, I., 1993. Collagen of accessory structures of organ of corti. *Connective Tissue Research,* 29(3), pp. 191-201.

Thompson, L.H. and Björklund, A., 2015. Reconstruction of brain circuitry by neural transplants generated from pluripotent stem cells. *Neurobiology of disease*, *79*, pp.28-40.

Tibbitt, M.W. and Anseth, K.S., 2009. Hydrogels as extracellular matrix mimics for 3D cell culture. *Biotechnology and bioengineering*, *103*(4), pp.655-663.

Tickle, J.A. and Furness, D.N., 2012. Breaking News: Stem Cells for Relieving Age-Related Hearing Loss. *The Hearing Journal*, *65*(6), pp.26-28.

Tsuprun, V. & Santi, P., 1997. Ultrastructural organization of proteoglycans and fibrillar matrix of the tectorial membrane. *Hearing Research,* 8, 110(1-2), pp. 107-118.

Tucker, S. J. et al., 2000. pH Dependence of the inwardly rectifying potassium channel, Kir5.1, and localization in renal tubular epithelia. *Journal of Biological Chemistry,* 2 6, 275(22), pp. 16404-16407.

Uccelli, A., Laroni, A. & Freedman, M. S., 2011. *Mesenchymal stem cells for the treatment of multiple sclerosis and other neurological diseases.* s.l.:s.n.

v. Békésy, G., 1951. DC Potentials and Energy Balance of the Cochlear Partition. *The Journal of the Acoustical Society of America,* 30 9, 23(5), pp. 576-582.

Van Laer, L., McGuirt, W.T., Yang, T., Smith, R.J. and Van Camp, G., 1999. Autosomal dominant nonsyndromic hearing impairment. *American journal of medical genetics*, *89*(3), pp.167-174.

Vats, A., Tolley, N.S., Polak, J.M. and Buttery, L.D.K., 2002. Stem cells: sources and applications. *Clinical Otolaryngology & Allied Sciences*, *27*(4), pp.227-232.

Vergara, C., Latorre, R., Marrion, N. V. & Adelman, J. P., 1998. Calcium-activated potassium channels. *Current Opinion in Neurobiology,* 8(3), pp. 321-329.

Verkman, A. S., 2003. Role of aquaporin water channels in eye function.. *Experimental eye research,* 2, 76(2), pp. 137-43.

Wallner, M., Meera, P. & Toro, L., 1999. Molecular basis of fast inactivation in voltage and Ca2+-activated K+ channels: A transmembrane -subunit homolog. *Proceedings of the National Academy of Sciences,* 26 7, 96(7), pp. 4137-4142.

Wallner, M., Meera, P., Ottolia, M., Kaczorowski, G.J., Latorre, R., Garcia, M.L., Stefani, E. and Toro, L., 1995. Characterization of and modulation by a beta-subunit of a human maxi KCa channel cloned from myometrium.. *Receptors & channels,* 3(3), pp. 185-99.

Wang, Z., Li, H., Moss, A.J., Robinson, J., Zareba, W., Knilans, T., Bowles, N.E. and Towbin, J.A., 2002. Compound heterozygous mutations in KvLQT1 cause Jervell and Lange-Nielsen syndrome. *Molecular genetics and metabolism*, *75*(4), pp.308-316.

Wangemann, P. and Schacht, J., 1996. Homeostatic mechanisms in the cochlea. In *The cochlea* (pp. 130-185). Springer New York.

Wangemann, P., 2002. K+ cycling and the endocochlear potential. *Hearing research*, *165*(1), pp.1-9.

Wangemann, P., 2006. Supporting sensory transduction: cochlear fluid homeostasis and the endocochlear potential. *The Journal of physiology*,*576*(1), pp.11-21.

Wangemann, P., Itza, E.M., Albrecht, B., Wu, T., Jabba, S.V., Maganti, R.J., Lee, J.H., Everett, L.A., Wall, S.M., Royaux, I.E. and Green, E.D., 2004. Loss of KCNJ10 protein expression abolishes endocochlear potential and causes deafness in Pendred syndrome mouse model. *BMC medicine*, *2*(1), p.30.

Willott, J.F., Turner, J.G., Carlson, S., Ding, D., Bross, L.S. and Falls, W.A., 1998. The BALB/c mouse as an animal model for progressive sensorineural hearing loss. *Hearing research*, *115*(1), pp.162-174.

Wollenberg, A.L., O'shea, T.M., Kim, J.H., Czechanski, A., Reinholdt, L.G., Sofroniew, M.V. and Deming, T.J., 2018. Injectable polypeptide hydrogels via methionine modification for neural stem cell delivery. *Biomaterials,* 1 9, Volume 178, pp. 527-545.

World Health Organization. 2019. Prevention of blindness and deafness. [Online]. [5 September 2019]. Available from: https://www.who.int/pbd/deafness/estimates/en/

Wozniak, M.A., Desai, R., Solski, P.A., Der, C.J. and Keely, P.J., 2003. ROCK-generated contractility regulates breast epithelial cell differentiation in response to the physical properties of a three-dimensional collagen matrix. *Journal of Cell Biology,* 10 11, 163(3), pp. 583-595.

Wright, J.L. and Schuknecht, H.F., 1972. Atrophy of the spiral ligament.*Archives of Otolaryngology—Head & Neck Surgery*, *96*(1), p.16.

Wu, T. and Marcus, D.C., 2003. Age-related changes in cochlear endolymphatic potassium and potential in CD-1 and CBA/CaJ mice. *Journal of the Association for Research in Otolaryngology*, *4*(3), pp.353-362.

Xia, A.P., Ikeda, K., Katori, Y., Oshima, T., Kikuchi, T. and Takasaka, T., 2000. Expression of connexin 31 in the developing mouse cochlea.*Neuroreport*, *11*(11), pp.2449-2453.

Xia, A.P., Katori, Y., Oshima, T., Watanabe, K., Kikuchi, T. and Ikeda, K., 2001. Expression of connexin 30 in the developing mouse cochlea. *Brain research*, *898*(2), pp.364-367.

Xia, A.P., Kikuchi, T., Hozawa, K., Katori, Y. and Takasaka, T., 1999. Expression of connexin 26 and Na, K-ATPase in the developing mouse cochlear lateral wall: functional implications. *Brain research*, *846*(1), pp.106-111.

Xia, A.P., Kikuchi, T., Minowa, O., Katori, Y., Oshima, T., Noda, T. and Ikeda, K., 2002. Late-onset hearing loss in a mouse model of DFN3 non-syndromic deafness: Morphologic and immunohistochemical analyses. *Hearing Research,* 166(1-2), pp. 150-158.

Xia, J.H., Liu, C.Y., Tang, B.S., Pan, Q., Huang, L., Dai, H.P., Zhang, B.R., Xie, W., Hu, D.X., Zheng, D. and Shi, X.L., 1998. Mutations in the gene encoding gap junction protein β-3 associated with autosomal dominant hearing impairment. *Nature genetics*, *20*(4), pp.370-373.

Xu, X. et al., 2012. Recreating the tumor microenvironment in a bilayer, hyaluronic acid hydrogel construct for the growth of prostate cancer spheroids. *Biomaterials,* 12, 33(35), pp. 9049-9060.

Yamaguchi, T., Nagashima, R., Yoneyama, M., Shiba, T. and Ogita, K., 2014. Disruption of Ion-Trafficking System in the Cochlear Spiral Ligament Prior to Permanent Hearing Loss Induced by Exposure to Intense Noise: Possible Involvement of 4-Hydroxy-2-Nonenal as a Mediator of Oxidative Stress. *PloS one*, *9*(7), p.e102133.

Yamaguchi, T., Yoneyama, M., Hinoi, E. and Ogita, K., 2015. Involvement of calpain in 4-hydroxynonenal-induced disruption of gap junction-mediated intercellular communication among fibrocytes in primary cultures derived from the cochlear spiral ligament. *Journal of pharmacological sciences*,*129*(2), pp.127-134.

Yoshida, T., Nin, F., Murakami, S., Ogata, G., Uetsuka, S., Choi, S., Nakagawa, T., Inohara, H., Komune, S., Kurachi, Y. and Hibino, H., 2016. The unique ion permeability profile of cochlear fibrocytes and its contribution to establishing their positive resting membrane potential. *Pflügers Archiv-European Journal of Physiology*, *468*(9), pp.1609-1619.

Yoshida, T., Nin, F., Ogata, G., Uetsuka, S., Kitahara, T., Inohara, H., Akazawa, K., Komune, S., Kurachi, Y. and Hibino, H., 2015. NKCCs in the fibrocytes of the spiral ligament are silent on the unidirectional K+ transport that controls the electrochemical properties in the mammalian cochlea.*Pflügers Archiv-European Journal of Physiology*, *467*(7), pp.1577-1589.

Yoshida, T., Sawamura, S., Ota, T., Higuchi, T., Ogata, G., Hori, K., Takashi, N., Doi, K., Sato, M.P., Nonomura, Y. and Horii, A., 2017. Fibrocytes in the cochlea of the mammalian inner ear: their molecular architecture, physiological properties, and pathological relevance. *Medical Research Archives*, *5*(6).

Yuge, I., Takumi, Y., Koyabu, K., Hashimoto, S., Takashima, S., Fukuyama, T., Nikaido, T. and Usami, S.I., 2004. Transplanted human amniotic epithelial cells express connexin 26 and Na-K-adenosine triphosphatase in the inner ear. *Transplantation*, *77*(9), pp.1452-1454.

Z Shen, F Liang, B. S., 2002. The membrane potential of type I fibrocytes is controlled by a Ca2+-dependent K conductance. *Abstr.-Ass. Res. ,* Otolaryngol(25), p. p. 389.

Zadeh, M.H., Storper, I.S. and Spitzer, J.B., 2003. Diagnosis and treatment of sudden-onset sensorineural hearing loss: a study of 51 patients.*Otolaryngology--Head and Neck Surgery*, *128*(1), pp.92-98.

Zdebik, A.A., Wangemann, P. and Jentsch, T.J., 2009. Potassium ion movement in the inner ear: insights from genetic disease and mouse models. *Physiology*, *24*(5), pp.307-316.

Zeng, F. G., 2004. Trends in Cochlear Implants. *Trends in Amplification,* 8(1), pp. 1-34.

Zhang, H. & Hornsby, P. J., 2002. Intradermal cell transplantation in soluble collagen.. *Cell transplantation,* 11(2), pp. 139-45.

Zhang, P.Z., He, Y., Jiang, X.W., Chen, F.Q., Chen, Y., Shi, L., Chen, J., Chen, X., Li, X., Xue, T. and Wang, Y., 2013. Stem cell transplantation via the cochlear lateral wall for replacement of degenerated spiral ganglion neurons. *Hearing research*, *298*, pp.1-9.
Zhuo, X.L., Wang, Y., Zhuo, W.L., Zhang, Y.S., Wei, Y.J. and Zhang, X.Y., 2008. Adenoviral-mediated up-regulation of Otos, a novel specific cochlear gene, decreases cisplatin-induced apoptosis of cultured spiral ligament fibrocytes via MAPK/mitochondrial pathway. *Toxicology*, *248*(1), pp.33-38.

Zidanic, M. & Brownell, W. E., 1990. Fine structure of the intracochlear potential field. I. The silent current. *Biophysical Journal,* 57(6), pp. 1253-1268.

Zietarska, M., Maugard, C.M., Filali-Mouhim, A., Alam-Fahmy, M., Tonin, P.N., Provencher, D.M. and Mes-Masson, A.M., 2007. Molecular description of a 3-D in vitro model for the study of epithelial ovarian cancer (EOC). *Molecular Carcinogenesis: Published in cooperation with the University of Texas MD Anderson Cancer Center*, *46*(10), pp.872-885.

Appendix

Appendix 1- video of cells included separately with electronic submission of thesis to Keele University library.